



UNIVERSITÀ  
DEGLI STUDI  
DI PADOVA

Sede Amministrativa: Università degli Studi di Padova

Dipartimento di *Scienze Cardiologiche, Toraciche e Vascolari*

---

SCUOLA DI DOTTORATO DI RICERCA IN : Scienze Mediche, Cliniche e Sperimentali

INDIRIZZO: Neuroscienze

CICLO XXVIII

## **MUSCLE MITOCHONDRIA DYSFUNCTIONS IN SPINAL AND BULBAR MUSCULAR ATROPHY**

**Direttore della Scuola:** Ch.mo Prof. Gaetano Thiene

**Coordinatore d'indirizzo:** Ch.ma Prof.ssa Elena Pegoraro

**Supervisore:** Ch.mo Dr. Gianni Sorarù

**Dottoranda:** Dott.ssa Doriana Borgia



## *Abstract*

Spinal and Bulbar Muscular Atrophy (SBMA), also known as Kennedy's Disease, is an X-linked recessive disorder, affecting only males, characterized by loss of motor neurons in the spinal cord and brainstem. Patients may also show signs of androgen insensitivity, including gynaecomastia, reduced fertility, and testicular atrophy. The molecular basis of SBMA is the expansion of a trinucleotide CAG repeat in the first exon of the *Androgen Receptor (AR)* gene, that results in an elongated polyglutamine (polyQ) tract in the translated protein. Recent reports suggest a primary role of muscle in SBMA pathogenesis and the presence of mitochondrial alteration in SBMA neuronal cells, knock-in mice and patients. The aim of this study was to investigate mutant *AR* effects on mitochondrial parameters in muscle tissue from 19 SBMA patients compared to sex and age-matched 18 control subjects. In SBMA muscle, AR protein levels were significantly increased in nuclei and significantly halved both in total lysate and in the cytosolic fraction as compared to controls. The altered distribution of AR in SBMA muscle tissue was associated with a 30-40% reduction of mitochondrial mass, measured as: mtDNA copy number, citrate synthase (CS) activity and dark blue area in muscle cross sections stained for NADH-DH. OXPHOS activity, normalised to CS, was normal. The reduced mitochondrial amount was correlated neither with atrophy and hypertrophy index nor with a decreased mitochondrial biogenesis. Rather, it was associated with an enhanced mitochondrial degradation through mitophagy, measured by biochemical and morphological assays. To explain mitophagy activation in SBMA muscle tissue, we evaluated mitochondria membranes composition through mass spectrometry. We found significant homogeneous decreased levels at 50% of all the cardiolipin molecular species in SBMA mitochondrial membranes, associated to a probably compensatory 1.5 and 2-fold increase in phosphatidylethanolamine and phosphatidylserine amount, respectively. The reduced cardiolipin levels was related to a decreased expression levels of *cardiolipin synthase* gene, involved in the biosynthesis of immature cardiolipin. In conclusion, for the first time, we showed a cause-effect mechanism of nuclear accumulation of polyQ AR linked to a reduction of mitochondrial mass in the muscle from SBMA patients, associated to an alteration of the mitochondrial membranes structure. Future studies will be needed to elucidate the exact

mechanism behind these abnormalities. Given the central role of mitochondria in cell bioenergetics and apoptosis, improvement of mitochondrial function is worth considering as a possible therapeutic approach to SBMA.

## *Riassunto*

L'Atrofia Muscolare Spino-Bulbare (SBMA), anche nota come malattia di Kennedy, è un disordine X-linked recessivo, che colpisce solo i soggetti di sesso maschile, caratterizzato dalla perdita dei motoneuroni inferiori del midollo spinale e del tronco encefalico. I pazienti, inoltre, possono presentare segni di insensibilità agli androgeni come la ginecomastia, la ridotta fertilità e l'atrofia testicolare. Essa è dovuta all'espansione del tratto polimorfico CAG presente nel primo esone del gene codificante per il *recettore degli androgeni (AR)*, che risulta in un tratto poliglutamminico più lungo nella proteina tradotta. Lavori recentemente pubblicati suggeriscono che il muscolo gioca un ruolo primario nella patogenesi della malattia di Kennedy e che ci sono alterazioni mitocondriali in cellule neuronali, topi knock-in e pazienti SBMA. Lo scopo di questo studio è stato quello di valutare l'effetto dell'espressione del recettore per gli androgeni mutato su alcuni parametri mitocondriali nel tessuto muscolare di 19 pazienti SBMA rispetto a 18 controlli di pari età e sesso. Nel muscolo SBMA, i livelli proteici di AR erano significativamente raddoppiati nei nuclei e significativamente dimezzati sia nel lisato totale che nella frazione citosolica rispetto ai controlli. L'alterata distribuzione del recettore per gli androgeni nel muscolo SBMA era associata ad una riduzione della massa mitocondriale di circa il 30-40%, misurata come: numero di copie di DNA mitocondriale, attività della citrato sintasi e area positiva all'attività dell'NADH-DH con un intenso segnale blu in sezioni trasversali di muscolo colorate per tale enzima. L'attività dei complessi della catena respiratoria, normalizzata per quella della citrato sintasi, è risultata normale. Questa riduzione della massa mitocondriale non è associata né ad una riduzione della biogenesi mitocondriale né agli elevati indici di atrofia ed ipertrofia, ma ad un'aumentata degradazione mitocondriale attraverso la mitofagia, misurata mediante analisi biochimiche e morfologiche. Per spiegare l'attivazione del processo mitofagico nel tessuto muscolare SBMA, abbiamo valutato la composizione lipidica delle membrane mitocondriali attraverso la spettrometria di massa. Abbiamo trovato un'omogenea riduzione del 50% di tutte le specie molecolari di cardiolipina nelle membrane mitocondriali SBMA, associata ad un aumento, probabilmente compensatorio, della quantità di fosfatidiletanolamina e fosfatidilserina, rispettivamente di 1.5 e 2 volte. La riduzione della quantità di cardiolipina era associata

ad una riduzione dei livelli di espressione del gene per la *cardiolipina sintasi*, coinvolto nella biosintesi della cardiolipina immatura. In conclusione, per la prima volta noi abbiamo mostrato un meccanismo causa-effetto di accumulo del recettore mutato nei nuclei del tessuto muscolare dei pazienti collegato ad una riduzione della massa mitocondriale, associata ad un'alterazione della struttura delle membrane mitocondriali. Successivi studi saranno necessari per spiegare l'esatto meccanismo alla base di queste anomalie. Dato il ruolo centrale dei mitocondri nella bioenergetica e nell'apoptosi, vale la pena considerare il miglioramento della funzione mitocondriale come un possibile approccio terapeutico per la malattia di Kennedy.

# Summary

Abstract .....	I
Riassunto .....	III
Summary .....	V
Abbreviations .....	IX
1. Introduction .....	1
PARTE I: SBMA .....	2
1.1. Clinical features .....	3
1.1.1. Female carriers.....	5
1.2. Diagnosis of Kennedy's Disease .....	6
1.3. Therapy.....	8
1.3.1. Targeting PolyQ AR mRNA Transcripts.....	9
1.3.2. Androgen Ablation Therapy.....	9
1.3.3. Heat Shock Proteins and UPS as Molecular Targets for Therapy .....	11
1.3.4. Autophagy-Mediated PolyQ AR Degradation .....	13
1.3.5. Allosteric Regulation of PolyQ AR Toxicity .....	15
1.3.6. Targeting PolyQ AR Aggregation and Nuclear Inclusion Formation ..	15
1.3.7. Regulation of Gene Expression .....	16
1.3.8. Mitochondrial Dysfunction .....	17
1.3.9. Trophic Support to Motor Neurons and Peripheral Tissues.....	17
1.4. Androgen Receptor .....	19
1.4.1. The <i>Androgen Receptor</i> Gene .....	19
1.4.2. The Androgen Receptor protein .....	20
1.4.3. Androgen functions.....	23
1.5. Pathogenesis .....	24
1.5.1. AR function in SBMA: Loss or gain of function?.....	24

1.5.2.	Nuclear accumulation of polyglutamine-expanded AR and cytoplasmic aggregates.....	25
1.5.3.	Ligand-dependent toxicity of polyglutamine-expanded AR .....	27
1.5.4.	Post-translational modification of AR.....	29
1.5.5.	Transcriptional dysregulation .....	29
1.5.6.	Disruption of axonal transport .....	30
1.5.7.	Mitochondrial dysfunction.....	31
1.5.8.	UPS and Autophagy in SBMA .....	33
1.5.9.	Non-cell autonomous toxicity: Muscle Matters in Kennedy’s Disease	35
1.6.	Animal models .....	36
PARTE II: MITOCHONDRIA .....		42
1.7.	Mitochondria.....	42
1.8.	Mitochondrial biogenesis.....	46
1.9.	Autophagy.....	49
1.9.1.	Lysosome biogenesis.....	53
1.10.	Mitophagy .....	54
1.10.1.	The PINK1/Parkin Pathway of Mitophagy .....	55
1.10.2.	Mitophagy in Erythrocyte Maturation, Hypoxia, and Embryogenesis	58
1.10.3.	Mitochondrial dynamics.....	60
1.11.	Mitochondrial membranes .....	63
1.11.1.	Cardiolipin biosynthesis .....	65
1.11.2.	Cardiolipin role .....	66
2.	Aims .....	73
3.	Material and Methods .....	75
3.1.	Tissue Samples.....	76
3.2.	Molecular analysis.....	78
3.2.1.	RT-PCR .....	78



3.3.	Biochemical analysis.....	79
3.3.1.	Total muscle lysates.....	79
3.3.2.	Nuclear and cytosolic fractions .....	80
3.3.3.	Mitochondria isolation .....	80
3.3.4.	Citrate synthase activity .....	80
3.3.5.	Protein quantization .....	81
3.3.6.	Western Blot analysis.....	82
3.3.7.	Blue Native PAGE.....	83
3.3.8.	OXPHOS Activity .....	83
3.3.9.	Mitochondria Lipid Extraction.....	84
3.3.10.	Nano Liquid Chromatography–Mass Spectrometry (LC–MS) Analysis .....	85
3.4.	Imaging.....	86
3.4.1.	Atrophy and Hypertrophy index.....	86
3.4.2.	Histoenzymatic NADH-DH assay .....	86
3.4.3.	Immunofluorescence.....	87
3.5.	Statistical analysis.....	88
4.	Results.....	89
4.1.	Normal polyQ AR transcript and abnormal protein levels and distribution in SBMA muscle tissue.....	90
4.2.	Reduction of mitochondrial abundance in SBMA muscle tissue .....	92
4.3.	Normal mitochondrial biogenesis in SBMA muscle tissue.....	94
4.4.	No correlation between Atrophy (AI) – Hypertrophy (HI) index and mtDNA copy number in SBMA muscle tissue. ....	96
4.5.	Increased autophagy in human SBMA muscle tissue.....	98
4.6.	Increased mitophagy in human SBMA muscle tissue.....	100
4.7.	Increased fission in the muscle tissue from SBMA patients .....	106

4.8.	Reduced biosynthesis and levels of cardiolipin in SBMA muscle tissue..	107
5.	Discussion.....	111
5.2.	Decreased mitochondrial mass in human SBMA muscle tissue.....	114
5.3.	Increased autophagy in human SBMA muscle tissue .....	116
5.4.	Increased mitophagy in human SBMA muscle tissue.....	118
5.5.	Mitochondrial dynamic in human SBMA muscle tissue.....	119
5.6.	Reduced cardiolipin amount in muscle mitochondria from SBMA patients .	120
	Conclusions .....	125
	References .....	127
	Relazione sull'attività svolta nel triennio di dottorato .....	143
	Curriculum vitae.....	151

# Abbreviations

17-AAG	17-allylamino-17-demethoxygeldanamycin
17-DMAG	17-(dimethylaminoethylamino)-17 demethoxygeldanamycin
AAC	ADP/ATP carrier
ACN	Acetonitrile
ADP	Adenosine diphosphate
AF	Activating function
AI	Atrophy index
ALCAT1	Acyl-CoA:lysoCL acyltransferase 1
AMPK	AMP-activated protein kinase
APP	Amyloid Precursor protein
AR	Androgen Receptor
ARE	Androgen responsive elements
ASC-J9	5-hydroxy-1,7-bis(3,4-dimethoxyphenyl)-1,4,6-heptatrien-3-one
ASOs	Antisense oligonucleotides
ATP	Adenosine triphosphate
AVs	Autophagic vacuoles
BH3	Bcl-2 homology 3
BNIP3	BCL2/Adenovirus E1B 19kDa Interacting Protein 3
BN-PAGE	Blue Native PAGE
BSA	Bovine serum albumin
CaMK	Calcium/calmodulin dependent protein kinases
cAMP	Cyclic adenosine monophosphate
CBP	CREB-binding protein
CDK1	Cyclin-dependent kinase 1
CDP-DG	CDP-diacylglycerol
CDR1 o CRLS1	Cardiolipin synthase
CHIP	C-terminus of heat shock cognate protein 70-interacting protein
CK	Creatine kinase
CL	Cardiolipin
CLD1	Cardiolipin deacylase
CLEAR	Coordinated Lysosomal Expression and Regulation
CMA	Chaperone-mediated autophagy
CNS	Central nervous system
CoA	Coenzyme A
COII	Cytochrome c oxidase subunit II
COX	Cytochrome c oxidase
CS	Citrate synthase
CS	Contact sites
CTE	C-terminal extension
Cyt c	Cytochrome c
DAPI	2-(4-amidinophenyl)-1H -indole-6-carboxamide
DBD	DNA-binding domain
DFCP1	Double FYVE domain-containing proteins
DHA	Docosahexaenoic acid
DHT	Dihydrotestosterone
DMC	Deuterated dichloromethane
Drp1	Dynamamin-related protein 1
DTNB	5,5-dithio-bis-2-nitrobenzoic acid
EGTA	Ethylene glycol tetraacetic acid

EMG	Electromyography
ER	Endoplasmic reticulum
ERRs	Estrogen-related receptors
ETC	Electron transport chain
FA	Fatty acids
FAM	6-carboxyfluorescein
FAO	Fatty acids oxidation
Fis1	Fission protein 1
FoxOs	Forkhead box
FUNDC1	FUN14 domain containing 1
GDNF	Glial cell line-derived neurotrophic factor
GnRH	Gonadotropin-releasing hormone
GRP75	Glucose-regulated protein
HAT	Histone acetyl transferase
HDAC	Histone deacetylase
HEPES	4-(2-hydroxyethyl)-1-piperazineethanesulfonic acid
HI	Hypertrophy
HIF-1	Hypoxia inducible factor-1
HPLC	High Performance Liquid Chromatography
HRP	Horseradish peroxidase
HSA	Human skeletal actin
hsc70	Heat shock cognate protein of 70 kDa
HSJ1	Hsp40 family members DnaJ-like-1
Hsp	Heat shock protein
ID	Inhibitory domain
IF	Immunofluorescence
IGF-1	Insulin-like growth factor 1
IM	Isolation membrane
IMM	Inner mitochondrial membrane
IMS	Intermembrane space
JNK	C-Jun N-terminal kinase
L4-CL	Tetralinoleoyl-CL
LAMP	lysosome-associated membrane protein
LBD	Ligand-binding domain
LC3	Microtubule associated protein 1 light chain 3
LC-MS	Liquid Chromatography–Mass Spectrometry
LIR	LC3-interacting regions
MEFs	Myocyte enhancing factors
MeOH	Methanol
Mfn	Mitofusins
MLCL	Monolyso-cardiolipin
MLCLAT1	Monolyso-cardiolipin acyltransferase-1
MOPS	3-(N-morpholino)propanesulfonic acid
MPP	Mitochondrial-processing protease
MPT	Mitochondrial permeability transition
Mt	Mitochondrial
mTOR	Mechanistic target of rapamycin
NADH	Nicotinamide adenine dinucleotide
NADH-DH	NADH dehydrogenase
Na-DOC	Sodium deoxycholate
NBT	Nitro-blue tetrazolium
NDUFB8	NADH:ubiquinone oxidoreductase subunit B8
NFL	Neurofilament light chain

NF-YA	Nuclear factor-YA
NIs	Nuclear inclusions
NLS	Nuclear localization signal
NP-40	Nonyl phenoxypolyethoxylethanol
NR	Nuclear receptor
NRF	Nuclear respiratory factors
NSE	Neuron-specific enolase
OMM	Outer mitochondrial membrane
Opa1	Optic atrophy 1
OXPPOS	Oxidative phosphorylation
PA	Phosphoatidic acid
PARP	poly(ADP-ribose) polymerase
PBS	Phosphate buffered saline
PC	Phosphatidilcholine
PCR	Polymerase chain reaction
PE	Phosphatidylethanolamine
PF	Paeoniflorin
PFA	Paraformaldehyde
PG	Phosphatidilglycerol
PGC-1	Peroxisome proliferator-activated receptor gamma coactivator-1
PGP	Phosphatidylglycerolphosphate
PI	Phosphatidilinositol
PI3K	Phosphoinositide3-kinase
PI3P	Phosphatidylinositol3-phosphate
PINK1	PTEN Induced Putative Kinase 1
PKA	Protein kinase A
polyG	Polyglycine
polyP	Polyproline
polyQ	Polyglutamine
PPAR- $\gamma$	Peroxisome proliferator-activated receptor- $\gamma$
PT	Permeability transition pore
Q-TOF	Time-of-Flight
RC	Respiratory Chain
RIPA	Radioimmunoprecipitation assay buffer
ROS	Reactive oxygen species
RPLPO	Large ribosomal protein
RT-PCR	Real-time polymerase chain reaction
SBMA	Spinal and Bulbar Muscular Atrophy
SE	Standard error
SIRT1	Sirtuin 1
SNB	Bulbocavernosus system
SOD	Superoxide dismutase
SQSTM1	Sequestosome
SRC-1	Steroid receptor coactivator-1
T	Testosterone
TAMRA	Tetramethylrhodamine
Taz	Tafazzin
TFAM	Transcription factor A mitochondrial
TFEB	Transcription factor EB
Tfm	Testicular feminization
Tg	Transgenic
TIS	Transcription initiation
TNB	5-thio-2-nitrobenzoic acid

UBA	Ubiquitin associated domain
ULK1	UNC-51-like kinase 1
UPS	Ubiquitin–proteasome system
UTR	Untranslated region
VDAC1	Voltage dependent anion channel 1
VEGF	Vascular endothelial growth factor
WB	Western Blot
WIPs	WD-repeat protein interacting with phosphoinoside
YY1	Yin-yang

# *1. Introduction*

## PARTE I: SBMA

Spinal and Bulbar Muscular Atrophy (SBMA), also known as Kennedy's Disease, was first recognized as a discrete syndrome by Dr. William Kennedy and his colleagues, who described a slowly progressive syndrome with muscle cramps in the 4th or 5th decade, progressing to generalized fasciculations and proximal muscle weakness, with bulbar involvement. The disease affects men only and is inherited in an X-linked recessive fashion (Kennedy et al., 1968). Affected males may show signs of androgen insensitivity, including gynaecomastia, reduced fertility, and testicular atrophy. The principal pathological manifestation of SBMA is the loss of motor neurons in the spinal cord and brainstem (Sobue et al. 1989). There is also a subclinical loss of sensory neurons in the dorsal root ganglia. The prevalence of this disease is estimated to be 1–2 per 100.000, whereas a considerable number of patients may have been misdiagnosed as other neuromuscular diseases including amyotrophic lateral sclerosis (Fischbeck, 1997). The molecular basis of SBMA is the expansion of a trinucleotide CAG repeat in the first exon of the *Androgen Receptor (AR)* gene on the long arm of the X chromosome (Xq11-12) (La Spada et al. 1991). The normal *AR* allele has 11–34 CAG repeats, whereas the expanded allele contains 38 to 66 (La Spada et al., 1992). In the translated protein, the CAG repeat codes for a polyglutamine (polyQ) tract, which is located in the N-terminal domain of the AR (starting from aa 58) (Fig. 1.1).

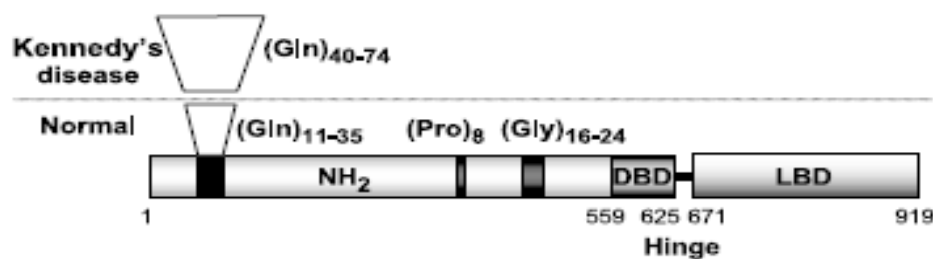


**Figure 1.1.** Schematic diagram of the structure of the androgen receptor (AR) protein including the domain structure and location of the polyglutamine (polyQ) repeat region. The AR has four functional domains: the N-terminal or transactivation domain, the DNA-binding domain (DBD), the hinge region and the ligand-binding domain (LBD). The N-terminal domain contains three different repeat regions: a polyQ region, a polyproline region and a polyglycine region. It is an expansion of the polyQ region that forms the basis of Kennedy's disease (Greenland and Zajac, 2004) (see section 1.4.2 for more details).



The identification of polyQ expansion in SBMA led to the discovery of a new class of neurodegenerative disorders. In fact, at least eight different polyQ-linked diseases, like Huntington's disease, spinal-cerebellar ataxia 1, 2, 3 or Machado-Joseph disease, 6 and 7, and dentatorubral and pallidoluysian atrophy, share a common molecular mechanism involving an expansion of a polyQ tract within different proteins (Piccioni et al., 2001). PolyQ diseases share several features. All of these diseases are neurodegenerative disorders with typically late onset, and all are inherited in an autosomal dominant fashion except SBMA, which is X-linked. There is a positive correlation between CAG repeat length and disease severity, and a negative correlation between repeat length and the age of disease onset (Doyu et al., 1992; Igarashi et al., 1992). Similar to other repeat expansion disorders, polyQ diseases show genetic anticipation, a phenomenon in which one generation shows a more severe phenotype and an earlier onset of disease compared with the previous generation, due to the fact that the repeat tends to expand when it is passed down from one generation to the next. Despite several common features shared by polyQ diseases, expansion of polyQ tracts in the different proteins causes degeneration only in specific neuronal subpopulations in each disease. This selective neuronal vulnerability results in clinically distinct disease phenotypes (Parodi and Pennuto, 2011). Expanded polyQ in AR selectively affects lower motor neuron function and maintenance.

### **1.1. Clinical features**

The major symptoms of SBMA are weakness, atrophy, and fasciculations of bulbar, facial, and limb muscles, which are attributable to degeneration of lower motor neurons in the spinal cord and brainstem (Kennedy et al., 1968; Harding et al., 1982). The disease progresses slowly; in a recent clinical trial, muscle strength as measured by quantitative muscle assessment declined by 2% per year in the placebo group (Fernandez-Rhodes et al, 2011). The majority of individuals with SBMA have a normal life expectancy and do not die from direct complications of the disease. Affected individuals are at risk of choking on food and aspiration pneumonia because of weakness of the bulbar muscles (Kennedy et al, 1968; Atsuta et al, 2006). Involvement is usually predominant in proximal musculature, and is occasionally asymmetric. The

onset is usually between 30 and 60 years of age. In a study on 26 patients the most frequent initial manifestations were premature exhaustion (62%), gynecomastia (52%), muscle cramps (38%), tremor (26%), and myalgia (24%). Weakness or bulbar involvement was the initial manifestation in only 4% of the patients each (Sperfeld et al., 2002). The initial site of weakness is lower limbs in more than half of patients (Atsuta et al., 2006; Rhodes et al., 2009). Limb weakness may result in gait disturbance, falls, or difficulty climbing stairs (La Spada et al., 1999). Typically, affected individuals require a wheelchair 15–20 years after the onset of weakness (Atsuta et al., 2006; Chahin and Sorenson, 2009). The extraocular muscles are typically spared. Fasciculations are not apparent at rest, but become conspicuous upon voluntary muscle movement. These contraction fasciculations are especially noticeable in the face, neck, and tongue. Neuromuscular symptoms are often worsened by coldness and by fatigue after exercise.

Since SBMA is X-chromosomal only males express the phenotype. X-chromosomal transmission also implies that affected men cannot pass the genetic trait on to their sons and that the risk to have a carrier as a daughter is 100%.

Affection of the brainstem motor nuclei results in involvement of the bulbar muscles. Bilateral facial and masseter muscle weakness, poor uvula and soft palatal movements, and atrophy of the tongue with fasciculations are often encountered. Tongue atrophy is usually associated with difficulty in chewing, vocal cord paresis resulting in dysarthria (unclear enunciation) or dysphonia, and pharyngeal paresis leading to dysphagia. Dysphagia is usually not so severe that it interferes with nutrition (Harding et al., 1982). Speech has a nasal quality in most cases due to reduced velopharyngeal closure. Patients occasionally experience laryngospasm, a sudden sensation of dyspnea (Sperfeld et al., 2005). Swallowing dysfunction is found in 80% of the cases and is characterised by incomplete food bolus clearance through the pharynx (Warnecke et al., 2009).

Muscle tone is usually hypotonic, and no pyramidal signs are detected. The deep tendon reflex is diminished or absent with no pathological reflex. Sensory involvement is largely restricted to a sense of vibration, which is affected distally in the legs (Sobue et al., 1989). Cerebellar symptoms are absent, while dysautonomia and mild cognitive impairment have been reported in a limited number of patients (Mirowska-Guzel et al., 2009; Rocchi et al., 2011).

Patients occasionally demonstrate signs of androgen insensitivity such as gynecomastia, testicular atrophy, dyserection, and decreased fertility, some of which are detected before the onset of motor symptoms (Nagashima et al., 1988; Sperfeld et al., 2002; Battaglia et al., 2003). Endocrinological examinations frequently reveal partial androgen resistance with elevated serum testosterone levels (Dejager et al., 2002). Although less common, hyperlipidemia, liver dysfunction and glucose intolerance are also detected. Abdominal obesity is common, whereas male pattern baldness is rare in patients with SBMA (Sinclair et al., 2007). Serum creatine kinase levels are elevated in the majority of patients (Sorarù et al., 2008; Chahin and Sorenson, 2009; Rhodes et al., 2009).

Muscle histopathology of SBMA patients is atypical for a motor neuron disease and shows both neurogenic and myopathic changes; there are groups of atrophic fibres with fibre type grouping as well as hypertrophic fibres, scattered basophilic fibres and central nuclei. Myogenic findings are consistent with the higher serum creatine kinase (CK) levels (Sorarù et al., 2008). Nerve biopsy may show moderate reduction of large myelinated fibers (Doyu et al., 1993). Scrotal skin biopsy may show the degree of nuclear accumulation of mutant AR and may be used to assess the efficacy of therapeutic trials (Banno et al., 2009). Nuclear accumulation of the pathogenic AR protein is observed in autopsied myocardium. Japanese physicians have recently reported an increased prevalence (11.8%) of Brugada-like ECG in their SBMA population; moreover 2 of their patients had a symptomatic Brugada syndrome and were affected by sudden death during follow-up (Araki et al., 2014).

### **1.1.1. Female carriers**

Females are usually heterozygous carriers of mutant expanded AR and they are generally asymptomatic. In detail, in about 50% of the cases female carriers of the mutation do not present with clinical manifestations. The other half may present with fasciculations, minimal distal weakness, muscle cramps, or hyper-CK-emia later in life (Tomik et al., 2006; Adachi et al., 2007). Two sisters, homozygous for the CAG-expansion, manifested with occasional muscle cramps, mild hand tremor, and occasional perioral fasciculations or twitches (Schmidt et al., 2002). The EMG may be normal or may show chronic denervation. Muscle biopsy in female carriers may show mild myopathic or neurogenic alterations (Sorarù et al., 2008).

The reason why female carriers are asymptomatic is not completely clear and the lyonization process seems to be not sufficient to explain it. In fact both X chromosome can be silenced, not only the one containing mutant *AR* (Paradas et al., 2008). Therefore it has been hypothesized that testosterone level could play a determinant role in the develop of the pathology. The binding between AR and its ligand is necessary to induce receptor translocation into the nucleus and begin the transcription of target genes. Having a lower amount of testosterone, females show a reduced activation of AR pathway in comparison with males, independently from the fact that AR is mutated or not and consequentially it is not sufficient to determine typical neurological features of SBMA. Animal studies support this hypothesis; indeed female AR-97Q mice treated with testosterone develop typical symptoms of SBMA (Katsuno et al., 2002).

## **1.2. Diagnosis of Kennedy's Disease**

Kennedy's Disease is thought to be a largely under-diagnosed condition. Its under-diagnosis results from a number of factors, including a lack of knowledge within the medical profession and similarities of presentation with other motor neuron degenerative disorders. The most common misdiagnosis for Kennedy's disease is amyotrophic lateral sclerosis. Correct diagnosis is imperative for appropriate counselling of affected individuals and family members. Kennedy's disease follows an X-linked mode of inheritance as the *AR* is located on the long arm of the X-chromosome. Other polyQ expansion diseases are autosomal dominant. The genetic diagnosis of Kennedy's disease is based on sizing of the CAG repeat region by amplification from genomic DNA using the technique of polymerase chain reaction (PCR). This is the standard technique for diagnosis of Kennedy's disease in symptomatic individuals, or presymptomatic individuals with a known family history. Heterozygous female carriers are also identifiable. In order to decide who undergoes to genetic analysis, clinical features play a central role. Indeed the presence of muscular cramps, hypostenia and atrophy in the proximal muscles, and bulbar involvement, particularly in association with tongue and perioral fasciculations are quite suggestive of SBMA. One of the main problem with SBMA is that for a long period symptoms are unspecific, often resulting in an important delay in the diagnosis. Some non-neural

features can be fundamental, such as gynecomastia, that is pathognomonic and the reduced fertility, especially if they are concomitant with neuromuscular symptoms. Even some endocrinal findings, for instance glucose intolerance or dyslipidemia, in association with lower motor neuron abnormalities, can support the diagnosis of SBMA. It is also important to consider family history of the patient, in order to investigate whether other family members have suffered from the disease.

Bulbar and spinal muscular atrophy is diagnosed upon the history, clinical neurologic examination, blood chemical investigations, nerve conduction studies, electromyography, evoked potentials, transcranial magnetic stimulation, and molecular genetic investigations. Nerve conduction velocities of motor and sensory nerves, compound muscle action potentials and sensory nerve action potentials may be reduced in SBMA, indicating an axonal degeneration in motor and sensory nerves. These abnormalities are usually more pronounced in the upper as compared with the lower limbs also confirmed by F-wave studies (Suzuki et al., 2008).

At last plasma levels of Creatine Kinase (CK) can be estimated. Creatine-kinase (CK) is usually elevated only in clinically manifesting male mutation carriers. However, it has been reported that non-manifesting male mutation carriers presented with idiopathic hyper-CK-emia 10 years before onset of the clinical manifestations (Sorenson and Klein, 2007).

In addition, biopsies from both muscle and scrotal tissue can be performed to assist in the diagnosis of SBMA. Muscle biopsy show both neuropathic and myopathic alterations. Indeed signs of neurogenic atrophy have been found: type I and II fibres aggregation, target fibres, atrophic fibres and subsarcolemmal nuclei clumping. On the other hand myopathic abnormalities are frequently present, such as a wide variability in fibres size (4-200 $\mu$ m), hugely hypertrophic fibres, spread basophilic fibres and necrotic fibres with vesicular nuclei. An increasing in connective tissue is usually detectable as well. Myopathic alterations are more incident in patients with a higher grade of disability in accordance with ADL scale or a late stage of disease (Sorarù et al., 2008). Scrotal skin biopsy may show the degree of nuclear accumulation of mutant AR, and may be used to assess the efficacy of therapeutic trials (Banno et al., 2009).

NMR in T1 measurement conducted on lower limb muscles highlights an increased signal. Moreover muscular atrophy can be detectable, showing a major involvement of flexor muscles (Hamano et al., 2004).

### 1.3. Therapy

Since a curative treatment for SBMA does not yet exist, only a palliative approach is possible. Severe preclinical studies have been shown to be beneficial, but the majority of them failed in the translation to clinical trials.

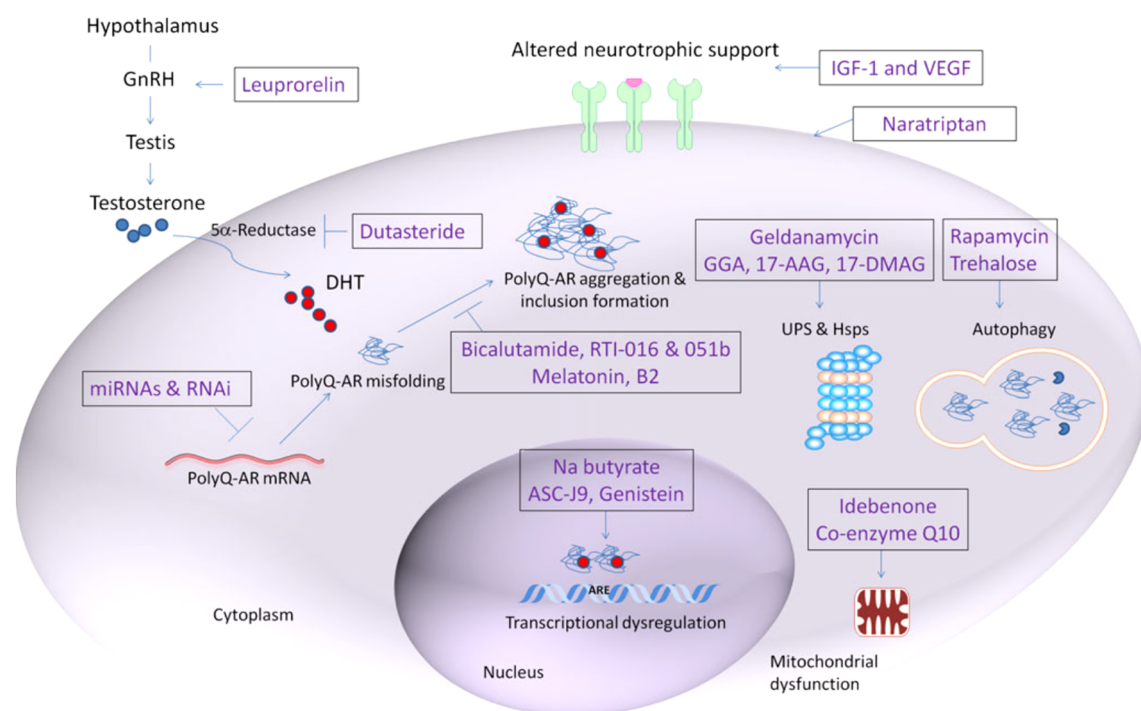


**Figure 1.2. Toxic pathways and therapeutic development for SBMA.** Multiple mechanisms of polyQ AR toxicity include loss of neurotrophic support, mitochondrial dysfunction, altered autophagy, protein aggregation, and transcriptional dysregulation. Therapeutic approaches to targeting polyQ AR toxicity include reduction of androgen availability through the use of antiandrogens; inhibition of polyQ AR mRNA transcription by RNAi and miRNA technology; trophic support with IGF-1 and VEGF; triptans; HDAC inhibition; overexpression of Hsps or treatment with agents to increase AR degradation by the UPS and autophagy; bicalutamine, melatonin, and B2 to target aggregation and inclusion formation; sodium butyrate and ASC-J9 to restore gene expression abnormalities; and antioxidants, such as Q10 and idebenone, to reduce oxidative stress (Rocchi and Pennuto, 2013).

### **1.3.1. Targeting PolyQ AR mRNA Transcripts**

Therapy designed to downregulate the expression of the disease protein may be effective. One strategy to reduce protein expression is post-transcriptional gene silencing based on the use of RNA interference (RNAi) technology. RNAi targeting the polyQ AR transcript has been shown to reduce the expression and toxicity of polyQ AR in mammalian and *Drosophila* cell models of SBMA (Caplen et al., 2002) (Fig. 1.2). Another approach to decrease the expression of *polyQ AR* was recently pursued in a transgenic mouse model of SBMA and was based on the use of microRNA technology (Miyazaki et al., 2012). In this case, an adeno-associated virus was used to deliver the microRNA miR-196a to motor neurons, where it reduced the stability of AR mRNA transcripts and attenuated disease manifestations in the transgenic SBMA mice (Fig. 1.2). These observations indicate that approaches targeting mutant protein transcript levels are effective in reducing toxicity and may therefore represent a therapeutic avenue worth pursuing.

Recently, Lieberman et al. developed antisense oligonucleotides that suppressed *AR* gene expression in the periphery but not the CNS in a mouse model of disease after subcutaneous administration. Suppression of polyQ AR in the periphery rescued deficits in muscle weight, fiber size, and grip strength, reversed changes in muscle gene expression, and extended the lifespan of mutant males. The therapeutic benefits documented here following peripheral administration of ASOs provide a compelling rationale for exploring treatments targeted to skeletal muscle in SBMA patients (Lieberman et al., 2014).

### **1.3.2. Androgen Ablation Therapy**

The ligand-dependent nature of SBMA offers the unique opportunity to develop a therapy based on the reduction of androgens in the serum. Testosterone levels in the serum are regulated by the hypothalamic–pituitary–testicular axis. The hypothalamus releases gonadotropin-releasing hormone (GnRH), which stimulates the anterior pituitary to release luteinizing hormone, which in turn stimulates secretion of testosterone from the testis. The hypothalamic–pituitary–testicular axis is regulated by negative feedback loops, and testosterone itself inhibits the hypothalamus and the anterior pituitary. Testosterone levels have been reported to be elevated in some SBMA

patients, suggesting that alterations in the hypothalamic–pituitary–testicular axis may contribute to SBMA pathogenesis (Dejager et al., 2002). Initially, assuming a loss of function of the mutated receptor that leads to the presence of signs of androgen insensitivity, it was thought to treat patients with testosterone. Testosterone had no negative effects on phenotypes in SBMA patients (Goldenberg and Bradley 1996; Neuschmid-Kaspar et al., 1996) or SBMA model mice (Chevalier-Larsen and Merry 2011). Notably, treatment of SBMA patients with testosterone was beneficial only when combined with physical exercise (Goldenberg and Bradley 1996). Conversely, surgical (Katsuno et al., 2002 e Chevalier-Larsen et al., 2004) or medical (Katsuno et al., 2003) castration has been demonstrated to prevent or improve the strength of male transgenic mice harbouring the human *androgen receptor* gene with expanded CAG repeats. In addition, female mutant mice without motor signs developed weakness after testosterone treatment (Katsuno et al., 2002). These findings suggest that ligand-dependent nuclear translocation of mutant AR and subsequent gain-of-toxic functions of these proteins in the nucleus play a key role in motor neuron dysfunction; therefore reduction of serum androgen levels may be therapeutically effective. Reduction of testosterone release can be achieved by treatment with gonadotropin-releasing hormone analogs, such as leuprorelin. Leuprorelin has been shown to inhibit nuclear accumulation of the polyglutamine-expanded AR, resulting in a marked improvement of neuromuscular phenotypes seen in the AR-97Q transgenic mice (Katsuno et al., 2003). Leuprorelin acts by preventing ligand-dependent nuclear translocation of the polyglutamine-expanded AR in the same way as castration (Fig. 1.2). In a phase 2 clinical trial, 12 months treatment with leuprorelin significantly diminished the serum level of creatine kinase, and suppressed the nuclear accumulation of the polyglutamine-expanded AR in the scrotal skin of patients. Of note is the observation that the frequency of AR-positive neurons in the anterior horn and brainstem of an autopsied patient, who received leuprorelin for 2 years, was less than in untreated SBMA patients (Banno et al., 2009). Nevertheless, no definite effects on motor functional scores or 6-minute walk test were observed in a 48-week randomized placebo-controlled multicentric clinical trial of this drug, although there was the improvement of swallowing function in a subgroup of patients whose disease duration was less than 10



years as well as the decrease of AR accumulation in scrotal skin biopsies and serum levels of creatine kinase (Katsuno et al., 2010).

Lack of positive results may be attributable to several factors: insensitiveness of the outcome measure utilized, antianabolic effects of leuprorelin, a relatively short observation period, and placebo-related improvement of motor function. The disease duration of the patients may also have influenced the effects of the androgen deprivation therapy. For these reasons, Yamamoto et al. evaluated the efficacy of medical castration maintained with leuprorelin on the muscle strength of SBMA patients over 3 years. It is noteworthy that most of the patients showed a 20–30% reduction in average leg strength despite the leuprorelin treatment for 3.5 years (Yamamoto et al., 2012). In conclusion, leuprorelin was not effective in this small long-term treatment trial in SBMA.

Testosterone is converted to its more potent derivative dihydrotestosterone by the activity of 5-alpha-reductase (Poletti, 2004; Parodi and Pennuto, 2011). Motor neurons express high levels of 5-alpha-reductase, suggesting the possibility that conversion of testosterone to dihydrotestosterone (DHT) is responsible for selective motor neuron degeneration in SBMA. The activity of 5-alpha-reductase can be inhibited by dutasteride (Fig. 1.2). Dutasteride efficacy has recently been evaluated in a phase-II clinical trial (Fernandez-Rhodes et al. 2011). Dutasteride treatment didn't give significant improvement of muscle strength and quality of life.

### **1.3.3. Heat Shock Proteins and UPS as Molecular Targets for Therapy**

Many components of the ubiquitin proteasome system and Hsps are known to co-localize with polyglutamine-containing nuclear inclusions (NIs), implying that failure of cellular defence mechanisms underlies neurodegeneration in polyglutamine diseases (Bauer and Nukina, 2009). A therapeutic strategy consists in the manipulation of expression of molecular chaperones, such as *Hsp90*, *Hsp70*, and the co-chaperone *Hsp40*. There is increasing evidence that Hsps abrogate polyglutamine-mediate cytotoxicity by refolding and solubilizing the pathogenic proteins (Nagai et al., 2010). Overexpression of *Hsp70*, together with *Hsp40*, inhibits toxic accumulation of the polyglutamine-expanded AR and suppresses cell death in a cellular model of SBMA (Kobayashi et al., 2000). *Hsp70* has also been shown to facilitate proteasomal degradation of the polyglutamine-expanded AR in another cell culture model of SBMA

(Bailey et al., 2002). Overexpression of the inducible form of human *Hsp70* markedly ameliorates symptomatic and histopathological phenotypes in a transgenic mouse model of SBMA (Adachi et al., 2003). C-terminus of heat shock cognate protein 70-interacting protein (CHIP) also prevents nuclear accumulation of the polyglutamine-expanded AR and thereby ameliorates motor symptoms in a transgenic mouse model of SBMA (Adachi et al., 2007). Overexpression of the *Hsp40* family members *DnaJ-like-1* (*HSJ1*), *HSJ1a* and *HSJ1b* in cultured cells also reduced polyQ AR aggregation through increased protein ubiquitination and degradation by the UPS in vitro (Howarth et al., 2007). Overexpression of *Hsp105alpha* has also been shown to reduce polyQ AR aggregation and neurotoxicity in cell models of SBMA (Ishihara et al., 2003).

*Hsps* expression can be manipulated pharmacologically. Hsp90 exists in two different complexes in the cell. The first complex includes Hsp70 and Hop, which target Hsp90 client proteins for degradation by the UPS; the other includes Cdc37 and p23, which stabilize the Hsp90 client protein. The Hsp90 inhibitor geldanamycin has been shown to reduce polyQ AR aggregation and promote degradation through a mechanism that involves inhibition of retrograde trafficking of polyQ AR (Thomas et al., 2006) (Fig. 1.2). Oral administration of acyclic isoprenoid geranylgeranylacetone GGA in transgenic SBMA mice increased the expression of *Hsp90*, *Hsp70*, and *Hsp105* and attenuated disease manifestations (Katsuno et al. 2005) (Fig. 1.2). Unfortunately, this compound is highly toxic and cannot be used for prolonged therapy in humans. The less toxic GGA derivative 17-allylamino-17-demethoxygeldanamycin (17-AAG) has been shown to induce mutant AR degradation and reduce motor neuron degeneration and death in SBMA cells and mice (Waza et al., 2005; Rusmini et al., 2011) (Fig. 1.2). Moreover, a more potent and water-soluble Hsp90 inhibitor named 17-(dimethylaminoethylamino)-17 demethoxygeldanamycin (17-DMAG) has also been proven effective in SBMA mice (Tokui et al., 2009) (Fig. 1.2). Recently was tested in mouse a ‘smart-drug’, arimoclomol, that, in contrast to drugs previously tested in models of spinal and bulbar muscular atrophy, only enhances the heat shock response in cells already under stress and in which the heat shock response is already activated (Kalmar et al., 2008), significantly reducing the likelihood of non-specific side effects in otherwise unstressed cells, which have been observed following the use of direct activators of the heat shock response (Kalmar et al., 2008). Treatment of AR100Q mice

with an oral dose of arimoclomol significantly delayed disease progression (Malik et al., 2013).

A therapeutic strategy that leads to AR degradation via UPS, consist in using Genistein, that promotes the dephosphorylation of AR at serine 515 via p44/42 MAPK inhibition, disrupting the interaction between AR and ARA70, a coregulator, and promotes AR protein clearance through the ubiquitin–proteasome system (Qiang et al., 2013) (Fig. 1.2).

#### **1.3.4. Autophagy-Mediated PolyQ AR Degradation**

Induction of autophagy, cellular machinery coping with abnormal protein toxicity, is also shown to mitigate the toxicity of the polyglutamine-expanded AR in cultured motor neurons (Montie et al., 2009). In the process of autophagy, degradation of proteins occurs through lysosomes. Autophagy activity is functionally and genetically linked to the UPS, as UPS impairment may lead to autophagy activation through a process that involves the activity of the histone deacetylase 6 (HDAC6). Importantly, overexpression of *HDAC6* in the eye of SBMA flies reduced neurodegeneration, suggesting that HDAC6-mediated activation of autophagy plays a protective role in SBMA pathogenesis (Pandey et al. 2007). A functional link between the UPS and autophagy is also supported by the finding that the protective effect of 17-AAG is associated with increased polyQ AR degradation by autophagy in cultured cells (Rusmini et al. 2011). In support of the neuroprotective role of autophagy, was demonstrated that depletion of p62 significantly increased the levels of monomeric mutant AR and mutant AR protein complexes in an SBMA mouse model via the impairment of autophagic degradation. In addition, *p62* overexpression improved SBMA mouse phenotypes by inducing cytoprotective inclusion formation. Thus, p62 provides two different therapeutic targets in SBMA pathogenesis: (1) autophagy-dependent degradation and (2) benevolent inclusion formation of the mutant AR (Doi et al., 2013). By contrast, inhibition of unfolded protein response, an endoplasmic reticulum stress response, exacerbates muscle pathology of SBMA via the activation of autophagy, suggesting that a fine tuning of protein quality controls system may be needed to mitigate the toxicity of polyglutamine-expanded AR. Genetic ablation of the autophagy-related gene *Beclin-1* in this mouse model attenuated some aspects of disease

pathogenesis, highlighting the complexity of the autophagy pathway in the context of disease pathogenesis (Yu et al., 2011). Autophagy has been shown to be activated in the skeletal muscle of a knock-in mouse model of SBMA (Yu et al., 2011).

Similar to Hsp activity, autophagy can also be pharmacologically manipulated. Activation of autophagy by rapamycin, an inhibitor of the autophagy regulator mechanistic target of rapamycin (mTOR), suppressed the neurodegenerative phenotype caused by polyQ AR in the eye of a *Drosophila* SBMA model (Pandey et al., 2007) (Fig. 1.2). Moreover, induction of autophagy by trehalose rescued primary SBMA motor neurons from polyQ AR-induced toxicity (Montie et al., 2009; Montie and Merry 2009) (Fig. 1.2). Rapamycin toxicity limits its applicability for treatment of chronic disorders. Recently was examined the effects of paeoniflorin (PF) in cultured cells and the transgenic mouse model of SBMA. PF administration inhibited the nuclear accumulation of the mutant AR and significantly ameliorated the motor phenotype of the SBMA mouse model without detectable toxicity. Mutant AR was preferentially degraded over wild-type AR in the presence of PF in both cell culture and mouse models of SBMA. PF significantly induced *nuclear factor-YA (NF-YA)*, resulting in the upregulation of the molecular chaperones *CHIP* and *TFEB* and consequent enhancement of the two major proteolysis systems, the molecular chaperone–UPS and the autophagy system. PF promoted the degradation of mutant AR to a greater extent than the induction of either the molecular chaperone–UPS or the autophagy system alone (Tohna et al., 2014). Furthermore, the last year was tested the combinatory treatment with trehalose and bicalutamide in motoneurons, that results very efficient in the removal of insoluble species of AR with a very long polyQ (Q112) tract, which typically aggregates into the cell nuclei. Using the antiandrogen bicalutamide (casodex), which slows down AR activation and nuclear translocation, and the disaccharide trehalose, an autophagy activator, was found that the two compounds together reduced PolyQ AR insoluble forms with higher efficiency than that obtained with single treatments. The PolyQ AR clearance was mediated by trehalose-induced autophagy combined with the longer cytoplasmic retention of PolyQ AR bound to Bicalutamide (Giorgetti et al., 2015).

### **1.3.5. Allosteric Regulation of PolyQ AR Toxicity**

Ligand binding induces a conformational change that leads to intramolecular or intermolecular N-term/C-term interactions. The observation that mutations that prevent the N/C interaction reduce the toxicity of polyQ AR suggests that this ligand-induced conformational change is a potential therapeutic target (Nedelsky et al., 2010; Orr et al., 2010). Flutamide is a non-steroidal anti-androgen known to reduce or prevent the N/C interaction, and is already used for prostate cancer treatment. In SBMA mice, flutamide had no effect on disease progression and manifestations (Katsuno et al., 2003). However, flutamide showed beneficial effects when administered at the prenatal stage in transgenic mice, suggesting a potential beneficial effect when administered in very early developmental stages (Johansen et al., 2010; Monks et al., 2007). Another anti-androgen that reduces the AR N/C interaction is bicalutamide, which has recently been shown to reduce polyQ AR aggregation and prevent DHT-dependent toxicity in PC12 cells expressing an AR with 112 glutamine residues and in primary motor neurons obtained from SBMA mice. The effect of these anti-androgens suggests that selective AR modulators (SARMs) with the ability to inhibit the AR N/C interaction may be effective in SBMA. Consistent with this idea, the two SARMs RTI-016 and RTI-051b that inhibit AR N/C interaction were shown to induce nuclear translocation of AR in the absence of aggregation and toxicity (Orr et al., 2010). Whether these SARMs will be effective in vivo is not yet known.

### **1.3.6. Targeting PolyQ AR Aggregation and Nuclear Inclusion Formation**

Expansion of polyQ tracts leads to protein misfolding and deposition of mutant protein in the forms of microaggregates/oligomers and inclusions (Walcott and Merry 2002; Jochum et al, 2012). The finding that inclusion formation can be associated with protection, rather than toxicity, has provided the rationale for identification of compounds that promote inclusion formation (Arrasate et al., 2004). Recently, it has been shown that treatment of cell and fly models of SBMA with B2 results in increased accumulation of mutant AR into inclusions and reduced toxicity, further supporting the idea that accumulation of polyQ expanded protein into inclusions is protective (Palazzolo et al., 2010) (Fig. 1.2). On the contrary, deposition of polyQ AR into microaggregates correlates with toxicity in cell and mouse models of the disease.

Interestingly, by atomic force microscopy, polyQ AR aggregates have been characterized as oligomeric fibrils of 300–600 nm in length, different from the annular species formed by wild-type AR (Jochum et al., 2012). From a therapeutic point of view, melatonin has been shown to shift the deposition of polyQ AR from oligomeric fibrils to annular oligomers, highlighting another potential avenue for treatment of SBMA (Jochum et al., 2012).

### **1.3.7. Regulation of Gene Expression**

Expression of *polyQ AR* alters gene transcription (Lieberman et al., 2002; Mo et al., 2010; Nedelsky et al., 2010). Transcription dysregulation is a primary pathogenic process in polyQ diseases. Altered gene expression is a consequence not only of sequestration of transcription factors and co-regulators, but also of altered chromatin remodeling. One of the major modifications of chromatin involves histone acetylases, such as CREB-binding protein (CBP), which is associated with gene expression, and histone deacetylases (HDAC), which is associated with gene silencing. PolyQ proteins has been shown to sequester CBP into inclusions and alter its activity and histone acetylation, defects that were rescued by overexpression of CBP (McCampbell et al., 2000; Taylor et al., 2003). Since suppression of HDAC activity results in augmentation of histone acetylation and subsequent restoration of gene transcription, HDAC inhibitors have been considered to be of therapeutic benefit in polyglutamine diseases (Butler and Bates, 2006). Butyrate, the first HDAC inhibitor to be discovered, has been shown to ameliorate symptomatic and histopathological phenotypes of the AR-97Q transgenic mouse model through upregulation of histone acetylation in nervous tissues (Minamiyama et al., 2004) (Fig. 1.2).

AR regulates gene expression through interaction with transcription cofactors, both co-activators and co-repressors. Genetic evidence obtained in a fly model of SBMA indicates that the interaction of polyQ AR with some transcriptional coregulators is pathogenetic and reveals amplification of the native function of the protein as a critical determinant of disease pathogenesis (Nedelsky et al., 2010). This evidence supports the idea that the gain of toxic function conferred by polyQ expansion to the mutant protein involves not only acquisition of a novel aberrant function, but also augmentation of normal protein function(s). This evidence implies an alternative approach to restore

normal gene expression, which consists in targeting the interaction of polyQ AR with co-regulators of transcription. Treatment of SBMA mice with the curcumin-related compound 5-hydroxy-1,7-bis(3,4-dimethoxyphenyl)-1,4,6-heptatrien-3-one (ASC-J9) disrupted the interaction between AR and its co-regulator ARA70 and improved disease symptoms by decreasing nuclear aggregation and increasing mutant AR clearance (Yang et al., 2007) (Fig. 1.2). Treatment of the mice with ASC-J9 did not alter the levels of testosterone in the serum of SBMA mice, thereby avoiding side effects on sexual activity and fertility.

### **1.3.8. Mitochondrial Dysfunction**

Several findings suggest a role for mitochondrial dysfunction in SBMA pathogenesis. Cytochrome c oxidase subunit Vb interacts with wild-type and polyQ AR and is sequestered into polyQ AR-positive inclusions (Beauchemin et al., 2001). Alteration of mitochondrial distribution and membrane depolarization, together with elevated levels of reactive oxygen species, has been observed in cell models of SBMA (Piccioni et al., 2002; Ranganathan et al., 2009). In addition, polyQ AR has been shown to repress the *transcription of peroxisome proliferator-activated receptor gamma co-activator-1 (PGC1 $\alpha$ )*, a transcriptional co-activator that regulates mitochondrial biogenesis and respiration (Ranganathan et al., 2009). Moreover, polyQ AR can alter mitochondrial function by inducing Bax-dependent cytochrome c release and apoptosis in primary cortical neurons (Young et al. 2009). Furthermore, alteration in the copy number of mitochondrial DNA in leucocytes of SBMA patients and carriers has been reported (Su et al., 2010). It is still debated whether mitochondrial dysfunction represents a consequence of cellular degeneration or if it plays a pathogenic role in SBMA. From a therapeutic perspective, antioxidants such as coenzyme Q10 and idebenone have been shown to reduce the levels of reactive oxygen species produced when polyQ AR is expressed in cultured cells (Ranganathan et al., 2009) (Fig. 1.2). However, it remains to be established whether this strategy is effective in animal models of the disease.

### **1.3.9. Trophic Support to Motor Neurons and Peripheral Tissues**

Altered gene expression as well as disruption of axonal transport may contribute to polyQ disease pathogenesis by decreasing trophic support for neurons. Among the

genes that have been shown to be down-regulated in mouse models of SBMA are the *vascular endothelial growth factor (VEGF)*, *insulin-like growth factor 1 (IGF-1)*, *glial cell line-derived neurotrophic factor (GDNF)*, *transforming growth factor-beta* and *neurotrophin-4* (Katsuno et al., 2010; Sopher et al., 2004; Yu et al., 2006). Activation of VEGF and IGF-1 signaling has been shown to be beneficial in SBMA mouse models, indicating this as a novel therapeutic strategy to attenuate disease manifestations (Palazzolo et al., 2009; Sopher et al., 2004) (Fig. 1.2). Recently was demonstrated that arimoclomol significantly enhances the survival of motor neurons, upregulating the expression of *VEGF* with a significant amelioration in the disease phenotype of mice with SBMA (Malik et al., 2013). Interestingly, muscle-restricted overexpression of a muscle-specific isoform of *IGF-1 (mIGF-1)* in SBMA mice protects from the toxicity of polyQ AR via a mechanism that involves direct modification of the disease protein (Palazzolo et al., 2009). MIGF-1 activated Akt in the muscle of SBMA mice, which then in turn stimulated the phosphorylation of polyQ AR and its turnover through proteasome. Activation of the IGF-1/Akt signaling in muscle not only resulted in a remarkable amelioration of muscle, but also of spinal cord pathology together with amelioration of motor dysfunction and increased survival. These findings support the idea that muscle represents a critical tissue target of polyQ AR toxicity and highlight that intervention in muscle may be therapeutically relevant for SBMA. Clenbuterol is a b<sub>2</sub>-agonist known to have anabolic effects on skeletal muscle, including the activation of PI3K/Akt signaling. An open trial suggests that clenbuterol may improve motor function in patients with SBMA without relevant adverse events. As compared with baseline, there was a mean increase of approximately 12% in 6MWD at 3 months and continuing to 12 months of treatment. These results are particularly intriguing because the natural history of SBMA is characterized by an 11.3% rate of decrease in 6MWD per year, regardless of the initial walking capacity of patients (Querin at al., 2008). Further in vitro and in vivo studies need to confirm the beneficial role of clenbuterol as SBMA treatment.



## 1.4. Androgen Receptor

### 1.4.1. The *Androgen Receptor* Gene

The action of both testosterone and 5 $\alpha$ -dihydrotestosterone is mediated by the intracellular androgen receptor. The androgen receptor is a member of the superfamily of nuclear receptors, which includes the steroid hormone receptors, thyroid hormone receptors and retinoic acid receptors (Beato et al., 1995). The androgen receptor is encoded by a messenger RNA of approximately 11 kb. The *AR* gene is localized in the long arm of the X chromosome, in its pericentromeric region at Xq11-q12 (Marcelli et al., 1990). Males have a single copy of the *AR* gene, while females possess two copies of the gene; however, in females, one allele undergoes random X-inactivation. The open reading frame, like those of the majority of the members of the steroid receptor superfamily, is separated over eight exons, and has a length of 2730 bp, encoding a protein of 910 amino acids, which are organized in several well-defined regions: (1) an N-terminal transactivation region, coded by exon 1, poorly conserved among the steroid nuclear receptor superfamily members; (2) a highly conserved DNA-binding domain, coded by exons 2 and 3, where each exon codes for one zinc (Zn) finger; and (3) a less conserved C-terminal ligand binding domain, coded by exons 4–8 (Fig. 1.3).

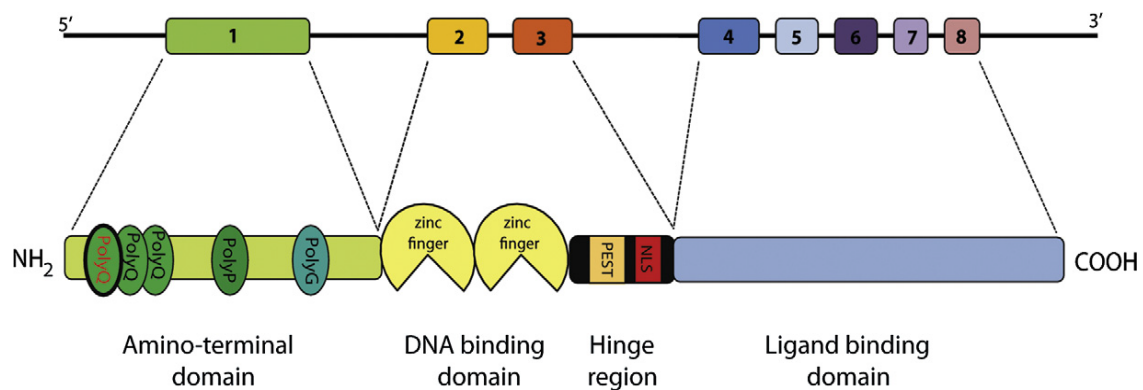


**Figure 1.3. Scheme of AR gene and protein.** The *AR* gene is composed of eight exons. The first exon encodes the amino-terminal domain, which contains three polyQ tracts (polyQ), a poly-proline tract (polyP) and a poly-glycine tract (polyG). The first polyQ tract (red) is expanded in SBMA. Exons 2 and 3 encode the DNA-binding domain, which is formed by two zinc fingers, and the hinge region, which contains the PEST sequence and the nuclear localization signal (NLS). Exons 4 through 8 encode the ligand-binding domain (Parodi and Pennuto, 2011).

In the amino-terminal domain, the human androgen receptor contains several polyamino-acid sequences that are polymorphic and responsible for the variability in the size of AR (Poletti et al., 2005). Two of these are very long: a glutamine stretch (Q stretch) starting at amino acid residue 58 and a glycine stretch (G stretch), starting at position 448. The Q stretch is encoded by a CAG repeat, and the G stretch by a GGT/C repeat. The DNA binding domain of the androgen receptor reveals approximately 80% homology with those of the glucocorticoid receptor, mineralocorticoid receptor and progesterone receptor. Central in the structure of the DNA binding domain are the interactions of four cysteine residues with a zinc ion in each of the two zinc clusters. The three amino acid residues which are important for specific recognition of the androgen response element are glycine-568, serine-569 and valine-572. The ligand binding domain of the androgen receptor is confined to a carboxy-terminal fragment of approximately 250 amino acids. The amino acid sequence of this domain is completely conserved between the human, rat and mouse receptors, indicating that its structure is very important in androgen receptor function (Trapman and Brinkmann, 1996). The promoter region of the *AR* gene is characterized by the absence of a canonic TATA box and CAAT box, but contains GC rich elements, a SP1 binding site, homopurine stretches, cAMP responsive elements and AP1 sites (Quigley et al., 1995). Two androgen responsive elements (ARE) have been identified in exons 4 and 5 of the *AR* gene (Grad et al., 2001); these selectively control the activation of the *AR* promoter, being responsible for androgen-mediated upregulation of AR messenger RNA in target cells. Two principal sites of transcription initiation (TIS I and TIS II) (Jenster et al., 1995) separated by 11 nucleotides have been identified approximately 1100 bp upstream to the translation-start site (Faber et al., 1993). The primary transcript is characterized by an unusually long 5'-untranslated region (5'-UTR), containing a short open reading frame driven by the first AUG in the 5'-UTR and coding for a peptide of nine amino acids whose functional roles remain to be determined. The translation into the AR protein starts at the second AUG (Chlenski et al., 2001).

#### **1.4.2. The Androgen Receptor protein**

The AR is a ligand-activated transcription factor that, in its inactive form, is confined in a multiheteromeric inactive complex in the cell cytoplasm (Tyagi et al., 2000). The

inactive complex contains several chaperones (Hsp90 and Hsp70), that dissociate from the receptor after the binding to the ligands (T or DHT), via the C-terminal ligand binding domain; this process allows a conformational change induced by the ligand that unmasks the nuclear localization signals in the region between the DNA binding domain (DBD) and the ligand binding domain (LBD) (residues 608-624) (Claessens et al., 1989). It has been proposed that this variation of the tertiary structure is also due to post-translational modifications, like the phosphorylation of specific serines (Brinkmann et al., 2001). The dissociation from the accessory proteins allows the translocation of AR into the cell nuclei, its dimerization, and, through the DNA-binding domain, the interaction with specific enhancer sequences, known as androgen responsive elements (ARE), located up- or downstream of the core promoter region of androgen-responsive gene. At this stage, the transcriptional control by AR is modulated by complex interactions between the receptor and positive (coactivator) or negative (corepressor) factors (Poletti et al., 2005) (Fig. 1.4).

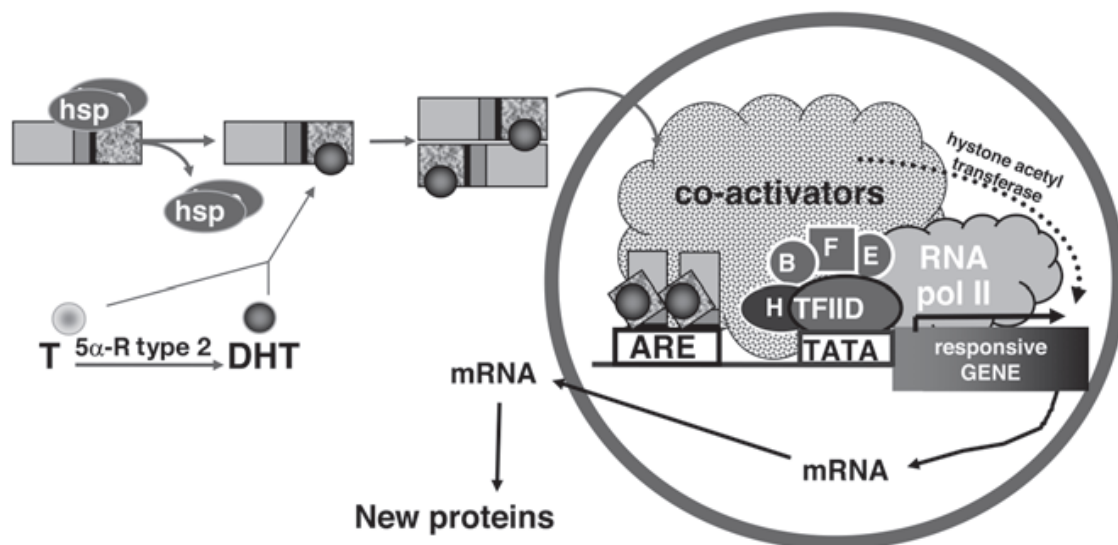


**Figure 1.4. Mechanism of androgen action.** See text for explanation. (Poletti et al., 2005).

Upon binding DNA, the AR undergoes DNA dependent dimerization mediated by its DBD (Dahlman-Wright et al., 1991). The DBD of all nuclear receptors is a highly conserved region arranged into three  $\alpha$ -helices containing two cysteine-rich zinc finger-like motifs and a C-terminal extension (CTE) (Glass et al., 1994). The first zinc finger

contains a stretch of five amino acids called the P-box that directly interacts with the major groove of DNA, conferring responsibility for sequence recognition and DNA binding (Umesono et al., 1989). Within the second zinc finger resides a five-amino acid region called the D-box, which contains the major residues involved in DNA-dependent dimerization between receptor monomers (Dahlman-Wright et al., 1991; Umesono et al., 1989). In addition, residues in the CTE (amino acids 625–636) provide an additional dimer interface for the AR-DBD that acts in concert with amino acids in the second zinc finger to mediate specific and high-affinity DNA binding (Schoenmakers et al., 2000). Whereas the core DBD of nuclear receptors is a highly conserved region, sequence homology is reduced within the CTE, resulting in unique residues that may potentiate specificity. Another potential contributor to AR dimerization is the AR N/C interaction. The N/C interaction was first identified using the mammalian two-hybrid assay system as an androgen-dependent interaction between the AR-LBD and the AR-Nterm domain (NTD) that results in receptor stabilization (Langley et al., 1995). Upon androgen binding, the AR-LBD undergoes a conformational rearrangement that results in the formation of a highly conserved protein-protein interaction surface known as activation function 2 (AF-2). Androgens induce a ligand-dependent intermolecular interaction between AF-2 in the AR-LBD and 23FQNL27 in the AR-NTD. AF-2 can also interact with 433WHTLF437 in the AR-NTD but with a much lower affinity than 23FQNL27 (He et al., 2000). Physiologically, the N/C interaction stabilizes the AR by slowing the rate of ligand dissociation and preventing receptor degradation (Langley et al., 1995). The dimeric receptor binds to the AREs sequences, composed of two symmetric 6 bp separated by a 3-bp spacer and oriented as direct or inverted repeat (GGTACAnnnTGTTCT sequence). When the AR dimer binds ARE, the transcriptional activity depends on the formation of specific transcription initiation complexes and the recruitment of other nuclear factors, driven by transcriptional activator domains of the AR (AF-1, AF-2, and AF-5) (Poletti et al., 2005). The AR N-terminal presents two out of three main transactivation regions (AF, activating functions). AF-1, the main AF in the N-terminal, spans between amino acids 51 and 211 (encompassing the PolyGln tract). It becomes active only after AR binding to ligand; in fact the region is hindered by the interaction of the AR with the Hsps complex bound to the LBD. The second N-terminal transactivation region AF-5 spans between residues 370 and 494. An inhibitory

domain (ID) is located upstream of the DNA-binding domain (DBD). The AF-2 is located in the C-terminus (Palazzolo et al., 2008). The AR-coactivators complex (a) recruits the general transcription factors to the TATA box and (b) exerts histone acetyltransferase activity destructuring the nucleosomes to allow RNA polymerase II to transcribe the genes (Spencer et al., 1997); these mechanisms act jointly and activate transcription of target genes.

The abnormal size of the polyGln tract in SBMA alters the transcriptional behaviour of the AR, probably because of its close integration into the AR transactivation domain. In fact, the highly polymorphic PolyGln tract apparently might act as a protein–protein interaction domain, and may be involved in the control of AR mediated transcription. Thus, very similar PolyGln tracts have been found in other transcription factor. (Palazzolo et al., 2008).

#### **1.4.3. Androgen functions**

Because of *AR* is expressed ubiquitously, androgen effects are wide spread, but they are predominantly detectable in androgen target tissues, such as skeletal muscle, liver, skin, central nervous system (CNS), adrenal gland, epididymis and prostate, where the highest levels can be found (Keller et al., 1996). One of the major targets of androgen action in the CNS are the motoneurons of the spinal nucleus of the bulbocavernosus (SNB) system (Matsumoto et al., 1988), known as Onuf's nucleus in humans. In this structure, androgens control the development and adult maintenance of SNB at different stages (Goldstain et al., 1992), by acting in two steps at time of birth (during sexual differentiation) and at the beginning of puberty, when androgens modulate the formation of synapses at neuromuscular junctions controlling the growth and maturation of SNB dendritic branches. In adulthood, androgens are involved in the maintenance of the size of motoneurons (Watson et al., 2001) and of their dendrites in SNB; moreover, androgens act also on the muscle fibers (Jordan et al., 2002), where have anabolic effects (Bhasin et al., 1997; Brodsky et al; 1996; Sinha-Hikim et al., 2004). It is known that androgen deprivation reduces the somatic size and the dendritic length of motoneurons, affecting also the number of chemical and electrical (gap junction) synapses; by contrast, androgen replacement therapy reverses these phenomena (Brooks et al., 1998). In addition, androgens promote the re-growth of several peripheral nerves

after resection, like the hypoglossal (Yu et al., 1989), facial, and sciatic (Kujawa et al., 1993) nerves.

The androgen receptor is a key molecule during development of male reproductive tissues. For example, the androgen receptor is essential for the maintenance of prostate structure and function. Orchiectomy or inhibition of androgen receptor activity by anti-androgens leads to a rapid loss of the secretory epithelial cells (Trapman and Brinkmann, 1996).

Mutations in the androgen receptor gene are found in several human diseases. Best documented so far are mutations which are the cause of androgen insensitivity. X-linked androgen insensitivity is associated with abnormalities in male sexual morphogenesis. These can range from genetic males with severe or mild defects in the development of the male phenotype (partial androgen insensitivity), to those with an apparent female phenotype (complete androgen insensitivity). Mutations can range from complete or partial deletion of the gene (which is a rare event) to point mutations or frame shift mutations in the open reading frame. Most point mutations are missense mutations that result in inhibition of ligand or DNA binding of the androgen receptor. Only a small number of mutations have been detected in the long N-terminal domain of the receptor; all of these are nonsense mutations or frame shifts, leading to the synthesis of a truncated protein (Trapman and Brinkmann, 1996). None of these mutations leads to neurodegeneration as polyQ expansion.

## **1.5. Pathogenesis**

### **1.5.1. AR function in SBMA: Loss or gain of function?**

The cause of SBMA is expansion of a trinucleotide CAG repeat, which encodes the polyglutamine tract, in the first exon of the *AR* gene (La Spada et al., 1991). The CAG repeat within the *AR* ranges in size from 9 to 34 in normal subjects, and from 38 to 62 in SBMA patients with a tissue-specific somatic mosaicism (La Spada et al., 1991; Tanaka et al., 1999). Multiple founder effects have been reported in Japan, Europe, and Australia (Tanaka et al., 1996; Lund et al., 2001). The expanded polyglutamine tract in AR has been implicated in the pathogenesis of SBMA in two different, but not mutually

exclusive, ways: (1) loss of normal AR function inducing neuronal degeneration, and (2) the polyglutamine-expanded AR acquiring toxic properties for motor neurons. Since AR possesses trophic effects on neuronal cells, one can assume that the loss of AR function may play a role in the pathogenesis of SBMA. For example, brain-derived neurotrophic factor signaling is regulated by AR in motor neurons (Verhovshek et al., 2010). Also, the endocrine abnormalities observed in SBMA patients indicate that polyQ expansion leads to a partial loss of AR function. However, a pure loss of function mechanism is difficult to reconcile with the observation that mutations that completely abolish AR function result in androgen insensitivity syndrome with no signs of neurodegeneration. Rather, expansion of polyQ is thought to confer a toxic gain of function to the mutant protein. Although this loss of function of AR may contribute to the androgen insensitivity in SBMA, the pivotal cause of neurodegeneration in SBMA is thought to be a gain of toxic function of the polyglutamine-expanded AR. This hypothesis is supported by the observation that motor impairment has never been observed in severe testicular feminization (Tfm) patients lacking AR function or in AR knockout mice (Brinkmann, 2001). Moreover, a transgenic mouse model carrying an elongated CAG repeat driven by human AR promoter demonstrated motor impairment, suggesting that the expanded polyglutamine tract itself is sufficient to induce the pathogenic process of SBMA (Adachi et al., 2001).

#### **1.5.2. Nuclear accumulation of polyglutamine-expanded AR and cytoplasmic aggregates**

A pathologic hallmark of polyglutamine diseases is the presence of nuclear inclusions (NIs). In SBMA, NIs containing the pathogenic AR are found in the residual motor neurons in the brainstem and spinal cord as well as in non-neuronal tissues including prostate, testis, and skin (Li et al., 1998). These inclusions are detectable using antibodies recognizing a small portion of the N-terminus of the AR protein, but not by those against the C-terminus of the protein. This observation implies that the C-terminus of AR is truncated or masked upon formation of NIs. A full-length AR protein with expanded polyglutamine tract is cleaved by caspase-3, liberating a polyglutamine-containing toxic fragment, and the susceptibility to cleavage is polyglutamine repeat length-dependent (Kobayashi et al., 1998). Thus, proteolytic cleavage is likely to

enhance the toxicity of the pathogenic AR protein. Although NIs are important histopathological findings, their role in the pathogenesis of polyQ diseases has been debated. Several studies indicate that NIs are likely formed as a result of cellular defence reactions coping with the pathogenic polyglutamine protein (Taylor et al., 2003). On the other hand, nuclear localization or accumulation of the abnormal proteins has been considered to be decisive for inducing neuronal cell dysfunction and degeneration in polyQ diseases including SBMA (Klement et al., 1998). An immunohistochemical study on autopsied SBMA patients, using an anti-polyglutamine antibody, 1C2, demonstrated that diffuse nuclear accumulation of the polyglutamine-expanded AR is more frequently observed than NIs in the anterior horn of the spinal cord (Adachi et al., 2005). The frequency of diffuse nuclear accumulation of the polyglutamine expanded AR in spinal motor neurons strongly correlates with the length of the CAG repeat in the *AR* gene (Adachi et al., 2005). No such correlation has been found between NIs occurrence and the CAG repeat length. Taken together, it appears that the polyglutamine-expanded AR principally accumulates within the nuclei of motor neurons in a diffusible form, leading to neuronal dysfunction and eventual cell death. Since the human *AR* is widely expressed in various organs, accumulation of the polyglutamine expanded AR protein is detected not only in the central nervous system, but also in non-neuronal tissues such as pancreas and scrotal skin (Li et al., 1998; Banno et al., 2006). Furthermore, inclusions containing mutant AR are positive for ubiquitin, supporting the hypothesis of a toxicity due to an abnormal response to the polyQ tract, that avoid degradation through the proteasome. Moreover several proteins are detectable in the inclusions, such as chaperones Hsp70, Hsp90, CREB Binding Protein (CBP) and other transcription factors. The loss of function of the proteins that are sequestered, could contribute to the disease pathogenesis (Poletti et al., 2004; Abel et al., 2001; Stenoien et al., 1999).

Another important observation is the presence of cytoplasmic mutant AR aggregates in neural and non-neural tissues (Adachi et al., 2005). Proteins with long polyGln sequences have a propensity to aggregate into high molecular weight insoluble protein complexes. Several hypotheses have been put forward to explain the formation of intracellular aggregates. Polyglutamine sequences can form stable  $\beta$ -pleated sheets ('polar zippers') that enable protein-protein interaction. Given that the AR is a



transcription factor, and that glutamine-rich domains of other transcription factors are thought to be involved in the protein-protein interactions that are required for assembling a transcription complex, the expanded glutamine repeat might lead to aberrant transcriptional regulation of target genes that leads to motor-neuron death. Alternatively, expansion of the repeat could exaggerate a normal interaction that is unrelated to transcription or promote formation of a novel protein complex that is toxic to neurons. Also, the expanded glutamine repeat might be a better substrate for transglutaminase, a ubiquitous enzyme that crosslinks glutamine residues in proteins with primary amines (for example, lysine residues in other proteins). The isodipeptide linkages that are formed by this enzyme are difficult for cells to degrade and, thus, could accumulate over time, leading to disruption of normal cellular function. Neurons, as long-lived, post-mitotic cells, might be particularly sensitive to this process (Brooks and Fischbeck, 1995). Aggregates are cytotoxic. For instance, sensory neurons within the dorsal root ganglion often show AR aggregates in the cytoplasm, that appear to be associated with axonal degeneration of sensory nerves in SBMA (Suzuki et al., 2008), while the cytoplasmic deposits of AR in the pancreas likely correspond to diabetes. Most important, also the wild-type AR form aggregates. The pathogenic AR mutants formed oligomeric fibrils up to 300–600 nm in length. These were clearly different from annular oligomers 120–180 nm in diameter formed by the non-pathogenic receptors (Jochum et al., 2012). In a mouse model of SBMA, soluble oligomers are detectable prior to the onset of neuromuscular symptoms (Li et al., 2007), suggesting that they play a role in pathogenesis of the disease. The aggregate formation and pathology of SBMA is strictly dependent on the presence of the androgen receptor's physiological ligand dihydrotestosterone (DHT), confirming the ligand-dependent nature of SBMA (Jochum et al., 2012).

### **1.5.3. Ligand-dependent toxicity of polyglutamine-expanded AR**

SBMA presents a unique feature, among PolyQ diseases, in that it is the only disorder in which a chemical compound (the AR ligands testosterone or DHT) is able to modify the protein localization, by favouring nuclear uptake, and aggregation (Poletti et al., 2004). This makes SBMA a ligand-dependent disorder, since the ligand-activated PolyQ AR exerts its effect by a toxic gain of function (Adachi et al., 2003; Katsuno et al., 2002;

Palazzolo et al., 2009) only after testosterone-induced conformational changes, which occur during the activation process of the receptor (Simeoni et al., 2000). In these conditions, the PolyQ AR accumulates into nuclear and cytoplasmic aggregates, both in neural and nonneural tissues (Adachi et al., 2005). Thus, the ligand-dependent intracellular trafficking of AR appears to play an important role in the pathogenesis of SBMA. In a transgenic mouse model of SBMA expressing the full-length human *AR* containing 97 CAGs (AR-97Q), neuromuscular symptoms are markedly pronounced and accelerated in the male mice, but either not observed or far less severe in the female counterparts (Katsuno et al., 2002). Androgen deprivation through surgical castration substantially improved the symptoms, histopathological findings, and nuclear accumulation of the polyglutamine-expanded AR in the male AR-97Q mice. In contrast, subcutaneous injection of testosterone causes significant aggravation of symptoms, histopathological features, and nuclear localization of the polyglutamine-expanded AR in the female AR-97Q mice. Since the nuclear translocation of AR is ligand-dependent, testosterone appears to show toxic effects by accelerating nuclear translocation of the polyglutamine-expanded AR. The ligand-dependent degeneration of motor neurons has also been reported in other animal models of SBMA (Takeyama et al., 2002; Yu et al., 2006). It should be noted that testosterone deprivation by castration reverses motor dysfunction in transgenic mice of SBMA (Chevalier-Larsen et al., 2004; Katsuno et al., 2006b). Lending support to the ligand-dependent hypothesis are the clinical observations that manifestation of symptoms is minimal even in the females homozygous for an expanded CAG repeat in the *AR* gene, and that testosterone administration may exacerbate neuromuscular symptoms of SBMA patients (Schmidt et al., 2002; Kinirons and Rouleau, 2008). Ligand binding results in the dissociation of the receptor from Hsps and translocation to the nucleus. To determine whether ligand converts polyQ AR into a toxic species because it brings the disease protein to the nucleus, several *AR* variants were generated with either mutations of the acetylation site KXKK, addition of a nuclear export signal, or deletion of the nuclear localization signal. These mutations block or reduce nuclear translocation without altering ligand binding. These *AR* variants suppress polyQ AR toxicity, indicating that nuclear translocation is a prerequisite for toxicity (Montie et al., 2009; Nedelsky et al., 2010; Takeyama et al., 2002). However, *polyQ AR* fused to a nuclear localization signal localizes to the nucleus

in the absence of ligand, but fails to trigger neurodegeneration, indicating that nuclear translocation is necessary, but not sufficient for toxicity (Montie et al., 2009; Nedelsky et al., 2010). This observation implies that events beyond ligand-induced nuclear translocation are central to disease pathogenesis.

#### **1.5.4. Post-translational modification of AR**

AR is substantially modified, in response to hormone binding, by phosphorylation, sumoylation, and acetylation. These post-translational modification has been implicated in the neurotoxicity of the polyglutamine-expanded AR. Akt-induced phosphorylation of AR at serines 215 and 792 blocks ligand binding and thereby mitigates toxicity in cultured motor neurons (Palazzolo et al., 2007). On the other hand, the phosphorylation of AR at 514 is shown to activate caspase-3, which in turn increases the amount of N-terminal fragment of AR via protein cleavage, resulting in the enhancement of the pathogenic AR toxicity in a cellular model of SBMA (LaFevre-Bernt and Ellerby, 2003). In addition to phosphorylation, acetylation and sumoylation are also shown to modify the toxicity of the polyglutamine-expanded AR. Acetylation at lysines 630/632/633 stabilizes the polyglutamine expanded AR and enhances its cytotoxicity (Montie et al., 2011). Sumoylation enhances the solubility of the polyglutamine expanded AR and inhibits the formation of insoluble aggregates and soluble oligomers in a manner that is independent of AR transcriptional activity (Mukherjee et al., 2009).

#### **1.5.5. Transcriptional dysregulation**

AR is a transcription factor that specifically regulates the expression of hormone-responsive genes. Transcription dysregulation is central to polyQ disease pathogenesis. It has been reported that nuclear inclusions frequently sequester other important proteins, including transcriptional co-activators, such as CBP, interfering with normal cell processes. The expression of genes regulated through CBP-mediated transcription is decreased in mouse models of polyglutamine diseases (Sugars and Rubinsztein, 2003). CBP functions as histone acetyltransferase, regulating gene transcription and chromatin structure. It has been demonstrated that acetylation of nuclear histone H3 is significantly diminished in SBMA mice (Minamiyama et al., 2004). Additionally, dysfunction of CBP results in a decreased expression of *vascular endothelial growth factor* and *type II*

*transforming growth factor-beta receptor* that are required for neuronal survival (Sopher et al., 2004; Katsuno et al., 2010a). Testosterone-dependant transcriptional dysregulation has also been studied using a *Drosophila* model of SBMA, in which the polyglutamine-expanded AR enhances an androgen-dependent association of AR with Retinoblastoma protein (Suzuki et al., 2009). This interaction appears to result in an aberrant E2F transactivation through the suppression of histone deacetylation. In HSA-AR Tg mouse model, overexpressing wild-type *AR* exclusively in myocyte, have been described many transcriptional changes that occur early and late in motor dysfunction progression and, importantly, are androgen-dependent (Halievski et al., 2014).

Increasing polyglutamine length can inhibit the interaction between AR and its coactivators, resulting in a partial loss of function (Irvine et al., 2000). Also, the polyQ tract can exacerbate the interaction of AR and other protein that normally regulate the function of the receptor. For example, NLK interacts with mutant AR at the N-terminal region of the protein, and, interestingly, polyQ expansion results in a more robust interaction between NLK and mutant AR in comparison to wild-type AR. The binding of NLK to AR, and its subsequent phosphorylation at S81, strongly inhibit the AR N/C interaction, and yet paradoxically increase AR-mediated gene transcription, exacerbating the transcriptional activity of the receptor (Todd et al., 2015).

#### **1.5.6. Disruption of axonal transport**

Motor neurons possess extremely long axon along which molecular motors transport essential components such as organelles, vesicles, cytoskeletons, and signal molecules. This implies that axonal trafficking plays a fundamental role in maintenance of normal function of motor neurons. Obstruction of axonal transport has gained attention as a cause of neuronal dysfunction in a variety of neurodegenerative diseases including SBMA (Gunawardena and Goldstein, 2005). The polyglutamine-expanded AR activates c-Jun N-terminal kinase (JNK), leading to the inhibition of kinesin-1 microtubule-binding activity and eventual disruption of anterograde axonal transport (Morfini et al., 2006). It is noteworthy that JNK inhibitors reverse the suppression of neurite outgrowth by pathogenic AR in cultured cells (Morfini et al., 2006). Piccioni et al. also demonstrate that cytoplasmic inclusions of the polyglutamine-expanded AR, when formed in the axons, alter the distribution of kinesin and interfere with axonal transport

of organelles, such as mitochondria (Piccioni et al., 2002). Furthermore, in the AR-97Q transgenic mouse model of SBMA, the mRNA level of dynactin 1 is substantially reduced, leading to the disruption of retrograde axonal transport (Katsuno et al., 2006). The defects in retrograde labeling of motor neurons and the blockade of endosomal trafficking are also documented in a knock-in mouse model of SBMA carrying *AR-113Q* (Kemp et al., 2011). Additionally, the deficits of retrograde axonal transport are also observed in mice over-expressing wild-type *AR* in muscle that demonstrate motor axonal degeneration mimicking SBMA (Monks et al., 2007; Kemp et al., 2011).

### 1.5.7. Mitochondrial dysfunction

In SBMA, mitochondrial dysfunction results from various interactions of elongated poly-Q AR with mitochondria, mitochondrial proteins, nuclear or mitochondrial DNA, causing oxidative stress, decreased mitochondrial membrane potential, or activation of the mitochondrial caspase pathway. In cell and animal models of SBMA mutant AR causes mitochondrial dysfunction by indirect effects on the transcription of nuclear-encoded mitochondrial genes or on mitochondrial proteins. It is now well established that poly-Q AR tracts are associated with lower levels of transcription of androgen-responsive, nuclear-encoded genes, including those that directly or indirectly influence mitochondrial functions. Genes down-regulated in MN-1 AR-65Q cells were those for *superoxide dismutase-1 (SOD-1)*, *SOD-2*, *catalase*, *NADH-dehydrogenase-1*, and *TFAM*, which is also controlled by PGC-1, resulting in increased ROS levels. Also in AR113Q knock-in mice transcript levels of *PGC-1* and *SOD-2* were significantly decreased (Ranganathan et al., 2009).

In an androgen-treated yeast two-hybrid system, COXVb colocalized to polyQ AR aggregates in a hormone-dependent manner providing a mechanism in which sequestration of mitochondrial proteins leads to mitochondrial dysfunction in SBMA (Beauchemin et al., 2001). There are also indications that mutant poly-Q AR results in decreased mitochondrial membrane potential (Ranganathan et al., 2009).

In leukocytes derived from SBMA patients and carriers was found a reduction in mtDNA copy number, that inversely correlated with the CAG-repeat length (Su et al., 2010). Furthermore, in these patients and carriers was found an increased frequency of the deletion mtDNA4977.

In MN-1 and PC-12 cells expressing the mutant polyQ AR, ligand-dependent activation of the mitochondrial caspase pathway with increased levels of key proteins of the apoptosis cascade, such as Bax, caspase 9, or caspase 3, and increased cell death were observed (Ranganatan et al., 2009). These effects were driven by altered expression of the *peroxisome proliferator-activated receptor- $\gamma$*  (*PPAR- $\gamma$* ). In another study on primary cortical neurons from mice it was found that N-terminal fragments of expanded poly-Q ARs activate apoptosis via activation of the c-Jun N-terminal kinase (JNK) (Young et al., 2009).

Presence of poly-Q AR also alters distribution of mitochondria within a cell. In transfected HeLa cells cytoplasmic AR48Q-aggregates sequestered mitochondria, HSPs, proteasome components, and steroid receptor co-activator (SRC-1), result in abnormal distribution of mitochondria within the cytoplasm and axons (Stenoien et al., 1999). One reason why mitochondria become aberrantly distributed could be an increased energy need in the vicinity of poly-Q AR aggregates. In fact, in a study on NCS34 cells, mitochondria were localised to neuronal processes containing poly-Q AR aggregates (neuropil aggregates) contrary to other cytosolic aggregates, which occurred peri-nuclearly. In some cells neuropil aggregates and accumulation of mitochondria corresponded to axonal swelling (Piccioni et al., 2002).

In a cell model of SBMA (MN-1 AR-65Q cells) the mitochondrial mass was reduced compared to MN-1 cells transfected with AR-20Q. Additionally, morphology of mitochondria was abnormal with cristae vesiculation, vacuolation, and fragmentation (Ranganatan et al., 2009).

There is increasing evidence that SBMA has a primary myopathic component and that mitochondrial dysfunction plays a role in the development of this myopathy (Orsucci et al., 2014). Speculations have been raised suggesting that myopathy starts before motor neuron degeneration in SBMA. Evidence for a mitochondrial contribution to myopathy in SBMA comes from animal and patients studies (Jordan et al., 2008). In two studies on AR-100Q transgenic mice muscle biopsy showed increased staining for NADH (Sopher et al., 2004; Monks et al., 2007). In a 55yo SBMA patient with exercise intolerance and hyper-CKemia, muscle biopsy showed mixed myopathic and neurogenic features together with “mitochondrial features”. Staining for oxidative enzymes revealed some COX-hypo-reactive fibers (Orsucci et al., 2014).

### **1.5.8. UPS and Autophagy in SBMA**

The PolyQ AR aggregates contain several chaperones, component of the ubiquitin–proteasome system (UPS), as well as transcription factors (Hdj2, Hsc70, Hsp70, Hsp90, the steroid receptor coactivator 1 (SRC-1), and the CREB-binding protein (CBP)) (Abel et al., 2001; Adachi et al., 2001, 2007; Stenoien et al., 1999). The colocalization of mutant polyQ proteins with molecules involved in protein refolding and degradation suggests the possibility of an involvement or a sequestration of these molecules into the aggregates. Protein catabolism is an essential protective event for the clearance of mutant and misfolded proteins. The two major intracellular degradative systems are the UPS and the autophagy. The UPS is a specific and selective proteolytic system for short-lived proteins. UPS degradation involves two steps: (i) the conjugation of ubiquitin moieties to the substrate and (ii) the degradation of the poly-ubiquitinated proteins by the 26S proteasome complex, followed by the recycling of ubiquitin and the release of short peptides (Ciechanover and Brundin, 2003). Macroautophagy, normally referred to as autophagy, is a highly conserved degradative process that removes cytoplasmic long-lived proteins, organelles, and portion of cytoplasm sequestered by a double membrane vesicle or autophagosome. These structures ultimately fuse with lysosome (Xie and Klionsky, 2007). In the absence of hormone, when cytoplasmic PolyQ AR is maintained inactivated by chaperones (Hsp70, and Hsp90), the soluble, non aggregated PolyQ AR impaired the UPS (Rusmini et al., 2007). UPS impairment could be the result of the unactivated-AR recruitment; in fact, UPS is unable to efficiently degrade the elongated polyQ regions of the proteins (Holmberg et al., 2004). PolyQ AR cytotoxicity correlated with UPS impairment (Pandey et al., 2007). Testosterone binding to AR induces posttranslational modifications that generate conformational changes resulting in AR dissociation from Hsps chaperones (Palazzolo et al., 2009; Poletti et al., 2004; Poletti et al., 2005). The release of the chaperones might unmask the polyQ tract; thus, testosterone-activated AR acquires the capability to self-aggregate (Rusmini et al., 2007). Surprisingly, the PolyQ AR activation correlated with proteasome desaturation (Rusmini et al., 2007). In theory, by clearing the cells from misfolded proteins, the UPS should prevent the formation of nuclear aggregates, but the overload of misfolded substrates impairs UPS activity leading to PolyQ AR accumulation also in the nuclei. Ligand-mediated PolyQ AR activation resulted in

nuclear aggregation (Pandey et al., 2007). Interestingly, in SBMA cellular models, the PolyQ AR retention in the cytoplasm may prevent the nuclear translocation, promoting cytoplasmic aggregates formation. The cytoplasmic sequestration of PolyQ AR into aggregates prevented the appearance of the PolyQ AR neurotoxicity (Montie et al., 2009; Montie and Merry, 2009; Rusmini et al., 2007). The aggregate-prone proteins, like PolyQ AR, seem to be substrates which can be degraded by macroautophagy. The activation of macroautophagy can be visualized using as marker the microtubule associated protein 1 light chain 3 (LC3), which, when autophagy is activated, associates to autophagosome vesicles membranes in its LC3-II lipidated form (Mizushima and Kuma, 2008; Mizushima, 2010). Overexpression of *polyQ AR* leads to the accumulation of LC3 puncta (Rusmini et al., 2010) and the formation of electron dense autophagic vacuoles (AVs) (Taylor et al., 2003). In a fly model of SBMA, expressing *polyQ AR* in the eye leads to classic degenerative phenotype, accompanied with AVs and multivesicular-body accumulation (Pandey et al., 2007). Additionally, motor neurons of a transgenic mouse model expressing 100 CAG repeats (AR100) have increased numbers of AVs at post-symptomatic stages, suggesting alterations in the autophagy pathway are indeed features of SBMA. Recently was uncovered a novel interaction between TFEB and polyQ AR. Dynamic measurements of autophagy markers revealed impairments in autophagic flux in SBMA cells, which correlated with marked deficits in TFEB target gene expression (Cortes et al., 2014). Importantly, Cortes et al. restored autophagy flux by overexpressing *TFEB* in patient-derived NPCs. Genetic ablation of autophagy in *Drosophila* exacerbates polyQ AR eye degeneration phenotypes (Pandey et al., 2007) and depletion of *p62* in AR97Q transgenic mice significantly worsens motor and neurological phenotypes (Doi et al., 2013). Conversely, pharmacological activation of autophagy through Rapamycin treatment suppresses polyQ AR eye degeneration, and this effect is dependent on functional autophagy and HDAC6 (Pandey et al., 2007). Like other aggregate prone proteins, cytosolic polyQ AR can be a substrate of autophagy (Montie et al., 2009). Although the nucleus has emerged as the principal site of polyQ disease pathogenesis, degradation of cytoplasmic polyQ AR oligomers would reduce nuclear polyQ AR available for aggregation and toxicity. Autophagy induction was detected in AR dNLS112Q cultured motor neurons, and inhibition of autophagy augmented testosterone-mediated toxicity in this model (Montie et al., 2009),



further suggesting that targeting of cytosolic polyQ AR for autophagy degradation could have important beneficial effects in SBMA.

Recently, was demonstrated that skeletal muscle plays a primary role in SBMA pathogenesis, superseding motor neurons as the key site of polyQ AR toxicity (Cortes et al., 2014; Lieberman et al., 2014; Sorarù et al., 2008). Interestingly, while TFEB activity in SBMA motor neurons and patient derived NPCs was significantly reduced, analysis of quadriceps muscle samples from symptomatic 14 month-old AR100Q transgenic mice yielded an opposite and dramatic up-regulation of TFEB target genes (Cortes et al., 2014), consistent with studies in SBMA knock-in AR113Q mice (Chua et al., 2014). This suggests a muscle-specific process of supraphysiological induction of *TFEB* in diseased SBMA muscle cells. Since uncontrolled autophagy is thought to underlie muscle wasting in models of muscular dystrophy (Sandri et al., 2013), excessive activation of autophagy could also be responsible for SBMA skeletal muscle phenotypes. In agreement with this hypothesis, global reduction of autophagic activity by Beclin-1 haploinsufficiency in SBMA knock-in AR113Q mice increased skeletal muscle fiber size and significantly extended lifespan in this model (Yu et al., 2011).

#### **1.5.9. Non-cell autonomous toxicity: Muscle Matters in Kennedy's Disease**

Traditionally, SBMA has been viewed as a cell-autonomous, primary motor neuron disease. Recently published reports challenge the traditional view of SBMA as a primary motor neuron disease. These studies establish muscle as a site of mutant AR toxicity and suggest targeting mutant protein expression in this tissue as an approach for treating the disorder. Several lines of evidence from previous studies support a primary contribution of skeletal muscle in the disease pathogenesis: (1) muscle biopsies of SBMA patients show features of both denervation and myofibers degeneration (Soraru' et al., 2008); (2) knockin mice expressing polyglutamine expanded AR develop early findings of myopathy with little or no motor neuron loss (Yu et al., 2006; Rocchi, Milioto et al., in revision); (3) muscle-specific overexpression of wildtype, non expanded *AR* in mice is sufficient to produce SBMA-like neuromuscular disease (Monks et al., 2007); (4) genetic overexpression of muscle-specific *IGF-1* or peripheral IGF-1 administration has been shown to mitigate SBMA symptoms in transgenic mice (Palazzolo et al., 2009; Rinaldi et al., 2012); (5) expression of polyglutamine-expanded

*AR* in all tissues except skeletal muscle is sufficient to prevent disease manifestations in transgenic mice (Cortes et al., 2014). Furthermore, the effects of antisense oligonucleotides (ASOs) mediated suppression of *AR* gene in the periphery but not in the CNS after subcutaneous administration, were recently tested by Lieberman et al. in two mouse models: AR113Q knock-in mice that have a CAG repeat expansion in the endogenous mouse *AR* locus and the fxAR121Q mice described by Cortes et al. in 2014 (see next section for more detail) (Lieberman et al., 2014). ASOs treatment rescued weight loss, muscle weakness, abnormal gene expression, and lethality in the mice, without altering testosterone levels. In conclusion, *AR* accumulation in motor neurons may not be sufficient for polyglutamine toxicity in SBMA models and targeting mutant *AR* in muscle can ameliorate the functional defects associated with SBMA.

## **1.6. Animal models**

Numerous animal models of SBMA have been created to elucidate the molecular pathogenesis and develop therapeutic approaches. All of the available animal models of SBMA are transgenic mice with truncated or full-length human *AR*. Early mouse models of SBMA failed to show phenotypes. Transgenic mice were first created using the full-length *AR* containing 45 CAGs, which is equivalent to the repeat length observed in SBMA patients, driven by the *interferon-inducible Mx* promoter or the *neuron-specific enolase (NSE)* promoter (Bingham et al., 1995). Expression of mutant *AR* was found in mice with the *inducible Mx* promoter, but at a lower level than normal endogenous expression. The mice demonstrated neither phenotype nor repeat length instability. Another transgenic mouse model was created with yeast artificial chromosomes (YACs) carrying the *AR* gene in the context of flanking non-coding sequences (La Spada et al., 1998). This model failed to show the expression of mutant *AR* in RT-PCR or Western blot analysis. In order to enhance the toxicity of mutant *AR*, a transgenic mouse model was created with human *AR* containing 66 CAGs, which was longer than the longest repeat observed in SBMA patients, driven by the *NSE* promoter or the *neurofilament light chain (NFL)* promoter (Merry et al., 1996). Although expression levels of mutant *AR* were 2–5 times the endogenous *AR* levels, these mice

showed no neurologic symptoms, presumably because the CAG repeat was not long enough.

In SBMA and other polyQ diseases, nuclear inclusions (NIs) are detected by antibodies against an N-terminal epitope, but not by antibodies against a C-terminal epitope (Li et al., 1998a, b). These findings suggest that truncated polyQ-containing proteins confer the toxicity in polyQ diseases. Additionally, in vitro translated full-length AR protein with an expanded polyQ tract is cleaved by caspase-3, liberating a polyQ-containing fragment, and the susceptibility to cleavage is polyQ repeat length-dependent (Kobayashi et al., 1998). For these reasons, was created a transgenic mouse model carrying 239 CAGs driven by the human *AR* promoter. These mice demonstrated motor impairment and revealed that the polyQ tract is sufficient to induce the pathogenic process of SBMA (Adachi et al., 2001). They exhibited small body size, weakness, truncal and limb incoordination, reduced activity and short lifespan. These phenotypes apparently developed within 4–8 weeks of birth, and gradually became severe at 8–16 weeks. The most striking pathologic observation was widespread occurrence of NIs, which were distributed in the neuronal cell nuclei in the cerebrum, cerebellum, brainstem and spinal cord, but to a lesser extent or not at all in the basal ganglia. This pathologic distribution was limited by the promoter used, and was more widely spread than that of human SBMA. These NIs were positive for ubiquitin and colocalized with proteasome components. Despite abundant NIs, there was no evidence of active neuronal degeneration or reactive astrogliosis. Thus neuronal dysfunction, rather than neuronal degeneration, is likely to be the pathogenesis of this mouse model. Expression of the transgene assessed by RT-PCR was revealed in the cerebrum, cerebellum, spinal cord, pituitary, lung, eye and skin; its distribution was compatible to that of NIs as well as mouse AR distribution. The mice showed subtle meiotic instability of the CAG repeat, in agreement with SBMA.

Simultaneously, another SBMA mouse model was created with truncated human *AR* containing 112 CAGs, driven by the *neurofilament light chain (NFL)* or *prion protein* promoter (Abel et al., 2001). The mice with the *prion protein* promoter showed non-specific features such as tremor, seizure and loss of body weight, whereas those with the *NFL* promoter demonstrated motor impairment similar to SBMA patients, accompanied by upper motor deficits. Widely expressed mutant *AR* may account for these

neurological phenotypes, because the distribution of histopathological involvement, which depended on the expression level of the transgene, was more extensive than that of SBMA. Immunohistochemical analysis of *AR* expression revealed transgenic AR positive nuclear inclusions in isolated neurons in several restricted regions of the central nervous system including the brainstem and the cortex and at lower frequency in spinal cord motor neurons. NIs were ubiquitinated and contained several molecular chaperones. About half of the NIs were positive for CREB-binding protein (McCampbell et al., 2000). In spite of neurologic symptoms and NIs, neither neuronal loss nor neurogenic muscle atrophy was demonstrated in this model.

Unlike the profound gender difference of phenotypes in SBMA patients, neither a transgenic (Tg) mouse model of SBMA expressing expanded *AR* with 239 CAGs (Adachi et al., 2001) nor another model carrying truncated *AR* with 112 CAGs (Abel et al., 2001) showed any remarkable phenotypic difference with gender, because the transgenes of these Tg mice did not contain the ligand-binding domain located in the C-terminus of AR. For these reasons, we generated Tg mice expressing the full-length human *AR* containing 24 or 97 CAGs under the control of the cytomegalovirus enhancer and the chicken  $\beta$ -actin promoter (Katsuno et al., 2002). This model recapitulated not only the neurologic disorder, but also the phenotypic difference with gender which is a specific feature of SBMA. Three out of five lines with 97 CAGs (*AR-97Q*) exhibited progressive motor impairment and no lines with 24 CAGs showed any manifested phenotypes. All symptomatic lines showed small body size, muscle atrophy, weakness, reduced activity and short lifespan; all of which were markedly pronounced and accelerated in the male *AR-97Q* mice, but either not observed or far less severe in the female *AR-97Q* mice regardless of the line. Early mortality of male mice, which is not common in SBMA, appears to be caused by cachexia. There was no significant difference in the expression of the transgene mRNA between the male and female *AR-97Q* mice. These observations indicate that the testosterone level plays important roles in the sexual difference of phenotypes, especially in the post-transcriptional stage of the mutant AR. The male *AR-97Q* mice showed markedly more abundant diffuse nuclear staining and NIs than females. Muscle histology revealed significant grouped atrophy and small angulated fibers in the male *AR-97Q* mice as well as mild myopathic change. The female *AR-97Q* mice showed no neurogenic change model. Castrated male *AR-*

97Q mice, which had a decreased testosterone level, showed significant improvement of symptoms, pathologic findings, and nuclear localization of the mutant AR compared with the sham-operated male AR-97Q mice. The life span was also significantly prolonged in the castrated male AR-97Q mice. Castration ameliorated muscle atrophy and body size reduction. In contrast to castration of the male mice, testosterone administered to the female AR-97Q mice caused significant exacerbation of symptoms, pathologic features, and nuclear localization of the mutant AR. These findings suggest that reduction of testosterone ameliorates phenotypic expression by preventing nuclear localization of the mutant AR, in addition castration may enhance the protective effects of heat shock proteins (HSPs), which are normally associated with AR and dissociate upon ligand binding.

Another Tg mouse model carrying the full-length *AR* with 120 CAGs driven by the cytomegalovirus promoter showed slowly progressive motor impairment and neurogenic muscle atrophy (McManamny et al., 2002). The affected mice also displayed a progressive reduction in sperm production consistent with androgen insensitivities in SBMA patients. Although this model showed no neuronal inclusions throughout the nervous system, loss of motor neurons was demonstrated in the spinal cord. Notably, as expected, mild but evident sexual difference of phenotypes was observed. This finding supports the hypothesis that testosterone level is implicated in the phenotypic expression of SBMA. These studies indicate that the C-terminus of mutant AR is necessary to recapitulate the testosterone-dependent pathogenesis of SBMA in mouse models.

Yu et al. (2006) developed a knock-in mouse model of Kennedy's disease, using gene targeting. They exchanged 1340 bp of coding sequence from mouse AR exon 1 with human exon 1 and in the process inserted 21, 48, or 113 CAG repeats. Mice with the targeted insertion of 21 or 48 CAG repeats (AR21Q and AR48Q, respectively) were similar to WT while those with an insertion of 113 CAG repeats (AR113Q) showed the systemic manifestations of Kennedy's disease. Expression of the targeted AR gene was under the control of the endogenous mouse regulatory elements, resulting in expression patterns that were similar to that of the WT allele. AR113Q mice exhibited testicular atrophy and decreased fertility, consistently with the mild androgen insensitivity in patients. Mutant males also exhibited androgen-dependent neuromuscular weakness.

Skeletal muscle pathology, including morphological changes in myofibers, preceded pathologic changes in spinal cord and showed evidence of both myopathic effects and neurogenic atrophy mediated by the expanded glutamine AR. AR and ubiquitin immunoreactive intranuclear inclusions was evident in males muscle by 3–5 months. In contrast, spinal cord pathology was detectable only in mutant males at 24 months. These data suggested that disease is initially characterized by myopathic effects in skeletal muscle combined with either functional denervation or distal axonopathy that is reflective of motor neuron dysfunction. Loss of lower motor neurons and spinal cord gliosis are late manifestations of this progressive disorder. Indeed, AR113Q hind-limb muscle expressed significantly lower levels of mRNAs encoding the neurotrophic factors NT-4 and GDNF, indicating that a loss of trophic support from the diseased muscle may hasten lower motor neuron dysfunction and degeneration, suggesting that muscle plays a primary role in SBMA pathogenesis. Testosterone-treated AR113Q females exhibit normal life span and developed small but statistically significant deficits in forelimb grip strength without altered body mass. These data suggest that, after testosterone treatment, AR113Q females develop androgen-dependent weakness but not exhibited the early death manifested by AR113Q males. AR113Q males unexpectedly died at 2–4 months, because of functional urinary tract obstruction (Yu et al., 2006).

According to the consideration that muscle play a primary role in SBMA pathogenesis, Monk et al. developed a Tg mouse models of SBMA, that overexpress *AR* with a WT number of Q repeats solely in skeletal muscle using the human skeletal actin (HSA) promoter. This promoter does not appear to be expressed in other muscle types, including cardiac or smooth muscle (Monks et al., 2007). No transgene expression was detected in other tissues. The males that survive are characterized by a neuromuscular phenotype, with reduced body weight, altered posture, decreased spontaneous locomotion, weakness and motor dysfunction, typical of the SBMA phenotype of polyQ mice. Along with these motor deficits, males have marked myopathy and reduced motor axon number, although motoneurons number does not differ between WT and Tg males, suggestive of axonopathy without motoneurons loss. Because the transgene is muscle specific, this neuropathology is secondary to muscle pathology. Indeed, castrating HSA-AR Tg males results in dramatic improvement of motor function. In further support of the androgen dependence of the HSA-AR phenotype, adult Tg females that

are treated with testosterone in the male range exhibit loss of body weight/muscle mass and motor dysfunction, similar to their male counterparts. This observation reinforces the notion that the transgene affects muscle primarily and that axon loss in males reflects more chronic, indirect, effects of androgen. The SBMA-like phenotype in males can be reversed upon cessation of testosterone treatment.

Recently, also Cortes et al. explore the contribution of muscle to SBMA pathogenesis with a new conditional mouse model of SBMA, BAC fxAR121Q, which expresses a full-length human *AR* transgene with 121 CAG repeats under the control of the endogenous *AR* promoter. The first exon of the human *AR* transgene is flanked by loxP sites, which allows removal of the transcription start site by Cre recombinase enzyme. In the absence of Cre, fxAR121Q mice show mutant AR transgene expression comparable to endogenous mouse AR in mRNA, protein, and tissue distribution. Male mice develop progressive muscle weakness, weight loss, and reduced survival, similar to other transgenic SBMA mouse models. Introduction of Cre recombinase under the control of a ubiquitous promoter (*CMV-Cre*) in fxAR121Q mice completely abrogated mutant *AR* transgene expression in all tissues. Double transgenic fxAR121Q/*CMV-Cre* mice were indistinguishable from non transgenic littermates and never developed SBMA manifestations, demonstrating complete mitigation of mutant AR toxicity through Cre-mediated recombination events in this model. Next, Cortes et al. introduced tissue-specific *Cre* expression driven by a human skeletal *actin* (HSA-Cre) promoter. fxAR121Q/HSA-Cre mice showed selective suppression of the *AR* transgene in skeletal muscle. Although *AR* was still expressed in the spinal cord, and reduced motor neuron soma size and accumulation of mutant AR in nuclear inclusions were unchanged in these mice, muscle-specific abrogation of *AR* increased survival, suppressed weight loss and weakness, and increased the diameter of motor axons. This study demonstrates a primary role of skeletal muscle in SBMA pathogenesis in these mice and justifies *AR* gene silencing in muscle tissues as a potential disease-modifying strategy in patients (Cortes et al., 2014).

## PARTE II: MITOCHONDRIA

### 1.7. Mitochondria

Mitochondria are the most specialized organelles with two membrane systems dividing the organelle in four compartments: the outer mitochondrial membrane (OMM), the intermembrane space (IMS), the inner mitochondrial membrane (IMM) and the matrix which are characterized by marker proteins and specific enzymes (Horvath and Daum, 2013). The numerous invaginations of the inner membrane are called cristae.

According to the endosymbiont hypothesis, mitochondria originated from the engulfment of aerobic eubacteria by a primordial anaerobic eukaryote. As a result, the organelle has its own genetic system with several bacteria-like features including a compact circular DNA genome (mtDNA), a simple transcription system that produces multigenic RNA transcripts, and a translational apparatus with antibiotic sensitivities similar to prokaryotic cells (Scarpulla et al., 2012). Human mitochondrial DNA (mtDNA) is a double stranded circular molecule of 16,569 bp encoding 2 ribosomal RNAs, 22 transfer RNAs and 13 messenger RNAs for polypeptides that form part of the multisubunits complexes of the oxidative phosphorylation system (OXPHOS) (7 subunits of complex I, 1 subunit of complex III, 3 subunits of complex IV and 2 subunits of complex V). The mammalian mtDNA contains few non-coding sequences: the largest being the D-loop or displacement loop, which contains promoters and origins of replication. Protein-coding genes have no intronic regions. Alkaline gradient centrifugation experiments allowed the separation of the mtDNA double strands into a heavy (H-strand) and a light (L-strand) due to their differential content of guanosine and cytidine (Fig. 1.5).



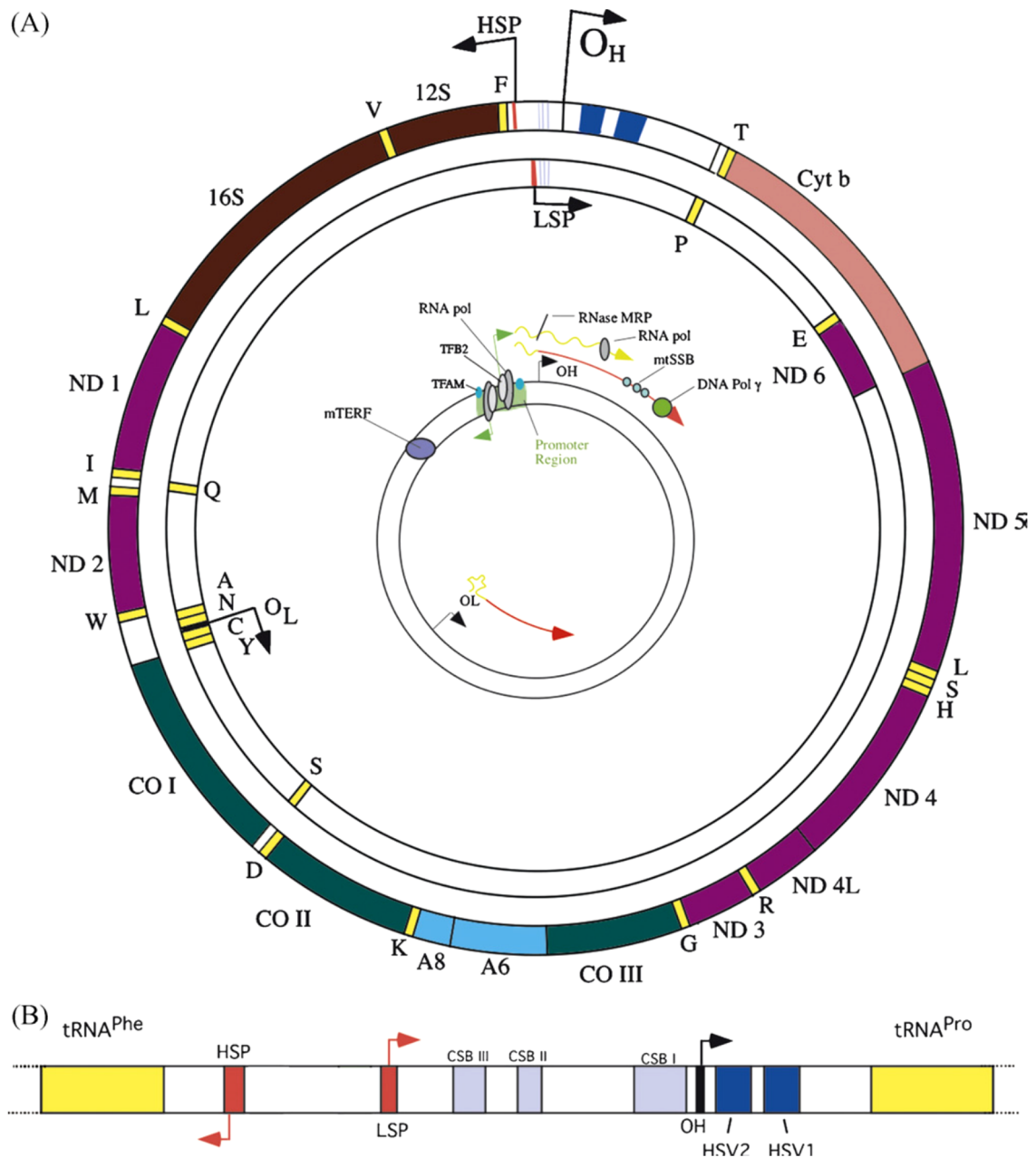


**Figure 1.5. Structure and expression of the human mitochondrial DNA.** The 16,569 bp human mtDNA (panel A) showing 13 protein-coding genes as well as 2 rRNA- and 22 tRNA-coding genes. Genes coding for subunits of complex I (*ND1–ND6*), complex III (*Cyt b*), complex IV (*COX I–COX III*) and complex V (*A8–A6*) are shown by different colours. The inset on panel A illustrates one of the mechanisms proposed for mtDNA replication. It also shows a consensus model of polycistronic transcription, including the approximately binding sites for the mitochondrial RNA polymerase, the mitochondrial transcription factor TFAM, the RNA processing enzyme RNase MRP and the transcription termination factor mTERF. The origins of replication for the H- and L-strands (OH and OL) are also shown. The structure of the regulatory D-loop region is shown in panel B, including the approximate position of the conserved sequence boxes believed to play a role in replication and RNA primer

processing. It also shows the location of the two hypervariable regions (HSV1 and HSV2) commonly used for evolutionary studies (Diaz and Moraes, 2008).

The genetic code of mitochondria differs from the nuclear universal code. The mitochondrial (mt)TGA codon codes for tryptophan instead of stop, the mtAGA and mtAGG code for stop instead of arginine and the mtATA codes for methionine instead of isoleucine. The mtDNA is associated with several proteins packed in structures denominated nucleoids, which are also associated with the inner mitochondrial membrane. Several studies showed that yeast nucleoids include proteins that bind DNA and are associated with replication and transcription such as the mitochondrial transcription factor A (TFAM). TFAM seems to be present at relatively high levels, and by itself is able to organize the mtDNA in “nucleoid-like” structures (Diaz and Moraes, 2008).

The transcription and translation of the mitochondrial genome is dependent upon a host of nucleus-encoded gene products (Scarpulla et al., 2012). Only 1% of mitochondrial proteins are translated on mitochondrial ribosomes in the matrix, whereas the bulk of mitochondrial proteins is encoded by nuclear genes, translated on cytosolic ribosomes and imported into mitochondria (Horvath and Daum 2013). Mitochondrial DNA (mtDNA) transcription requires a single RNA polymerase (POLRMT), two stimulatory transcription factors (TFAM, TFB2M), and a termination factor (MTERF1). Transcription takes place bidirectionally from divergent promoters, within the D-loop regulatory region (Scarpulla et al., 2012).

Mitochondria are capable of synthesizing some lipids on their own, but depend at the same time on the transfer and assembly of lipids mainly formed in the endoplasmic reticulum (ER). The continuous supply and exchange of lipids is required for maintaining mitochondrial membrane integrity and overall cellular function (Horvath and Daum, 2013).

Mitochondria have further roles in cell maintenance and survival, including calcium signaling and storage, metabolite synthesis, and apoptosis. In addition, cellular homeostasis depends highly on the energy provided by mitochondria, the cellular power plants responsible for aerobic production of ATP by the mitochondrial electron transport chain (ETC) in a process called oxidative phosphorylation (OXPHOS) (Novak, 2012). The (ETC) comprises four large protein complexes, which along with

the F<sub>0</sub>F<sub>1</sub> ATP synthase and mobile electron carriers (cytochrome c and coenzyme Q) constitute the machinery for converting metabolic energy into ATP. They are multi-subunit enzymatic complexes, all located in the inner mitochondrial membrane (Paradies et al., 2013). The electron donors, NADH and FADH<sub>2</sub>, derived from the oxidation of acetyl-CoA, are utilized by the ETC of the mitochondrial inner membrane to establish an electrochemical proton gradient across the membrane. The resulting proton motive force, comprising both a voltage potential and a pH gradient, is used by the membrane-bound ATP synthase to drive the synthesis of ATP, or by uncoupling proteins to generate heat or for the active transport of ions and metabolites. The mitochondrial ETC efficiently delivers electron pairs to molecular oxygen, the terminal acceptor (Scarpulla et al., 2012). In detail, Complex I (NADH-ubiquinone oxidoreductase) catalyzes electron transfer from the NADH to ubiquinone. The redox reaction is coupled to proton translocation across the membrane, contributing to proton motive force. The activity of this enzyme complex is considered the rate limiting step for mitochondrial respiratory chain and, therefore, an important factor in the regulation of OXPHOS process. Complex I is also considered an important site of superoxide anion generation in mitochondria. Complex II (succinate dehydrogenase) serves as a link between the tricarboxylic acid cycle and the electron transport chain. This enzyme participates in oxidative phosphorylation but not in the proton-gradient during ATP synthesis. It catalyzes the oxidation of succinate to fumarate with the reduction of ubiquinone to ubiquinol. Complex III (ubiquinol-cytochrome c oxido-reductase) is a central enzyme in oxidative phosphorylation which catalyzes electron transfer from membrane-localized ubiquinol to water-soluble cytochrome c. This redox reaction is coupled to the translocation of protons across the IMM. Complex IV (cytochrome c oxidase) receives an electron from four cytochrome c molecules, and transfers them to one oxygen molecule, converting molecular oxygen to two molecules of water. Finally, F<sub>0</sub>F<sub>1</sub> ATP-synthase (complex V) uses the energy created by the proton electrochemical gradient to phosphorylate ADP to ATP (Paradies et al., 2013). Two alternative models of organization of the mitochondrial electron transport chain have been elaborated: the solid model or the random collision model. The random collision model proposes that Complexes I–IV do not interact physically and that electrons are transferred between them by coenzyme Q and cytochrome c, the solid model proposes that all complexes

super-assemble in the so-called respirasome and the substrate is channelled directly from one enzyme to the next (Enriquez and Lenaz, 2014). Several models of supercomplexes, involving components of the electron transport chain (complexes I, II, III and IV), and complex V and ADP/ATP carrier, have been proposed. By using blue native electrophoresis after mild solubilisation of mitochondria with digitonin, the existence of two supercomplexes composed by complexes I, III and IV with a stoichiometry of I1, III2, and IV4, and by complexes III and IV with a stoichiometry of III2 and IV4, was demonstrated (Paradies et al., 2013). Four major roles have been attributed to the supercomplexes organization of the ETC: (a) increased efficiency of electron flux, through substrate channeling or enhanced catalysis, (b) sequestration of reactive intermediates to prevent generation of ROS, (c) structural stabilization of individual respiratory complexes, and (d) structures in which Complex I is assembled and activated (Enriquez and Lenaz 2014). Recently, it was proposed that the respirasome is a dynamic assembly, the aggregation states of which can respond to variations in the demand for energy under different physiopathological conditions (Paradies et al., 2013)

## **1.8. Mitochondrial biogenesis**

Normally, mitochondrial biogenesis is activated by changes that require increases in the rates of ATP utilization. Such events include thermogenesis, exercise, calorie restriction, hypoxia and several others (Piantadosi and Suliman, 2012). Mitochondrial biogenesis is very complex and requires numerous processes: besides synthesis of mtDNA encoded protein, biogenesis of new organellar structures includes synthesis and import of nuclear encoded proteins, assembly of the dual genetic origin derived proteins and mtDNA replication. Nuclear encoded mitochondrial proteins are synthesized in the cytoplasm and are then imported into mitochondria. mtDNA encoded proteins are synthesized within the organelle itself. mtDNA transcription generates 13 mRNA as well as 2 rRNAs and 22 tRNAs needed for the translation of mitochondrial mRNAs. The core machinery of mitochondrial gene expression consists of the mitochondrial transcription factor A (TFAM), the RNA polymerase  $\gamma$  (Polrmt) and the mitochondrial transcription factor B2 (TFB2). These factors form the crucial core and are sufficient for

mtDNA transcription. A second homologue of TFB2, namely TFB1, is involved in mitochondrial translation and regulates the methylation state of the mitochondrial ribosome. TFAM has an additional role in packaging of mtDNA and is necessary for mtDNA maintenance (Wenz et al., 2012).

The regulation of mitochondrial biogenesis is governed by nuclear factors in a hierarchical structure. Several nuclear transcription factors regulate the expression of nuclear encoded mitochondrial proteins: the first identified transcription factors are nuclear respiratory factors 1 and 2 (NRF1 and NRF2), which control the expression of genes encoding for *cytochrome c* and *cytochrome c oxidase* subunits. NRF2 belongs to the family of GA binding proteins, which bind DNA sequences rich in guanine and adenine (GA). NRF1 governs the expression of nuclear OXPHOS genes as well as the expression of nuclear encoded factors involved in mitochondrial transcription, protein import and protein assembly, such as *TFAM*. Human NRF-2 was identified as a multisubunit transcriptional activator of the *cytochrome oxidase subunit IV* (COXIV) promoter (Scarpulla et al., 2012). NRF2 binding sites have been also identified in several other mitochondrial genes including OXPHOS subunits, the mitochondrial protein import machinery and mitochondrial translation factors (Wenz et al., 2012). Several additional nuclear transcription factors have been linked to the expression of the respiratory apparatus, including YY1, MEF2 and c-myc. YY1 was first associated with the expression of *cytochrome oxidase subunits Vb and VIc*, and subsequent analysis of 723 human core promoters revealed a preponderance of YY1 sites in nuclear genes encoding ribosomal subunits and mitochondrial proteins. Tissue-specific expression of at least some muscle-specific *cytochrome oxidase subunits* depends upon MEF2/Ebox recognition sites. NRF-1 regulates *MEF2A* in muscle. Finally, c-myc acts on the expression of particular NRF-1 target genes through a canonical NRF-1 binding site, resulting in the sensitization of cells to apoptosis (Morrish et al., 2003).

Most nuclear receptors (NR) are involved in the regulation of mitochondrial genes. The first was the peroxisome proliferator-activated receptor  $\alpha$  (PPAR $\alpha$ ). PPAR $\alpha$  is now known to coordinately regulate nuclear genes encoding mitochondrial fatty acid oxidation (FAO) enzymes. The activation of PPAR $\alpha$  and PPAR $\beta$  by lipid ligands provides a mechanism for transducing changes in cellular lipid metabolism to the transcriptional control of mitochondrial FAO, a key source of ATP production in heart

and muscle. A second family of NRs, the estrogen-related receptors or ERRs (ERRa, ERRb, and ERRg), have also been shown to regulate nuclear genes encoding mitochondrial proteins involved in FAO, in the TCA cycle, in the respiratory chain, and oxidative phosphorylation. In addition, ERRa can regulate the transcription of the *PPARa* gene. All three *ERRs* are expressed in mitochondrion-rich tissues such as heart and skeletal muscle (Narkar et al., 2011).

Mitochondrial biogenesis is controlled also by a family of coactivators including PGC-1 $\alpha$  and PGC-1  $\beta$  (peroxisome proliferator-activated receptor- $\gamma$  coactivator-1 $\alpha$  and  $\beta$ ). PGC-1 $\alpha$  interacts directly with transcriptional factors, recruits the histone acetyl transferase (HATs) and interacts with the transcriptional machinery. Different transcription factors, including *PPARs*, *nuclear respiratory factors (NRFs)*, *myocyte enhancing factors (MEFs)*, *estrogen-related receptor (ERR)*, *forkhead box (FoxOs)* and *yin-yang (YYI)* are modulated by PGC1 $\alpha$  (Romanello and Sandri, 2012). An important regulator of *PGC-1 $\alpha$*  gene expression is the cAMP response element-binding protein (CREB), which activates *PGC-1 $\alpha$*  in liver in response to glucagon. In brown adipose tissue, CREB induces *PGC-1 $\alpha$*  expression in response to altered cytosolic calcium homeostasis and in response to cold temperature (Scarpulla et al., 2008). PGC1 family members are preferentially expressed in tissues with high-capacity mitochondrial function like heart, adipose tissue and slow-twitch skeletal muscle. PGC-1 $\alpha$  coordinately increases mitochondrial biogenesis as well as the uptake and utilization of substrates for energy production, being crucial in the maintenance of energy homeostasis. PGC-1 $\alpha$  is a powerful coactivator of NRF-1 and NRF-2 enhancing the expression of *mitochondrial transcription factor A (TFAM)*, mitofusins and of different nuclear genes encoding mitochondrial proteins. Both TFAM and nuclear gene products are imported into mitochondria where they regulate the expression of mitochondrial proteins required for ATP synthesis (Olesen et al., 2010). In skeletal muscle, there is compelling evidence that PGC-1 $\alpha$  is a key regulator of multiple pathways coordinating tissue adaptation to exercise. Transgenic mice that expressed *PGC-1 $\alpha$*  specifically in fast glycolytic muscles show a switch to oxidative metabolism, increased mitochondrial content and improvements in endurance exercise (Lin et al., 2002). During contraction, cytoplasmic calcium concentration transiently increases, as well as ROS production and ATP consumption. The alteration in calcium homeostasis activates calcium-sensitive

signaling such as calcium/calmodulin dependent protein kinases (CaMK) and calcineurin/NFAT pathways. On the other side ATP depletion modifies the AMP/ATP ratio, activating the energy sensor AMP-activated protein kinase (AMPK). Both the calcium-dependent pathways and AMPK modulate the activity and the expression of *PGC-1 $\alpha$* . During aging, mitochondrial biogenesis, mitochondrial content and *PGC-1 $\alpha$*  levels decrease. Importantly, maintaining *PGC-1 $\alpha$*  high levels in aged muscles preserves mitochondrial function and content (Romanello and Sandri, 2012). Metabolic signaling through *PGC-1a* takes place, in part, through post-translational modifications. For example, *PGC-1a* is directly regulated by deacetylation (SIRT1) and phosphorylation (AMPK) in response to changes in nutrient or energy depletion. The SIRT1 and AMPK pathways can also cooperate in promoting calcium-dependent mitochondrial biogenesis in myocytes (Scarpulla et al., 2012).

## **1.9. Autophagy**

Autophagy (from Greek, meaning self-eating) is an evolutionarily conserved eukaryotic process that can be initiated in response to both external and intracellular factors, including amino acid starvation, endoplasmic reticulum (ER) stress, hypoxia, oxidative stress, pathogen infection, and organelle signaling, which are beneficial to cell survival under adverse conditions (Wang et al., 2015). It is a self-eating system, in which cellular components including organelles are entrapped into a double membrane structure called the autophagosome and then degraded by lysosomal hydrolases. In addition to its role in supplying amino acids in response to nutrient starvation, autophagy is involved in quality control to maintain cell health. Thus, inactivation of autophagy causes the formation of cytoplasmic protein inclusions, which comprise misfolded proteins and the accumulation of many degenerated organelles, resulting in liver injury, diabetes, myopathy and neurodegeneration (Komatsu and Ichimura, 2010). There are three types of autophagic pathways: macroautophagy, microautophagy and chaperone-mediated autophagy (CMA) (Mizushima and Kuma, 2008). Microautophagy is accompanied by membrane extensions of a vacuole as well as invagination of the vacuole, in which cytoplasmic components close to the vacuole are sequestered and then degraded. CMA targets specific cytosolic proteins, with a KFERQ amino-acid

motif, that are trapped by the heat shock cognate protein of 70 kDa (hsc70) and, through the interaction with lysosome-associated membrane protein type 2A (LAMP-2A), they are translocated into the lysosomal lumen for rapid degradation. Macroautophagy (here after referred to as autophagy) is the prototype of autophagy, in which isolation membranes/phagophores engulf a portion of the cytoplasm by double membrane vesicles, called autophagosomes, which deliver their contents to the lysosomes. Fusion of the autophagosome with the lysosome triggers the breakdown of the inner autophagosomal membrane followed by degradation of the contents (Komatsu and Ichimura, 2010) (Fig. 1.6).

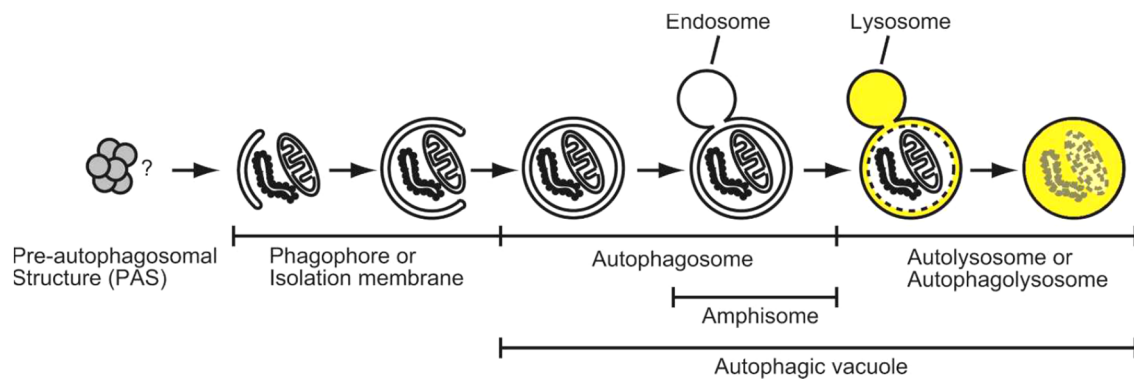


**Figure 1.6. The process of macroautophagy in mammalian cells.** A portion of cytoplasm, including organelles, is enclosed by a phagophore or isolation membrane to form an autophagosome. The outer membrane of the autophagosome subsequently fuses with the endosome and then the lysosome, and the internal material is degraded. In yeast, autophagosomes are generated from the PAS, which has not yet been identified in mammalian cells. The nomenclature for various autophagic structures is indicated (Mizushima, 2007).

Thus, autophagy consists of several sequential steps: induction, autophagosome formation, degradation of the engulfed cytoplasm-derived materials and reuse of the monomeric units (Mizushima, 2007). The most typical trigger of autophagy is nutrient starvation. One candidate sensor of amino acid concentration is Beclin1. Beclin1 was originally identified as an interaction partner of Bcl-2, an anti-apoptotic protein. This Bcl-2–Beclin1 interaction is mediated through a BH3 domain in Beclin1 and is reduced upon starvation, freeing Beclin1 to activate autophagy. The starvation-induced dissociation of Beclin1 and Bcl-2 (or Bcl-XL) could be one manner in which nutrient starvation induces autophagy. After induction, cytoplasmic constituents, including



organelles, are sequestered by a unique membrane called the phagophore or isolation membrane, which is a very flat organelle like a Golgi cisterna. Complete sequestration by the elongating phagophore results in formation of the autophagosome, which is typically a double-membraned organelle (Mizushima, 2007). The autophagosome is a globular organelle with a diameter of approximately 1  $\mu\text{m}$  and with volume of  $0.5 \times 10^{-18} \text{ m}^3$  (Komatsu and Ichimura, 2010). In the next step, autophagosomes fuse with endosomes to become amphisomes before fusion with lysosomes. The inner membrane of the autophagosome and the cytoplasm-derived materials contained in the autophagosome are then degraded by lysosomal hydrolases. These degrading structures are often called “autolysosomes” or “autophagolysosomes”. The definition of autophagosomes, amphisomes, and autolysosomes is based on their function, not on morphology. In such cases, the term “autophagic vacuoles” may be used because it covers all autophagic structures. The average half-life of AVs appears to be  $<10$  min. Once macromolecules have been degraded in the lysosome/vacuole, monomeric units (for example, amino acids) are exported to the cytosol for reuse (Mizushima, 2007).

Autophagy is precisely regulated by many different proteins. The *autophagy-related* gene (*ATG*) family provides the infrastructure for autophagy; until recently, 40 *ATG* genes had been identified, primarily through genetic studies in yeast. In mammals, autophagosome assembly requires activation of the ULK1 (UNC-51-like kinase 1) complex (including ULK1, ATG13, focal adhesion kinase family interacting protein of 200 kDa and ATG101) and recruitment of the class III phosphoinositide3-kinase (PI3K) Vps34 complex (including Beclin-1, Atg14, Ambra1, Vps34 and Vps15) for producing phosphatidylinositol3-phosphate (PI3P). Formation of PI3P recruits the PI3P-binding proteins double FYVE domain-containing proteins (DFCP1) and WD-repeat protein interacting with phosphoinoside (WIPIs) to generate the omegasome and the isolation membrane (IM). Atg9 seems to shuttle between IM and cytosol and provides membranes needed for elongation of the IM. Atg12–Atg5–Atg16 L1 complex and LC3–phosphatidylethanolamine (PE) conjugate are crucial for the elongation and closure of the IM. LC3 is first cleaved by a cysteine protease (Atg4/autophagin) to expose a C-terminal glycine, generating LC3-II, after recruiting by the oligomeric protein complex containing Atg12-Atg5 and Atg16 to the pre-autophagosome membrane (Zeng et al., 2006). LC3-II is localized in the inner and outer membranes of the isolation

membrane/phagophore and is essential for the membrane biogenesis and/or closure of the membrane. LC3-II localized on the outer membrane is efficiently re-cleaved by Atg4 after completion of autophagosome formation and recycled, whereas LC3-II present on the inner membrane is degraded together with other cellular constituents by lysosomal proteases (Komatsu and Ichimura, 2010). LC3 bind cargo receptors and promotes their entry into the autophagy cascade via interaction with the LC3-interacting regions (LIR) of the receptors (Wang et al., 2015). An LC3-interacting protein is p62. It is an ubiquitin-associated protein that localized to the autophagosome via LC3 interaction and is constantly degraded by the autophagy–lysosome system. Ablation of autophagy leads to marked accumulation of p62, resulting in the formation of p62-positive inclusions. p62 is a receptor for ubiquitinated proteins necessary for their degradation in the lysosomes. As a receptor, p62 contributes in autophagic degradation of various cargos such as Parkin-mediated ubiquitinated mitochondria, peroxisomes and microbes, that recognized with its ubiquitin associated domain (UBA). Thus, all inclusions in autophagy-deficient cells are positive for both ubiquitin and p62 (Komatsu and Ichimura, 2010).

Beclin1 is a 60 kDa protein that has been implicated as an important regulator of macroautophagy. Beclin is an interacting partner for the mammalian class III PI3-kinase mVps34, important for macroautophagy in nutrient-starved cells, for normal lysosomal enzyme sorting and protein trafficking in the endocytic pathway. Beclin is required for the formation of LC3-II, thus it functions in the earliest steps required for autophagosome biogenesis. Since inhibitors of PI3-kinase have been reported to cause a reduction in LC3-II production, Zeng et al. believe that the attenuated production of LC3-II observed in starved or ceramide-treated Beclin1 knock down cells is related to an impaired ability of hVps34 to function in the autophagy pathway without Beclin1. They propose that a primary function of Beclin1 is to facilitate the interaction of hVps34 PI3-kinase with specific effectors on the pre-autophagosomal isolation membrane in response to pro-autophagic conditions or death signals (Zeng et al., 2006). In fact, recruitment of PI3K–Beclin1 complexes together with Atg12–Atg5 is an initial step in autophagosome formation (Tassa et al., 2003).

### **1.9.1. Lysosome biogenesis**

The lysosome is often described as a “cellular garbage” (Mizushima and Komatsu, 2011). Lysosomes are acidic, membrane-bound organelles rich in hydrolytic enzymes. Lysosomes are responsible for the degradation of macromolecules derived from the extracellular space through endocytosis or phagocytosis, as well as from the cytoplasm through autophagy. One crucial role of the membrane limiting late endosomes and lysosomes is to separate the potent activities of lysosomal acid hydrolases from other cellular constituents. Protein components of the lysosomal membrane also mediate a number of essential functions of this compartment, including the acidification of the lysosomal lumen, transport of amino acids, fatty acids, and carbohydrates resulting from the hydrolytic degradation, as well as other nutrients generated by lysosomal hydrolases (Eskelinen et al., 2003). In addition, lysosomal membrane proteins may be involved in the interaction and fusion of the lysosomes with themselves as well as with other cell components, including endosomes, phagosomes and the plasma membrane (Fukuda, 1991). Lysosome associated membrane protein-1 (LAMP-1) and LAMP-2 are estimated to contribute to about 50% of all proteins of the lysosome membrane. They are type I transmembrane proteins with a large luminal domain, one transmembrane domain and a C-terminal cytoplasmic tail. Despite their 37% amino acid sequence homology, LAMP-1 and LAMP-2 are distinct proteins which most likely diverged relatively early in evolution as evidenced by their localisation on different chromosomes (Fukuda, 1991). The presence of LAMP molecules is one of the major definitions of the lysosomal compartment (Kornfeld and Mellman, 1989). Both LAMPs were originally thought to protect the lysosomal membrane against the action of the hydrolytic enzymes. LAMP-2 undergoes alternative splicing which leads to the isoforms LAMP-2A, B, and C (Eskelinen et al., 2005). LAMP-2B is the principal isoform in skeletal muscle (Konecki et al., 1995). In the double LAMP1 and LAMP2 deficient cells the amount of early autophagic vacuoles was comparable to control cells, but the amount of late vacuoles was increased. This suggests that although initial maturation of autophagosomes including fusion with endosomes is functional, the final maturation step of the late autophagic vacuoles, probably including fusion with lysosomes, is retarded (Eskelinen et al., 2004). In these cells, mutual disruption of both LAMPs is associated with an increased accumulation of autophagic vacuoles and unesterified cholesterol, while

protein degradation rates are not affected. These results clearly show that the LAMP proteins fulfil functions far beyond the initially suggested roles in maintaining the structural integrity of the lysosomal compartment.

### **1.10. Mitophagy**

Alongside the critical metabolic functions of mitochondria in fatty acid oxidation, the Krebs cycle, and oxidative phosphorylation, mitochondria can also potentially damage cells. Reactive oxygen species (ROS), in particular superoxide anion, hydrogen peroxide, and hydroxyl radical are toxic products of oxidative phosphorylation. ROS causes oxidative damage to mitochondrial lipids, DNA, and proteins, making mitochondria further prone to ROS production (Ashrafi and Schwarz, 2013). For these reasons, mitochondria homeostasis needs to be highly regulated. Elaborate mechanisms of mitochondrial quality control have evolved to maintain a functional mitochondrial network and avoid cell damage. The crucial role of these defence pathways for cellular homeostasis and survival is supported by the fact that mitochondrial dysfunction is related to aging, cancer and a wide range of neurological pathologies (Campello et al., 2014). Autophagy has emerged as a key mechanism in this quality control, responsible of the elimination of superfluous or damaged mitochondria (Gomes and Scorrano, 2013). Two types of macroautophagy have been identified to date. Nonselective autophagy occurs on nutrient deprivation to supply cells with essential metabolic building blocks and energy until nutrients can once again be obtained from the extracellular environment. By contrast, cargo-specific autophagy occurs under nutrient-rich conditions to mediate the removal of superfluous or damaged organelles and protein aggregates that otherwise could be toxic. This can occur following changes in nutrient sources and during developmental processes. A well-studied type of cargo-specific autophagy is mitophagy, which mediates the selective removal of mitochondria. Lemasters and colleagues coined the term “mitophagy” to describe the engulfment of mitochondria into vesicles that are coated with the autophagosome marker LC3, a process that can occur within 5 minutes (Youle and Narendra, 2011). Mitochondria are dynamic organelles that continuously fuse and fragment during cell life, appearing in situ as short round-shaped or elongated organelles, with a major axis that can reach 5

$\mu\text{m}$ . On the other hand, autophagosomes are globular organelles with a diameter of approximately  $1 \mu\text{m}$ , posing a sterical problem to mitochondrial engulfment by autophagosomes (Gomes and Scorrano, 2013). Indeed, it has been suggested that mitochondrial fragmentation (fission) precedes mitophagy, which divides elongated mitochondria into pieces of manageable size for encapsulation and also quality control segregation of damaged mitochondrial material for selective removal by mitophagy (Youle and Narendra, 2011). Mitochondrial permeability transition (MPT) has been proposed to be responsible for the mitophagy of depolarized mitochondria in mammalian cells (Lemasters et al., 2002). MPT is mediated by the permeability transition (PT) pore. Mitochondria become permeable to all solutes up to a molecular mass of about 1500 Da after the onset of MPT, which can lead to mitochondrial depolarization. When cultured hepatocytes were deprived of nutrition, depolarized mitochondria could be found to colocalized with acidic vesicles. Some of the mitochondria were enveloped by GFP-LC3-positive autophagosomes (Kim et al., 2007). The removal of damaged mitochondria through mitophagy is thus critical for maintaining proper cellular functions. Furthermore, mitophagy has been recently proposed to play critical roles in terminal differentiation of red blood cells, paternal mitochondrial degradation and hypoxia. Removal of mitochondria through autophagy requires three steps: fission, induction of general autophagy and priming specific mitochondria for selective autophagic recognition. Mitochondrial priming is mediated either by the Pink1-Parkin signaling pathway or the mitophagic receptors NIX and BNIP3 (Ding and Yin, 2012).

### **1.10.1. The PINK1/Parkin Pathway of Mitophagy**

PINK1 encodes the PTEN-induced putative kinase, a serine/threonine kinase, whereas Parkin is an E3 ubiquitin ligase. The intracellular location of Parkin is regulated by mitochondrial function. Parkin normally resides in the cytosol but it translocates to mitochondria upon mitochondrial depolarization. Mitochondrial-localized Parkin promotes the colocalization of mitochondria with the autophagy marker LC3. Mitochondrial translocation of Parkin is dependent on PINK1 (Ding and Yin, 2012). PINK1 contains a mitochondrial targeting sequence allowing for its mitochondrial localization. In healthy mitochondria, PINK1 is constitutively imported, probably via

the TIM/TOM complex, to the inner membrane where it is cleaved by several proteases including the mitochondrial-processing protease (MPP) and the inner membrane presenilin-associated rhomboid-like protease PARL, and ultimately proteolytically degraded. Loss of mitochondrial membrane potential precludes import of PINK1 to the inner membrane, thereby stabilizing intact PINK1 on the mitochondrial outer membrane where it interact with TOM20 (Ashrafi and Schwarz, 2013). Therefore, the bioenergetic state of mitochondria can regulate PINK1 levels as well as the subsequent Parkin recruitment to the mitochondria. PINK1 directly phosphorylates Parkin on Thr175 and Thr217 at the linker region of Parkin, which promotes Parkin mitochondrial translocation (Ding and Yin, 2012). After recruitment, Parkin mediates selective engulfment of depolarized mitochondria by autophagosomes (Gomes and Scorrano, 2013). Because Parkin has E3 ligase activity, it is not surprising to find that Parkin positive mitochondria are also positive for ubiquitin staining (Ding and Yin, 2012). Different Parkin isoforms have been described, but their specific roles and tissue distribution are still unknown (La Cognata et al., 2014; Scuderi et al., 2014). Parkin participates in ubiquitination of the mitochondrial fusion proteins MFN1 and MFN2, that being degraded in a proteasome and p97-dependent manner (Gomes and Scorrano, 2013). Removal of mitofusins is necessary for proper mitophagy induction and selective removal of damaged mitochondria because mitochondria, that lack mitofusins, are not able to fuse with healthy mitochondria as a repair mechanism, called functional complementation. This programmed imbalance of mitochondrial morphology can thus function to isolate the pool of damaged mitochondria for subsequent selective autophagic sequestration and degradation. Furthermore, the mitochondrial outer membrane-localized VDAC1 (voltage dependent anion channel 1) is a Parkin target during mitophagy. In contrast to mitofusin ubiquitination, Parkin generates Lys 27 polyubiquitin chains on VDAC1 whose role is not to recruit proteasome and degrade VDAC1, but instead to engage the autophagy machinery by attracting the autophagy receptor p62. Recognition of polyubiquitinated substrates by p62 occurs via the ubiquitin binding UBA domain on one side and the LIR (LC3-interacting region) motif, which binds LC3 proteins that are essential for autophagy initiation. This interaction thus generates the bridge between mitochondria and newly forming autophagosome (Fig. 1.7). However, the role and requirement for p62 in mitophagy are controversial.

Whereas p62 recruitment is shown to be necessary for PINK1/Parkin-induced mitophagy, the mitophagy can occur even in the absence of p62 at the mitochondria (Narendra et al., 2010), thanks to the presence of others ubiquitin-binding autophagic adaptors, such as NBR1 and optineurin (Novak, 2012). In addition, ubiquitinated mitochondria recruit not only p62 but also HDAC6, an ubiquitin-binding protein deacetylase that mediates transport of damaged mitochondria, facilitating their clustering at the perinuclear region for subsequent clearance (Gomes and Scorrano, 2013).

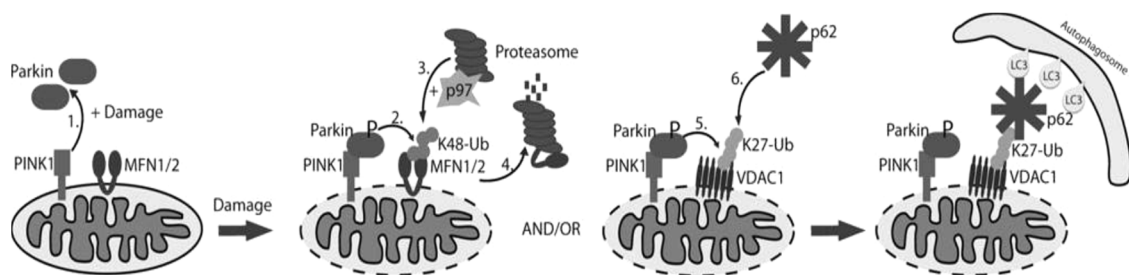


**Figure 1.7. Damage-induced mitophagy.** Upon mitochondrial damage, mitochondria-localized PINK1 recruits E3-ligase Parkin to mitochondria (1). PINK1-phosphorylated Parkin ubiquitinates mitofusins (2). Ubiquitinated mitofusins are then degraded by proteasome (4) that is recruited to mitochondria together with p97 (3). Mitofusin degradation blocks fusion events and mitophagy can be activated. At the same time, Parkin can polyubiquitinate VDAC1 creating K27-linked Ub-chains (5) that recruit p62 (6). Binding of p62 to VDAC1 on the mitochondria and ATG8/LC3/GABARAP on the developing autophagosome, results in mitochondrial sequestration and removal by autophagic machinery (Novak, 2012).

Parkin is not the only E3 ubiquitin ligase found on mitochondria: MARCH5/ MITOL, or MULAN belong to the same family and are associated with the mitochondrial outer membrane, opening the interesting possibility that they might be involved in mitophagy. In addition, the cytoplasmic E3 ubiquitin ligase SMURF1 has also been found to be required for mitophagy (Ashrafi and Schwarz, 2013). In addition to the ubiquitination of mitochondrial proteins, in the vertebrate central nervous system, Parkin also interacts with Ambra1, a protein that promotes general autophagy by activating the class III phosphatidylinositol3-kinase complex. The Parkin-Ambra1 interaction is increased during prolonged mitochondrial depolarization. Ambra1 is recruited to perinuclear clusters of depolarized mitochondria in a Parkin-dependent manner, activates autophagy

around these mitochondria, and contributes to their selective autophagic clearance (Ding and Yin, 2012).

### **1.10.2. Mitophagy in Erythrocyte Maturation, Hypoxia, and Embryogenesis**

Removal of mitochondria occurs during development of some specialized cells and is essential for correct organ or tissue development. Unlike PINK1/Parkin-mediated mitophagy, mitophagy induced during differentiation is not a quality control mechanism for degradation of unhealthy mitochondria, but a programmed complete or almost complete mechanism for elimination of the mitochondrial population. The best-studied differentiation-induced mitophagy is the removal of mitochondria in red blood cells. Mature erythrocytes of mammals do not contain any mitochondria, allowing them to maximize their oxygen-carrying capacity and to live longer in the circulation because of lower risk of damage induced by reactive oxygen species (ROS) produced by mitochondria (Novak, 2012). NIX (also named BNIP3L) is a mammalian mitophagy receptor important for selective removal of damaged mitochondria as well as complete removal of mitochondria during reticulocyte maturation (Novak and Dikic, 2011). NIX, as is homolog BNIP3, contains a Bcl-2 homology 3 (BH3) domain and acts as a proapoptotic mitochondrial protein. Both BNIP3 and NIX are inserted into the outer mitochondrial membrane through their C-terminal transmembrane domains, while their N-terminal domains are exposed to the cytoplasm (Ding and Yin, 2012). It was shown that NIX directly interacts with LC3, through an LC3-interacting region (LIR) on the N-terminal part of NIX, the tetrapeptide WxxL motif found in other receptors involved in autophagic cargo recognition (Novak, 2012). Thus, it may be directly involved in the recruitment of the autophagy machinery to mitochondria (Ding and Yin, 2012). The function of NIX may not be restricted to erythrocyte maturation. NIX could also be involved in depolarization-induced mitophagy (Ashrafi and Schwarz, 2013). In muscle wasting disorders, where autophagy is implicated in the pathogenesis, *BNIP3* and *NIX* are upregulated and the expression of either in skeletal muscle induces autophagosome formation. BNIP3 and NIX can trigger mitochondrial depolarization and cause mitophagy (Zhang and Ney, 2009). NIX and BNIP3, are also involved in hypoxia-induced mitophagy. Removal of mitochondria during hypoxia is important to reduce ROS production and maintain oxygen homeostasis (Ashrafi and Schwarz, 2013). Under



hypoxia conditions, both BNIP3 and NIX are highly induced. Their expression levels are regulated by hypoxia inducible factor-1 (HIF-1) (Ding and Yin, 2012). BNIP3 and NIX, both BH3- only proteins, through binding to Bcl-2 and/or Bcl-xL disrupt the interaction between Bcl-2 or Bcl-XL and Beclin1, thus freeing Beclin1 to induce autophagy. Beclin1 activates the Atg6/PIK3-class III complex important for autophagosome membrane construction and is therefore essential for autophagy initiation (Novak, 2012) (Fig. 1.8).

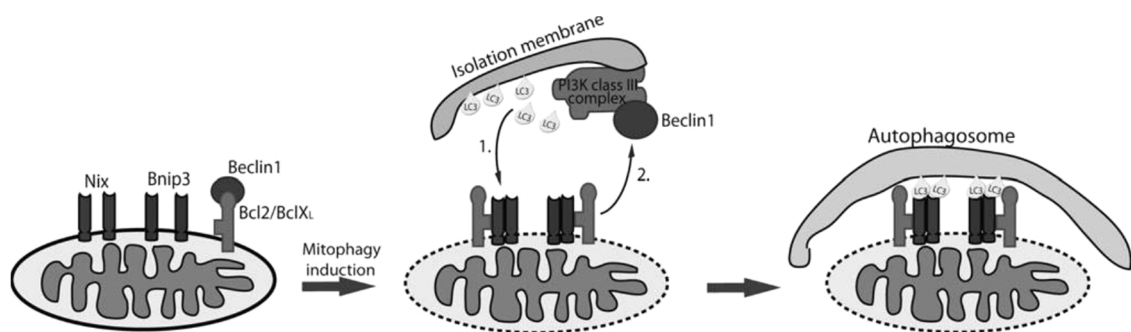


**Figure 1.8. Development-induced mitophagy—role of mitochondrial receptors.** Upon mitophagy induction, mitochondrial receptors Nix and Bnip3 recruit ATG8/LC3/GABARAP and mediate tethering of the nascent autophagosome to the target mitochondria (1). Dimerization of the receptors could enhance Nix and Bnip3 interaction with ATG8/LC3/GABARAP. Concurrently, Nix and Bnip3 interaction with Bcl-2/Bcl-XL releases Beclin1 (bound to Bcl-2/Bcl-XL to block autophagy). Free Beclin1 activates basic autophagic machinery to form autophagosomes (2) (Novak, 2012).

Further, NIX initiates mitophagy by preparing mitochondria for recognition by the autophagic machinery. When mitochondria get depolarized, NIX influences translocation of the E3 ligase Parkin to mitochondria in order to ubiquitinate mitochondrial proteins and, thus, mark mitochondria for degradation by autophagy (Novak and Dikic, 2011). NIX is upstream of both mitochondrial “priming” by Parkin/p62 and autophagy machinery recruitment, thus linking PINK1/Parkin-mediated mitophagy with hypoxia/NIX/BNIP3-mediated mitophagy (Novak, 2012).

In addition to NIX and BNIP3, an outer mitochondrial membrane protein, FUNDC1, has recently been reported to have an essential role in hypoxia-induced mitophagy. FUNDC1 interacts with LC3 through the characteristic LIR motif YXXL. Under normoxia conditions, FUNDC1 is constantly phosphorylated by the Src kinase. Src can be inactivated under hypoxia conditions, leading to the dephosphorylation of FUNDC1, which has a higher affinity binding with LC3 than the phosphorylated form (Ding and

Yin, 2012). It is attractive to hypothesize that NIX, BNIP3, and FUNDC1 function in a coordinate manner during hypoxia with the consequence that FUNDC1 selectively targets mitochondria to autophagosomes formed through NIX- and BNIP3-mediated activation of Beclin1. FUNDC1 has also role in the elimination of paternal mitochondria from fertilized oocytes through mitophagy. In most eukaryotes, only maternal mitochondrial DNA is inherited, although sperms do contain mitochondria that are present in the oocyte immediately after fertilization. These paternal mitochondria are rapidly destroyed, although the evolutionary advantage this confers is unclear (Ashrafi and Schwarz, 2013).

### **1.10.3. Mitochondrial dynamics**

Mitochondria are morphologically highly dynamic organelles, undergoing constant fission and fusion events. There are many intracellular and extracellular signals that regulate fusion and fission events, including oxidative stress, membrane potential, mtDNA quality and apoptosis (Novak, 2012). Fusion of isolated mitochondria induces the formation of an extended interconnected mitochondrial network. This change enables mitochondria to mix their contents within the network allowing for the redistribution of metabolites, proteins and mtDNA. Moreover, fusion into a network prevents the local accumulation of defective/abnormal mitochondria which is advantageous under conditions of high energy demand. Conversely, mitochondrial fission or fragmentation is a mechanism that segregates components of the mitochondrial network which are dysfunctional or damaged, allowing for their removal via mitophagy. Excessive fission generates isolated mitochondria which are not only less efficient in ATP production than fused ones but are dysfunctional, consuming cytosolic ATP to maintain their membrane potential. Hence, dynamic regulation of fission–fusion events adapts mitochondrial morphology to the bioenergetic requirements of the cell (Romanello and Sandri, 2012). The most-studied proteins involved in mitochondrial fusion are mitofusins (Mfn1 and Mfn2), outer mitochondrial membrane proteins that enable fusion through their cytoplasm-exposed GTPase domain, thus allowing tethering of the opposing mitochondrial membranes. Opa1 (optic atrophy 1), instead, is responsible for the fusion of inner mitochondrial membranes (Novak, 2012) (Fig. 1.9). It is anchored to the IMM by a transmembrane domain at the N-

terminus but most of the protein is exposed to the intermembrane space (Romanello and Sandri, 2012). Mammalian OPA1 has eight isoforms that are generated by alternative splicing and alternative processing at two cleavage sites. OPA1 isoforms are constitutively cleaved by the intermembrane space AAA protease Yme1 to generate the short and long forms of OPA1 (S- and L-OPA1) under normal conditions. When cells were treated with CCCP, a mitochondria uncoupler that depolarizes mitochondria, L-OPA1 was further cleaved by an inducible protease OMA1. This cleavage resulted in mitochondrial fragmentation (Ding and Yin, 2012).

Fission is regulated by proteins including Drp1 (dynamin-related protein 1) and Fis1 (fission protein 1) (Fig. 1.9). In contrast to mitofusins and Opa1, Drp1 is predominantly localized in cytoplasm. Only when recruited to the mitochondria does Drp1 associate with Fis1, its receptor, localized to the outer mitochondrial membrane to form a complex that allows the fission of mitochondria (Novak, 2012). It was shown that rise of cytosolic  $Ca^{2+}$ , associated with mitochondrial depolarization, leads to Drp1 dephosphorylation by calcineurin at serine 637 and concomitant translocation of Drp1 to mitochondria, where it is stabilized by sumoylation and participates in fission. Conversely, protein kinase A (PKA) phosphorylates Drp1 at serine 637, restraining fission. Alternatively, Drp1 can be phosphorylated also at serine 637 by calcium/calmodulin-dependent protein kinase Ialpha (CAMKI $\alpha$ ) or at serine 616 by cyclin-dependent kinase 1 (CDK1). However, when phosphorylated by these two kinases, Drp1 drives mitochondrial fission (Gomes and Scorrano, 2013). Other possible Drp1 receptors are: Mff (the OMM anchored mitochondrial fission factor), and human MIEF1/MiD51 (the OMM-bound mitochondrial elongation factor1/mitochondrial dynamics) with its variant MiD49 (Campello 2013). Accumulating evidence emphasizes the requirement of mitochondrial fragmentation prior to mitophagy. Conceptually, this is not surprising given that an organelle that is going to be engulfed and degraded by the autophagosome needs to fit into this forming structure. Considering that individual mitochondrial length averages 5  $\mu$ m, and that autophagosomes display a diameter of around 1  $\mu$ m, a role for mitochondria-shaping proteins in solving this sterical hindrance could have been anticipated. Inhibition of mitochondrial fission also impairs mitophagy, suggesting a role for the shape of the organelle in the process (Gomes and Scorrano, 2013). Furthermore, an entire mitochondrial network is sterically

far from being engulfed by autophagosomes during autophagy. Thus, mitochondria protect themselves from autophagic removal by blocking the fission machinery and promoting fusion (Campello et al., 2014). Gomes and Scorrano (2008) found that overexpression of *Fis1* itself can induce general autophagy in HeLa cells. Moreover, a conserved mutation in *Fis1* (*hFis1 K148R*) induced mitochondrial fission but was unable to induce mitochondrial dysfunction and did not induce autophagy (Gomes and Scorrano, 2008). These observations suggest that mitochondrial dysfunction, rather than mitochondrial fragmentation, is responsible for the induction of autophagy (Ding and Yin, 2012). Fragmentation per se does not seem to represent a signal to target mitochondria to the autophagosome. Often a fission event gives rise to uneven daughter mitochondria in respect to their membrane potential: one displays high  $\Delta\psi_m$ , the other low  $\Delta\psi_m$  and has a reduced probability to fuse. This population of fragmented mitochondria with decreased  $\Delta\psi_m$  is removed by mitophagy. Blocking fission, however, impaired mitophagy, resulting in the accumulation of dysfunctional mitochondria. In conclusion, mitophagy requires efficient fission that helps segregating the bad organelles and prepares them to fit into the autophagosomes. However, fission per se is not the trigger of mitophagy, for which a concomitant dysfunction of the organelle, or other yet unclear signals, are required (Gomes and Scorrano, 2013).

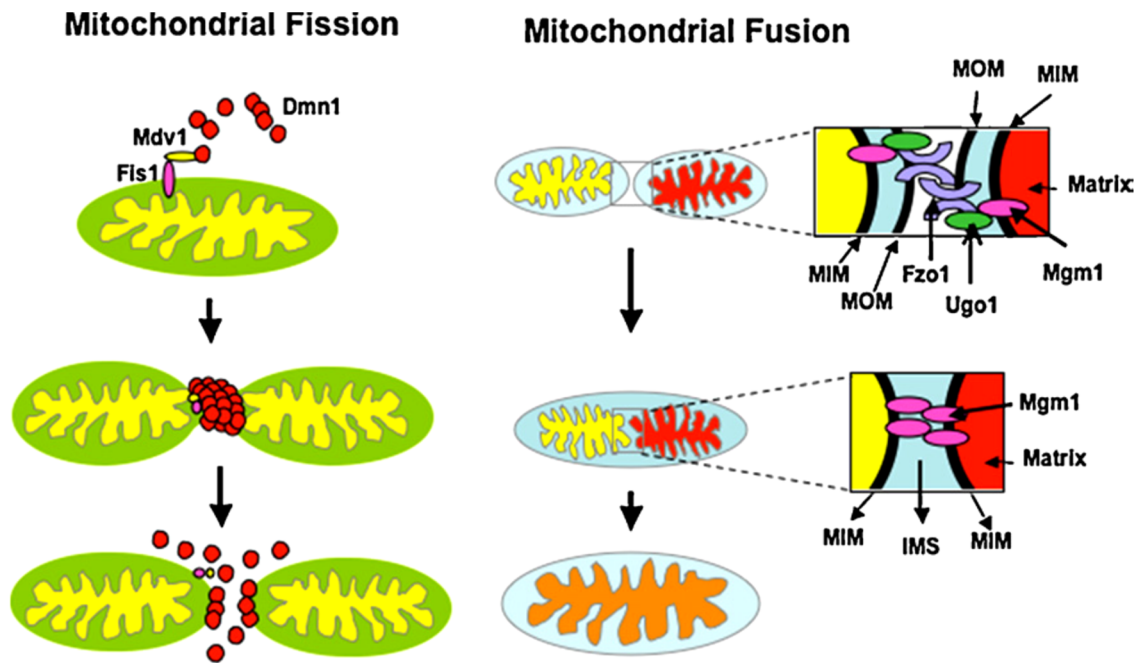


**Figure 1.9. Mitochondrial fission and fusion.** In yeast, mitochondria fission involves the action of Dmn1, that can self-assemble into polymeric spirals and is recruited into the mitochondrial membrane by Fis1 and Mdv1. Dmn1 polymers wrap around the organelle and constrict the membrane until fission occurs. In humans, Drp1 and hFis1 are the homologs of Dmn1 and Fis1 whereas no homolog of Mdv1 has been found yet. Mitochondrial fusion involves the interaction of Fzo1/Ugo1 molecules located in the outer membrane of two mitochondria until outer membrane fuses, and then inner membrane fusion occurs through the interaction of Mgm1 molecules. In mammals, there are two homologs of Fzo1, the mitofusins 1 and 2 (Mfn1 and Mfn2) whereas the homolog of Mgm1 is OPA1. MIM, mitochondrial inner membrane; MOM, mitochondrial outer membrane (Diaz and Moraes, 2008).

### 1.11. Mitochondrial membranes

Biological membranes are multifunctional cellular constituents not only protecting the cell from external sources but also assigning specific processes to certain compartments. The main building blocks of most membranes are phospholipids which provide a matrix for embedding proteins, sphingolipids and sterols. Lipids are not randomly distributed among biological membranes. Furthermore, they are highly specific and characteristic for each organelle influencing their shape, structure and function. Mitochondrial membrane from different cell types share the following specific characteristics: (i) phospholipid to protein and sterol to protein ratios are low compared to membranes of

other subcellular fractions; (ii) phosphatidylcholine (PC) and phosphatidylethanolamine (PE) are the major phospholipids which account for about 80% of total phospholipids; (iii) have high cardiolipin (CL) content in the range of 10–15%; (iv) sterols and sphingolipids are only found at low amounts. Mitochondria membranes from heart, brain, kidney, adrenal cortex and spleen additionally contain also PC and PE plasmalogens in the range of 5–30% of total phospholipids. Plasmalogens are a class of phospholipids carrying a vinyl ether bond in the sn-1 and an ester bond in the sn-2 position of the glycerol backbone (Horvath and Daum, 2013). The majority of lipids are synthesized in the endoplasmic reticulum (ER) and transported to the mitochondria, but the synthesis of cardiolipin and phosphatidylethanolamine occurs in the inner membrane of mitochondria. The maintenance of the lipid complement of mitochondrial membranes therefore depends on lipid transfer from the ER. Consequently, extensive lipid transfer occurs between the ER and the mitochondrial OMM and between both mitochondrial membranes (Tatsuta et al., 2014). The OMM forms a smooth lipid rich surface of mitochondria envelope with high membrane fluidity. In contrast, the IMM is highly folded and exhibits an elevated protein level and lower lipid content compared to the OMM (Horvath and Daum, 2013). The lipid composition of the OMM and the IMM differs significantly. The mitochondria-specific diglycerophospholipid cardiolipin (CL), for instance, is enriched in the IMM but present at low concentrations in the OMM (Tatsuta et al., 2014). Also PE is enriched in the IMM of mammalian cells, on the contrary phosphatidylinositol (PI) is present at a large amount in the OMM. In mammalian cells, the OMM and IMM are in close contact to each other through junctions called contact sites (CS). These junctions were considered as possible sites of protein import as well as phospholipid translocation. CS display an increased level of non-bilayer forming lipids such as PE and CL promoting hexagonal phase structures and therefore stabilizing the local arrangement of membrane junctions (Horvath and Daum, 2013).

Mitochondria harbor a certain set of enzymes involved in lipid biosynthesis. The capacity of mitochondria to synthesize their own lipids is limited to CL, PE, phosphatidylglycerol (PG) and phosphoatidic acid (PA) (Horvath and Daum, 2013). Here, I will focus only on the biosynthesis and the role of CL.

### 1.11.1. Cardiolipin biosynthesis

CL was first isolated and purified from beef heart in 1942. It is structurally unique: in contrast to the other membrane phospholipids, in which a single glycerol backbone is acylated to two fatty acid chains, CL contains two phosphatidyl groups (linked to a glycerol backbone) and four fatty acyl chains. Synthesis of CL occurs at the inner mitochondrial membrane (Houtkooper et al., 2006) (Fig. 1.10).

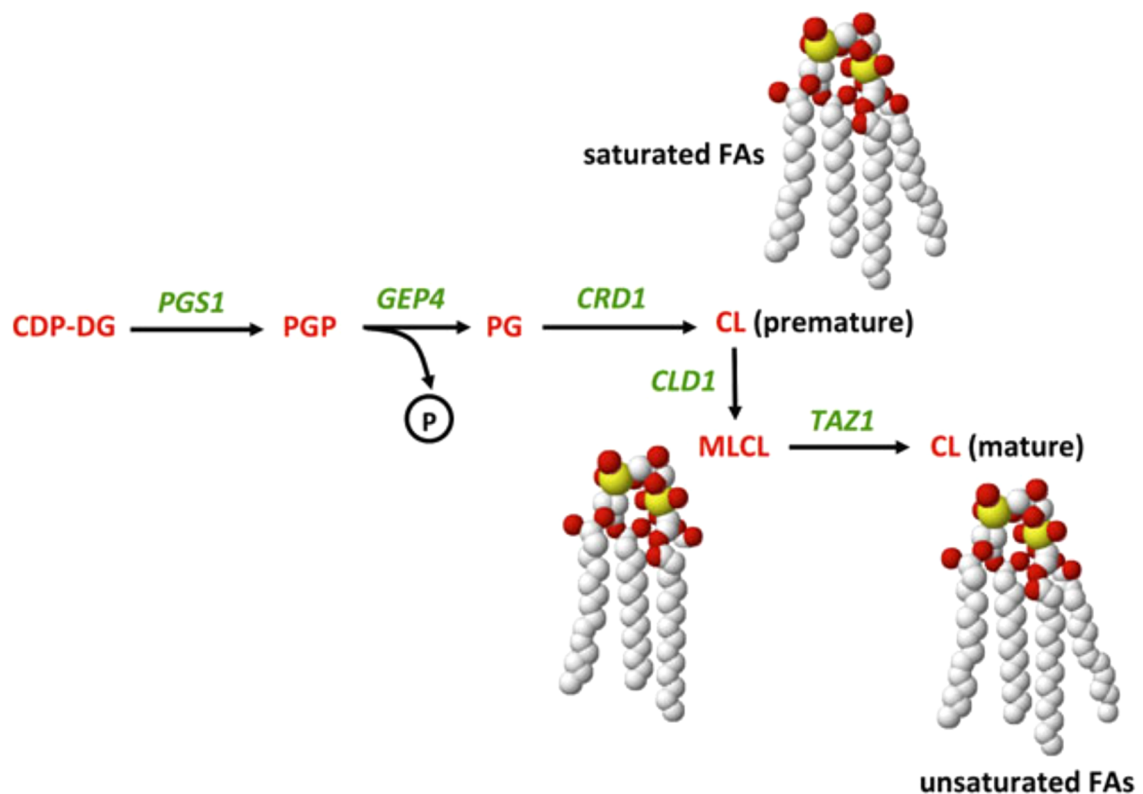


**Figure 1.10. Synthesis and remodeling of CL in yeast.** CL synthesis begins with the conversion of CDPdiacylglycerol (CDP-DG) to phosphatidylglycerolphosphate (PGP) by PGP synthase (encoded by PGS1). PGP is dephosphorylated to phosphatidylglycerol (PG) by GEP4- encoded PGP phosphatase. CL synthase (encoded by CRD1) converts PG to premature CL containing primarily saturated fatty acids (FA). CL is deacylated by CL deacylase (encoded by CLD1) to monolyso-CL (MLCL), which is reacylated by the TAZ1- encoded enzyme tafazzin to mature CL containing unsaturated fatty acids. The yeast gene names are depicted in green, while phospholipids and their intermediates are shown in red (Patil and Greenberg, 2013).

The first step is catalyzed by phosphatidylglycerolphosphate (PGP) synthase (Pgs1), which converts CDPdiacylglycerol (DAG) and glycerol-3-phosphate (G-3-P) to PGP.

PGP is dephosphorylated to phosphatidylglycerol (PG) by PGP phosphatase (Gep4). The mammalian homologue of the yeast *GEP4* gene was recently identified as protein tyrosine phosphatase localized in the mitochondrion (PTPMT1). CL synthase (CRLS1) catalyzes an irreversible condensation reaction in which the phosphatidyl group of CDP-DAG is linked to PG via cleavage of a high-energy anhydride bond to form CL (Patil and Greenberg, 2013). This conversion of PG into CL is so effective that mitochondrial membranes only contain trace amounts of PG (Houtkooper et al., 2006). CL synthase does not show strong preference for specific fatty acyl chains (Patil and Greenberg, 2013). Houtkooper et al., in 2006, first identified a human candidate gene/cDNA for *cardiolipin synthase*, C20orf155. The human *CRLS1* gene is localized at chromosome 20p13-p12.3 and encodes a protein of 301 amino acids. The protein contains a C-terminal transmembrane segment and belongs to the CDP-alcohol phosphatidyltransferase class-I family. It contains also an N-terminal mitochondrial targeting sequence (Houtkooper et al., 2006).

After biosynthesis, the newly synthesized immature CL undergoes deacylation by a CL-specific deacylase (Cld1). Cld1 removes one saturated fatty acyl chain from CL to form monolysocardiolipin (MLCL) (Patil and Greenberg, 2013). CL remodeling critically depends on tafazzin, a phospholipid–lysophospholipid transacylase. Tafazzin can catalyze both the removal and the re-attachment of fatty acids, which results in an exchange of acyl groups between CL and other phospholipids (Ren et al., 2014). CL in the normal human heart is primarily tetralinoleoyl-CL (L4-CL). Two other enzymes in addition to tafazzin remodel CL in mammalian cells: MLCL acyltransferase-1 (MLCLAT1), that shows specificity for linoleate, and acyl-CoA:lysoCL acyltransferase 1 (ALCAT1), that incorporate long chain polyunsaturated fatty acyl chains such as docosahexaenoic acid (DHA) fatty acyl chains in CL, makes it more susceptible to oxidative damage by ROS, causing early peroxidation (Patil and Greenberg, 2013).

### **1.11.2. Cardiolipin role**

Cardiolipin has been shown to interact with a number of inner mitochondrial membrane (IMM) proteins, enzymes and metabolite carriers. The list of proteins that bind cardiolipin with high affinity is long and includes, among others, the electron transport chain complexes involved in oxidative phosphorylation (OXPHOS), pyruvate carrier,



carnitine:acylcarnitine translocase and ADP/ATP carrier (AAC). CL is required for optimal activity of complex I, III, IV, and V (Fig. 1.11). It is not a passive component, but it is functionally required for normal electron transport and proton translocation activity of these enzymes. In fact, their removal from complex IV destabilizes its subunits interactions which are essential for its full activity. Removal of CL decreases electron-transport activity of Complex IV by around 50%. Moreover CL is essential for catalytic function of complex III, stabilizing the fully active conformation of this complex. CL molecule appears to stabilize the architecture of the proton conduction environment at this site and may be involved in proton uptake. Treatment of bovine heart submitochondrial particles with nonylacridine orange, a compound that interacts specifically with CL, resulted in a marked inactivation of complex I and exogenous added CL fully prevented this inactivation, while addition of other phospholipids such as PC and PE was ineffective. F<sub>0</sub>F<sub>1</sub> ATP synthase has been shown to form dimers as well as higher oligomeric assemblies. It plays an essential role for cristae formation (Allen, 1995). CL is critical for the degree of oligomerization and the degree of order in these ATP synthase assemblies, which is likely to affect cristae morphology and energy efficiency (Acehan et al., 2011). It has been hypothesized that this CL effect could either result from direct interaction with the enzyme, or from physical constraints associated with membrane curvature. Due to its molecular shape, CL is known to partition into high-curvature membrane segments and to adopt a specific orientation with respect to the intrinsic curvature, due to its inherent anisotropy. Thus, CL and ATP synthase might act in concert to reduce the free energy imposed by membrane curvature, together stabilizing these high-curvature folds.

CL seems to participate in the structural organization and stabilization of the respiratory chain complexes in high order structure of functional importance (Wenz et al., 2009; Claypool et al., 2008; Claypool, 2009) (Fig. 1.11). About 200 CLs were estimated to be present in the purified bovine respirasome (I<sub>1</sub>III<sub>2</sub>IV<sub>1</sub>), and about 50 CLs in the III<sub>2</sub>IV<sub>2</sub> supercomplex from *Saccharomyces cerevisiae*. Thus, CL seems to be essential for supercomplexes formation in addition to its occurrence as in integral part of individual complexes.

It is estimated that approximately 0.2–2% of the oxygen taken up by a cell is converted by mitochondria to ROS. Within mitochondria, the electron transport chain is

considered the main source of ROS. The two major sites of  $O_2^{2-}$  production are complex I and complex III. Cardiolipin molecules are particularly susceptible to ROS induced oxidation, either for their fatty acyl composition or for their proximity to the ROS generating centers. Oxidative damage to CL may have deleterious effect on respiratory chain complex activity and mitochondrial function. ROS-induced CL oxidation may also affect OXPHOS supercomplexes formation and/or stabilization (Paradies et al., 2013).

What is unique about CL in contrast to other phospholipids can be traced back to a single structural feature, namely the bonding of two phosphatidyl moieties with a single glycerol group. This feature results in a small, relatively immobile head group, which in turn promotes negative curvature, cohesive effects between hydrocarbon chains, and electrostatic interactions. The reason why such properties are of particular importance to mitochondria may be related to the high protein density of cristae membranes, the need for extensive membrane folds, or the need for continuous fission and fusion, which requires non-bilayer lipid phases with high negative curvature (Fig. 1.11). Thus, the likely role of CL in mitochondria is (i) to support membrane dynamics and (ii) to stabilize the lateral organization of protein-rich membranes (Ren et al., 2014). CL is critical for fusion of the inner membrane via its interaction with the dynamin-related protein Opa1, a GTPase which mediates inner membrane fusion. Opa1 is found in long and short isoforms that are inactive when monomeric but exhibit GTPase activity as dimers and drive mitochondrial fusion. The dimerization is dependent on the presence of CL and the GTPase activity is enhanced on liposomes composed of lipids matching that of the mitochondrial inner membrane, again in a manner dependent on CL (DeVay et al., 2009; Ban et al., 2010).

Cardiolipin is transferred from the inner membrane to the outer membrane by a specific protein machinery, thus facilitating processes such as apoptosis and mitochondrial fission. The most obvious role for CL in the fission pathway involves Drp1, the protein that directly mediates the fission process. CL has been shown to mediate both Drp1 recruitment to membrane surfaces and to activate Drp1's GTPase activity, similar to the role it undertakes for Opa1. Anyway, CL seems to predominantly function as a pro-fusion lipid, since CL deficiency leads to fragmented mitochondria (Frohman, 2015).

CL has an important role for mitochondrial bioenergetic function; but in addition, recent studies are now revealing that CL has a much broader impact on mitochondrial physiology and pathophysiology. Cardiolipin has been implicated in the process of apoptosis in animal cells through its interaction with a variety of death-inducing proteins, including cytochrome c (Cyt c) (Paradies et al., 2013) (Fig. 1.11). During apoptosis initiation, CL is the only phospholipid in mitochondria that undergoes peroxidation, catalyzed by a cardiolipin-specific peroxidase activity of CL-bound cytochrome c. Cytochrome c-catalyzed peroxidation of CL utilizes polyunsaturated molecular species, whereas saturated and monounsaturated CL molecules do not undergo peroxidation. In its native structure, cytochrome c functions as an electron shuttle between respiratory complexes III and IV in mitochondria. Upon binding of CL, cytochrome c undergoes a structural reconfiguration and transforms into a CL-specific peroxidase (Kagan et al., 2009). The structural reconfiguration of cytochrome c appears to involve both electrostatic interactions of one or more positively charged amino acid (lysine) residues with negatively charged phosphate groups of CL as well as hydrophobic interactions of one or more of CL's fatty acid residues with nonpolar sites of the protein. The peroxidase function of cytochrome c requires its direct physical interaction with CL. Normally, CL is present primarily in the inner leaflet of the inner membrane, whereas cytochrome c is confined to the intermembrane space. Thus, binding of cytochrome c to CL depends on the availability of the latter in the outer leaflet of the inner membrane. Moreover, significant demand for high-affinity CL binding by other mitochondrial proteins such as mitochondrial respiratory complexes I, III, and IV, and ADP/ATP carriers, also limits access of cytochrome c to CL. It appears that mitochondrial injuries (metabolic or chemical) generate reactive oxygen species, such as superoxide radicals, which cause (through an as yet unknown mechanism) a significant amount of CL to flip to the outer leaflet facing the intermembrane space where cytochrome c is located. Upon binding of CL, cytochrome c is transformed into a CL-specific peroxidase, which catalyzes CL peroxidation in the presence of sufficient supply of H<sub>2</sub>O<sub>2</sub>, a product of superoxide dismutation. After, cardiolipin go to the outer leaflet of the OMM (Ren et al., 2014). A diverse set of apoptotic proteins such as t-Bid, Bax, Bak, and caspase-8 are recruited to the mitochondrial surface of cells undergoing apoptosis in a CL-dependent manner. Upon activation, caspase-8 migrates to the

mitochondrial outer membrane in regions where CL is present (Patil and Greenberg, 2013). In a further step, caspase-8 cleaves Bid (a BH3-only protein) to a truncated form (tBid) which is directed to the OMM and induces Bax/Bak oligomerization thereby permeabilizing the membrane and releasing cytochrome c. Targeting of tBid to mitochondria occurs in a CL-dependent manner and plays a crucial role in apoptosis associated processes including cristae remodeling and mitochondrial fragmentation (Horvath and Daum, 2013).

Recent studies revealed the physiological significance of the appearance of externalized CL as an “eat-me-signal” for the autophagic machinery resulting in targeted removal of damaged mitochondria (Chu et al., 2013) (Fig. 1.11). The mitophagy mechanisms include specific recognition of externalized CL by microtubule-associated protein 1 light chain 3 (LC3), a component of the autophagic machinery which mediates both autophagosome formation and cargo recognition. RNAi knockdown of *cardiolipin synthase* or of *phospholipid scramblase-3*, which transports cardiolipin to the outer mitochondrial membrane, decreased the delivery of mitochondria to autophagosomes. LC3 contains cardiolipin-binding sites important for the engulfment of mitochondria by the autophagic system. Mutation of LC3 residues predicted as cardiolipin-interaction sites by computational modelling inhibited its participation in mitophagy. The unique structure of CL includes a compact, negative charged head group, whereas mammalian LC3 contains basic surface patches. Importantly, autophagic machinery recognizes CLs more effectively than its metabolites, including mono- and di-lyso-CLs as well as CL oxidation products. This implies that CL oxidation is not a requirement for mitophagic elimination of injured mitochondria (Chu et al., 2013). This seems to be contradictory to the accepted opinion that oxidative stress and lipid peroxidation are inherent to mitochondrial injury and mitophagy. Thus, although CL is found mostly in the inner membrane of normally functioning mitochondria, upon mitochondrial injury and depolarization, a significant portion of CL becomes exposed on the mitochondrial surface, where it serves as either pro-mitophagic or pro-apoptotic signals, depending on the extent of mitochondrial injury (Ren et al., 2014).

Due to the role played by CL in mitochondrial bioenergetics as well as in apoptosis, mitophagy and mitochondria morphology, it is conceivable that CL abnormalities may have important implications in mitochondrial dysfunction and hence, in cellular

pathophysiology. Alterations in CL structure, content and acyl chain composition, associated with mitochondrial dysfunction, have been described in several pathophysiological conditions, such as hypo–hyperthyroid states, heart ischemia–reperfusion, nonalcoholic fatty liver disease, diabetes, Barth syndrome and aging (Paradies et al., 2013).

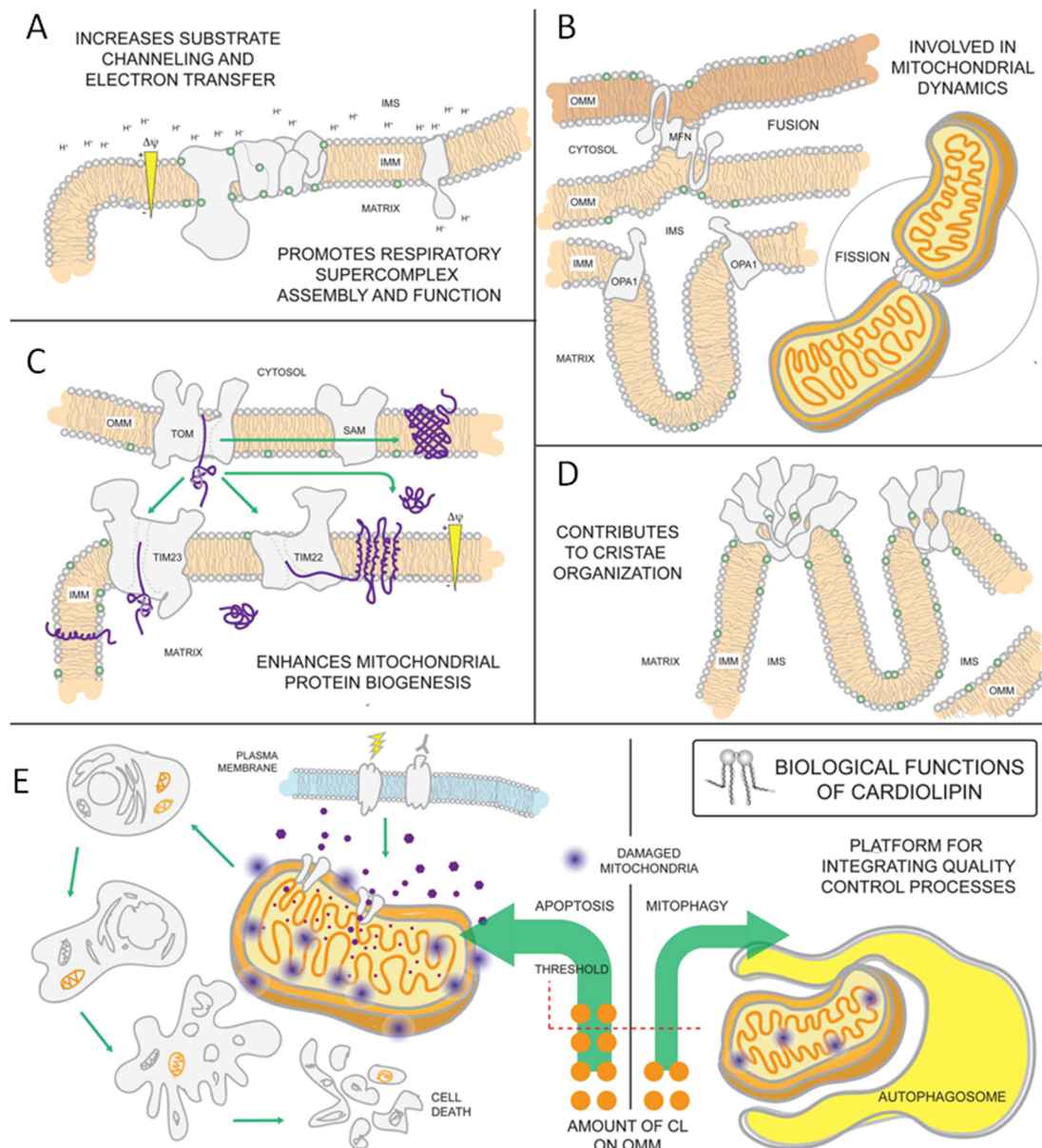


**Figure 1.11. Biological functions of cardiolipin.** As the signature phospholipid of the mitochondrion, CL is intimately involved in a number of mitochondrial processes. **(A)** Anionic CL on the IMM can function as a proton trap by attracting (and providing) a local pool of protons that can be funnelled towards the ATP synthase. Moreover, CL is associated with every OXPHOS component and can promote

their assembly in to respiratory supercomplexes. Such supramolecular assemblies are thought to enhance electrontransfer and reduce ROS leakage from the electron transport chain. **(B)** CL associates with dynamin-related GTPases that are intimately involved in fusion and fission and **(C)** contributes to the assembly and function of IMM and OMM translocases vital for mitochondrial biogenesis. **(D)** Besides enhancing OXPHOS by stabilizing SCs, CL also promotes the assembly of ATPsynthase oligomers that provide a structural scaffold required for establishing the characteristics shape of mitochondrial cristae. **(E)** Externalization of CL on the surface of the mitochondrion is involved in signaling the execution of either mitophagy or apoptotic cell death (Lu and Claypool, 2015).

## *2. Aims*

This study rests on the primary role of skeletal muscle dysfunction in SBMA pathogenesis and on the hypothesis that mitochondrial alterations may play a role in the development of SBMA myopathy.

To verify if the muscle tissue of our SBMA patients presents mitochondrial abnormalities and how these abnormalities are related to the presence of polyQ expanded *androgen receptor* gene, we aimed to evaluate:

1. transcript, protein levels and cellular distribution of polyglutamine-expanded androgen receptor.
2. a set of mitochondrial parameters, included mitochondrial (i) activity, (ii) mass, (iii) biogenesis and (iv) degradation (mitophagy).



### *3. Material and Methods*

### **3.1. Tissue Samples**

We studied 19 SBMA patients followed at our Neuromuscular Clinic of the University of Padua (Table 2.1). The mean age at onset was 42.7 years (range 26 - 64 years) and the mean delay from first symptoms to time of biopsy was 11,2 years (range -6 – 49 years). In all of them we recorded main clinical data including age at disease onset, age at biopsy and first clinical symptoms. At the time of biopsy patients underwent standard neurological examination and electrophysiological studies (EMG, nerve conduction studies and sensory evoked potentials). Genomic DNA was extracted from peripheral blood using standard protocol. PolyQ (CAG repeats) alleles were amplified by PCR as previously described (Querin et al., 2015). Repeats fragment sizing was performed on an ABI PRISM 3700 DNA Sequencer (Applied Biosystems, Foster City, CA). The specific length of CAG repeats was further verified via Sanger sequencing. Muscle biopsies were obtained with informed consent by open biopsy procedure with the resultant collection of 100-200 mg of muscle tissue. All biopsies were immediately frozen in liquid nitrogen for histopathology and biochemical analysis and stored at -80°C until analysed. Muscle biopsies from 18 age- and sex-matched healthy subjects, free from neuromuscular diseases and with normal creatine kinase levels (Table 2.2) were used as controls. The mean age at biopsy for controls was 44,6 years (range 19 – 79 years).

Patient	Sex	Biopsied muscle	Age at onset (years)	Age at biopsy (years)	CAG repeats number
1	M	Quadriceps	50	52	43
2	M	Quadriceps	31	80	41
3	M	Quadriceps	60	54	43
4	M	Quadriceps	50	59	46
5	M	Quadriceps	26	57	45
6	M	Quadriceps	38	61	44
7	M	Quadriceps	41	45	46
8	M	Quadriceps	64	71	43
9	M	Quadriceps	49	57	44
10	M	Quadriceps	45	61	46
11	M	Quadriceps	37	44	49
12	M	Quadriceps	46	55	48
13	M	Quadriceps	27	28	43
14	M	Quadriceps	29	39	46
15	M	Quadriceps	45	54	48
16	M	Quadriceps	49	55	44
17	M	Quadriceps	43	64	41
18	M	Quadriceps	48	51	44
19	M	Quadriceps	34	37	49

Table 2.1. Clinical data of SBMA patients.

Control	Sex	Biopsied muscle	Age at biopsy (years)
1	M	Quadriceps	52
2	M	Quadriceps	42
3	M	Quadriceps	55
4	M	Quadriceps	53
5	M	Quadriceps	63
6	M	Quadriceps	36
7	M	Quadriceps	45
8	M	Quadriceps	28
9	M	Quadriceps	42
10	M	Quadriceps	32
11	M	Quadriceps	45
12	M	Quadriceps	45
13	M	Quadriceps	44
14	M	Quadriceps	79
15	M	Quadriceps	38
16	M	Quadriceps	38
17	M	Quadriceps	19
18	M	Quadriceps	47

Table 2.2. Clinical data of male controls.

## **3.2. Molecular analysis**

### **3.2.1. RT-PCR**

Total DNA was isolated from muscle tissue using DNeasy Blood & Tissue Kit (Qiagen). Quantitative polymerase chain reaction (qPCR) was performed in ABI PRISM 7000 light cycler, using Platinum quantitative PCR SuperMix-UDG with ROX (Invitrogen). The mtDNA copy number was estimated as described in Malena et al., (2009). Briefly a portion of the cytochrome c oxidase (COII) gene of mtDNA was amplified and compared to the amplification profile of a nuclear single copy gene, Amyloid Precursor Protein (APP). The relative level for each gene was calculated using the “ $2^{-\Delta\Delta Ct}$  method”. In all experiments, each sample was analysed in triplicate. Probes were labelled with FAM and TAMRA.

Total RNA was isolated from muscle biopsies using TRIzol Reagent (Life Technologies). First-Strand cDNA synthesis was performed using High-Capacity cDNA Reverse Transcription Kit (Life Technologies) and transcript levels were quantified by SYBER Green Real-Time PCR (Life Technologies) using the ABI PRISM 7000 sequence detection system.

Primer sequences are listed in the following table (Table 2.3):

	Forward primer	Reverse primers	Probe
APP	5'-TTTTTGTGTGCTCTCCAGGTCT-3'	5'-TGGTCACTGGTTGGTTGGC-3'	5'-CCCTGAACTGCAGATCACCAATGTGGTAG-3'
AR	5'-TTGTCCACCGTGTCTTCTCTGC-3'	5'-TGCACCTCCATCCTTGAGCTGGC-3'	
Beclin-1	5'-AGGTTGAGAAAGGCGAGACA-3'	5'-GCTTTTGTCCAATGCTCCTC-3'	
BNIP3	5'-GCATGAGTCTGGACGGAGTA-3'	5'-GTTTCAGAAGCCCTGTTGGT-3'	
COII	5'-CGTCTGAACTATCCTGCCCG-3'	5'-TGGTAAGGGAGGGATCGTTG-3'	5'-CGCCCTCCCATCCCTACGCATC-3'
COX4	5'-CATGTGGCAGAAGCACTATGTGT-3'	5'-GCCACCCACTCTTTGTCAAAG-3'	
CRLS1	5'-CCCAGTTCTGGGCTATTTGA-3'	5'-TCTTTGATTGGCCAGTTTC-3'	
Drp1	5'-CTGACGCTTGTGGATTACC-3'	5'-CCCTCCCATCAATACATCC-3'	
ERR $\alpha$	5'-TTCTCATCGCTGCTGCTGTCT-3'	5'-CAGCCGCCGCACTAGTTG-3'	
hFis1	5'-GGAGGACCTGCTGAAGTTTG-3'	5'-ACGATGCCCTTACGGATGTC-3'	
LAMP-1	5'-TCTCAACATCAACCCCAACA-3'	5'-AACTTGCAATTCATCCGAAC-3'	
LAMP-2B	5'-GGGTTCAGCCTTCAATGTG-3'	5'-CCTGAAAGACCAGCACCAAC-3'	
LC3	5'-CATGAGCGAGTTGGTCAAGA-3'	5'-CTCGTCTTCTCCTGCTCGT-3'	
MFN1	5'-TGTTTTGGTCGCAAACTCTG-3'	5'-CTGTCTGCTACGTCTTCCA-3'	
MFN2	5'-ATGCATCCCCACTTAAGCAC-3'	5'-CCAGAGGGCAGAACTTTGTC-3'	
MnSOD	5'-CTTCAGCCTGCACTGCCGTTCAAT-3'	5'-CTGAAGGTAGTAAGCGTGCTCCC-3'	
NRF1	5'-GGTGCAGCACCTTTGGAGAA-3'	5'-CCAGAGCAGACTCCAGGTCTTC-3'	
p62	5'-GTGGTAGGAACCCGCTACAA-3'	5'-GAGAAGCCCTCAGACAGGTG-3'	
Parkin	5'-AAAGGCCCTGTCAAAGAGT-3'	5'-ATCATCCCAGCAAGATGGAC-3'	
PGC-1 $\alpha$	5'-TCAGTCTCACTGGTGGACA-3'	5'-TGCTTCGTGTCAAAAACAG-3'	
PGC-1 $\beta$	5'-CTGCTGGCCAGATACACTGA-3'	5'-ATCCATGGCTTCATACTTGCT-3'	
PINK1	5'-CCAAGTTTGTGTGACCCGGC-3'	5'-CTTCATAACGAGGAACAGCGTCC-3'	
RPLPO	5'-GTGATGTGCAGCTGATCAAGACT-3'	5'-GATGACCCAGCCAAAAGGAGA-3'	
TFAM	5'-GAACAACATCCCATATTTAAAGCTCA-3'	5'-GAATCAGGAAGTCCCTCCA-3'	

**Table 2.3. Primers used for RT-PCR analysis.**

### **3.3. Biochemical analysis**

#### **3.3.1. Total muscle lysates**

Total muscle lysates were obtained by thirty 20  $\mu$ m thick fresh-frozen sections of muscle biopsies, maintained on ice for 30 min with 200  $\mu$ l of RIPA buffer (65 mM Tris, 150 mM NaCl, 1 % NP-40, 0.25 % Na-DOC, 1 mM EDTA, pH 7.4) and 2 $\mu$ l of a cocktail of protease inhibitors (Sigma). The muscle lysate was centrifuged at 20000g for 20 minutes at 4°C and the supernatant stored at -80°C until use. Protein concentration was determined by BCA assay (Pierce) (see section 2.3.5).

### **3.3.2. Nuclear and cytosolic fractions**

Nuclear and cytosolic fractions were obtained treating fifty 20 µm thick fresh-frozen sections of muscle biopsies with the NE-PER Nuclear and Cytoplasmic Extraction kit (Thermo Scientific), supplemented with protease inhibitor cocktail (Sigma). Briefly, the Kit contains three reagents: Cytoplasmic Extraction Reagent I (CER I), Cytoplasmic Extraction Reagent II (CER II) and Nuclear Extraction Reagent (NER). Addition of the first two reagents to muscle slices caused cell membrane disruption and release of cytoplasmic contents. After centrifugation at 13000 rpm for 5 minutes at 4°C, the cytoplasmic extract (supernatant) was transferred into a new tube and stored at -80°C until use, while intact nuclei (pellet) were suspended in the third reagent and centrifuged at 13000 rpm for 10 minutes at 4°C. Nuclear extract (supernatant) was transferred into a new tube and stored at -80°C until use. Protein concentration was determined by BCA assay (Pierce) (see section 2.3.5).

### **3.3.3. Mitochondria isolation**

For mitochondria isolation, 50-100mg of muscle biopsies were washed and homogenized by 10 strokes using a Velp Scientifica homogenizer in Buffer A (20mM HEPES, 100mM KCl, 1mM EDTA, 2mM β-mercaptoethanol, 0.3% BSA) and then centrifuged at 800g for 10 min at 4°C. The supernatant (S1) was stored at 4°C and the pellet was again washed and homogenized in Buffer A and then centrifuged at 800g for 10 min at 4°C, to increase the yield of mitochondria. The supernatants (S1+S2) were centrifuged at 10000g for 10 min at 4°C. The pellet containing the mitochondria were washed using MSEM buffer (220mM Mannitol, 70 mM sucrose, 1mM EDTA, 2mM β-mercaptoethanol, 5mM MOPS), aliquoted in several tubes and centrifuged at 20000g for 10 min at 4°C. The pellets were stored at -80°C until use.

### **3.3.4. Citrate synthase activity**

Citrate synthase (CS) activity was quantified as previously described (Spinazzi et al., 2012). Briefly, mitochondria pellets (see section 3.3.3) were lysed using a 10 mM KP buffer pH 7. Then, mitochondrial membranes were breaking mechanically with a glass syringe and by thermal shock (liquid nitrogen - 37°C). CS catalyses the reaction between acetyl coenzyme A and oxaloacetic acid to form citric acid. The hydrolysis of

the thioester of acetyl CoA results in the formation of CoA with a thiol group (CoA-SH). The thiol reacts with DTNB in the reaction mixture (200 mM Tris with 0,2% (vol/vol) Triton X-100, 1 mM DTNB, 10 mM Acetyl-coA and 10 mM Oxaloacetic acid) to form 5-thio-2-nitrobenzoic acid (TNB). This yellow product (TNB) is observed spectrophotometrically by measuring the increase in absorbance at 412 nm for 5 minutes at 37°C. Spectrophotometric assays were conducted using micro cuvettes for spectrophotometry with optimal transparency along the spectral range from 340 to 800 nm. The mix of each reaction, with a final volume of 1 ml, was prepared directly into cuvettes and left for 5 minutes inside the spectrophotometer before starting the reaction with the addition of sample. The enzymatic activity of CS was calculated using the extinction coefficient of DTNB ( $\epsilon_{412} = 13.6 \text{ mmol}^{-1} \text{ cm}^{-1}$ ) and expressed in  $\text{nmol min}^{-1} \text{ mg}^{-1}$  of protein, through the following formula.

$$\text{Activity} = \frac{\Delta OD}{\text{min}} \times \frac{1}{13.6} \times \frac{1}{\text{mg.protein}}$$

2500, 4000 or 5000 activities of CS were loaded for the different analysis. Protein concentration was determined by Bradford assay (Sigma) (see section 2.3.5).

### **3.3.5. Protein quantization**

Protein concentration was determined by BCA assay (Pierce) or Bradford assay (Sigma), supplemented with BSA ( $2 \mu\text{g}/\mu\text{l}$ ). In each case, bovine serum albumin (BSA) standard curve was assayed to determine sample protein concentrations.

The BCA Protein Assay consists in two steps. In the first, peptides containing three or more amino acid residues form a colored chelate complex with cupric ions in an alkaline environment containing sodium potassium tartrate. In the second step, bicinchoninic acid (BCA) reacts with the reduced cuprous cation formed in step one. The intense purple-colored reaction product results from the chelation of two molecules of BCA with one cuprous ion. The BCA/copper complex is water-soluble and exhibits a strong linear absorbance at 562 nm with increasing protein concentrations. The kit contains two reagents (A and B): 1 ml of solution was prepared for each samples and standard ( $980 \mu\text{l}$  of reagent A +  $20 \mu\text{l}$  of reagent B). After incubation at 37°C for 30 minutes, spectrophotometric assay was performed, by using the same micro cuvettes for CS activity evaluation. Absorbance was measured at 562nm at 37°C.

For Bradford assay, Coomassie Brilliant Blue G-250 was diluted 1:5 and 1ml of this solution was used for each sample and standard. The assay is up to be read at the spectrophotometer after 5 minutes and is stable until 1 hour. Reacting with amino and carboxylic groups of proteins, its absorbance maximum shifts from 465 (red) to 595nm (blue) in acid solutions.

From the standard BSA curve 1 $\mu$ g of proteins' Optical Density (O.D.<sub>1 $\mu$ g</sub>) was obtained and protein concentration of each sample was calculated using the following equation:

$$mg\ of\ proteins = O.D._{sample} \div O.D._{1mg} \div used\ sample\ ml \times total\ sample\ ml$$

### **3.3.6. Western Blot analysis**

30  $\mu$ g of protein from each sample was separated into 7.5 or 10 % Criterion precast gels (Bio-Rad Laboratories) and transferred onto a nitrocellulose membrane (Whatman). Membranes were blocked in 5 % (w/v) fat-free milk in 0.02 M Tris/HCl pH 7.5, 137mM NaCl, and 0.1 % (v/v) Tween-20 for 1 h at room temperature. Membranes were then incubated overnight at 4 °C with the primary antibodies. After 1 h incubation with secondary HRP-conjugated antibodies, signals were visualized by chemiluminescence (GE HealthCare) and exposition to films (Kodak). Integrated optical density of each band was calculated with commercial software (Gel Pro Analyzer).

The primary antibodies used were: anti-AR polyclonal (Santa Cruz, N-20, sc-816, 1:1000), anti-actin monoclonal (Chemicon International, MAB1501, 1:20000), anti-PARP-1 polyclonal (Santa Cruz, H-250, 1:2000), anti- $\beta$  tubulin polyclonal (Santa Cruz, H-235, 1:1000), anti-LC3 monoclonal (Sigma, L7543, 1:1000), anti-Beclin-1 polyclonal (Cell Signaling, 3738, 1:1000), anti-BNIP3 polyclonal (Sigma, B7931, 1:1000), anti-PINK1 monoclonal (Cell Signaling, D8G3, 1:1000), anti-TOM20 polyclonal (Santa Cruz, Sc-11415, 1:1000), anti-LAMP-1 monoclonal (DSHB, H4A3, 1:400), anti-Ubiquitin monoclonal (Millipore, MAB1510, 1:1000), anti-p62 monoclonal (Sigma, 041M4812 1:2000), anti-Parkin monoclonal (Santa Cruz, Sc-32282, 1:1000), anti-DLP1 monoclonal (BD Biosciences, 611112, 1:1000), anti-Fis1 polyclonal (Alexis, ALX-210-907, 1:1000), anti-COX IV polyclonal (Cell Signaling, #4844, 1:1000); anti-NRF1 polyclonal (Rockland Immunochemicals, 200-401-869, 1:1000); anti-Mitofusin-1 monoclonal (Abnova GmbH, H00055669-M04, 1:1000); anti-Mitofusin-2 polyclonal (Abnova GmbH, PAB7989; 1:1000); COXIV (Santa Cruz Biotechnology, CA, USA),



anti-ATPase polyclonal (home-made), generous gift of Prof. F. Dabbeni-Sala from University of Padua and .

### **3.3.7. Blue Native PAGE**

For Blue Native PAGE (BN-PAGE) human muscle mitochondria were isolated as previously described. Mitochondrial pellets were suspended at 10 $\mu$ g/ $\mu$ l on Native Buffer (Invitrogen) with 4% Digitonin (Sigma) during 1 hour on ice and centrifuged 20 min 16,000 x g at 4°C. Supernatant was collected and 1% G250 sample buffer additive (Invitrogen) was added. 10 $\mu$ g of mitochondrial membrane proteins were applied and run on a 3-12% Bis-Tris gel (Invitrogen) as described elsewhere (NativePAGE™ Novex® Bis-Tris Gel System manual).

Visualization of antibody protein complexes was achieved by enhanced chemiluminescence (LiteAblot-Turbo, Euroclone) and the ChemiDoc™ XRS+ System (Bio-Rad). Densitometry was performed with the Gel-Pro Analyzer software.

The primary antibodies used were: anti-MTCO1 monoclonal (Abcam, ab14705, 1:5000), anti-Complex I subunit NDUFB8 monoclonal (Molecular Probes, 459210, 1:5000) and anti-GRP75 polyclonal (Santa Cruz, sc-13967, 1:5000).

### **3.3.8. OXPHOS Activity**

For fresh muscle homogenate, 20-30mg of muscle biopsies were washed and homogenized by 15 strokes at 500 rpm using a Velp Scientifica homogenizer in Sucrose buffer 250 mM (0.121 g Tris, 0.15 g KCl and 0.038 g EGTA in a final volume of 50 ml; on the same day of the experiment 0,854 g of sucrose was added to 10 ml of this buffer) and then centrifuged at 600g for 10 min at 4°C. The supernatant was transferred into a new tube on ice for Respiratory Chain (RC) analysis. The enzymatic activities of Respiratory Chain complexes I–IV were assayed in duplicate or triplicate with a single-wavelength, temperature-controlled spectrophotometer at 37°C for few minutes as described in Spinazzi et al. (2012). Spectrophotometric assays were conducted using the same micro cuvettes for CS activity (see section 3.3.4). Similarly, the mix of each reaction, with a final volume of 1 ml, was prepared directly into cuvettes and left for 5 minutes inside the spectrophotometer before starting the reaction with the addition of sample. Total protein concentration was determined by Bradford assay (Biorad) (see

section 3.3.5). The enzymatic activities for each mitochondrial enzyme was calculated as  $\text{nmol min}^{-1} \text{mg}^{-1}$  of protein using different extinction coefficient depending on substrate/electron acceptors used in the reaction and also normalized to the activity of CS, a mitochondrial matrix enzyme, used as a marker of the abundance of mitochondria within a tissue/cell. For more details, see Table 2.4.

	CI	CII	CIII	CIV	CI+III	CII+III	CS
Option in Step 2	A	B	C	D	E	F	G
$\lambda$ (nm)	340	600	550	550	550	550	412
$\epsilon$ ( $\text{mmol}^{-1} \text{cm}^{-1}$ )	6.2	19.1	18.5	18.5	18.5	18.5	13.6
Buffer	KP, 50 mM	KP, 25 mM	KP, 25 mM	KP, 50 mM [25 mM]	KP, 50 mM	KP, 20 mM [100 mM]	Tris, 100 mM
pH	7.50	7.50	7.50	7.00	7.50	7.50	8.00
Substrates/ electron acceptors	NADH, 100 $\mu\text{M}$ Ub <sub>1</sub> , 60 $\mu\text{M}$	Succinate, 20 mM DCPIP, 80 $\mu\text{M}$ DUB, 50 $\mu\text{M}$	DubH <sub>2</sub> , 100 $\mu\text{M}$ Cyt c, 75 $\mu\text{M}$	Cyt c H <sub>2</sub> , 60 $\mu\text{M}$ [50 $\mu\text{M}$ ]	NADH, 200 $\mu\text{M}$ Cyt c, 50 $\mu\text{M}$	Succinate, 10 mM Cyt c, 50 $\mu\text{M}$	DTNB, 100 $\mu\text{M}$ Ac CoA, 300 $\mu\text{M}$
Detergent	—	—	Tween-20 (0.025% (vol/vol))	—	—	—	Triton X-100 (0.1% (vol/vol))
Other reagent(s)	BSA, 3 $\text{mg ml}^{-1}$ KCN, 300 $\mu\text{M}$	BSA, 1 $\text{mg ml}^{-1}$ KCN, 300 $\mu\text{M}$	KCN, 500 $\mu\text{M}$ EDTA, 100 $\mu\text{M}$	—	BSA, 1 $\text{mg ml}^{-1}$ KCN, 300 $\mu\text{M}$	KCN, 300 $\mu\text{M}$	—
Specific Inhibitor	Rotenone 10 $\mu\text{M}$	Malonate, 10 mM, or TTFA, 500 $\mu\text{M}$	Antimycin A, 10 $\mu\text{g ml}^{-1}$	KCN, 300 $\mu\text{M}$	Rotenone, 10 $\mu\text{M}$	Malonate, 10 mM	—

**Table 2.4. Conditions for spectrophotometric assays of respiratory chain enzymes and citrate synthase activities in tissues and cells** (Spinazzi et al., 2012).

### 3.3.9. Mitochondria Lipid Extraction

Isolated mitochondria were obtained as described in section 3.3.3. 100  $\mu\text{l}$  aliquots of mitochondria suspension (containing 10  $\mu\text{g}$  of protein) were used for lipids extraction. Lipids were extracted according to the method of Bligh and Dyer (Bligh and Dyer, 1959) substituting deuterated dichloromethane (DMC) for chloroform (Cequier-Sanchez et al., 2008). First, 320  $\mu\text{l}$  of methanol (MeOH) was added to each 100  $\mu\text{l}$  sample. Samples were then vortexed for 60 s. Next, 630  $\mu\text{l}$  of DCM was added, the sample was again vortexed for 60 s and 200  $\mu\text{l}$  of water was added to induce phase separation. The samples were then vortexed for 60 s and allowed to equilibrate at room temperature for 10 min before centrifugation at 8000g for 10 min at 10 C. A total of 10  $\mu\text{l}$  of the lower

lipid-rich DCM layer was then collected and diluted in 990  $\mu\text{L}$  of acetonitrile (ACN)/DCM/H<sub>2</sub>O (80:15:5 v/v/v) before (Liquid Chromatography–Mass Spectrometry) LC-MS analysis. One microliter of sample (equivalent to 200 pg of proteins) was injected onto the nano LC-MS system.

### **3.3.10. Nano Liquid Chromatography–Mass Spectrometry (LC–MS) Analysis**

The LC/MS analyses were run on an Agilent (Agilent, Santa Clara, CA, US) 6520 accurate mass Quadrupole Time-of-Flight (Q-TOF) LC-MS system governed by Agilent MassHunter software (B.05.00 version). The LC system consists of a 1200 series High Performance Liquid Chromatography (HPLC) system coupled on-line to MS through a Chip Cube Interface (Agilent Technologies, CA, USA). Each sample (1  $\mu\text{L}$ ) was loaded onto a large capacity chip-column filled with 3  $\mu\text{m}$  Merck ZIC-HILIC, integrating a 500 nL capacity trap-column, a 75  $\mu\text{m}$   $\times$  150 mm column, connection capillaries, and a nano-spray emitter. Solvent A was ACN/DCM/MET/H<sub>2</sub>O (60:10:10:20 v/v/v/v), containing 5 mM ammonium formate, while solvent B was ACN/DCM/H<sub>2</sub>O (80:15:5 v/v/v) containing 5 mM ammonium formate. Peptides were separated with a linear gradient of 0 – 100 % of solvent A in 30 min at a flow rate of 0.35  $\mu\text{L min}^{-1}$ . The LC effluents were introduced into the Q-TOF spectrometer by Agilent Chip Cube Interface that operated in negative mode ( $V_{\text{ap}}=1700\text{V}$ ) with nitrogen as desolvating gas at 325  $^{\circ}\text{C}$  and 4.0L/min; fragmentor, skimmer, and octapole were set at 150, 65, and 750 V, respectively. The Q-TOF operates in MS mode at 2 GHz, extend dynamic range with two reference ions (mass accuracy 5 ppm, resolution about 0.05 Da). Mass spectra were acquired in a data dependent mode: MS/MS spectra of the 5 most intense ions were acquired for each MS scan in the 140 – 1700 Da range. Scan speed was set to 3 MS spectra  $\text{s}^{-1}$  and 5 MS/MS spectra  $\text{s}^{-1}$ .

Lipids identification and quantification was performed, after conversion of the raw data in XML format, by the software LipidXplorer (Herzog et al., 2012).

### **3.4. Imaging**

#### **3.4.1. Atrophy and Hypertrophy index**

Atrophy and Hypertrophy index (AI-HI) were measured in routine hematoxylin-eosin stained muscle sections of 8 controls and 11 SBMA patients (Olympus BX60), according to Dubowitz (Dubowitz and Sewry, 2006), by using ImageJ software. We have measured the minor diameter of each fiber (almost 50 for each muscle samples), because this is not altered by oblique sectioning or kinking of the fibers, both common occurrences in muscle biopsy. Considering that normal males have a minor diameter of 40-80µm, Atrophy and Hypertrophy index were calculated giving different importance to fibers with mild or severe change in size (in males normal values AI: 0-150 ; HI: 0-500), through the following equations:

$$\begin{aligned}
 \mathbf{AI} &= (\text{n}^\circ \text{ of fibers with a minor diameter } <10\mu\text{m}) * 4 & + \\
 &(\text{n}^\circ \text{ of fibers with a minor diameter of } 10\text{-}20\mu\text{m}) * 3 & + \\
 &(\text{n}^\circ \text{ of fibers with a minor diameter of } 20\text{-}30\mu\text{m}) * 2 & + \\
 &(\text{n}^\circ \text{ of fibers with a minor diameter of } 30\text{-}40\mu\text{m}) * 1
 \end{aligned}$$

$$\begin{aligned}
 \mathbf{HI} &= (\text{n}^\circ \text{ of fibers with a minor diameter of } 80\text{-}90\mu\text{m}) * 4 & + \\
 &(\text{n}^\circ \text{ of fibers with a minor diameter of } 90\text{-}100\mu\text{m}) * 3 & + \\
 &(\text{n}^\circ \text{ of fibers with a minor diameter of } 100\text{-}110\mu\text{m}) * 2 & + \\
 &(\text{n}^\circ \text{ of fibers with a minor diameter } >110\mu\text{m}) * 1
 \end{aligned}$$

#### **3.4.2. Histoenzymatic NADH-DH assay**

For the histoenzymatic NADH-DH mitochondrial assay, frozen 8 µm cryosections of 5 controls and 6 SBMA patients were brought to room temperature and then incubated for 40 min at 37°C with the NADH incubation mixture. The NADH solution consisted of 25 ml of 0.2 M TRIS/HCl buffer pH 7.4, 25 ml of distilled water, 25 mg of nitro-blue tetrazolium (NBT) (Sigma N-6876) and 20 mg NADH (Sigma N-8129). Percentage of dark blue Area for field was calculated in NADH-DH stained sections (Olympus BX60) by using ImageJ software, measuring the number of pixel for field with a dark blue staining. The used procedure divided the image into objects and background by taking an initial threshold. Then the averages of the pixels at or below the threshold and pixels above were computed. The averages of those two values were computed, the threshold

is incremented and the process was repeated until the threshold is larger than the composite average. The used formula is:

$$\text{threshold} = (\text{average background} + \text{average objects})/2$$

After, number of pixel for field with a value above threshold was measured.

### **3.4.3. Immunofluorescence**

For immunofluorescence (IF), muscle 8  $\mu\text{m}$  cryosections were collected on Superfrost slides, fixed with 4% paraformaldehyde (PFA), treated with 0.5% Triton-X-100, incubated in blocking solution (10% Fetal Bovine Serum in PBS) for 30 min and then incubated overnight at 4 °C with primary antibodies to rabbit LC3 (Cell Signaling, polyclonal, #2775, 1:200) and to mouse ATP5A (Abcam, monoclonal, ab110273, 1:200) in 10% FBS+PBS. Each primary antibody was sequentially incubated at 4 °C in separately overnight sections. After incubation with the first primary antibody (LC3), the appropriate secondary fluorescent antibody (Alexa-Fluor-488, Invitrogen) was used for 1 h at room temperature. Next, muscle cryosections were washed in PBS, incubated again in blocking solution for 30 min and incubated overnight at 4 °C with ATP5A. The appropriate secondary fluorescent antibody (Alexa-Fluor-647, Invitrogen) was used for 1 h at room temperature. Slides were mounted using Vectashield medium with DAPI stain (Vector) and examined on a confocal microscope (Leica TCS SP5). In the z-axis stacks acquired, each image was separated by 0.5  $\mu\text{m}$  along the z-axis. By using Fiji program, the number of object-voxel was analysed in each green and red slide of the z-stack. A voxels (volumetric pixel or, more precisely, volumetric picture element) is an element of volume that represents a value of signal intensity or colour in a three dimensional space, similarly to pixel that represents a data in two-dimensional images. Considering the autophagosome diameter about 1 $\mu\text{m}$ , were kept only the element-object with that size or greater, expressed in voxel. To evaluate the LC3-ATPase colocalization signal, we used the following formula, measuring the distance between two objects:  $\sqrt{(x_1 - x_2)^2 + (y_1 - y_2)^2 + (z_1 - z_2)^2}$  and were considered colocalized objects only when the green (LC3-autophagosome) was bigger than the red one (ATPase-mitochondria).

### **3.5. Statistical analysis**

Data were expressed as mean values  $\pm$  SE. Differences between groups were assessed using analysis of variance (Student's *t*-test) and linear regression analysis. We considered a *p*-value  $<0.05$  to be significant.

## *4. Results*

#### 4.1. Normal polyQ AR transcript and abnormal protein levels and distribution in SBMA muscle tissue

We determined for the first time expression, protein levels and distribution of polyglutamine-expanded androgen receptor (polyQ AR) in muscle samples of seven SBMA and seven age matched control subjects, by RT-PCR and WB. PolyQ AR protein levels were significantly decreased of 60% of control in SBMA total muscular lysates (Fig. 4.1A,B). The higher molecular weight of mutant polyQ AR validated the analyzed bands (Fig. 4.1A,B). The normal transcript levels of *AR* in SBMA muscle indicated that this reduction was not due to a lower expression of the *polyQ AR* gene, as shown in figure 4.1C. Next the cytosolic and nuclear fractions of the same muscle samples were separated (see material and methods, section 3.3.2) and immunoblotted against AR, the cytosolic marker  $\beta$ -tubulin and the nuclear marker poly (ADP-ribose) polymerase-1 (PARP-1, also designated PARP). In SBMA cytosolic fraction, polyQ AR protein levels were significantly reduced of 60% of controls, as found in total lysate. On the contrary, in SBMA nuclei we found a significant twofold accumulation of the mutated receptor (Fig. 4.1A,B); this result is in line with the reported PolyQ AR increase in nuclei of SBMA primary differentiated myotubes (Malena et al., 2013). Interesting this accumulation was inversely correlated with the age at biopsy of the patients (Fig. 4.1D). To validate these data, we quantified the purity of the nuclear extract by WB, evaluating the nuclear enrichment as ratio between PARP (nuclear marker) and  $\beta$ -tubulin (cytosolic marker) in total lysate, cytosolic and nuclear fractions from muscle samples of two SBMA subjects and one control. As shown in figure 4.2, this procedure yielded six-fold enrichment of nuclear fraction compare to total lysate and cytosol, indicating a good purification of nuclei.



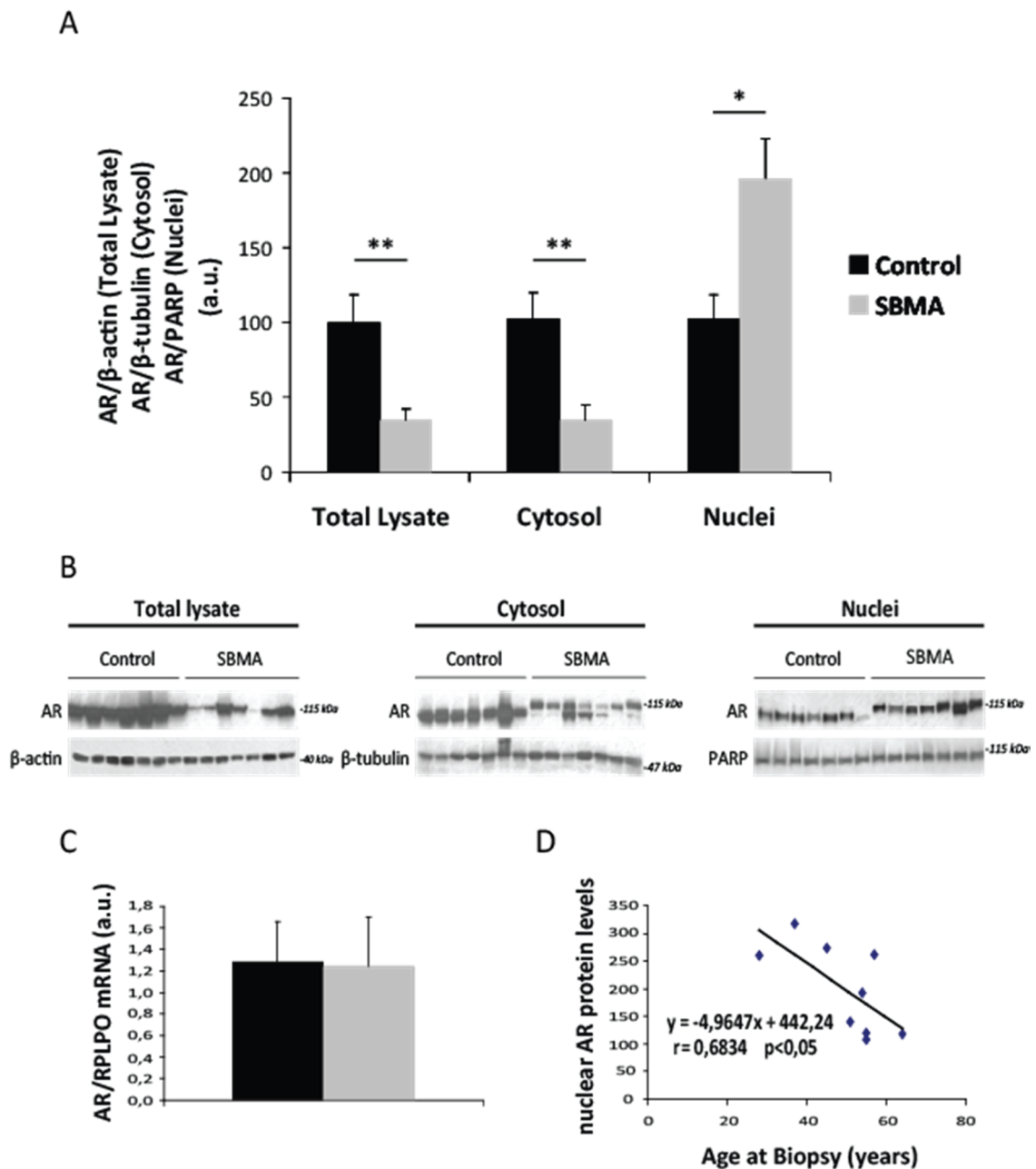


**Figure 4.1. Expression, protein levels and distribution of androgen receptor (AR) in muscle tissue from SBMA and control subjects.** **A, B** Representative WB analysis of AR in muscle total lysate, cytosolic and nuclear fractions from muscle samples of seven SBMA patients and seven controls.  $\beta$ -actin,  $\beta$ -tubulin and PARP protein levels were used as loading control in total lysate, cytosolic and nuclear fractions, respectively. Values expressed as mean  $\pm$  SE of at least three independent experiments. **C**, Normal AR expression. The values expressed as ratio between AR and housekeeping large ribosomal protein (RPLPO) mRNA. The data given as mean  $\pm$  SE of two independent experiments of RT-PCR (carried out in triplicate). **D**, Significant inverse correlation between nuclear PolyQ AR protein levels and SBMA patient's age at biopsy. Significance by Student *t* test: \* $p < 0.05$ , \*\* $p < 0.01$ .

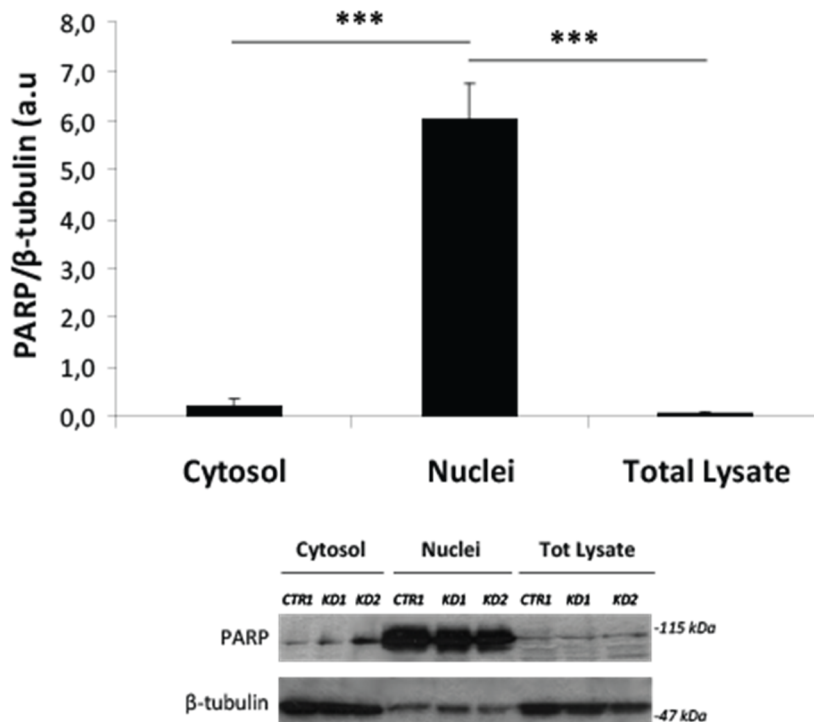


**Figure 4.2. Purity of nuclear extract.** WB analysis of PARP (nuclear), and β-tubulin (cytosolic marker), in cytosolic fraction (cytosol), nuclear fraction (nuclei) and total lysate from two SBMA patients and one control muscle samples. Nuclear enrichment, evaluated as ratio between PARP and β-tubulin protein amount. Values expressed as mean ± SE. \*\*\*p < 0.001 by Student's t test.

## 4.2. Reduction of mitochondrial abundance in SBMA muscle tissue

To investigate if the abnormal distribution of polyQ AR was associated to altered mitochondrial parameters, we firstly evaluated the mitochondrial mass by molecular, biochemical and morphological assays. Mitochondrial DNA (mtDNA) copy number, index of mitochondrial abundance, assayed by RT-PCR, resulted significantly reduced of about 40% in SBMA muscle tissue compare to controls (Fig. 4.3A). Next, activities of respiratory chain complexes (OXPHOS) were quantified with a single-wavelength, temperature-controlled spectrophotometer, following the reaction of the single enzymes at 37 °C for a few minutes. The enzymatic activities for each mitochondrial enzyme were expressed as  $\text{nmol min}^{-1} \text{mg}^{-1}$  of protein and then normalized to the activity of Citrate synthase (CS), a mitochondrial matrix enzyme, used as marker of the abundance

of mitochondria within a tissue/cell. Similar to mtDNA copy number data, CS and OXPHOS (data not shown) activities significantly decreased of 35% in SBMA muscle compare to control (Fig. 4.3B). However OXPHOS rates, when normalised to CS, were normal (Fig. 4.3E). All together these results indicated that SBMA muscle had a diminished amount of well-functioning mitochondria. The decreased mitochondrial mass in SBMA muscle was further corroborated by Nicotinamide adenine dinucleotide (NADH) staining in cryosections of muscle quadriceps femoris. Mitochondrial mass was assessed in images, captured by the microscope Olympus BX60, and expressed as percentage-of-Dark-Blue-(NADH positive)-Area-for-field by using ImageJ software (see material and methods, section 3.4.2). Consistent with the previous results, also imaging analysis demonstrated a significant reduction of the mitochondrial amount of 48% in SBMA muscle compare to controls (Fig. 4.3C). Moreover, NADH histoenzymatic staining revealed an abnormal mitochondrial distribution in SBMA muscle. In fact the fibers were: (i) intensely stained only in the periphery and/or (ii) with the central area devoid of mitochondria and/or (iii) moth-eaten fibers. At difference, control fibers showed an homogeneous NADH staining (Fig. 4.3D). In conclusion in SBMA muscle three different analysis (molecular, biochemical and morphological) showed a decreased mitochondrial network, with normal OXPHOS activity.

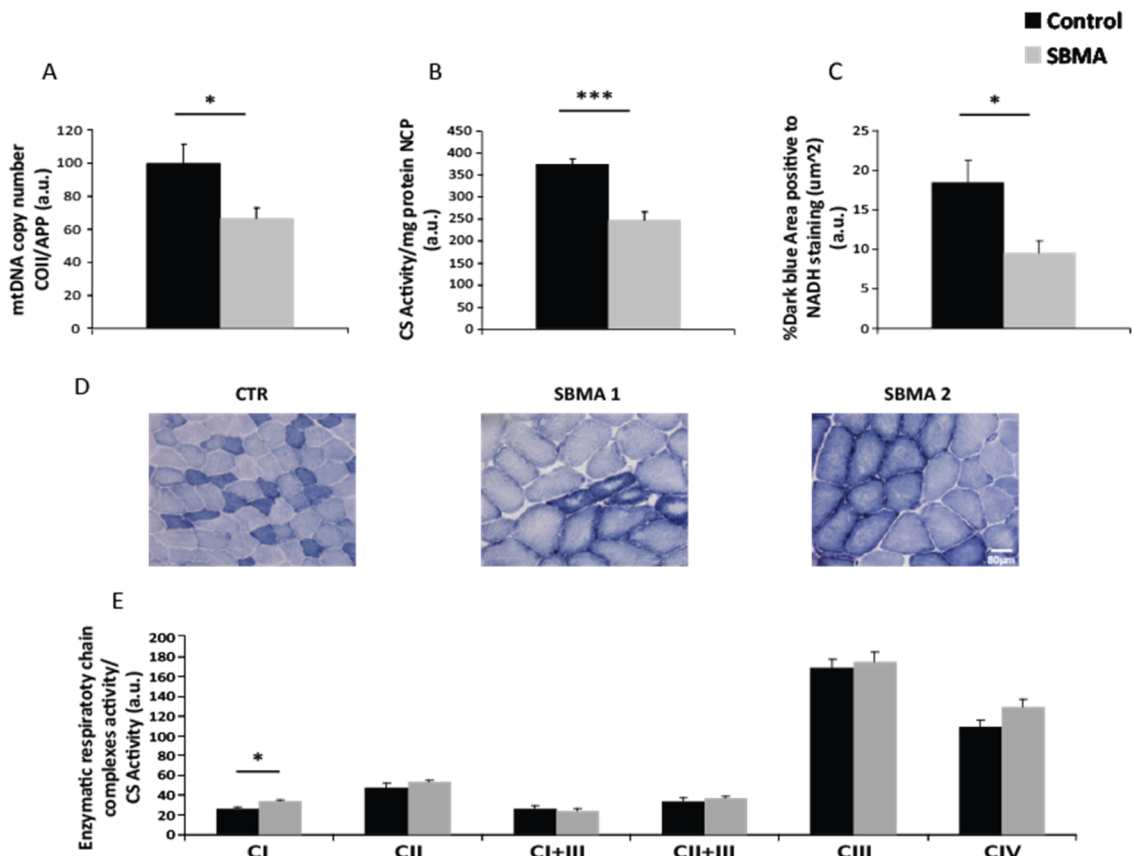


**Figure 4.3. Reduction of normal functional mitochondria in muscle tissue from SBMA patients.** **A**, mtDNA copy number, determined by RT-PCR in muscle of 13 SBMA and 14 control subjects, was expressed as ratio of mitochondrial *cytochrome c oxidase II* gene (*COII*) amplification with nuclear *amyloid precursor protein* gene (*APP*). The data expressed as mean  $\pm$  SE of three independent experiments (carried out in triplicate). The values were given as arbitrary units (a.u.). **B**, Citrate synthase (CS) activity, expressed as  $\text{nmol min}^{-1} \text{mg}^{-1}$  of protein, determined in 6 SBMA and 4 controls muscle. **C**, Mitochondrial mass expressed as percentage-of-Dark-Blue-Area in NADH stained muscle cross sections of 6 SBMA and 5 control subjects. **D**, Representative NADH staining in control and SBMA subjects. **E**, Activity of the Respiratory Chain complexes I–IV normalized to the CS activity. Scale bar 80  $\mu\text{m}$ . \* $p < 0.05$ , \*\*\* $p < 0.001$  by Student's t test.

### 4.3. Normal mitochondrial biogenesis in SBMA muscle tissue

It is known that expression of *polyQ AR* leads to transcription dysregulations (Suzuki et al., 2009; Halievski et al., 2014; Irvine et al., 2000; Todd et al., 2015). Altered gene expression is a consequence of sequestration of transcription factors and co-regulators or altered chromatin remodeling (Sugars and Rubinsztein, 2003; Minamiyama et al.,

2004; Sopher et al., 2004; Katsuno et al., 2010). To investigate if the reduction of mitochondrial mass was due to dysregulation of genes related to mitochondrial biogenesis and function, transcript levels of *peroxisome proliferator-activated receptor-gamma coactivator 1 alpha* and *1 beta* (*PGC-1 $\alpha$*  and *PGC1- $\beta$* ), *transcription factor A mitochondrial* (*TFAM*), *estrogen-related receptor alpha* (*ERR $\alpha$* ), *nuclear respiratory factor 1* (*NRF1*), *cytochrome c oxidase 4* (*COX4*), *manganese-dependent superoxide dismutase* (*MnSOD*) and *mitofusin 1* and *2* (*MFN1* and *MNF2*), were assessed by RT-PCR. As shown in figure 4.4A, no altered expression levels were found in 14 SBMA muscle compare to 18 controls. PolyQ AR can also influence cellular homeostasis directly interacting and sequestering proteins, preventing them to carry out their functions (Beauchemin et al., 2001). For this reason, the protein amount of NRF1, COX4 and MFNs was evaluated and found unaffected by PolyQ AR in 13 SBMA muscle (Fig. 4.4B) compare to 14 controls.

In conclusion, at difference of SBMA knock-in mice (Ranganathan et al., 2009), in SBMA muscle tissue the reduction of mitochondrial abundance, was not due to an impaired mitochondrial biogenesis.

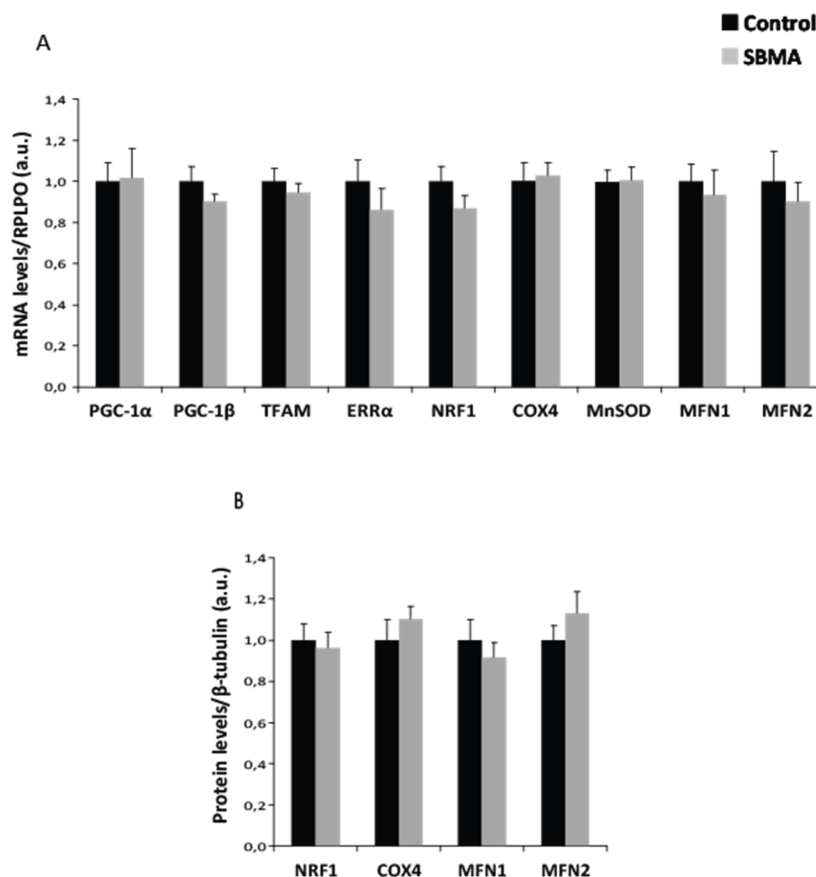


**Figure 4.4. Normal mitochondrial biogenesis in muscle tissue from SBMA patients.** **A**, RT-PCR analysis of the transcript levels and **B**, WB analysis of protein levels of genes involved in mitochondrial biogenesis, normalized to *large ribosomal protein (RPLPO)* and to  $\beta$ -tubulin, respectively, in SBMA and control muscle tissues. Data expressed as mean  $\pm$  SE of two independent experiments of RT-PCR (carried out in triplicate) and of three WB analysis ask to Prof. Aaron P. Russell of Deakin University.

#### **4.4. No correlation between Atrophy (AI) – Hypertrophy (HI) index and mtDNA copy number in SBMA muscle tissue.**

It is known in literature that muscle biopsies from SBMA patients show both signs of neurogenic atrophy, such as type I and II fibers aggregation, target fibers, atrophic fibers and subsarcolemmal nuclei clumping, and myopathic abnormalities, such as a wide variability in fibers size (4-200 $\mu$ m), hypertrophic fibers, spread basophilic fibers and necrotic fibers with central nuclei (Soraru et al., 2008). We hypothesized that processes that lead to muscle atrophy and/or hypertrophy could be involved in the reduction of

mtDNA copy number. For these reason, we evaluated atrophy (AI) and hypertrophy (HI) index in cross sections of quadriceps femoris stained for hematoxylin and eosin (EE) from eleven SBMA patients and eight controls (Fig. 4.5A,B), as previously described (Dubowitz and Sewry, 2006). Figure 4.5A show the huge AI and HI found in most SBMA muscle biopsies (7/11), determined as described in material and methods, section 3.4.1. However, we did not find correlation between the reduction of mtDNA copy number and atrophy or hypertrophy values, suggesting that atrophic and/or hypertrophic processes are not involved in reduction of mitochondrial mass (Fig. 4.5C).

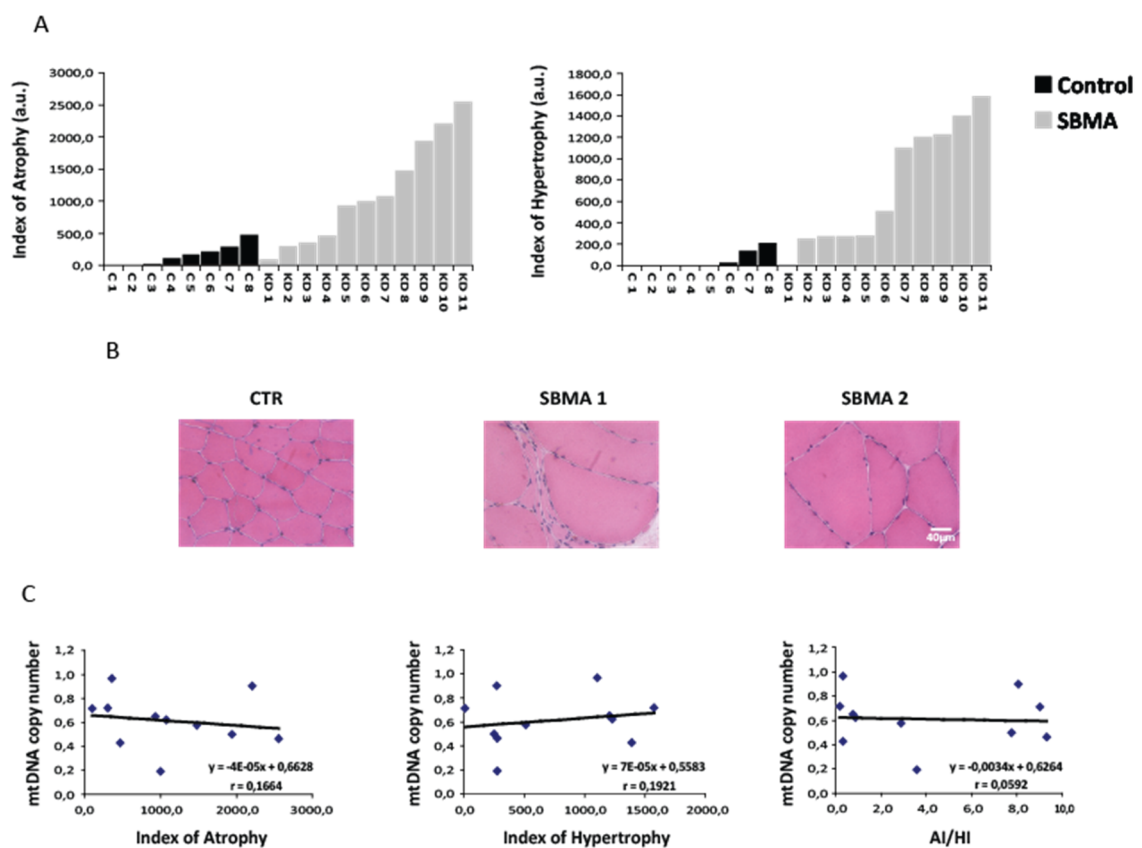


**Figure 4.5. Fiber size analysis and correlation with mtDNA copy number in SBMA muscle tissue.** A, Histograms showing the values of Atrophy (AI) and Hypertrophy (HI) Index in eleven SBMA and eight control subjects. The values, quantified as described in material and methods section 3.4.1, are expressed as arbitrary units (a.u.). B, Representative images of hematoxylin-eosin stained cryosections of control and SBMA muscle tissue, showing the wide variability in SBMA muscle fiber size. Scale bar 40 µm. C, No significant correlation between mtDNA copy number and AI, HI and AI/Hi ratio, assessed in eleven SBMA muscle biopsies.

#### 4.5. Increased autophagy in human SBMA muscle tissue

Since the reduction of mitochondrial mass (Fig. 4.3) is neither due to an impaired mitochondrial biogenesis (Fig. 4.4), nor to atrophy-hypertrophy related processes (Fig. 4.5), we asked if it was associated to an increased degradation of these organelles. In the cell, the removal of damaged or superfluous subcellular organelles can take place through autophagy (Gomes and Scorrano, 2013; Youle and Narendra, 2011) (see introduction, section 1.9, for details). For this reason, we evaluated the transcript and protein levels of genes involved in autophagic process (*LC3*, *Beclin-1*) and lysosomal biogenesis (*LAMP1*, *LAMP2B*) by RT-PCR and WB analysis, normalized respectively to *large ribosomal protein (RPLPO)* and  $\beta$ -actin. The expression levels of *microtubule-associated protein 1A/1B-light chain 3 (LC3)* and *Beclin-1* and *lysosomal-associated membrane protein 1 and 2B (LAMP1 and LAMP2B)* were normal (Fig. 4.6A) in respectively 20 and 6 SBMA muscle compare to 10 and 4 controls. On the contrary, the protein levels of the lipidated form of LC3 (LC3-II) and Beclin-1 were significantly increased respectively by 49% and 174% in the muscle tissue from 10 SBMA patients compare to 5 controls (Fig. 4.6B,C) and the protein levels of LAMP1 was significantly increased by 529% in the muscle tissue from 9 SBMA patients compare to 9 controls.

To further confirm these data, we performed an immunohistochemical assay, by using antibody against LC3, to mark autophagosomes (Fig. 4.6D). Images were obtained by using a confocal microscope (Leica TCS SP5). The number of autophagosomes/fiber, expressed as puncta/fiber, was measured as number of positive green objects by using a dedicated software (program Fiji), as described in material and methods section 3.4.3. Consistently, we found that the number of autophagosomes/fiber was about 205% greater in the muscle tissue from 11 SBMA patients compare to 10 controls (Fig. 4.6E). This increase was not correlated with the number of CAG repeats present in the N-term domain of AR (Fig. 4.7A). Furthermore, no correlation was found with the age at biopsy of patients (Fig. 4.7B).

In conclusion both the biochemical and morphological assays indicated an increased autophagic process in SBMA muscle tissue.



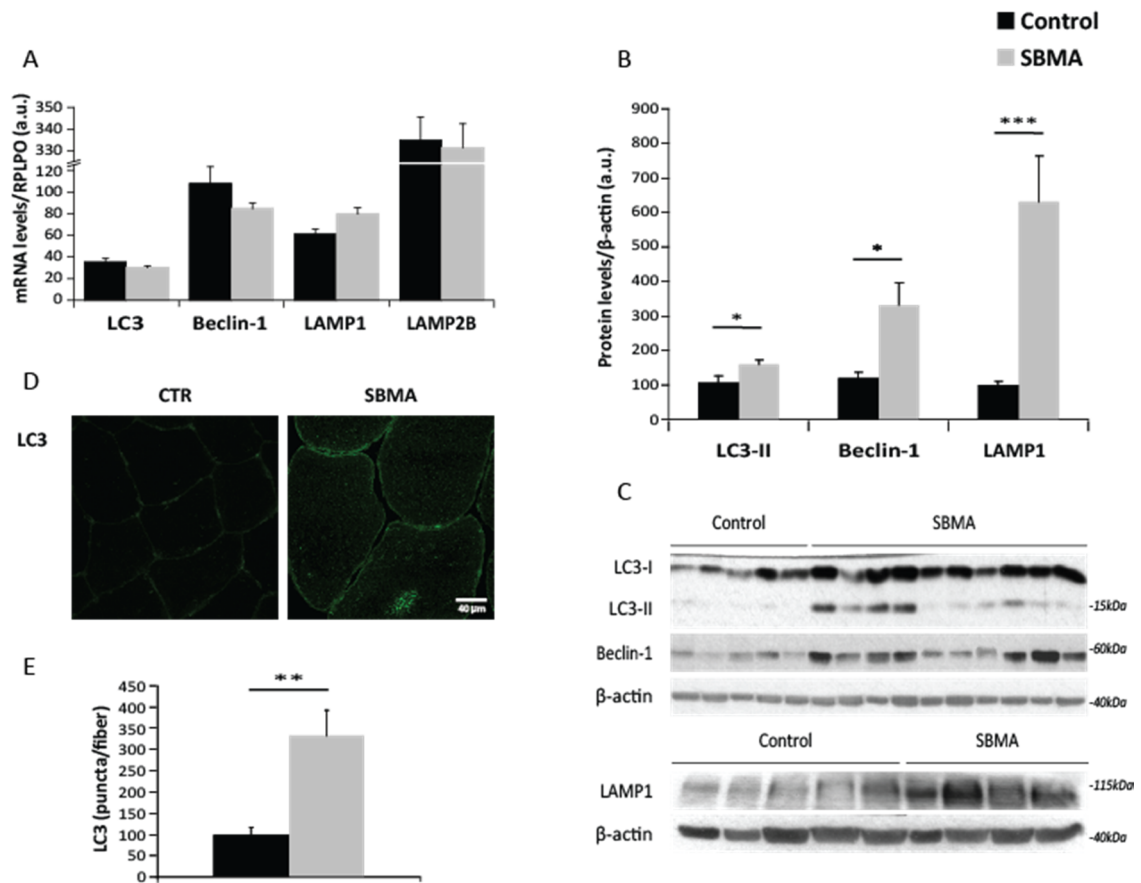


**Figure 4.6. Increased autophagy in SBMA muscle tissue.** **A**, RT-PCR analysis of the transcript levels and **B**, **C** WB analysis of the protein levels of genes involved in autophagy normalized respectively to *RPLPO* and  $\beta$ -actin. The data are expressed as mean  $\pm$  SE of two independent experiments of RT-PCR (carried out in triplicate) and three WB analysis. **D**, Representative images of anti-LC3 immunostaining of control and SBMA muscle tissue. **E**, Immunofluorescence assay of muscle cryosections from eleven patients and ten controls was performed, by using antibody against LC3, to mark autophagosomes. The number of autophagosomes for fiber was measured as number of green object- for fiber (puncta/fiber) by using dedicated Fiji software. The data, expressed as mean  $\pm$  SE of almost 50 fibers, were scored for each analyzed muscle sample. Scale bar 40  $\mu$ m. \* $p < 0.05$ , \*\* $p < 0.01$ , \*\*\* $p < 0.001$  by Student's t test.

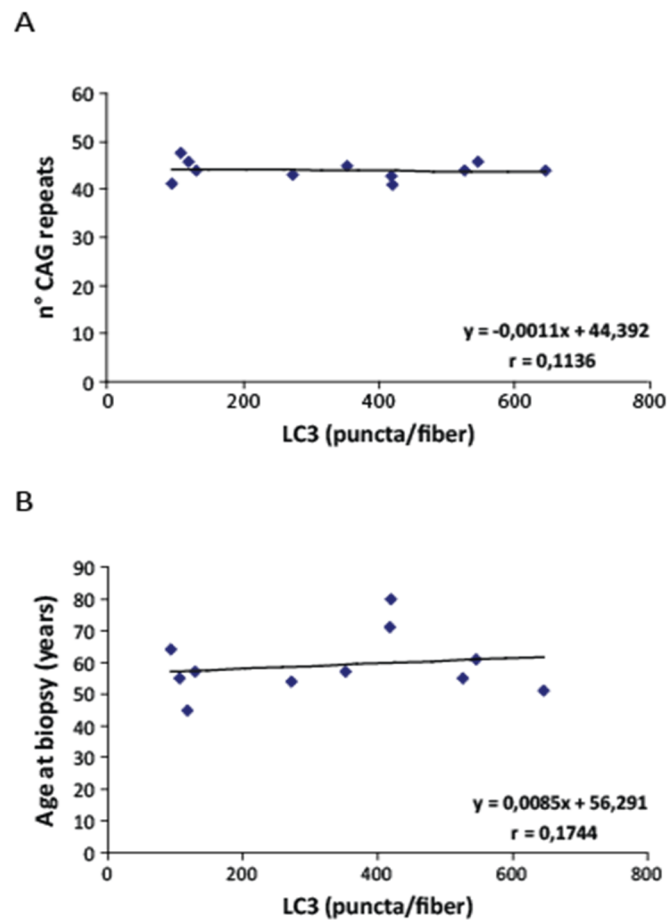


**Figure 4.7. No correlation between clinical features of SBMA patients and the increased number of autophagosomes found in the respective muscle.** No correlation between autophagosomes' number, expressed as LC3 puncta/fiber, in the muscle tissue from eleven SBMA patients and **A** the number of CAG repeats in their androgen receptor gene; **B** age at biopsy, expressed in years.

#### 4.6. Increased mitophagy in human SBMA muscle tissue

Activation of the autophagic process in the muscle tissue of SBMA patients may be related to the previously observed reduction of mitochondrial mass. The removal of mitochondria in cells takes place through two types of autophagy: non selective and selective autophagy. *Non selective autophagy* occurs on nutrient deprivation to supply cells with essential metabolic building-blocks and energy, until nutrients can once again be obtained from the extracellular environment. *Selective-cargo-specific autophagy or mitophagy* occurs under nutrient-rich conditions to mediate the removal of superfluous or damaged organelles that otherwise could be harmful and/or toxic. Mitophagy has a

mechanistically separate induction and regulation from non-selective autophagy. PTEN Induced Putative Kinase 1 (PINK1), Parkin and BCL2/Adenovirus E1B 19kDa Interacting Protein 3 (BNIP3) are the major players of the mitophagic process (Ding and Yin, 2012; Ashrafi and Schwarz, 2013), together with the mitochondrial recruitment of the effector proteins LC3 and p62 (Gomes and Scorrano, 2013; Novak, 2012). Therefore, we wanted to test whether there was an increase of the mitophagic process in SBMA muscle, that could explain the mitochondrial reduction in SBMA muscle (Fig. 4.3). With this aim in mind, we performed molecular, biochemical and morphological assays, focused to mitophagic parameters.

Biochemically mitophagy was estimated by monitoring the recruitment of sequestosome 1/p62 (SQSTM1/p62), PINK1, Parkin, BNIP3 and ubiquitin on isolated mitochondria of five SBMA and five control muscle by WB analysis.

We quantified the purity of the mitochondrial extract by WB, evaluating the mitochondrial enrichment as ratio between TOM20 (mitochondrial marker) and  $\beta$ -tubulin (cytosolic marker) in total lysate and isolated mitochondria of two SBMA and two control muscle samples. As shown in figure 4.10, this procedure yielded eight-fold enrichment of mitochondrial fraction compare to total lysate, indicating a good purification of mitochondria.

The mitochondrial protein levels of PINK1 (mtPINK), BNIP3 (mtBNIP3) and ubiquitin (mtUbiq) from 5 SBMA muscle were significantly increased respectively by 338%, 187% and 200% compare to 5 control samples (Fig. 4.8B,C,D). These data were suggestive of an enhanced mitophagic process in SBMA muscle tissue. However, Parkin mitochondrial protein levels were not increased (Fig. 4.9B), suggesting the involvement of other E3 ligases, that target SBMA mitochondria to autophagosomes via ubiquitination (Ashrafi and Schwarz, 2013). Another possibility is the presence of Parkin muscle specific isoform(s), recognized by other specific antibodies (La Cognata et al., 2014; Scuderi et al., 2014). Also p62 protein levels in isolated mitochondria from SBMA patients resulted similar to controls. These data may be due either to absence of blocks-impairments in SBMA autophagic flux or to the involvement of other adaptor proteins in the mitophagic process in muscle (Fig. 4.9B).

The expression levels of *BNIP3*, *PINK1*, *Parkin* and *p62* were normal in 20 SBMA compare to 10 control muscle samples (Figs. 4.8A, 4.9A), indicating that their transcription was not influenced by PolyQ AR.

To further confirm the increased mitophagy observed by WB analysis, we performed an immunohistochemical assay on quadriceps femoris cryosections from eleven SBMA patients and ten controls, using antibody against LC3 (green), to mark autophagosomes, and antibody against ATPase (red), to mark mitochondria (Fig. 4.8E). This morphological method quantified mitophagy as number of autophagosomes that colocalized with mitochondria (yellow), measured with Fiji program and expressed as number of yellow puncta/fiber (see material and methods, section 3.4.3). In line with the WB data, we found that the autophagosomes-mitochondria colocalization was significantly 3,5 increased in SBMA muscle tissue compared to controls (Fig. 4.8F). These data confirmed that in SBMA but not in control muscle many mitochondria were trapped in autophagosomes and successively degraded through the autophagic machinery. Interesting, we had a visual impression of this phenomenon in some SBMA muscle fibers, where we observed area devoid of mitochondria and rich in autophagic vacuoles, indicating a mitophagic process that led to removal of mitochondria (Fig. 4.8E). Increased mitophagy, in SBMA patients, was neither correlate with the number of CAG repeats present in the N-term domain of polyQ *AR* gene (Fig. 4.11A) nor with their age at biopsy (Fig. 4.11B). In summary both biochemical and morphological analysis confirmed an augmented mitophagy in SBMA muscle that explained the previously observed reduction of mitochondrial mass. Furthermore the activation of BNIP3 and PINK1 mediated mitophagy suggested the presence of latent mitochondrial alterations, able to recruit auto-mitophagic apparatus.

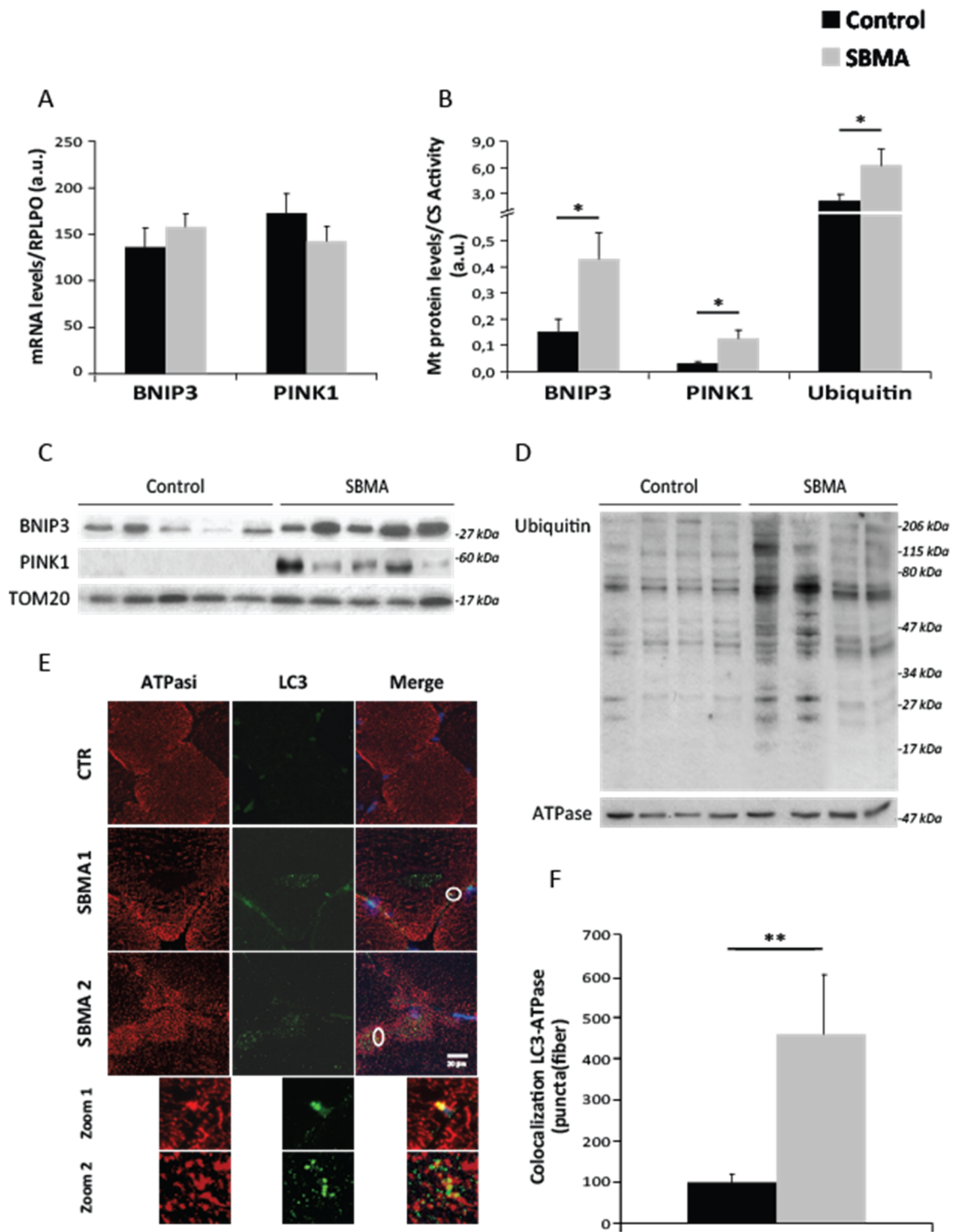


**Figure 4.8. Increased mitophagy in SBMA muscle tissue.** A, RT-PCR analysis of *BNIP3* and *PINK1* transcript levels in 20 SBMA and 10 control muscle samples. Data, normalized to *RPLPO*, are expressed as mean  $\pm$  SE of two independent RT-PCR experiments (carried out in triplicate). B, C, D WB analysis of BNIP3 (mtBNIP3), PINK1 (mtPINK1) and ubiquitin (mtUbiquitin) protein levels in muscle isolated mitochondria from 5 SBMA patients and 5 controls, normalized to CS activity. Data are expressed as mean  $\pm$  SE of three independent WB experiments. Membranes were immunoblotted against TOM20 and

ATPase, as mitochondrial loading controls. **E**, Representative images of anti-LC3 (green) and anti-ATPase (red) immunostaining of control and SBMA muscle tissue. Zoom: magnification of the marked areas. **F**, Number of colocalized autophagosome-mitochondria (yellow puncta), measured as number of yellow puncta/fiber in 11 SBMA and 10 controls. The data are expressed as mean  $\pm$  SE. Almost 50 fibers were scored in each analyzed muscle sample. Scale bar 20  $\mu$ m. \* $p < 0.05$ , \*\* $p < 0.01$  by Student's t test.

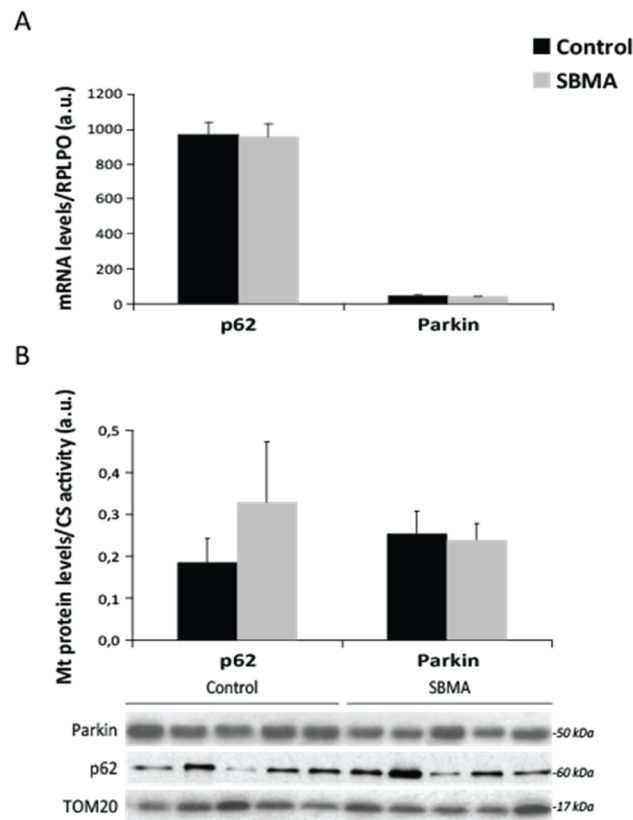


**Figure 4.9. p62 and Parkin expression and mitochondrial protein levels in SBMA and control muscle.** **A**, RT-PCR analysis of *p62* and *Parkin* transcript levels in 20 SBMA and 10 control muscle samples. Data, normalized to *RPLPO*, expressed as mean  $\pm$  SE of two independent RT-PCR experiments (carried out in triplicate). **B**, WB analysis of p62 (mtp62) and Parkin (mtParkin) protein levels in muscle isolated mitochondria from 5 SBMA patients and 5 controls, normalized to CS activity. Data are expressed as mean  $\pm$  SE of three WB independent experiments. Membranes were immunoblotted against TOM20 and ATPase, as mitochondrial loading controls

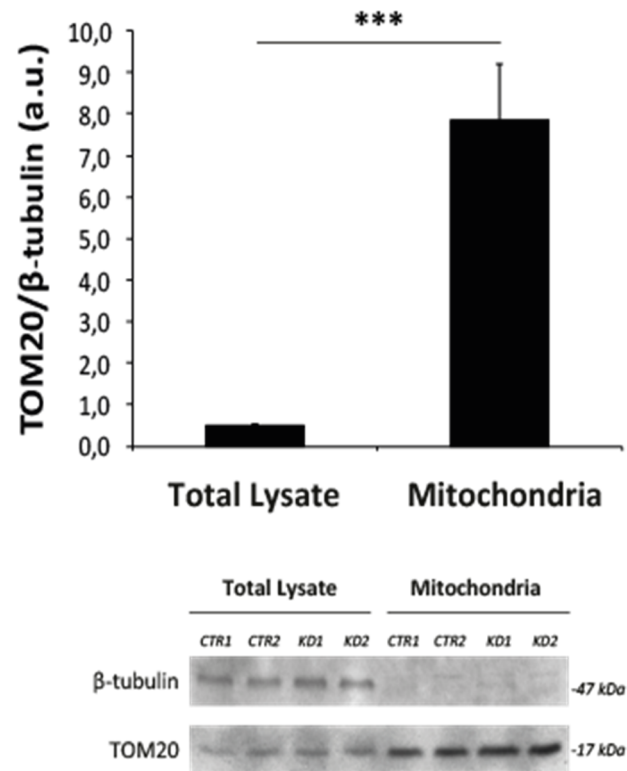


**Figure 4.10. Purity of mitochondrial extract.** Representative WB analysis of TOM20 (mitochondrial) and  $\beta$ -tubulin (cytosolic marker) in muscle total lysate and isolated mitochondria from two SBMA patients and two control samples. Mitochondrial purification, evaluated as ratio between TOM20 and  $\beta$ -tubulin protein amount. The graph represents the mean  $\pm$  SE. \*\*\* $p < 0.001$  by Student's t test.

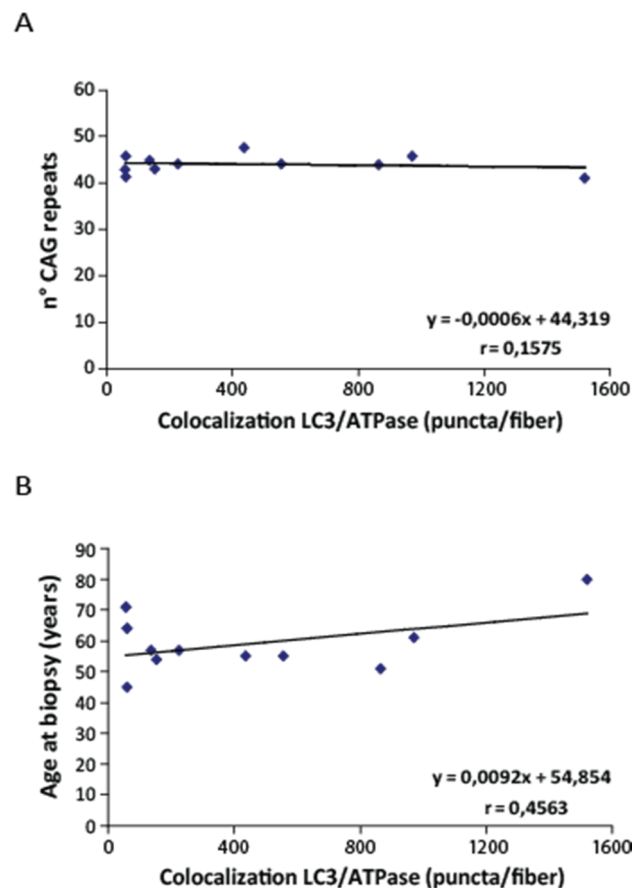


**Figure 4.11. Absence of correlation between clinical features of SBMA patients and the increased mitophagy found in their respective muscle.** **A**, Linear regression analysis between mitophagy, expressed as mitochondria-autophagosomes colocalization signal (puncta/fiber), and the number of CAG repeats in AR gene from the respective muscle tissue of eleven SBMA patients. **B**, Linear regression analysis between mitophagy, expressed as mitochondria-autophagosomes colocalization signal (puncta/fiber), and age at biopsy of eleven patients.

#### 4.7. Increased fission in the muscle tissue from SBMA patients

Accumulating evidences emphasize the requirement of mitochondrial fragmentation (fission) prior to mitophagy (Gomes and Scorrano, 2013; Youle and Narendra, 2011). Fission divides elongated mitochondria into pieces of manageable size, that can be engulfed by autophagosomes and then degraded into lysosome. For this reason, we evaluated mRNA and protein content of the main actors of the mitochondrial fragmentation process: Drp1 and hFis1. The expression levels of both were normal in



the muscle from four SBMA patients compare to four controls (Fig. 4.12A). On the contrary, in respectively 9 and 5 SBMA muscle isolated mitochondria we found an increased protein amount of both Drp1 that hFis1 (37% and 72%, respectively), but only hFis1 values were significant higher (Fig. 4.12B) compare 9 and 4 controls. These data suggested an increase of fission events in the muscle of SBMA patients, in line with increased mitophagy, although further studies will be necessary to confirm these data.

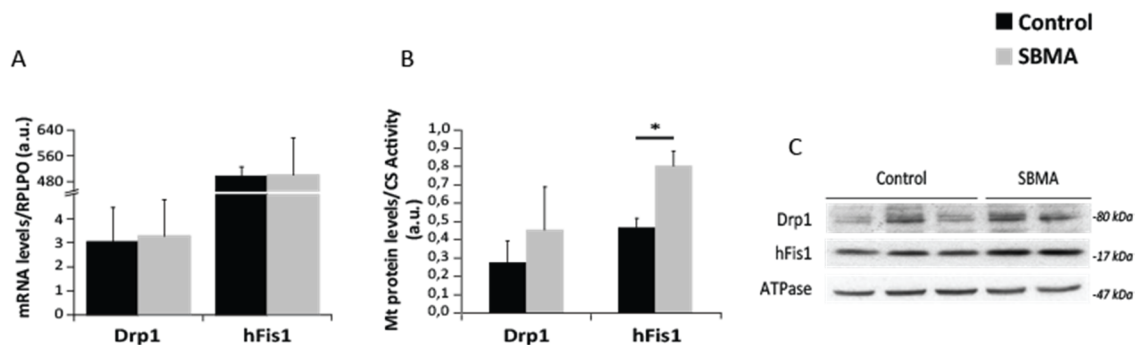


**Figure 4.12. Increased fission in SBMA muscle tissue.** A, RT-PCR analysis of *Drp1* and *hFIS1* transcript levels in SBMA and control muscle. Data, normalized to *RPLPO*, are expressed as mean  $\pm$  SE of two independent RT-PCR experiments (carried out in triplicate). B, C Representative WB analysis of Drp1 and hFis1 protein levels in isolated mitochondria from SBMA and control muscle, normalized to CS activity. Data are expressed as mean  $\pm$  SE of three independent WB experiments. Membranes were immunoblotted against ATPase, as mitochondrial loading controls. \* $p < 0.05$  by Student's t test.

#### 4.8. Reduced biosynthesis and levels of cardiolipin in SBMA muscle tissue

Previous results showed an increased mitophagy in the muscle from SBMA patients (Fig. 4.8), and suggested an underlying mitochondrial dysfunction, that could explain why mitochondria were degraded in muscle tissue, that normally needs a lot of energy for its normal function. For this reason, we evaluated the lipid composition of mitochondrial membranes by mass spectrometry in muscle isolated mitochondria from four SBMA patients and four controls. Interesting, we found that cardiolipin (CL) amount, the structural unique phospholipid of the inner mitochondrial membrane (IMM), was halved (52%) (Fig. 4.13A), in parallel with a significant increase of

phosphatidylethanolamine (PE) (149%) and of the PE- precursor- phosphatidylserine (PS) (204%) levels in SBMA muscle mitochondria compare to control (Fig. 4.13A). All together these data suggested a compensatory response to an underlying alteration in lipid mitochondrial homeostasis. However, in SBMA muscle the composition of CL was not altered (Fig. 4.13B), in fact there was an homogeneous reduction of all the CL molecular species and not of a single as observed in Barth Syndrome, characterized by the reduction of tetralinoleoyl-CL (L4-CL) ([McKenzie et al., 2006](#)). These data suggested an anomaly in the initial steps in CL synthesis. Cardiolipin synthase (CRLS1) is a key enzyme involved in the biosynthesis of immature CL (see introduction, section 1.11.1, for more details) ([Patil and Greenberg, 2013](#)). CRLS1 catalyzes an irreversible condensation reaction in which the phosphatidyl group of CDP-diacylglycerol (CDP-DAG) is linked to phosphatidylglycerol (PG). After this biosynthetic step, immature CL undergoes deacylation and remodeling, to generate the different molecular species with diverse acyl group composition. For these reasons, we hypothesized that the decreased levels of cardiolipin in SBMA mitochondrial membranes could be related to downregulation of *CRLS1* gene. Therefore, we evaluate expression levels of *CRLS1* gene by RT-PCR in muscle tissue from six control and five SBMA patients. *CRLS1* expression levels were decreased of 51% in SBMA muscle tissue compare to controls. This reduction explained the decreased CL levels in SBMA mitochondria (Fig. 4.13C). This result may represent the connection between the accumulation of polyQ AR in the nucleus of SBMA muscle and the elimination of mitochondria through the auto-mitophagic machinery.

It is known in literature that one of the most important role of cardiolipin is to stabilize some respiratory chain (RC) complexes (CI, CIII and CIV) and their super-assembling in the so called “Respirasome” ([Paradies et al., 2013](#)). So we thought that the CL reduction could create a mitochondrial damage through supercomplexes disassembling, although singularly the individual enzymes worked properly (Fig. 4.3E). For these reasons, we analyzed mitochondrial supercomplexes composition in isolated mitochondria from muscle of four controls and four SBMA patients by using a Blue Native PAGE (BN-PAGE) technique, based on a mild membrane solubilization with digitonin, that preserves the interactions between the RC complexes (see material and methods, section 3.3.7). However, we did not find any difference in the supercomplexes

amount between SBMA muscle and control (Fig. 4.13D). We can conclude that CL decreased levels affect muscle SBMA mitochondria without a valuable supercomplexes disassembling, probably for the concomitant compensatory increase of PE. In summary the present data reveal in SBMA muscle a novel relationship among PolyQ AR, mitophagy and reduced CL levels.

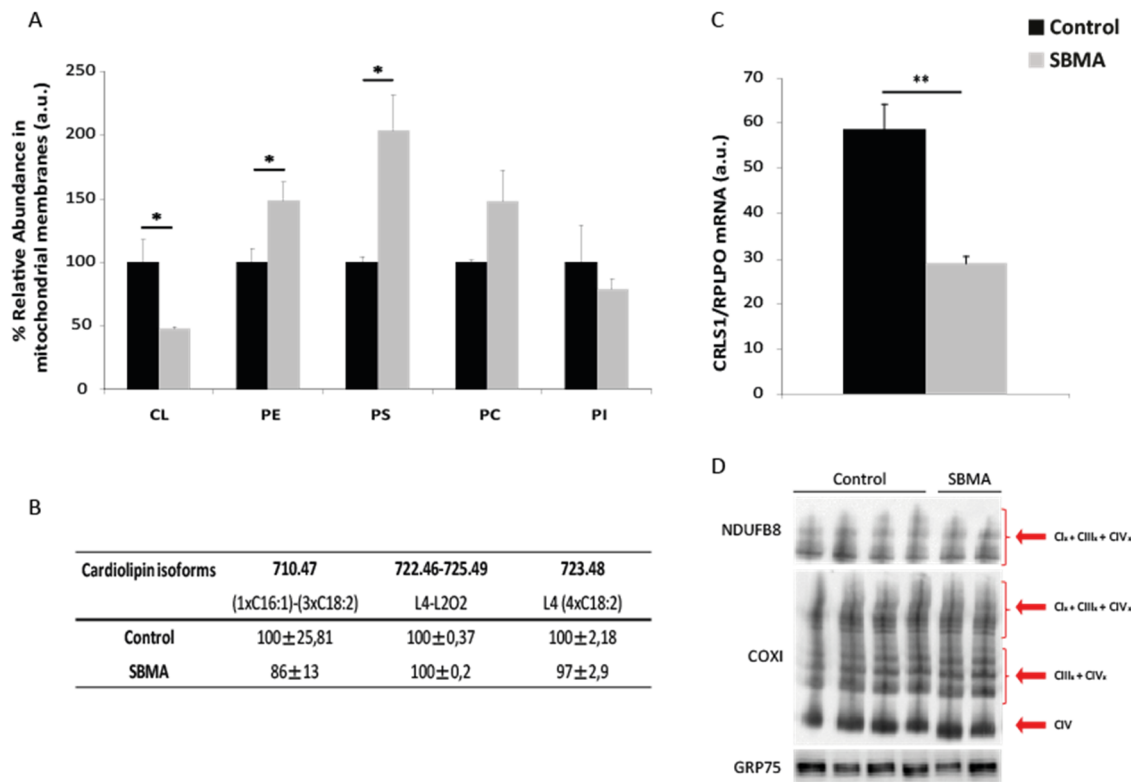


**Figure 4.13. Reduced cardiolipin level and biosynthesis in SBMA muscle tissue.** **A**, Lipid composition of mitochondrial membranes by mass spectrometry in muscular isolated mitochondria from four SBMA patients and four controls. Cardiolipin (CL), phosphatidylethanolamine (PE), phosphatidylserine (PS), phosphatidylcholine (PC) and phosphatidylinositol (PI) amount were normalized to CS activity and expressed as mean  $\pm$  SE of two independent experiment. **B**, Composition of the different CL species in control and SBMA muscle samples. **C**, Decreased transcript levels of *cardiolipin synthase* (*CRLS1*) normalized to *RPLPO* in the muscle tissue from five SBMA patients compare to six controls. The values expressed as mean  $\pm$  SE of two independent experiments of RT-PCR (carried out in triplicate). **D**, Representative Blue Native PAGE (BN-PAGE) of mitochondrial supercomplexes in muscle isolated mitochondria from four controls and four SBMA patients. Mitochondrial supercomplexes were recognized with antibody against a subunit of Complex I (NDURFB8) and of Complex IV (COXI). Antibody against GRP75, a marker of mitochondrial matrix, used as loading control. \* $p < 0.05$ , \*\* $p < 0.01$  by Student's t test.



## *5. Discussion*

Traditionally, SBMA has been viewed as a cell-autonomous, primary motor neuron disease. Recently published reports challenge the traditional view, suggesting a primary role of muscle in SBMA pathogenesis (Yu et al., 2006; Rocchi, Milioto et al., in revision; Sorarù et al., 2008; Monks et al., 2007; Palazzolo et al., 2009; Rinaldi et al., 2012; Cortes et al., 2014). *Androgen receptor (AR)* is expressed in muscle tissue, where mediates the anabolic effects of androgens. In fact, administration of androgens to hypogonadal men resulted in increased muscle strength and size, together with enhanced lean body mass and performance (Bhasin et al., 1997; Brodsky et al., 1996; Sinha-Hikim et al., 2004). It was shown that there is a loss of androgens anabolic effects in SBMA primary myotubes, in a polyQ related manner (Malena et al., 2013). This process can be especially harmful in aging, when skeletal muscle undergoes to sarcopenia (Glass et al., 2010; Sakuma and Yamaguchi, 2010; Haehling et al., 2012). However, till now a direct measure of polyQ AR expression, amount and distribution in human SBMA muscle tissue was not available.

### **5.1. Nuclear accumulation of PolyQ AR in human SBMA muscle tissue**

In the present study, for the first time we showed that there was a significant reduction of the protein amount of AR in total lysate and cytosolic fraction of SBMA muscle tissue (Fig. 4.1 A,B). It is known that *AR* gene contains AREs and that AR can regulate its expression (Grad et al., 2001). So, we hypothesized that a loss of function of PolyQ AR may led to a decrease in its expression and consequently in its protein content. However, we found normal polyQ AR transcript levels in SBMA muscle samples (Fig. 4.1C). Therefore, the cytosolic decrease of PolyQ AR could be probably due to a cellular defence carried out by the affected muscle tissue in order to eliminate the abnormal PolyQ AR proteins by ubiquitin proteasome system (UPS) or autophagic processes (Rusmini et al., 2007; Rusmini et al., 2010; Taylor et al., 2003; Pandey et al., 2007; Yu et al., 2011). Consistently, a decreased cellular amount of polyQ AR protein was found in several cells and tissues, different from muscle (Nakamura et al., 1994; Warner et al., 1992; Danek et al., 1994; Matsuura et al., 1992). A post mortem study,

carried out by Nakamura et al. (1994), showed a decreased polyQ AR protein amount (by WB) and expression levels (by RT-PCR) in the spinal cord of one SBMA patient compared to ALS and lung cancer subjects. Both Warner et al. (1992) and Danek et al. (1994) also found decreased levels of *polyQ AR* expression in genital skin fibroblasts from SBMA patients. Similarly, Matsuura et al. (1992) were not able to demonstrate AR immunoreactivity in genital skin biopsies from SBMA patients. Since some of these studies showed decreased polyQ AR transcript levels, associated to reduced protein levels, it was suggested that SBMA could be considered a loss-of-function disease.

More importantly were the increased levels of the monomeric polyQ AR soluble form in quadriceps femoris nuclei of our SBMA patients (Fig. 4.1A,B). This accumulation is inversely correlate with the age at biopsy of patients, probably due to the reduction in testosterone levels that occur in aging. Nuclear localization and accumulation of the abnormal proteins were considered to be decisive for inducing neuronal cell dysfunction and degeneration in all the polyQ diseases, i.e. spinocerebellar ataxia (Klement et al., 1998). Indeed, it was shown in several tissues and primary cells that one of the main pathophysiological processes of SBMA disease is the accumulation of polyQ AR in nuclei both in a diffusible form and/or in nuclear inclusions (NIs) (Adachi et al., 2005, Li et al., 1998; Banno et al., 2006; Malena et al., 2013). Consistently, increased nuclear polyQ AR levels were found in SBMA primary differentiated human myotubes, but not in proliferating primary myoblasts, indicating that the process of differentiation of SBMA myoblasts to myotubes is associated with an abnormal accumulation of polyQ AR (Malena et al., 2013). An immunohistochemical study on autopsies of SBMA patients showed that diffuse nuclear accumulation of the polyglutamine-expanded AR was more frequently observed than NIs in the anterior horn of the spinal cord and was correlated to the length of the CAG repeat in *AR* gene (Adachi et al., 2005). Furthermore, it was shown that NIs are likely formed as a result of cellular defence reactions coping with the pathogenic polyglutamine protein (Taylor et al., 2003).

In conclusion, for the first time, we demonstrated accumulation of monomeric polyQ AR in skeletal muscle nuclei from SBMA patients, indicating muscle primary involvement in SBMA pathogenesis.

## 5.2. Decreased mitochondrial mass in human SBMA muscle tissue

The myopathic component of SBMA can be mitochondrial. Accumulating evidences suggest that polyQ AR interferes with mitochondria either indirectly via the nucleus or cytoplasm or directly via the organelle (Ranganathan et al., 2009; Beauchemin et al., 2001; Piccioni et al., 2002; Stenoien et al., 1999; Su et al., 2010; Orsucci et al., 2014). In the nucleus down-regulation of various nuclear-DNA-encoded mitochondrial proteins (e.g. PPAR- $\gamma$ , SOD-I, SOD-II, catalase, NADH-dehydrogenase-I, TFAM) by expanded polyQ AR was observed (Ranganathan et al., 2009). In the cytoplasm co-localization of polyQ AR with various mitochondrial proteins (e.g. COXVb) was reported (Beauchemin et al., 2001). Direct affection of mitochondria with polyQ aggregates results in abnormal distribution of mitochondria (Piccioni et al., 2002; Stenoien et al., 1999), damage of mtDNA in form of mtDNA depletion or multiple mtDNA deletions (Su et al., 2010; Orsucci et al., 2014), ligand-dependent mitochondrial membrane depolarization, increase in ROS, or activation of the mitochondrial caspase pathway with increased levels of key proteins of the mitochondrial apoptosis cascade (Ranganathan et al., 2009). However, almost none of these studies were conducted in human tissues. The aim of this study was to investigate if many of these mitochondrial abnormalities were present in the muscle tissue from SBMA patients.

In this study, we demonstrated, through three different methods, that in the muscle tissue from our SBMA patients the mitochondrial mass was reduced compare to controls (Fig. 4.3). Firstly, we found a 40% reduction in mtDNA copy number in SBMA muscle tissue (Fig. 4.3A). Similarly, in leukocytes derived from SBMA patients and carriers was found a reduction in mtDNA copy number, that inversely correlated with the CAG-repeat length (Su et al., 2010). In these patients and carriers was found also an increased frequency of mtDNA4977 deletion, the most common “aging-deletion”, and a higher mtDNA  $\Delta$ CT value, a biomarker of mtDNA oxidative stress. Furthermore, multiple mtDNA deletions were detected in the skeletal muscle of a 55yo SBMA patient with exercise intolerance and hyper-CKemia ranging from 1000 to 1400 U/l (Orsucci et al., 2014). These data showed a link between polyQ AR and mtDNA damage and degradation.



The decreased mitochondrial amount was confirmed by the 40% reduction of Citrate synthase (CS) activity in total SBMA muscle homogenate (Fig. 4.3B), and by the 48% reduction of NADH positive area/field in SBMA muscle fibers (Fig. 4.3C,D). In addition, the histochemical NADH-DH staining revealed altered mitochondrial distribution and/or absence of oxidative enzyme activity in the central region of SBMA muscle fibers as previously reported in several morphological studies of muscle tissue from patients and knock-in mice (Orsucci et al., 2014; Sorarù et al., 2008; Harding et al., 1982; Sopher et al., 2004). In a 55yo SBMA patient with exercise intolerance and hyper-CKemia, muscle biopsy staining for oxidative enzymes revealed some COX-hypo-reactive fibers (Orsucci et al., 2014). In two studies of muscle specimens from SBMA patients and carriers stained for NADH-DH, lobulated fibers, moth-eaten fibers and fibers with a loss of oxidative enzyme activity in the central regions were observed (Sorarù et al., 2008; Harding et al., 1982), as well as in one study on AR-100Q transgenic mice (Sopher et al., 2004).

OXPHOS activity was normal in SBMA muscle tissue if normalized to CS activity (Fig. 4.3E). This means that in the quadriceps femoris of SBMA patients there were mitochondria that worked properly, but present in a reduced abundance compare to controls.

We found normal expression and protein levels of NRF1, COX4 and MFNs (Fig. 4.4A,B) and normal expression levels of *PGC-1 $\alpha$* , *PGC-1 $\beta$* , *TFAM* and *ERR $\alpha$*  (Fig. 4.4A). Most of these genes encode transcription factors, while others encode mitochondrial proteins. PGC-1 $\alpha$  is a coactivator, as PGC-1 $\beta$ . It interacts directly with transcriptional factors, recruits the histone acetyl transferase (HATs) and interacts with the transcriptional machinery. The expression of all genes evaluated is modulated by PGC1 $\alpha$  (Romanello and Sandri, 2012). TFAM is a mitochondrial transcription factor and therefore promotes the transcription of mitochondrial genome. Its expression is modulates also by PGC-1 $\alpha$ . Thus, our results show that reduction of mitochondrial mass in SBMA muscle tissue is not due to reduced mitochondrial biogenesis, as observed in SBMA knock-in mice (Ranganathan et al., 2009).

Subsequently, we hypothesized that muscle atrophy or hypertrophy processes could be implied in the mitochondrial mass reduction. The growth of skeletal muscle mass depends on protein and cell turnover, controlled by two different pathways (Sartorelli

and Fulco, 2004). Cellular turnover plays a major role during muscle development in embryo. Moreover, satellite cell incorporation into the growing fibers takes place during postnatal muscle growth (Moss and Leblond, 1971), concomitantly with increased protein synthesis. The activation of satellite cells is important for maintaining a constant size of each nuclear domain (quantity of cytoplasm/number of nuclei). Unlike young muscle, the contribution of cellular turnover to homeostasis of adult fibers is minor (Rehfeldt et al., 2007). In adult muscle, tissue growth take place by increasing protein synthesis and decreasing protein degradation. Whereas satellite cells are activated in compensatory hypertrophy (Schiaffino et al., 1976). On the contrary, atrophy is a decrease in cell size mainly caused by loss of organelles, cytoplasm, and proteins, through activation of UPS or autophagy (Sandri, 2008). We evaluated for the first time the atrophy (AI) and hypertrophy (HI) index in hematoxylin and eosin stained cross sections of SBMA and control quadriceps femoris (Fig. 4.5A,B). Whereas both AI and HI were increased in most of SBMA muscle samples, any correlation was found between the reduction of mtDNA copy number with neither AI nor HI (Fig. 4.5C). These data indicate that AI and HI underlying processes could be not involved in the reduction of mitochondrial mass.

### **5.3. Increased autophagy in human SBMA muscle tissue**

The process through with entire subcellular organelles are removed is called autophagy. It is a self-eating quality-control system, in which cellular components, including organelles, are entrapped into a double membrane structures, autophagosome, and then degraded by lysosomal hydrolases. We found that the expression levels of *LC3* and *Beclin-1*, involved in autophagosomes biogenesis, and *LAMP1* and *LAMP2B*, involved in lysosome biogenesis, were normal in SBMA muscle tissues compare to controls (Fig. 4.6A). On the contrary, the protein amount of LC3-II, Beclin-1 and LAMP1 was significantly increased in SBMA muscle homogenate (Fig. 4.6B,C). Furthermore, we found an increased number of autophagosomes in muscle SBMA cryosections immunostained for LC3, expressed as puncta/fiber (Fig. 4.6D,E).

All together, the data showed an enhanced autophagic process in SBMA muscle tissue in line with previously results (Chua et al., 2014; Cortes et al., 2014; Yu et al., 2011).

Indeed, recently analysis of quadriceps muscle samples from symptomatic 14 month-old AR100Q transgenic mice yielded a dramatic up-regulation of TFEB target genes (Cortes et al., 2014). TFEB is a transcription factor, which directs the expression of hundreds of autophagy- and lysosomal-related genes as part of the Coordinated Lysosomal Expression and Regulation (CLEAR) network (Settembre et al., 2011; Settembre and Ballabio, 2011; Palmieri et al., 2011). Consistently, in SBMA patients and knock-in AR113Q mice muscle were observed increased biochemical, morphological and molecular parameters of autophagy (Chua et al., 2014). Uncontrolled autophagy is thought to underlie muscle wasting; therefore the excessive activation of autophagy could also be responsible for SBMA skeletal muscle atrophic phenotype. In agreement with this hypothesis, global reduction of autophagic activity by Beclin-1 haploinsufficiency in SBMA knock-in AR113Q mice increased skeletal muscle fiber size and significantly extended lifespan (Yu et al., 2011). Furthermore, activation of the autophagic repressor Akt, by genetic and pharmacologic upregulation of insulin-like growth factor 1, mitigated SBMA muscle specific phenotype in mice (Palazzolo et al., 2009).

Paradoxically in motor neurons, contrarily to skeletal muscle, *polyQ AR* expression inhibits autophagy activation. Indeed, TFEB activity was significantly reduced both in SBMA motor neurons and patients derived neuronal progenitor cells (NPCs), with a consequent reduced autophagy. In addition, genetic ablation of autophagy in *Drosophila* exacerbates polyQ AR eye degeneration phenotypes (Pandey et al., 2007) and depletion of p62 in AR97Q transgenic mice significantly worsened motor and neurological phenotypes (Doi et al., 2013). Therefore pharmacological activation of autophagy in neuronal cells had beneficial effects, as shown in rapamycin (Pandey et al., 2007) and bicalutamide-trehalose treatments (Giorgetti et al., 2015). Indeed, rapamycin treatment suppressed polyQ AR-mediated eye degeneration in *drosophila* (Pandey et al., 2007); and trehalose-induced autophagy combined with the longer cytoplasmic retention of polyQ AR bound to Bicalutamide, enhanced polyQ AR clearance in motoneurons (Giorgetti et al., 2014). Thus, autophagy activation has important positive effects in SBMA motoneurons; at the opposite autophagy inhibition is beneficial in SBMA skeletal muscle.

The increased number of autophagosomes observed were unaffected by CAG repeat number in AR gene and by age at biopsy of SBMA patients (Fig. 4.7A,B), indicating that in our SBMA patients the autophagy induction is determined only by polyQ AR.

#### 5.4. Increased mitophagy in human SBMA muscle tissue

This study for the first time reported increased mitophagy in SBMA muscle tissue by biochemical and morphological assays. In SBMA muscle isolated mitochondria was significantly increased the presence of PINK1, BNIP3 and ubiquitin protein levels compare to control samples (Fig. 4.8B,C,D). These data suggested activation of PINK1 and BNIP3 mediated mitophagic pathways. In parallel, the transcript levels of *BNIP3* and *PINK1* were normal in SBMA samples compare to controls (Fig. 4.8A). As specified in introduction (section 1.10.1), PINK1 is stabilized on the OMM (Ashrafi and Schwarz, 2013) by mitochondrial depolarization. Therefore, the bioenergetic state can regulate mitochondrial PINK1 levels and the subsequent mitochondrial Parkin recruitment (Ding and Yin, 2012). The E3 ligase Parkin mediates selective engulfment of depolarized mitochondria by autophagosomes through ubiquitination (Gomes and Scorrano, 2013). Ubiquitin binds to different autophagy receptors, such as p62, NBR1 and optineurin (Novak, 2012), that in turn recruit the autophagic machinery through LC3 binding. The increased mtPINK1 and mtUbiquitin protein levels indicated a probable dysfunction-damage of SBMA mitochondria. The normal mtParkin and increased mtUbiquitin protein levels is difficult to explain. It could be due to the presence-involvement of other E3 ligases in the targeting of SBMA mitochondria (Ashrafi and Schwarz, 2013) or to different Parkin isoforms (La Cognata et al., 2014; Scuderi et al., 2014), not recognised by the used antibodies. Therefore other analysis will be necessary to clarify this point. We did not find increased protein levels of p62 in SBMA mitochondria. However, whereas p62 recruitment is shown to be necessary for PINK1/Parkin-induced mitophagy, the mitophagy can occur even in the absence of p62, as shown in mitochondria of MEF cells p62 knockout or p62 siRNA depleted (Narendra et al., 2010).

Furthermore, we found increased mtBNIP3 protein levels. BNIP3 (BCL2 and adenovirus E1B 19 kDa-interacting protein 3) contains an LC3-interacting region (LIR)

in the N-terminal domain, through which directly interact with LC3 recruiting the autophagic machinery on damaged mitochondria (Ding and Yin, 2012). In muscle wasting disorders, where autophagy is implicated in the pathogenesis, BNIP3 is upregulated, and its expression in skeletal muscle induces autophagosomes formation (Zhang and Ney, 2009). BNIP3 is also involved in hypoxia-induced mitophagy. Removal of mitochondria during hypoxia is important to reduce ROS production and maintain oxygen homeostasis (Ashrafi and Schwarz, 2013). BNIP3, with its BH3 domain, also can bind Bcl-2/Bcl-Xl disrupting the interaction between Bcl-2/Bcl-XL and Beclin-1, thus freeing Beclin-1 to induce autophagy (Novak, 2012).

The increased mitophagy, observed by WB analysis, was confirmed by morphological analysis that showed many mitochondria trapped in autophagosomes (Fig. 4.8E,F). This increase of the autophagosomes-mitochondria colocalization signal was not correlate with the CAG repeat number in *AR* gene or with patient's age at biopsy (Fig. 4.11A,B), indicating that in our SBMA patients the mitophagic induction is determined only by nuclear polyQ AR localization.

Interesting, we observed that some mitochondria-free-area in SBMA muscle fibers were rich in autophagic vacuoles, indicating the presence of a residual mitophagic activity that previously removed mitochondria (Fig. 4.8E). These images corresponded to the negative-NADH-DH stained area observed by histoenzymatical assay (Fig. 4.3D).

In conclusion, for the first time, we demonstrated in SBMA muscle an increased mitophagy, linked to reduced mitochondrial mass, probably related to a masked mitochondrial dysfunction.

## 5.5. Mitochondrial dynamic in human SBMA muscle tissue.

Removal of mitochondria through mitophagy requires three steps: mitochondria fragmentation (fission), induction of general autophagy and priming specific mitochondria for mitophagic recognition. Accumulating evidence emphasizes the requirement of fission prior to mitophagy (Gomes and Scorrano, 2013; Youle and Narendra, 2011). Mitochondrial dynamic is regulated by fusion and fission events. The most-studied proteins involved in mitochondrial fusion are mitofusins (MFN1 and MFN2), outer mitochondrial membrane proteins that enable fusion through their

cytoplasm-exposed GTPase domain, thus allowing tethering of the opposing mitochondrial membranes. Fission is regulated by proteins including Drp1 (dynamin-related protein 1) and Fis1 (fission protein 1). Drp1 is predominantly localized in cytoplasm. When recruited to mitochondria Drp1 associates with its receptors, such as Fis1, that localized to the outer mitochondrial membrane, to form a complex that allows the fission of mitochondria (Novak, 2012).

In SBMA muscle compare to controls we found: i) normal expression and protein levels of MFNs (Fig. 4.4A,B); ii) normal Drp1 and hFis1 expression levels (Fig. 4.12A): interesting, hFis1 transcript levels were 150-fold increased compare to Drp1 both in SBMA and control muscle samples (Fig. 4.12A), suggesting a greater role of hFis1 in muscular mitochondrial dynamic; iii) increased Drp1 and hFis1 protein amount in SBMA muscle mitochondria. Gomes and Scorrano (2008) found that overexpression of Fis1 itself can induce mitochondrial fragmentation and general autophagy in HeLa cells. Moreover, they show that mitochondrial dysfunction, rather than mitochondrial fragmentation, is responsible for the induction of autophagy (Ding and Yin, 2012).

In conclusion, all together the mitophagic and dynamic data suggested an increased mitochondrial quality control in SBMA muscle.

## **5.6. Reduced cardiolipin amount in muscle mitochondria from SBMA patients**

As previously discuss, induction of mitophagy may account for the decreased mitochondrial mass in our SBMA muscle samples (Figs. 4.8). However, activated mitophagy is probably related to a masked mitochondrial dysfunction. For this reason, we evaluated by mass spectrometry lipid composition of mitochondrial membranes in muscle isolated mitochondria from our SBMA patients and controls. Interesting, we found a significant reduction of cardiolipin (CL) amount and a probably compensatory increased levels of phosphatidylethanolamine (PE) and phosphatidylserine (PS) (Fig. 4.13A). Importantly the composition and proportion of the different cardiolipin species is normal (Fig. 4.13B). In mammalian cells, there are two biosynthetic routes of PE formation: PS decarboxylation, that occur in mitochondria, and the CDP-ethanolamine pathways, that occur in cytosol and ER (Horvath and Daum, 2013). PE and

phosphatidylcholine (PC) are the most abundant lipid in mitochondrial membranes, accounting for 80% of total mitochondrial phospholipids (Horvath and Daum, 2013). Mitochondria have also high CL content. It is exclusively synthesized in mitochondria, accounts for 10-15% of total mitochondrial phospholipids and it is mainly located in the inner mitochondrial membrane (Horvath and Daum, 2013). CL was shown to stabilize and interact with a number of mitochondrial proteins, such as pyruvate carrier and carnitine:acylcarnitine translocase, necessary to provide cells of metabolites essential for the production of ATP, and ADP/ATP carrier (AAC). CL is also required for optimal activity of complex I, III, IV, and V of Respiratory Chain and for supercomplexes assembling (Paradies et al., 2013). Luévano-Martínez et al. showed that CL binds mitochondrial nucleoids and is necessary for the maintenance of mtDNA stability under stress conditions (Luévano-Martínez et al., 2015), suggesting a link between the reduced mtDNA copy number (Fig.4.3A) and decreased CL levels (Fig. 4.13A). Furthermore, it was shown that CL is implicated in apoptosis, mitophagy and fusion processes (see introduction, section 1.11.2, for more details). Thus, a reduction of CL content in mitochondria could be extremely detrimental for the cellular homeostasis. Since we not found decreased levels of a single molecular specie of cardiolipin, we thought that probably there was an anomaly in initial steps in CL synthesis, included the cardiolipin synthase (CRLS1) reaction. CRLS1 is a key enzyme involved in the biosynthesis of immature CL. It catalyzes the irreversible condensation reaction in which the phosphatidyl group of Cytidine diphosphate diacylglycerol (CDP-DAG) is linked to phosphatidylglycerol (PG). After biosynthesis, immature CL undergoes deacylation and remodeling, to generate the different molecular species with diverse fatty acid composition.

We evaluated *CRLS1* mRNA levels by RT-PCR in SBMA muscle tissue and controls. The significant reduction of 51% of *CRLS1* expression levels found in SBMA muscle samples compare to controls, may explain the decreased CL levels (Fig. 4.13C), suggesting polyQ AR involvement in *CRLS1* regulation. Two different studies supported our data, showing that androgen exposure of human prostate cancer cells leads to *CRLS1* upregulation (De Primo et al., 2002; Wang et al., 2006).

We are not able to define if *CRLS1* downregulation was due to loss or gain of PolyQ AR functions. The data from prostate cancer cells sustained a probable direct bound of

AR to *CRLS1* gene promoter by ARE, therefore a loss of function of polyQ AR. However is not to exclude an indirect polyQ AR interference, due to the sequester of transcription factors or co-regulators involved in the expression of *CRLS1* gene by NIs containing the mutant protein . The ARE presence in *CRLS1* gene promoter may solve this point.

It was shown that chronic denervation significantly decreases CL concentration in muscle (Wicks and Hood, 1991; Ostojić et al. 2012) and increases mRNA encoding both *CRLS1* and CTP:PA-cytidylyltransferase-1 (Ostojić et al. 2012) biosynthesis enzymes of CL. This compensatory response during chronic muscle denervation differs from our results. Therefore we can conclude that the underlying mechanisms of CL reduction in SBMA muscle may be unrelated to denervation-induced muscle disuse. However in SBMA muscle tissue there were less mitochondria (Fig. 4.3 A,B,C,D), with normal OXPHOS activity (Fig. 4.3E), normal supercomplexes assembling (Fig. 4.13E) and an increased autophagosomes-mitochondria colocalization (Fig. 4.8E,F). Since in SBMA muscle tissue *CRLS1* expression and cardiolipin synthesis were not completely suppressed, it is possible the coexistence of decreased functioning mitochondria, that fuse and redistribute their contents, and dysfunctional mitochondria, that are separated from the mitochondrial network and removed via mitophagy. Moreover, accordingly to the fact that muscle is a high energy required tissue, the increment in PE and PS amount could be a partial compensatory response of SBMA muscle cells to save mitochondrial from mitophagic degradation. Several studies support this idea (Joshi et al., 2012; Jiang et al., 2000; Trotter et al., 1993; Rietveld et al., 1993; Zhonget al., 2004; Gu et al., 2004). It was shown that CL and PE have redundant functions and that each can compensate for the loss of the other. Depletion of CL or PE (in *crd1* or *psd1* mutants, respectively) results in similar phenotypes (Joshi et al., 2012; Jiang et al., 2000; Trotter et al., 1993). In the PE-lacking *Escherichia coli* strain AD93, CL levels are increased (Rietveld et al., 1993). Similar compensation is observed in yeast cells (Zhonget al., 2004; Gu et al., 2004), in which PE levels increase in the CL deficient mutants *crd1* and *taz1*. Collectively, these studies indicate a specific requirement for mitochondrial PE in cells lacking CL to carry out shared essential function(s), such as OPA1 stabilization, a pro-fusion inner mitochondrial membrane protein (Joshi et al., 2012). In fact, in *Saccharomyces cerevisiae* CL lack does not lead to defects in the mitochondrial network



for the PE compensatory role in the maintenance of mitochondrial tubular morphology and fusion (Joshi et al., 2012). Consistently, cells, lacking of both CL and mitochondrial PE, had reduced levels of all Mgm1p (OPA1 in mammals) isoforms and exhibited excessive mitochondrial fragmentation and defects in mitochondrial fusion (Joshi et al., 2012).

In conclusion, all together our data suggest that in muscle isolated mitochondria from SBMA patients the increased PE levels, in response to CL reduction, promote a temporary fusion of dysfunctional SBMA mitochondria, saving them from mitophagy. The PE compensative role may be insufficient in stress conditions, when dysfunctional mitochondria appear, with consequent activation of mitophagy and mitochondrial removal.



## Conclusions

Our findings provided evidence of a mitochondrial component in SBMA myopathy. Molecular (mtDNA copy number) (Fig. 4.3A), biochemical (activity of citrate synthase) (Fig. 4.3B) and morphological (imaging of muscle cryosections stained for NADH-DH) (Fig. 4.3C,D) analysis in muscle tissue from SBMA patients showed decreased amount of well functioning mitochondria, with normal OXPHOS activity (Fig. 4.3E) and supercomplexes' amount (Fig. 4.13D). The decreased mitochondrial mass was neither due to altered mitochondrial biogenesis (Fig. 4.4) nor to increased muscular atrophy and hypertrophy (Fig. 4.5). For the first time, we observed that mitophagy accounts for the enhanced removal of mitochondria (Fig. 4.8). Biochemical and morphological analysis indicated an increased autophagic process in SBMA muscle (Fig. 4.6), consistent with previous results, in parallel with an increased mitophagy. In SBMA muscle these alterations were associated with:

1. nuclear accumulation of the monomeric soluble form of polyQ AR (Fig. 4.1A,B);
2. decreased polyQ AR protein levels in total muscle lysate and cytosolic fraction (Fig. 4.1 A,B);
3. reduced expression levels of *cardiolipin synthase*, the only gene whose transcription was found altered in this study (Fig. 4.13C);
4. significant reduction of cardiolipin amount in mitochondrial membranes, together with a probably compensatory significant increase of phosphatidylethanolamine levels (Fig. 4.13A).

These data show nuclear accumulation of polyQ AR associated with reduction of mitochondrial mass, increased mitophagy and altered mitochondrial membrane lipid composition in the muscle from SBMA patients. Future studies will be needed to elucidate the exact mechanism behind these abnormalities. Anyway, our data indicated the mitochondrial involvement in SBMA pathogenesis. Not only in SBMA but also in other neurodegenerative disorders it has been shown that mitochondrial dysfunctions and oxidative stress are implicated in the pathophysiological mechanism of these disorders (Trushina et al., 2007; Di Filippo et al., 2010). Given the central role of

mitochondrial integrity in bioenergetics and cell death pathways, improvement of mitochondrial function is worth considering as a therapeutic approach to SBMA.

## *References*

1. Abel, A., Walcott, J., Woods, J., Duda, J., Merry, D.E., 2001. Expression of expanded repeat androgen receptor produces neurologic disease in transgenic mice. *Hum Mol Genet* 10, 107-16.
2. Adachi, H., Waza, M., Katsuno, M., Tanaka, F., Doyu, M., Sobue, G., 2007. Pathogenesis and molecular targeted therapy of spinal and bulbar muscular atrophy. *Neuropathol Appl Neurobiol* 33, 135-51
3. Adachi, H., Waza, M., Tokui, K., Katsuno, M., Minamiyama, M., Tanaka, F., Doyu, M., Sobue, G., 2007. CHIP overexpression reduces mutant androgen receptor protein and ameliorates phenotypes of the spinal and bulbar muscular atrophy transgenic mouse model. *J Neurosci* 27, 5115-26.
4. Adachi, H., Katsuno, M., Minamiyama, M., Sang, C., Pagoulatos, G., Angelidis, C., Kusakabe, M., Yoshiki, A., Kobayashi, Y., Doyu, M., Sobue, G., 2003. Heat shock protein 70 chaperone overexpression ameliorates phenotypes of the spinal and bulbar muscular atrophy transgenic mouse model by reducing nuclear-localized mutant androgen receptor protein. *J Neurosci* 23, 2203-11.
5. Adachi, H., Katsuno, M., Minamiyama, M., Waza, M., Sang, C., Nakagomi, Y., Kobayashi, Y., Tanaka, F., Doyu, M., Inukai, A., Yoshida, M., Hashizume, Y., Sobue, G., 2005. Widespread nuclear and cytoplasmic accumulation of mutant androgen receptor in SBMA patients. *Brain* 128, 659-70.
6. Adachi, H., Kume, A., Li, M., Nakagomi, Y., Niwa, H., Do, J., Sang, C., Kobayashi, Y., Doyu, M., Sobue, G., 2001. Transgenic mice with an expanded CAG repeat controlled by the human AR promoter show polyglutamine nuclear inclusions and neuronal dysfunction without neuronal cell death. *Hum Mol Genet* 10, 1039-48
7. Acehan, D., Malhotra, A., Xu, Y., Ren, M., Stokes, D.L., Schlame, M., 2011. Cardiolipin affects the supramolecular organization of ATP synthase in mitochondria. *Biophys. J.* 100, 2184–2192.
8. Allen, R.D., 1995. Membrane tubulation and proton pumps, *Protoplasma* 189, 1–8.
9. Araki, A., Katsuno, M., Suzuki, K., Banno, H., Suga, N., Hashizume, A., Mano, T., Hijikata, Y., Nakatsuji, H., Watanabe, H., Yamamoto, M., Makiyama, T., Ohno, S., Fukuyama, M., Morimoto, S., Horie, M., Sobue, G., 2014. Brugada syndrome in spinal and bulbar muscular atrophy. *Neurology* 82, 1813-21.
10. Arrasate, M., Mitra, S., Schweitzer, E.S., Segal, M.R., Finkbeiner, S., 2004. Inclusion body formation reduces levels of mutant huntingtin and the risk of neuronal death. *Nature* 431, 805-10.
11. Ashrafi, G., Schwarz, T.L., 2013. The pathways of mitophagy for quality control and clearance of mitochondria. *Cell Death Differ* 20, 31-42.
12. Atsuta, N., Watanabe, H., Ito, M., Banno, H., Suzuki, K., Katsuno, M., Tanaka, F., Tamakoshi, A., Sobue, G., 2006. Natural history of spinal and bulbar muscular atrophy (SBMA): a study of 223 Japanese patients. *Brain* 129, 1446-55.
13. Bailey, CK., Andriola, I.F., Kampinga, H.H., Merry, D.E., 2002. Molecular chaperones enhance the degradation of expanded polyglutamine repeat androgen receptor in a cellular model of spinal and bulbar muscular atrophy. *Hum Mol Genet* 11, 515-23.
14. Ban, T., Heymann, J.A., Song, Z., Hinshaw, J.E., Chan, D.C., 2010. OPA1 disease alleles causing dominant optic atrophy have defects in cardiolipin-stimulated GTP hydrolysis and membrane tubulation. *Hum Mol Genet* 19, 2113–2122
15. Banno, H., Adachi, H., Katsuno, M., Suzuki, K., Atsuta, N., Watanabe, H., Tanaka, F., Doyu, M., Sobue, G., 2006. Mutant androgen receptor accumulation in spinal and bulbar muscular atrophy scrotal skin: a pathogenic marker. *Ann Neurol* 59, 520-6.

16. Banno, H., Katsuno, M., Suzuki, K., Takeuchi, Y., Kawashima, M., Suga, N., Takamori, M., Ito, M., Nakamura, T., Matsuo, K., Yamada, S., Oki, Y., Adachi, H., Minamiyama, M., Waza, M., Atsuta, N., Watanabe, H., Fujimoto, Y., Nakashima, T., Tanaka, F., Doyu, M., Sobue, G., 2009. Phase 2 trial of leuprorelin in patients with spinal and bulbar muscular atrophy. *Annals of Neurology* 65, 140–150.
17. Battaglia, F., Le Galudec, V., Cossee, M., Tranchant, C., Warter, J.M., Echaniz-Laguna, A., 2003. Kennedy's disease initially manifesting as an endocrine disorder. *Journal of Clinical Neuromuscular Disease* 4, 165–167.
18. Bauer, P.O., Nukina, N., 2009. The pathogenic mechanisms of polyglutamine diseases and current therapeutic strategies. *Journal of Neurochemistry* 110, 1737–1765.
19. Beato, M., Herrlich, P., Schütz, G., 1995. Steroid hormone receptors: many actors in search of a plot. *Cell* 83, 851-7.
20. Beauchemin, A.M., Gottlieb, B., Beitel, L.K., Elhaji, Y.A., Pinsky, L., Trifiro, M.A., 2001. Cytochrome c oxidase subunit Vb interacts with human androgen receptor: a potential mechanism for neurotoxicity in spinobulbar muscular atrophy. *Brain Res Bull* 56, 285-97.
21. Bhasin, S., Storer, T.W., Berman, N., Yarasheski, K.E., Clevenger, B., Phillips, J., Lee, W.P., Bunnell, T.J., Casaburi, R., 1997. Testosterone replacement increases fat-free mass and muscle size in hypogonadal men. *J Clin Endocrinol Metab* 82, 407–413.
22. Bligh, E.G., Dyer, W.J., 1959. *Can J Biochem Physiol* 37, 911–917.
23. Brodsky, I.G., Balagopal, P., Nair, K.S., 1996. Effects of testosterone replacement on muscle mass and muscle protein synthesis in hypogonadal men—a clinical research center study. *J Clin Endocrinol Metab* 81, 3469–3475.
24. Bingham, P.M., Scott, M.O., Wang, S., McPhaul, M.J., Wilson, E.M., Garbern, J.Y., Merry, D.E., Fischbeck, K.H., 1995. Stability of an expanded trinucleotide repeat in the androgen receptor gene in transgenic mice. *Nat Genet* 9, 191-6.
25. Brinkmann, A.O., 2001. Lessons to be learned from the androgen receptor. *European Journal of Dermatology* 11, 301–303.
26. Brooks, B.P., Fischbeck, K.H., 1995. Spinal and bulbar muscular atrophy: a trinucleotide-repeat expansion neurodegenerative disease. *Trends Neurosci* 18, 459-61.
27. Brooks, B.P., Merry, D.E., Paulson, H.L., Lieberman, A.P., Kolson, D.L., Fischbeck, K.H., 1998. A cell culture model for androgen effects in motor neurons. *J Neurochem* 70, 1054-60.
28. Butler, R., Bates, G.P., 2006. Histone deacetylase inhibitors as therapeutics for polyglutamine disorders. *Nature Reviews Neuroscience* 7, 784–796.
29. Campello, S., Strappazon, F., Cecconi, F., 2014. Mitochondrial dismissal in mammals, from protein degradation to mitophagy. *Biochim Biophys Acta* 1837, 451-60.
30. Caplen, N.J., Taylor, J.P., Statham, V.S., Tanaka, F., Fire, A., Morgan, R.A., 2002. Rescue of polyglutamine-mediated cytotoxicity by double-stranded RNA-mediated RNA interference. *Hum Mol Genet* 11, 175-84.
31. Cequier-Sanchez, E., Rodriguez, C., Ravelo, A.G., Zarate, R.J., 2008. *Agric Food Chem* 56, 4297–4303.
32. Chahin, N., Sorenson, E.J., 2009. Serum creatine kinase levels in spinobulbar muscular atrophy and amyotrophic lateral sclerosis. *Muscle and Nerve* 40, 126–129.
33. Chevalier-Larsen, E.S., O'Brien, C.J., Wang, H., Jenkins, S.C., Holder, L., Lieberman, A.P., Merry, D.E., 2004. Castration restores function and neurofilament alterations of aged symptomatic males in a transgenic mouse model of spinal and bulbar muscular atrophy. *Journal of Neuroscience* 24, 4778–4786.
34. Chevalier-Larsen, E.S., Merry, D.E., 2012. Testosterone treatment fails to accelerate disease in a transgenic mouse model of spinal and bulbar muscular atrophy. *Dis Model Mech* 5, 141-5.
35. Chlenski, A., Nakashiro, K., Ketels, K.V., Korovaitseva, G.I., Oyasu, R., 2001. Androgen receptor expression in androgen-independent prostate cancer cell lines. *Prostate* 47, 66-75.

36. Chu, C.T., Ji, J., Dagda, R.K., Jiang, J.F., Tyurina, Y.Y., Kapralov, A.A., Tyurin, V.A., Yanamala, N., Shrivastava, I.H., Mohammadyani, D., Qiang Wang, K.Z., Zhu, J., Klein-Seetharaman, J., Balasubramanian, K., Amoscato, A.A., Borisenko, G., Huang, Z., Gusdon, A.M., Cheikhi, A., Steer, E.K., Wang, R., Baty, C., Watkins, S., Bahar, I., Bayir, H., Kagan, V.E., 2013. Cardiolipin externalization to the outer mitochondrial membrane acts as an elimination signal for mitophagy in neuronal cells. *Nat Cell Biol* 15, 1197-205.
37. Chua, J.P., Reddy, S.L., Merry, D.E., Adachi, H., Katsuno, M., Sobue, G., Robins, D.M., Lieberman A.P., 2014. Transcriptional activation of TFEB/ZKSCAN3 target genes underlies enhanced autophagy in spinobulbar muscular atrophy. *Hum Mol Genet* 23, 1376-86.
38. Ciechanover, A., Brundin, P., 2003. The ubiquitin proteasome system in neurodegenerative diseases: sometimes the chicken, sometimes the egg. *Neuron* 40, 427-46.
39. Claessens, F., Celis, L., Peeters, B., Heyns, W., Verhoeven, G., Rombauts, W., 1989. Functional characterization of an androgen response element in the first intron of the C3(1) gene of prostatic binding protein. *Biochem Biophys Res Commun* 164, 833-40.
40. Claypool, S.M., Oktay, Y., Boonthung, P., Loo J.A., Koehler, C.M., 2008. Cardiolipin defines the interactome of the major ADP/ATP carrier protein of the mitochondrial inner membrane. *J. Cell Biol* 182, 937-950.
41. Claypool, S.M., 2009. Cardiolipin, a critical determinant of mitochondrial carrier protein assembly and function. *Biochim. Biophys. Acta* 1788, 2059-2068.
42. Cortes, C.J., Miranda, H.C., Frankowski, H., Batlevi, Y., Young, J.E., Le, A., Ivanov, N., Sopher, B.L., Carromeu, C., Muotri, A.R., Garden, G.A., La Spada, A.R., 2014. Polyglutamine-expanded androgen receptor interferes with TFEB to elicit autophagy defects in SBMA. *Nat Neurosci* 17, 1180-9.
43. Cortes, C.J., Ling, S.C., Guo, L.T., Hung, G., Tsunemi, T., Ly, L., Tokunaga, S., Lopez, E., Sopher, B.L., Bennett, C.F., Shelton, G.D., Cleveland, D.W., La Spada, A.R., 2014. Muscle expression of mutant androgen receptor accounts for systemic and motor neuron disease phenotypes in spinal and bulbar muscular atrophy. *Neuron* 82, 295-307.
44. Dahlman-Wright, K., Grandien, K., Nilsson, S., Gustafsson, J.A., Carlstedt-Duke, J., 1993. Protein-protein interactions between the DNA-binding domains of nuclear receptors: influence on DNA-binding. *J Steroid Biochem Mol Biol* 45, 239-50.
45. Danek, A., Witt, T.N., Mann, K., Schweikert, H.U., Romalo, G., La Spada, A.R., Fischbeck, K.H., 1994. Decrease in androgen binding and effect of androgen treatment in a case of X-linked bulbospinal neuronopathy. *Clin Investig* 72 892-7.
46. Dejager, S., Bry-Gauillard, H., Bruckert, E., Eymard, B., Salachas, F., LeGuern, E., Tardieu, S., Chadarevian, R., Giral, P., Turpin, G., 2002. A comprehensive endocrine description of Kennedy's disease revealing androgen insensitivity linked to CAG repeat length. *Journal of Clinical Endocrinology and Metabolism* 87, 3893-3901.
47. DePrimo, S.E., Diehn, M., Nelson, J.B., Reiter, R.E., Matese, J., Fero, M., Tibshirani, R., Brown, P.O., Brooks, J.D., 2002. Transcriptional programs activated by exposure of human prostate cancer cells to androgen. *Genome Biol* 3, RESEARCH0032.
48. DeVay, R.M., Dominguez-Ramirez, L., Lackner, L.L., Hoppins, S., Stahlberg, H., Nunnari, J., 2009. Coassembly of Mgm1 isoforms requires cardiolipin and mediates mitochondrial inner membrane fusion. *J Cell Biol* 186, 793-803
49. Diaz, F., Moraes, C.T., 2008. Mitochondrial biogenesis and turnover. *Cell Calcium* 44, 24-35.
50. DiFiglia, M., Sapp, E., Chase, K.O., Davies, S.W., Bates, G.P., Vonsattel, J.P., Aronin, N., 1997. Aggregation of huntingtin in neuronal intranuclear inclusions and dystrophic neurites in brain. *Science* 277, 1990-3.
51. Di Filippo, M., Chiasserini, D., Tozzi, A., Picconi, B., Calabresi, P., 2010. Mitochondria and the link between neuroinflammation and neurodegeneration. *J Alzheimers Dis* 20 Suppl 2:S369-79.

52. Ding, W.X., Yin, X.M., 2012. Mitophagy: mechanisms, pathophysiological roles, and analysis. *Biol Chem* 393, 547-64.
53. Doi, H., Adachi, H., Katsuno, M., Minamiyama, M., Matsumoto, S., Kondo, N., Miyazaki, Y., Iida, M., Tohnai, G., Qiang, Q., Tanaka, F., Yanagawa, T., Warabi, E., Ishii, T., Sobue, G., 2013. p62/SQSTM1 differentially removes the toxic mutant androgen receptor via autophagy and inclusion formation in a spinal and bulbar muscular atrophy mouse model. *J Neurosci* 33, 7710-27.
54. Doyu, M., Sobue, G., Mukai, E., Kachi, T., Yasuda, T., Mitsuma, T., Takahashi, A., 1992. Severity of X-linked recessive bulbospinal neuronopathy correlates with size of the tandem CAG repeat in androgen receptor gene. *Annals of Neurology* 32, 707-710.
55. Doyu M., Sobue, G., Mitsuma, T., Uchida, M., Iwase, T., Takahashi, A., 1993. Very late onset X-linked recessive bulbospinal neuronopathy: mild clinical features and a mild increase in the size of tandem CAG repeat in androgen receptor gene. *J Neurol Neurosurg Psychiatry* 56, 832-3.
56. Dubowitz, V., Sewry, C. A., 2006. *Muscle biopsy: A practical approach*. Third edition. Saunders, Elsevier.
57. Enriquez, J.A., Lenaz, G., 2014. Coenzyme q and the respiratory chain: coenzyme q pool and mitochondrial supercomplexes. *Mol Syndromol* 5, 119-40.
58. Eskelinen, E.L., Tanaka, Y., Saftig, P., 2003. At the acidic edge: emerging functions for lysosomal membrane proteins. *Trends Cell Biol* 13, 137-45.
59. Eskelinen, E.L., Cuervo, A.M., Taylor, M.R., Nishino, I., Blum, J.S., Dice, J.F., Sandoval, I.V., Lippincott-Schwartz, J., August, J.T., Saftig, P., 2005. Unifying nomenclature for the isoforms of the lysosomal membrane protein LAMP-2. *Traffic* 6, 1058-61.
60. Eskelinen, E.L., Schmidt, C.K., Neu, S., Willenborg, M., Fuertes, G., Salvador, N., Tanaka, Y., Lüllmann-Rauch, R., Hartmann, D., Heeren, J., von Figura, K., Knecht, E., Saftig, P., 2004. Disturbed cholesterol traffic but normal proteolytic function in LAMP-1/LAMP-2 double-deficient fibroblasts. *Mol Biol Cell* 15, 3132-45.
61. Faber, P.W., van Rooij, H.C., Schipper, H.J., Brinkmann, A.O., Trapman, J., 1993. Two different, overlapping pathways of transcription initiation are active on the TATA-less human androgen receptor promoter. The role of Sp1. *J Biol Chem* 268, 9296-301.
62. Fernandez-Rhodes, L.E., Kokkinis, A.D., White, M.J., Watts, C.A., Auh, S., Jeffries, N.O., Shrader, J.A., Lehky, T.J., Li, L., Ryder, J.E., Levy, E.W., Solomon, B.I., Harris-Love, M.O., La Pean, A., Schindler, A.B., Chen, C., Di Prospero, N.A., Fischbeck, K.H., 2011. Efficacy and safety of dutasteride in patients with spinal and bulbar muscular atrophy: a randomised placebo-controlled trial. *The Lancet Neurology* 10, 140-147.
63. Finsterer, J., Mishra, A., Wakil, S., Pennuto, M., Soraru, G., 2015. Mitochondrial implications in bulbospinal muscular atrophy (Kennedy disease). *Amyotroph Lateral Scler Frontotemporal Degener* 1, 1-7.
64. Fischbeck, K.H., 1997. Kennedy disease. *Journal of Inherited Metabolic Disease* 20, 152-158.
65. Frohman, M.A., 2015. Role of mitochondrial lipids in guiding fission and fusion. *J Mol Med (Berl)* 93, 263-9.
66. Fukuda, M., 1991. Lysosomal membrane glycoproteins. Structure, biosynthesis, and intracellular trafficking. *J Biol Chem* 266, 21327-30.
67. Giorgetti, E., Rusmini, P., Crippa, V., Cristofani, R., Boncoraglio, A., Cicardi, M.E., Galbiati, M., Poletti, A., 2015. Synergic prodegradative activity of Bicalutamide and trehalose on the mutant androgen receptor responsible for spinal and bulbar muscular atrophy. *Hum Mol Genet* 24, 64-75.
68. Glass, D., Roubenoff, R., 2010. Recent advances in the biology and therapy of muscle wasting. *Ann N Y Acad Sci* 1211, 25-36.
69. Goldenberg, J.N., Bradley, W.G., 1996. Testosterone therapy and the pathogenesis of Kennedy's disease (X-linked bulbospinal muscular atrophy). *J Neurol Sci* 135, 158-61.



70. Goldstein, L.A., Sengelaub, D.R., 1992. Timing and duration of dihydrotestosterone treatment affect the development of motoneuron number and morphology in a sexually dimorphic rat spinal nucleus. *J Comp Neurol* 326, 147-57.
71. Gomes, L.C., Scorrano, L., 2013. Mitochondrial morphology in mitophagy and macroautophagy. *Biochim Biophys Acta* 1833, 205-12.
72. Gomes, L.C., Scorrano, L., 2008. High levels of Fis1, a pro-fission mitochondrial protein, trigger autophagy. *Biochim Biophys Acta*. 1777, 860-6.
73. Grad, J.M., Lyons, L.S., Robins, D.M., Burnstein, K.L., 2001. The androgen receptor (AR) amino-terminus imposes androgen-specific regulation of AR gene expression via an exonic enhancer. *Endocrinology* 142, 1107-16.
74. Greenland, K.J., Zajac, J.D., 2004. Kennedy's disease: pathogenesis and clinical approaches. *Intern Med J* 34, 279-86.
75. Gu, Z., Valianpour, F., Chen, S., Vaz, F.M., Hakkaart, G.A., Wanders, R.J., Greenberg, M.L., 2004. Aberrant cardiolipin metabolism in the yeast *taz1* mutant: a model for Barth syndrome. *Mol Microbiol* 51, 149-58.
76. Gunawardena, S., Goldstein, L.S., 2005. Polyglutamine diseases and transport problems: deadly traffic jams on neuronal highways. *Arch Neurol* 62, 46-51.
77. Haehling, S., Morley, J.E., Anker, S.D., 2012. From muscle wasting to sarcopenia and myopenia: update 2012. *J Cachexia Sarcopenia Muscle*. 3, 213–217.
78. Halievski, K., Mo, K., Westwood, J.T., Monks, D.A., 2015. Transcriptional profile of muscle following acute induction of symptoms in a mouse model of Kennedy's disease/spinobulbar muscular atrophy. *PLoS One* 10, e0118120.
79. Hamano, T., Mutoh, T., Hirayama, M., Kawamura, Y., Nagata, M., Fujiyama, J., Kuriyama, M., 2004. Muscle MRI findings of X-linked spinal and bulbar muscular atrophy. *J Neurol Sci* 222, 93-7.
80. Harding, A.E., Thomas, P.K., Baraitser, M., Bradbury, P.G., Morgan-Hughes, J.A., Ponsford, J.R., 1982. X-linked recessive bulbospinal neuronopathy: a report of ten cases. *Journal of Neurology, Neurosurgery and Psychiatry* 45, 1012–1019.
81. He, B., Kempainen, J.A., Wilson, E.M., 2000. FXXLF and WXXLF sequences mediate the NH<sub>2</sub>-terminal interaction with the ligand binding domain of the androgen receptor. *J Biol Chem* 275, 22986-94.
82. Herzog, R., Schuhmann, K., Schwudke, D., Sampaio, J.L., Bornstein, S.R., Schroeder, M., Shevchenko, A., 2012. *PLoS One* 7, e29851.
83. Holmberg, C.I., Staniszewski, K.E., Mensah, K.N., Matouschek, A., Morimoto, R.I., 2004. Inefficient degradation of truncated polyglutamine proteins by the proteasome. *EMBO J*. 23, 4307-18.
84. Horvath, S.E., Daum, G., 2013. Lipids of mitochondria. *Prog Lipid Res* 52, 590-614.
85. Houtkooper, R.H., Akbari, H., van Lenthe, H., Kulik, W., Wanders, R.J., Frentzen, M., Vaz, F.M., 2006. Identification and characterization of human cardiolipin synthase. *FEBS Lett* 580, 3059-64.
86. Howarth, J.L., Kelly, S., Keasey, M.P., Glover, C.P., Lee, Y.B., Mitrophanous, K., Chapple, J.P., Gallo, J.M., Cheetham, M.E., Uney, J.B., 2007. Hsp40 molecules that target to the ubiquitin-proteasome system decrease inclusion formation in models of polyglutamine disease. *Mol Ther* 15, 1100-5.
87. Igarashi, S., Tanno, Y., Onodera, O., Yamazaki, M., Sato, S., Ishikawa, A., Miyatani, N., Nagashima, M., Ishikawa, Y., Sahashi, K., 1992. Strong correlation between the number of CAG repeats in androgen receptor genes and the clinical onset of features of spinal and bulbar muscular atrophy. *Neurology* 42, 2300-2302
88. Irvine, R.A., Ma, H., Yu, M.C., Ross, R.K., Stallcup, M.R., Coetzee, G.A., 2000. Inhibition of p160-mediated coactivation with increasing androgen receptor polyglutamine length. *Hum Mol Genet* 9, 267-74.

89. Ishihara, K., Yamagishi, N., Saito, Y., Adachi, H., Kobayashi, Y., Sobue, G., Ohtsuka, K., Hatayama, T., 2003. Hsp105alpha suppresses the aggregation of truncated androgen receptor with expanded CAG repeats and cell toxicity. *J Biol Chem* 278, 25143-50.
90. Jenster, G., van der Korput, H.A., Trapman, J., Brinkmann, A.O., 1995. Identification of two transcription activation units in the N-terminal domain of the human androgen receptor. *Journal of Biological Chemistry* 270, 7341–7346.
91. Jiang, F., Ryan, M.T., Schlame, M., Zhao, M., Gu, Z., Klingenberg, M., Pfanner, N., Greenberg, M.L., 2000. Absence of cardiolipin in the *crd1* null mutant results in decreased mitochondrial membrane potential and reduced mitochondrial function. *J Biol Chem* 275, 22387-94.
92. Jochum, T., Ritz, M.E., Schuster, C., Funderburk, S.F., Jehle, K., Schmitz, K., Brinkmann, F., Hirtz, M., Moss, D., Cato, A.C., 2012. Toxic and non-toxic aggregates from the SBMA and normal forms of androgen receptor have distinct oligomeric structures. *Biochimica et Biophysica Acta* 1822, 1070–1078.
93. Johansen, J.A., Troxell-Smith, S.M., Yu, Z., Mo, K., Monks, D.A., Lieberman, A.P., Breedlove, S.M., Jordan, C.L., 2010. Prenatal flutamide enhances survival in a myogenic mouse model of spinal bulbar muscular atrophy. *Neurodegener Dis* 8, 25-34.
94. Johansen, J.A., Yu, Z., Mo, K., Monks, D.A., Lieberman, A.P., Breedlove, S.M., Jordan, C.L., 2009. Recovery of function in a myogenic mouse model of spinal bulbar muscular atrophy. *Neurobiol Dis* 34, 113-20.
95. Jordan, C.L., Price, R.H. Jr, Handa, R.J., 2002. Androgen receptor messenger RNA and protein in adult rat sciatic nerve: implications for site of androgen action. *J Neurosci Res* 69, 509-18.
96. Joshi, A.S., Thompson, M.N., Fei, N., Hüttemann, M., Greenberg, M.L., 2012. Cardiolipin and mitochondrial phosphatidylethanolamine have overlapping functions in mitochondrial fusion in *Saccharomyces cerevisiae*. *J Biol Chem* 287, 17589-97.
97. Kagan, V.E., Bayir, H.A., Belikova, N.A., Kapralov, O., Tyurina, Y.Y., Tyurin, V.A., et al., 2009. Cytochrome *c*/cardiolipin relations in mitochondria: a kiss of death. *Free Radic Biol Med* 46, 1439–53.
98. Katsuno, M., Adachi, H., Kume, A., Li, M., Nakagomi, Y., Niwa, H., Sang, C., Kobayashi, Y., Doyu, M., Sobue, G., 2002. Testosterone reduction prevents phenotypic expression in a transgenic mouse model of spinal and bulbar muscular atrophy. *Neuron* 35, 843–854.
99. Katsuno, M., Adachi, H., Doyu, M., Minamiyama, M., Sang, C., Kobayashi, Y., Inukai, A., Sobue, G., 2003. Leuprorelin rescues polyglutamine-dependent phenotypes in a transgenic mouse model of spinal and bulbar muscular atrophy. *Nature Medicine* 9, 768–773.
100. Katsuno, M., Sang, C., Adachi, H., Minamiyama, M., Waza, M., Tanaka, F., Doyu, M., Sobue, G., 2005. Pharmacological induction of heat-shock proteins alleviates polyglutamine-mediated motor neuron disease. *Proceedings of the National Academy of Sciences of the United States of America* 102, 16801–16806.
101. Katsuno, M., Adachi, H., Waza, M., Banno, H., Suzuki, K., Tanaka, F., Doyu, M., Sobue, G., 2006a. Pathogenesis, animal models and therapeutics in spinal and bulbar muscular atrophy (SBMA). *Experimental Neurology* 200, 8–18.
102. Katsuno, M., Adachi, H., Minamiyama, M., Waza, M., Tokui, K., Banno, H., Suzuki, K., Onoda, Y., Tanaka, F., Doyu, M., Sobue, G., 2006b. Reversible disruption of dynactin 1-mediated retrograde axonal transport in polyglutamine-induced motor neuron degeneration. *Journal of Neuroscience* 26, 12106–12117.
103. Katsuno, M., Adachi, H., Minamiyama, M., Waza, M., Doi, H., Kondo, N., Mizoguchi, H., Nitta, A., Yamada, K., Banno, H., Suzuki, K., Tanaka, F., Sobue, G., 2010a. Disrupted transforming growth factor-beta signaling in spinal and bulbar muscular atrophy. *Journal of Neuroscience* 30, 5702–5712.
104. Katsuno, M., Banno, H., Suzuki, K., Takeuchi, Y., Kawashima, M., Yabe, I., Sasaki, H., Aoki, M., Morita, M., Nakano, I., Kanai, K., Ito, S., Ishikawa, K., Mizusawa, H., Yamamoto, T., Tsuji, S., Hasegawa, K., Shimohata, T., Nishizawa, M., Miyajima, H.,

- Kanda, F., Watanabe, Y., Nakashima, K., Tsujino, A., Yamashita, T., Uchino, M., Fujimoto, Y., Tanaka, F., Sobue, G., 2010b. Efficacy and safety of leuprorelin in patients with spinal and bulbar muscular atrophy (JASMITT study): a multicentre, randomised, double-blind, placebo-controlled trial. *The Lancet Neurology* 9, 875–884.
105. Kalmar, B., Novoselov, S., Gray, A., Cheetham, M.E., Margulis, B., Greensmith, L., 2008. Late stage treatment with arimocloleol delays disease progression and prevents protein aggregation in the SOD1 mouse model of ALS. *J Neurochem* 107, 339–50.
106. Keller, E.T., Ershler, W.B., Chang, C., 1996. The androgen receptor: a mediator of diverse responses. *Front Biosci* 1:d59–71.
107. Kemp, M.Q., Poort, J.L., Baqri, R.M., Lieberman, A.P., Breedlove, S.M., Miller, K.E., Jordan, C.L., 2011. Impaired motoneuronal retrograde transport in two models of SBMA implicates two sites of androgen action. *Human Molecular Genetics* 20, 4475–4490.
108. Kennedy, W.R., Alter, M., Sung, J.H., 1968. Progressive proximal spinal and bulbar muscular atrophy of late onset. A sex-linked recessive trait. *Neurology* 18, 671–680.
109. Kim, I., Rodriguez-Enriquez, S., Lemasters, J.J., 2007. Selective degradation of mitochondria by mitophagy. *Arch Biochem Biophys* 462, 245–253.
110. Kinirons, P., Rouleau, G.A., 2008. Administration of testosterone results in reversible deterioration in Kennedy's disease. *Journal of Neurology, Neurosurgery and Psychiatry* 79, 106–107.
111. Klement, I.A., Skinner, P.J., Kaytor, M.D., Yi, H., Hersch, S.M., Clark, H.B., Zoghbi, H.Y., Orr, H.T., 1998. Ataxin-1 nuclear localization and aggregation: role in polyglutamine-induced disease in SCA1 transgenic mice. *Cell* 95, 41–53.
112. Kobayashi, Y., Kume, A., Li, M., Doyu, M., Hata, M., Ohtsuka, K., Sobue, G., 2000. Chaperones Hsp70 and Hsp40 suppress aggregate formation and apoptosis in cultured neuronal cells expressing truncated androgen receptor protein with expanded polyglutamine tract. *Journal of Biological Chemistry* 275, 8772–8778.
113. Kobayashi, Y., Miwa, S., Merry, D.E., Kume, A., Mei, L., Doyu, M., Sobue, G., 1998. Caspase-3 cleaves the expanded androgen receptor protein of spinal and bulbar muscular atrophy in a polyglutamine repeat length-dependent manner. *Biochem Biophys Res Commun* 252, 145–50.
114. Komatsu, M., Ichimura, Y., 2010. Selective autophagy regulates various cellular functions. *Genes Cells* 15, 923–33.
115. Konecki, D.S., Foetisch, K., Zimmer, K.P., Schlotter, M., Lichter-Konecki, U., 1995. An alternatively spliced form of the human lysosome-associated membrane protein-2 gene is expressed in a tissue-specific manner. *Biochem Biophys Res Commun* 215, 757–67.
116. Kornfeld, S., Mellman, I., 1989. The biogenesis of lysosomes. *Annu Rev Cell Biol* 5, 483–525.
117. Kujawa, K.A., Jacob, J.M., Jones, K.J., 1993. Testosterone regulation of the regenerative properties of injured rat sciatic motor neurons. *J Neurosci Res* 35, 268–73.
118. La Cognata, V., Iemmolo, R., D'Agata, V., Scuderi, S., Drago, F., Zappia, M., et al., 2014. Increasing the Coding Potential of Genomes Through Alternative Splicing: The Case of PARK2 Gene. *Current genomics* 15, 203–16.
119. LaFevre-Bernt, M.A., Ellerby, L.M., 2003. Kennedy's disease. Phosphorylation of the polyglutamine-expanded form of androgen receptor regulates its cleavage by caspase-3 and enhances cell death. *Journal of Biological Chemistry* 278, 34918–34924.
120. Lagouge, M., Argmann, C., Gerhart-Hines, Z., Meziane, H., Lerin, C., Daussin, F., Messadeq, N., Milne, J., Lambert, P., Elliott, P., Geny, B., Laakso, M., Puigserver, P., Auwerx, J., 2006. Resveratrol improves mitochondrial function and protects against metabolic disease by activating SIRT1 and PGC-1 $\alpha$ . *Cell* 127, 1109–22.
121. Langley, E., Zhou, Z.X., Wilson, E.M., 1995. Evidence for an anti-parallel orientation of the ligand-activated human androgen receptor dimer. *J Biol Chem* 270, 29983–90.

122. La Spada, A.R., Wilson, E.M., Lubahn, D.B., Harding, A.E., Fischbeck, K.H., 1991. Androgen receptor gene mutations in X-linked spinal and bulbar muscular atrophy. *Nature* 352, 77–79.
123. La Spada, A.R., Roling, D.B., Harding, A.E., Warner, C.L., Spiegel, R., Hausmanowa-Petrusewicz, I., Yee, W.C., Fischbeck, K.H., 1992. Meiotic stability and genotype-phenotype correlation of the trinucleotide repeat in X-linked spinal and bulbar muscular atrophy. *Nature Genetics* 2, 301-304.
124. La Spada, A.R., Peterson, K.R., Meadows, S.A., McClain, M.E., Jeng, G., Chmelar, R.S., Haugen, H.A., Chen, K., Singer, M.J., Moore, D., Trask, B.J., Fischbeck, K.H., Clegg, C.H., McKnight, G.S., 1998. Androgen receptor YAC transgenic mice carrying CAG 45 alleles show trinucleotide repeat instability. *Hum Mol Genet* 7, 959-67.
125. La Spada, A., Spinal and Bulbar Muscular Atrophy, 1999. Source: GeneReviews® [Internet].
126. Lemasters, J.J., Qian, T., He, L., Kim, J.S., Elmore, S.P., Cascio, W.E., Brenner, D.A., 2002. Role of mitochondrial inner membrane permeabilization in necrotic cell death, apoptosis, and autophagy. *Antioxid Redox Signal* 4, 769-81.
127. Li, M., Chevalier-Larsen, E.S., Merry, D.E., Diamond, M.I., 2007. Soluble androgen receptor oligomers underlie pathology in a mouse model of spinobulbar muscular atrophy. *Journal of Biological Chemistry* 282, 3157–3164.
128. Li, M., Miwa, S., Kobayashi, Y., Merry, D.E., Yamamoto, M., Tanaka, F., Doyu, M., Hashizume, Y., Fischbeck, K.H., Sobue, G., 1998a. Nuclear inclusions of the androgen receptor protein in spinal and bulbar muscular atrophy. *Annals of Neurology* 44, 249–254.
129. Li, M., Nakagomi, Y., Kobayashi, Y., Merry, D.E., Tanaka, F., Doyu, M., Mitsuma, T., Hashizume, Y., Fischbeck, K.H., Sobue, G., 1998b. Nonneural nuclear inclusions of androgen receptor protein in spinal and bulbar muscular atrophy. *American Journal of Pathology* 153, 695–701.
130. Lieberman, A.P., Yu, Z., Murray, S., Peralta, R., Low, A., Guo, S., Yu, X.X., Cortes, C.J., Bennett, C.F., Monia, B.P., La Spada, A.R., Hung, G., 2014. Peripheral androgen receptor gene suppression rescues disease in mouse models of spinal and bulbar muscular atrophy. *Cell Rep* 7, 774-84.
131. Lieberman, A.P., Harmison, G., Strand, A.D., Olson, J.M., Fischbeck, K.H., 2002. Altered transcriptional regulation in cells expressing the expanded polyglutamine androgen receptor. *Hum Mol Genet* 11, 1967-76.
132. Lin, J., Wu, H., Tarr, P.T., Zhang, C.Y., Wu, Z., Boss, O., Michael, L.F., Puigserver, P., Isotani, E., Olson, E.N., Lowell, B.B., Bassel-Duby, R., Spiegelman, B.M., 2002. Transcriptional co-activator PGC-1 alpha drives the formation of slow-twitch muscle fibres. *Nature* 418, 797-801.
133. Lu, Y.W., Claypool, S.M., 2015. Disorders of phospholipid metabolism: an emerging class of mitochondrial disease due to defects in nuclear genes. *Front Genet* 6, 3.
134. Luévano-Martínez, L.A., Forni, M.F., dos Santos, V.T., Souza-Pinto, N.C., Kowaltowski, A.J., 2015. Cardiolipin is a key determinant for mtDNA stability and segregation during mitochondrial stress. *Biochim Biophys Acta* 1847, 587-98.
135. Lund, A., Udd, B., Juvonen, V., Andersen, P.M., Cederquist, K., Davis, M., Gellera, C., Kolmel, C., Ronnevi, L.O., Sperfeld, A.D., Sorensen, S.A., Tranebjaerg, L., Van Maldergem, L., Watanabe, M., Weber, M., Yeung, L., Savontaus, M.L., 2001. Multiple founder effects in spinal and bulbar muscular atrophy (SBMA, Kennedy disease) around the world. *European Journal of Human Genetics* 9, 431–436.
136. McCampbell, A., Taylor, J.P., Taye, A.A., Robitschek, J., Li, M., Walcott, J., Merry, D., Chai, Y., Paulson, H., Sobue, G., Fischbeck, K.H., 2000. CREB-binding protein sequestration by expanded polyglutamine. *Hum Mol Genet* 9, 2197-202.
137. McKenzie, M., Lazarou, M., Thorburn, D.R., Ryan, M.T., 2006. Mitochondrial respiratory chain supercomplexes are destabilized in Barth Syndrome patients. *J Mol Biol* 361, 462-9.

138. McManamny, P., Chy, H.S., Finkelstein, D.I., Craythorn, R.G., Crack, P.J., Kola, I., Cheema, S.S., Horne, M.K., Wreford, N.G., O'Bryan, M.K., De Kretser, D.M., Morrison, J.R., 2002. A mouse model of spinal and bulbar muscular atrophy. *Hum Mol Genet* 11, 2103-11.
139. Malena, A., Loro, E., Di Re, M., Holt, I.J., Vergani, L., 2009. Inhibition of mitochondrial fission favours mutant over wild-type mitochondrial DNA. *Hum Mol Genet* 18, 3407-16.
140. Malena, A., Pennuto, M., Tezze, C., Querin, G., D'Ascenzo, C., Silani, V., Cenacchi, G., Scaramozza, A., Romito, S., Morandi, L., Pegoraro, E., Russell, A.P., Sorarù, G., Vergani, L., 2013. Androgen-dependent impairment of myogenesis in spinal and bulbar muscular atrophy. *Acta Neuropathol* 126, 109-21.
141. Malik, B., Nirmalanathan, N., Gray, A.L., La Spada, A.R., Hanna, M.G., Greensmith, L., 2013. Co-induction of the heat shock response ameliorates disease progression in a mouse model of human spinal and bulbar muscular atrophy: implications for therapy. *Brain* 136, 926-43.
142. Matsumoto, A., Micevych, P.E., Arnold, A.P., 1988. Androgen regulates synaptic input to motoneurons of the adult rat spinal cord. *J Neurosci.* 8, 4168-76.
143. Matsuura, T., Demura, T., Aimoto, Y., Mizuno, T., Moriwaka, F., Tashiro, K., 1992. Androgen receptor abnormality in X-linked spinal and bulbar muscular atrophy. *Neurology* 42, 1724-6.
144. Merry, D. E., McCampbell, A., Taye, A. A., Winston, R. L., Fischbeck, K. H., 1996. Toward a mouse model for spinal and bulbar muscular atrophy: effect of neuronal expression of androgen receptor in transgenic mice (abstract). *Am. J. Hum. Genet.* 59, A271.
145. Minamiyama, M., Katsuno, M., Adachi, H., Waza, M., Sang, C., Kobayashi, Y., Tanaka, F., Doyu, M., Inukai, A., Sobue, G., 2004. Sodium butyrate ameliorates phenotypic expression in a transgenic mouse model of spinal and bulbar muscular atrophy. *Human Molecular Genetics* 13, 1183–1192.
146. Mirowska-Guzel, D., Seniow, J., Sulek, A., Lesniak, M., Czlonkowska, A., 2009. Are cognitive and behavioural deficits a part of the clinical picture in Kennedy's disease? A case study. *Neurocase* 15, 332–337.
147. Miyazaki, Y., Adachi, H., Katsuno, M., Minamiyama, M., Jiang, Y.M., Huang, Z., Doi, H., Matsumoto, S., Kondo, N., Iida, M., Tohnai, G., Tanaka, F., Muramatsu, S., Sobue, G., 2012. Viral delivery of miR-196a ameliorates the SBMA phenotype via the silencing of CELF2. *Nat Med* 18, 1136-41
148. Mizushima, N., 2010. Autophagy. *FEBS Lett* 584, 1279.
149. Mizushima, N., 2007. Autophagy: process and function. *Genes Dev* 21, 2861-73.
150. Mizushima, N., Kuma, A., 2008. Autophagosomes in GFP-LC3 Transgenic Mice. *Methods Mol Biol* 445, 119-24.
151. Mizushima, N., Komatsu, M., 2011. Autophagy: renovation of cells and tissues. *Cell* 147, 728-41.
152. Mo, K., Razak, Z., Rao, P., Yu, Z., Adachi, H., Katsuno, M., Sobue, G., Lieberman, A.P., Westwood, J.T., Monks, D.A., 2010. Microarray analysis of gene expression by skeletal muscle of three mouse models of Kennedy disease/spinal bulbar muscular atrophy. *PLoS One* 5, e12922.
153. Monks, D.A., Johansen, J.A., Mo, K., Rao, P., Eagleson, B., Yu, Z., Lieberman, A.P., Breedlove, S.M., Jordan, C.L., 2007. Overexpression of wild-type androgen receptor in muscle recapitulates polyglutamine disease. *Proceedings of the National Academy of Sciences of the United States of America* 104, 18259–18264.
154. Montie, H.L., Cho, M.S., Holder, L., Liu, Y., Tsvetkov, A.S., Finkbeiner, S., Merry, D.E., 2009. Cytoplasmic retention of polyglutamine-expanded androgen receptor ameliorates disease via autophagy in a mouse model of spinal and bulbar muscular atrophy. *Human Molecular Genetics* 18, 1937–1950.

155. Montie, H.L., Pestell, R.G., Merry, D.E., 2011. SIRT1 modulates aggregation and toxicity through deacetylation of the androgen receptor in cell models of SBMA. *Journal of Neuroscience* 31, 17425–17436
156. Morfini, G., Pigino, G., Szebenyi, G., You, Y., Pollema, S., Brady, S.T., 2006. JNK mediates pathogenic effects of polyglutamine-expanded androgen receptor on fast axonal transport. *Nature Neuroscience* 9, 907–916.
157. Morrish, F., Giedt, C., Hockenbery, D., 2003. c-MYC apoptotic function is mediated by NRF-1 target genes. *Genes Dev* 17, 240-55.
158. Moss, F.P., Leblond, C.P., 1971. Satellite cells as the source of nuclei in muscles of growing rats. *Anat Rec* 170, 421–435.
159. Mukherjee, S., Thomas, M., Dadgar, N., Lieberman, A.P., Iniguez-Lluhi, J.A., 2009. Small ubiquitin-like modifier (SUMO) modification of the androgen receptor attenuates polyglutamine-mediated aggregation. *Journal of Biological Chemistry* 284, 21296–21306.
160. Nagai, Y., Fujikake, N., Popiel, H.A., Wada, K., 2010. Induction of molecular chaperones as a therapeutic strategy for the polyglutamine diseases. *Current Pharmaceutical Biotechnology* 11, 188–197.
161. Nagashima, T., Seko, K., Hirose, K., Mannen, T., Yoshimura, S., Arima, R., Nagashima, K., Morimatsu, Y., 1988. Familial bulbo-spinal muscular atrophy associated with testicular atrophy and sensory neuropathy (Kennedy-Alter-Sung syndrome). Autopsy case report of two brothers. *Journal of the Neurological Sciences* 87, 141–152.
162. Nakamura, M., Mita, S., Murakami, T., Uchino, M., Watanabe, S., Tokunaga, M., Kumamoto, T., Ando, M., 1994. Exonic trinucleotide repeats and expression of androgen receptor gene in spinal cord from X-linked spinal and bulbar muscular atrophy. *J Neurol Sci* 122, 74-9.
163. Narendra, D., Kane, L.A., Hauser, D.N., Fearnley, I.M., Youle, R.J., 2010. p62/SQSTM1 is required for Parkin-induced mitochondrial clustering but not mitophagy; VDAC1 is dispensable for both. *Autophagy* 6, 1090-106.
164. Narkar, V.A., Fan, W., Downes, M., Yu, R.T., Jonker, J.W., Alaynick, W.A., Banayo, E., Karunasiri, M.S., Lorca, S., Evans, R.M., 2011. Exercise and PGC-1 $\alpha$ -independent synchronization of type I muscle metabolism and vasculature by ERR $\gamma$ . *Cell Metab* 13, 283-93.
165. Nedelsky, N.B., Pennuto, M., Smith, R.B., Palazzolo, I., Moore, J., Nie, Z., Neale, G., Taylor, J.P., 2010. Native functions of the androgen receptor are essential to pathogenesis in a *Drosophila* model of spinobulbar muscular atrophy. *Neuron* 67, 936–952.
166. Neuschmid-Kaspar, F., Gast, A., Peterziel, H., Schneikert, J., Muigg, A., Ransmayr, G., Klocker, H., Bartsch, G., Cato, A.C., 1996. CAG-repeat expansion in androgen receptor in Kennedy's disease is not a loss of function mutation. *Mol Cell Endocrinol* 117, 149-56.
167. Novak, I., 2012. Mitophagy: a complex mechanism of mitochondrial removal. *Antioxid Redox Signal* 17, 794-802.
168. Novak, I., Dikic, I., 2011. Autophagy receptors in developmental clearance of mitochondria. *Autophagy* 7, 301-3.
169. Olesen, J., Kiilerich, K., Pilegaard, H., 2010. PGC-1 $\alpha$ -mediated adaptations in skeletal muscle. *Pflugers Arch* 460, 153-62.
170. Orr, C.R., Montie, H.L., Liu, Y., Bolzoni, E., Jenkins, S.C., Wilson, E.M., Joseph, J.D., McDonnell, D.P., Merry, D.E., 2010. An interdomain interaction of the androgen receptor is required for its aggregation and toxicity in spinal and bulbar muscular atrophy. *Journal of Biological Chemistry* 285, 35567–35577.
171. Orsucci, D., Rocchi, A., Caldarazzo Ienco, E., Ali, G., LoGerfo, A., Petrozzi, L., Scarpelli, M., Filosto, M., Carlesi, C., Siciliano, G., Bonuccelli, U., Mancuso, M., 2014. Myopathic involvement and mitochondrial pathology in Kennedy disease and in other motor neuron diseases. *Curr Mol Med*. 14,598-602.

172. Ostojic, O., O'Leary, M.F., Singh, K., Menzies, K.J., Vainshtein, A., Hood, D.A., 2012. The effects of chronic muscle use and disuse on cardiolipin metabolism. *J Appl Physiol* 114, 444-52.
173. Palazzolo, I., Burnett, B.G., Young, J.E., Brenne, P.L., La Spada, A.R., Fischbeck, K.H., Howell, B.W., Pennuto, M., 2007. Akt blocks ligand binding and protects against expanded polyglutamine androgen receptor toxicity. *Human Molecular Genetics* 16, 1593-1603.
174. Palazzolo, I., Gliozzi, A., Rusmini, P., Sau, D., Crippa, V., Simonini, F., Onesto, E., Bolzoni, E., Poletti, A., 2008. The role of the polyglutamine tract in androgen receptor. *Journal of Steroid Biochemistry and Molecular Biology* 108, 245-253.
175. Palazzolo, I., Stack, C., Kong, L., Musaro, A., Adachi, H., Katsuno, M., Sobue, G., Taylor, J.P., Sumner, C.J., Fischbeck, K.H., Pennuto, M., 2009. Overexpression of IGF-1 in muscle attenuates disease in a mouse model of spinal and bulbar muscular atrophy. *Neuron* 63, 316-328.
176. Palmieri, M., Impey, S., Kang, H., di Ronza, A., Pelz, C., Sardiello, M., Ballabio, A., 2011. Characterization of the CLEAR network reveals an integrated control of cellular clearance pathways. *Hum Mol Genet* 20, 3852-66.
177. Pandey, U.B., Nie, Z., Batlevi, Y., McCray, B.A., Ritson, G.P., Nedelsky, N.B., Schwartz, S.L., DiProspero, N.A., Knight, M.A., Schuldiner, O., Padmanabhan, R., Hild, M., Berry, D.L., Garza, D., Hubbert, C.C., Yao, T.P., Baehrecke, E.H., Taylor, J.P., 2007. HDAC6 rescues neurodegeneration and provides an essential link between autophagy and the UPS. *Nature* 447, 859-863.
178. Palazzolo, I., Nedelsky, N.B., Askew, C.E., Harmison, G.G., Kasantsev, A.G., Taylor, J.P., Fischbeck, K.H., Pennuto, M., 2010. B2 attenuates polyglutamine-expanded androgen receptor toxicity in cell and fly models of spinal and bulbar muscular atrophy. *J Neurosci Res* 88, 2207-16.
179. Paradas, C., Solano, F., Carrillo, F., Fernández, C., Bautista, J., Pintado, E., Lucas, M., 2008. Highly skewed inactivation of the wild-type X-chromosome in asymptomatic female carriers of spinal and bulbar muscular atrophy (Kennedy's disease). *J Neurol* 255, 853-7.
180. Paradies, G., Paradies, V., De Benedictis, V., Ruggiero, F.M., Petrosillo, G., 2014. Functional role of cardiolipin in mitochondrial bioenergetics. *Biochim Biophys Acta* 18374, 08-17.
181. Parodi, S., Pennuto, M., 2011. Neurotoxic effects of androgens in spinal and bulbar muscular atrophy. *Frontiers in Neuroendocrinology* 32, 416-425.
182. Patil, V.A., Greenberg, M.L., 2013. Cardiolipin-mediated cellular signaling. *Adv Exp Med Biol* 991, 195-213.
183. Piantadosi, C.A., Suliman, H.B., 2012. Redox regulation of mitochondrial biogenesis. *Free Radic Biol Med* 53, 2043-53.
184. Piccioni, F., Pinton, P., Simeoni, S., Pozzi, P., Fascio, U., Vismara, G., Martini, L., Rizzuto, R., Poletti, A., 2002. Androgen receptor with elongated polyglutamine tract forms aggregates that alter axonal trafficking and mitochondrial distribution in motor neuronal processes. *FASEB Journal* 16, 1418-1420.
185. Piccioni, F., Simeoni, S., Andriola, I., Armatura, E., Bassanini, S., Pozzi, P., Poletti, A., 2001. Polyglutamine tract expansion of the androgen receptor in a motoneuronal model of spinal and bulbar muscular atrophy. *Brain Res Bull* 56, 215-20.
186. Poletti, A., 2004. The polyglutamine tract of androgen receptor: from functions to dysfunctions in motor neurons. *Frontiers in Neuroendocrinology* 25, 1-26.
187. Poletti, A., Negri-Cesi, P., Martini, L., 2005. Reflections on the diseases linked to mutations of the androgen receptor. *Endocrine* 28, 243-62.
188. Qiang, Q., Adachi, H., Huang, Z., Jiang, Y.M., Katsuno, M., Minamiyama, M., Doi, H., Matsumoto, S., Kondo, N., Miyazaki, Y., Iida, M., Tohnai, G., Sobue, G., 2013. Genistein, a natural product derived from soybeans, ameliorates polyglutamine-mediated motor neuron disease. *J Neurochem* 126, 122-30.

189. Querin, G., D'Ascenzo, C., Peterle, E., Ermani, M., Bello, L., Melacini, P., Morandi, L., Mazzini, L., Silani, V., Raimondi, M., Mandrioli, J., Romito, S., Angelini, C., Pegoraro, E., Sorarù, G., 2013. Pilot trial of clenbuterol in spinal and bulbar muscular atrophy. *Neurology* 80, 2095-8.
190. Quigley, C.A., De Bellis, A., Marschke, K.B., el-Awady, M.K., Wilson, E.M., French, F.S., 1995. Androgen receptor defects: historical, clinical, and molecular perspectives. *Endocr Rev* 16, 271-321.
191. Ranganathan, S., Harmison, G.G., Meyertholen, K., Pennuto, M., Burnett, B.G., Fischbeck, K.H., 2009. Mitochondrial abnormalities in spinal and bulbar muscular atrophy. *Human Molecular Genetics* 18, 27-42.
192. Rehfeldt, C., Mantilla, C.B., Sieck, G.C., Hikida, R.S., Booth, F.W., Kadi, F., Bodine, S.C., Lowe, D.A., 2007. Satellite cell addition is/is not obligatory for skeletal muscle hypertrophy. *J Appl Physiol* 103, 1104-1106.
193. Ren, M., Phoon, C.K., Schlame, M., 2014. Metabolism and function of mitochondrial cardiolipin. *Prog Lipid Res* 55, 1-16.
194. Rhodes, L.E., Freeman, B.K., Auh, S., Kokkinis, A.D., La Pean, A., Chen, C., Lehky, T.J., Shrader, J.A., Levy, E.W., Harris-Love, M., Di Prospero, N.A., Fischbeck, K.H., 2009. Clinical features of spinal and bulbar muscular atrophy. *Brain* 132, 3242-3251.
195. Rietveld, A.G., Killian, J.A., Dowhan, W., de Kruijff, B., 1993. Polymorphic regulation of membrane phospholipid composition in *Escherichia coli*. *J Biol Chem* 268, 12427-33.
196. Rinaldi, C., Bott, L.C., Chen, K.L., Harmison, G.G., Katsuno, M., Sobue, G., Pennuto, M., Fischbeck, K.H., 2012. Insulinlike growth factor (IGF)-1 administration ameliorates disease manifestations in a mouse model of spinal and bulbar muscular atrophy. *Mol Med* 18, 1261-8.
197. Rocchi, C., Greco, V., Urbani, A., Di Giorgio, A., Priori, M., Massa, R., Bernardi, G., Marfia, G.A., 2011. Subclinical autonomic dysfunction in spinobulbar muscular atrophy (Kennedy disease). *Muscle and Nerve* 44, 737-740.
198. Rocchi, A., Pennuto, M., 2013. New routes to therapy for spinal and bulbar muscular atrophy. *J Mol Neurosci* 50, 514-23.
199. Romanello, V., Sandri, M., 2013. Mitochondrial biogenesis and fragmentation as regulators of protein degradation in striated muscles. *J Mol Cell Cardiol* 55, 64-72.
200. Rusmini, P., Simonini, F., Crippa, V., Bolzoni, E., Onesto, E., Cagnin, M., Sau, D., Ferri, N., Poletti, A., 2011. 17-AAG increases autophagic removal of mutant androgen receptor in spinal and bulbar muscular atrophy. *Neurobiology of Disease* 41, 83-95.
201. Rusmini, P., Sau, D., Crippa, V., Palazzolo, I., Simonini, F., Onesto, E., Martini, L., Poletti, A., 2007. Aggregation and proteasome: the case of elongated polyglutamine aggregation in spinal and bulbar muscular atrophy. *Neurobiol Aging* 28, 1099-1111.
202. Rusmini, P., Bolzoni, E., Crippa, V., Onesto, E., Sau, D., Galbiati, M., Piccolella, M., Poletti, A., 2010. Proteasomal and autophagic degradative activities in spinal and bulbar muscular atrophy. *Neurobiol Dis* 40, 361-9.
203. Sakuma, K., Yamaguchi, A., 2010. The functional role of calcineurin in hypertrophy, regeneration, and disorders of skeletal muscle. *J Biomed Biotechnol* 721219.
204. Sandri, M., Coletto, L., Grumati, P., Bonaldo, P., 2013. Misregulation of autophagy and protein degradation systems in myopathies and muscular dystrophies. *J Cell Sci* 126, 5325-33.
205. Sandri, M., 2008. Signaling in Muscle Atrophy and Hypertrophy. *PHYSIOLOGY* 23, 160-170.
206. Sartorelli, V., Fulco, M., 2004. Molecular and cellular determinants of skeletal muscle atrophy and hypertrophy. *Sci STKE* 2004: re11.
207. Scarpulla, R.C., Vega, R.B., Kelly, D.P., 2012. Transcriptional integration of mitochondrial biogenesis. *Trends Endocrinol Metab* 23, 459-66.
208. Scarpulla, R.C., 2008. Transcriptional paradigms in mammalian mitochondrial biogenesis and function. *Physiol Rev* 88, 611-38.



209. Schiaffin, S., Bormioli, S.P., Aloisi, M., 1976. The fate of newly formed satellite cells during compensatory muscle hypertrophy. *Virchows Arch B Cell Pathol* 21, 113–118.
210. Schmidt, B.J., Greenberg, C.R., Allingham-Hawkins, D.J., Spriggs, E.L., 2002. Expression of X-linked bulbospinal muscular atrophy (Kennedy disease) in two homozygous women. *Neurology* 59, 770–772.
211. Schoenmakers, E., Verrijdt, G., Peeters, B., Verhoeven, G., Rombauts, W., Claessens, F., 2000. Differences in DNA binding characteristics of the androgen and glucocorticoid receptors can determine hormone-specific responses. *Biol Chem* 275, 12290-7.
212. Scuderi, S., La Cognata, V., Drago, F., Cavallaro, S., D'Agata, V., 2014. Alternative splicing generates different parkin protein isoforms: evidences in human, rat, and mouse brain. *BioMed research international* 2014:690796.
213. Settembre, C., Ballabio, A., 2011. TFEB regulates autophagy: an integrated coordination of cellular degradation and recycling processes. *Autophagy* 7, 1379-81.
214. Settembre, C., Di Malta, C., Polito, V.A., Garcia Arencibia, M., Vetrini, F., Erdin, S., Erdin, S.U., Huynh, T., Medina, D., Colella, P., Sardiello, M., Rubinsztein, D.C., Ballabio, A., 2011. TFEB links autophagy to lysosomal biogenesis. *Science* 332, 1429-33.
215. Simeoni, S., Mancini, M.A., Stenoien, D.L., Marcelli, M., Weigel, N.L., Zanisi, M., Martini, L., Poletti, A., 2000. Motoneuronal cell death is not correlated with aggregate formation of androgen receptors containing an elongated polyglutamine tract. *Human Molecular Genetics* 9, 133–144.
216. Sinclair, R., Greenland, K.J., Egmond, S., Hoedemaker, C., Chapman, A., Zajac, J.D., 2007. Men with Kennedy disease have a reduced risk of androgenetic alopecia. *British Journal of Dermatology* 157, 290–294.
217. Sinha-Hikim, I., Taylor, W.E., Gonzalez-Cadavid, N.F., Zheng, W., Bhasin, S. 2004. Androgen receptor in human skeletal muscle and cultured muscle satellite cells: up-regulation by androgen treatment. *J Clin Endocrinol Metab* 89, 5245–5255.
218. Sobue, G., Hashizume, Y., Mukai, E., Hirayama, M., Mitsuma, T., Takahashi, A., 1989. X-linked recessive bulbospinal neuronopathy. A clinicopathological study. *Brain* 112 (Pt 1), 209–232.
219. Sopher, B.L., Thomas Jr., P.S., LaFevre-Bernt, M.A., Holm, I.E., Wilke, S.A., Ware, C.B., Jin, L.W., Libby, R.T., Ellerby, L.M., La Spada, A.R., 2004. Androgen receptor YAC transgenic mice recapitulate SBMA motor neuronopathy and implicate VEGF164 in the motor neuron degeneration. *Neuron* 41, 687–699.
220. Soraru, G., D'Ascenzo, C., Polo, A., Palmieri, A., Baggio, L., Vergani, L., Gellera, C., Moretto, G., Pegoraro, E., Angelini, C., 2008. Spinal and bulbar muscular atrophy: skeletal muscle pathology in male patients and heterozygous females. *Journal of the Neurological Sciences* 264, 100–105.
221. Sorenson, E.J., Klein, C.J., 2007. Elevated creatine kinase and transaminases in asymptomatic SBMA. *Amyotroph Lateral Scler* 8, 62-4.
222. Spencer, T.E., Jenster, G., Burcin, M.M., Allis, C.D., Zhou, J., Mizzen, C.A., McKenna, N.J., Onate, S.A., Tsai, S.Y., Tsai, M.J., O'Malley, B.W., 1997. Steroid receptor coactivator-1 is a histone acetyltransferase. *Nature* 389, 194-8.
223. Sperfeld, A.D., Karitzky, J., Brummer, D., Schreiber, H., Haussler, J., Ludolph, A.C., Hanemann, C.O., 2002. X-linked bulbospinal neuronopathy: Kennedy disease. *Archives of Neurology* 59, 1921–1926.
224. Sperfeld, A.D., Hanemann, C.O., Ludolph, A.C., Kassubek, J., 2005. Laryngospasm: an underdiagnosed symptom of X-linked spinobulbar muscular atrophy. *Neurology* 64, 753–754.
225. Spinazzi, M., Casarin, A., Pertegato, V., Salviati, L., Angelini, C., 2012. Assessment of mitochondrial respiratory chain enzymatic activities on tissues and cultured cells. *Nat protoc* 7, 1235-46.
226. Stenoien, D.L., Cummings, C.J., Adams, H.P., Mancini, M.G., Patel, K., DeMartino, G.N., Marcelli, M., Weigel, N.L., Mancini, M.A., 1999. Polyglutamine-expanded androgen

- receptors form aggregates that sequester heat shock proteins, proteasome components and SRC-1, and are suppressed by the HDJ-2 chaperone. *Hum Mol Genet* 8, 731-41.
227. Su, S., Jou, S., Cheng, W., Lin, T., Li, J., Huang, C., Lee, Y., Soong, B., Liu, C., 2010. Mitochondrial DNA damage in spinal and bulbar muscular atrophy patients and carriers. *Clin Chim Acta* 411, 626-30.
  228. Sugars, K.L., Rubinsztein, D.C., 2003. Transcriptional abnormalities in Huntington disease. *Trends Genet* 19, 233-8.
  229. Suzuki, E., Zhao, Y., Ito, S., Sawatsubashi, S., Murata, T., Furutani, T., Shirode, Y., Yamagata, K., Tanabe, M., Kimura, S., Ueda, T., Fujiyama, S., Lim, J., Matsukawa, H., Kouzmenko, A.P., Aigaki, T., Tabata, T., Takeyama, K., Kato, S., 2009. Aberrant E2F activation by polyglutamine expansion of androgen receptor in SBMA neurotoxicity. *Proceedings of the National Academy of Sciences of the United States of America* 106, 3818–3822.
  230. Suzuki, K., Katsuno, M., Banno, H., Takeuchi, Y., Atsuta, N., Ito, M., Watanabe, H., Yamashita, F., Hori, N., Nakamura, T., Hirayama, M., Tanaka, F., Sobue, G., 2008. CAG repeat size correlates to electrophysiological motor and sensory phenotypes in SBMA. *Brain* 131, 229–239.
  231. Takeyama, K., Ito, S., Yamamoto, A., Tanimoto, H., Furutani, T., Kanuka, H., Miura, M., Tabata, T., Kato, S., 2002. Androgen-dependent neurodegeneration by polyglutamine-expanded human androgen receptor in *Drosophila*. *Neuron* 35, 855–864.
  232. Tanaka, F., Doyu, M., Ito, Y., Matsumoto, M., Mitsuma, T., Abe, K., Aoki, M., Itoyama, Y., Fischbeck, K.H., Sobue, G., 1996. Founder effect in spinal and bulbar muscular atrophy (SBMA). *Human Molecular Genetics* 5, 1253–1257.
  233. Tanaka, F., Reeves, M.F., Ito, Y., Matsumoto, M., Li, M., Miwa, S., Inukai, A., Yamamoto, M., Doyu, M., Yoshida, M., Hashizume, Y., Terao, S., Mitsuma, T., Sobue, G., 1999. Tissue-specific somatic mosaicism in spinal and bulbar muscular atrophy is dependent on CAG-repeat length and androgen receptor–gene expression level. *American Journal of Human Genetics* 65, 966–973.
  234. Tassa, A., Roux, M.P., Attaix, D., Bechet, D.M., 2003. Class III phosphoinositide 3-kinase–Beclin1 complex mediates the amino acid-dependent regulation of autophagy in C2C12 myotubes. *Biochem J* 376, 577-86.
  235. Tatsuta, T., Scharwey, M., Langer, T., 2014. Mitochondrial lipid trafficking. *Trends Cell Biol* 24, 44-52.
  236. Taylor, J.P., Tanaka, F., Robitschek, J., Sandoval, C.M., Taye, A., Markovic-Plese, S., Fischbeck, K.H., 2003. Aggresomes protect cells by enhancing the degradation of toxic polyglutamine-containing protein. *Human Molecular Genetics* 12, 749–757.
  237. Thomas, P.S. Jr, Fraley, G.S., Damian, V., Woodke, L.B., Zapata, F., Sopher, B.L., Plymate, S.R., La Spada, A.R., 2006. Loss of endogenous androgen receptor protein accelerates motor neuron degeneration and accentuates androgen insensitivity in a mouse model of X-linked spinal and bulbar muscular atrophy. *Hum Mol Genet* 15, 2225-38.
  238. Tilley, W.D., Wilson, C.M., Marcelli, M., McPhaul, M.J., 1990. Androgen receptor gene expression in human prostate carcinoma cell lines. *Cancer Res* 50, 5382-6.
  239. Todd, T.W., Kokubu, H., Miranda, H.C., Cortes, C.J., La Spada, A.R., Lim, J., 2015. Nemo-like kinase is a novel regulator of spinal and bulbar muscular atrophy. *Elife* 4, e08493.
  240. Tohnai, G., Adachi, H., Katsuno, M., Doi, H., Matsumoto, S., Kondo, N., Miyazaki, Y., Iida, M., Nakatsuji, H., Qiang, Q., Ding, Y., Watanabe, H., Yamamoto, M., Ohtsuka, K., Sobue, G., 2014. Paeoniflorin eliminates a mutant AR via NF- $\kappa$ B-dependent proteolysis in spinal and bulbar muscular atrophy. *Hum Mol Genet* 23, 3552-65.
  241. Tomik, B., Partyka, D., Sulek, A., Kurek-Gryz, E.A., Banach, M., Ostrowska, M., Zaremba, J., Figlewicz, D.A., Szczudlik, A., 2006. A phenotypic-genetic study of a group of Polish patients with spinal and bulbar muscular atrophy. *Amyotroph Lateral Scler.* 7, 72-9.

242. Tokui, K., Adachi, H., Waza, M., Katsuno, M., Minamiyama, M., Doi, H., Tanaka, K., Hamazaki, J., Murata, S., Tanaka, F., Sobue, G., 2009. 17-DMAG ameliorates polyglutamine-mediated motor neuron degeneration through well-preserved proteasome function in an SBMA model mouse. *Human Molecular Genetics* 18, 898–910.
243. Trapman, J., Brinkmann, A.O., 1996. The androgen receptor in prostate cancer. *Pathol Res Pract* 192,752-60.
244. Trotter, P.J., Pedretti, J., Voelker, D.R., 1993. Phosphatidylserine decarboxylase from *Saccharomyces cerevisiae*. Isolation of mutants, cloning of the gene, and creation of a null allele. *J Biol Chem* 268, 21416-24.
245. Trushina, E., McMurray, C.T., 2007. Oxidative stress and mitochondrial dysfunction in neurodegenerative diseases. *Neuroscience* 145, 1233-48.
246. Tyagi, R.K., Lavrovsky, Y., Ahn, S.C., Song, C.S., Chatterjee, B., Roy, A.K., 2000. Dynamics of intracellular movement and nucleocytoplasmic recycling of the ligand-activated androgen receptor in living cells. *Mol Endocrinol* 14, 1162-74.
247. Umesono, K., Evans, R.M., 1989. Determinants of target gene specificity for steroid/thyroid hormone receptors. *Cell* 57, 1139-46.
248. Verhovshek, T., Cai, Y., Osborne, M.C., Sengelaub, D.R., 2010. Androgen regulates brain-derived neurotrophic factor in spinal motoneurons and their target musculature. *Endocrinology* 151, 253–261.
249. von Mikecz, A., 2009. PolyQ fibrillation in the cell nucleus: who's bad? *Trends Cell Biol* 19, 685-91.
250. Walcott, J.L., Merry, D.E., 2002. Ligand promotes intranuclear inclusions in a novel cell model of spinal and bulbar muscular atrophy. *J Biol Chem* 27, 50855-9.
251. Wang, D.W., Peng, Z.J., Ren, G.F., Wang, G.X., 2015. The different roles of selective autophagic protein degradation in mammalian cells. *Oncotarget* 6, 37098-116.
252. Wang, G., Jones, S.J., Marra, M.A., Sadar, M.D., 2006. Identification of genes targeted by the androgen and PKA signaling pathways in prostate cancer cells. *Oncogene* 25, 7311-23.
253. Warnecke, T., Oelenberg, S., Teismann, I., Suntrup, S., Hamacher, C., Young, P., Ringelstein, EB., Dzielwas, R., 2009. Dysphagia in X-linked bulbospinal muscular atrophy (Kennedy disease). *Neuromuscul Disord* 19, 704-8.
254. Warner, C.L., Griffin, J.E., Wilson, J.D., Jacobs, L.D., Murray, K.R., Fischbeck, K.H., Dickoff, D., Griggs, R.C., 1992. X-linked spinomuscular atrophy: a kindred with associated abnormal androgen receptor binding. *Neurology* 42, 2181-4.
255. Watson, N.V., Freeman, L.M., Breedlove, S.M., 2001. Neuronal size in the spinal nucleus of the bulbocavernosus: direct modulation by androgen in rats with mosaic androgen insensitivity. *J Neurosci* 21, 1062-6.
256. Waza, M., Adachi, H., Katsuno, M., Minamiyama, M., Sang, C., Tanaka, F., Inukai, A., Doyu, M., Sobue, G., 2005. 17-AAG, an Hsp90 inhibitor, ameliorates polyglutamine-mediated motor neuron degeneration. *Nature Medicine* 11, 1088–1095.
257. Wenz, T., Hielscher, R., Hellwig, P., Schägger, H., Richers, H., Hunte, C., 2009. Role of phospholipids in respiratory cytochrome bc(1) complex catalysis and supercomplex formation. *Biochim. Biophys. Acta* 1787, 609–616.
258. Wenz, T., 2013. Regulation of mitochondrial biogenesis and PGC-1 $\alpha$  under cellular stress. *Mitochondrion* 13, 134-42.
259. Wicks, K.L., Hood, D.A., 1991. Mitochondrial adaptations in denervated muscle: relationship to muscle performance. *Am J Physiol* 260, C841-50.
260. Xie, Z., Klionsky, D.J., 2007. Autophagosome formation: core machinery and adaptations. *Nat Cell Biol* 9, 1102-9.
261. Yamamoto, T., Yokota, K., Amao, R., Maeno, T., Haga, N., Taguri, M., Ohtsu, H., Ichikawa, Y., Goto, J., Tsuji, S., 2013. An open trial of long-term testosterone suppression in spinal and bulbar muscular atrophy. *Muscle Nerve* 47, 816-22.

262. Yang, Z., Chang, Y.J., Yu, I.C., Yeh, S., Wu, C.C., Miyamoto, H., Merry, D.E., Sobue, G., Chen, L.M., Chang, S.S., Chang, C., 2007. ASC-J9 ameliorates spinal and bulbar muscular atrophy phenotype via degradation of androgen receptor. *Nature Medicine* 13, 348–353.
263. Youle, R.J., Narendra, D.P., 2011. Mechanisms of mitophagy. *Nat Rev Mol Cell Biol* 12, 9-14.
264. cc, J.E., Garden, G.A., Martinez, R.A., Tanaka, F., Sandoval, C.M., Smith, A.C., Sopher, B.L., Lin, A., Fischbeck, K.H., Ellerby, L.M., Morrison, R.S., Taylor, J.P., La Spada, A.R., 2009. Polyglutamine-expanded androgen receptor truncation fragments activate a Bax-dependent apoptotic cascade mediated by DP5/Hrk. *Journal of Neuroscience* 29, 1987–1997.
265. Yu, Z., Dadgar, N., Albertelli, M., Gruis, K., Jordan, C., Robins, D.M., Lieberman, A.P., 2006. Androgen-dependent pathology demonstrates myopathic contribution to the Kennedy disease phenotype in a mouse knock-in model. *Journal of Clinical Investigation* 116, 2663–2672.
266. Yu, Z., Wang, A.M., Adachi, H., Katsuno, M., Sobue, G., Yue, Z., Robins, D.M., Lieberman, A.P., 2011. Macroautophagy is regulated by the UPR-mediator CHOP and accentuates the phenotype of SBMA mice. *PLoS Genetics* 7, e1002321.
267. Yu, W.H., 1989. Administration of testosterone attenuates neuronal loss following axotomy in the brain-stem motor nuclei of female rats. *J Neurosci* 9, 3908-14.
268. Zhang, J., Ney, P.A., 2009. Autophagy-dependent and -independent mechanisms of mitochondrial clearance during reticulocyte maturation. *Autophagy* 5, 1064-5.
269. Zeng, X., Overmeyer, J.H., Maltese, W.A., 2006. Functional specificity of the mammalian Beclin-Vps34 PI 3-kinase complex in macroautophagy versus endocytosis and lysosomal enzyme trafficking. *J Cell Sci* 119, 259-70.
270. Zhong, Q., Gohil, V.M., Ma, L., Greenberg, M.L., 2004. Absence of cardiolipin results in temperature sensitivity, respiratory defects, and mitochondrial DNA instability independent of pet56. *J Biol Chem* 279, 32294-300.

*Relazione sull'attività svolta nel triennio di*  
*dottorato*

## RELAZIONE SULL'ATTIVITÀ SVOLTA NEL TRIENNIO DI DOTTORATO

DOTTORANDO: Dr.ssa DORIANA BORGIA - TUTOR: Dr. GIANNI SORARU'  
Scuola di Dottorato in SCIENZE MEDICHE, CLINICHE E SPERIMENTALI  
Indirizzo NEUROSCIENZE

### Introduzione

L'Atrofia Muscolare Spino-Bulbare (SBMA) è una malattia dei motoneuroni dovuta all'espansione del tratto CAG nel primo esone del gene per il recettore degli androgeni (AR). Recentemente sono stati riscontrati un interessamento primario del muscolo (Malena et al., *Acta Neuropathol.* 2013,126:109-21; Cortes et al., *Neuron*, 2014,82:295-307; Sorarù et al., *J Neurol Sci.* 2008, 264:100-105) e alterazioni mitocondriali in topi Knock-in e leucociti di pazienti SBMA (Ranganathan et al., *HMG* 2009,18:27-42; Su et al., *Clin Chim Acta* 2010,411:626-630).

### Scopo

Lo scopo del mio studio è stato quello di valutare l'effetto di AR mutato su parametri mitocondriali nel tessuto muscolare di 19 pazienti SBMA e 18 controlli di pari età e sesso.

### Risultati

1. Ho trovato una normale espressione di AR nel tessuto dei pazienti, associata a un accumulo significativo della proteina mutata nel nucleo degli stessi (2 volte superiore a quanto trovato nei controlli). L'incremento di AR nei nuclei dei pazienti è risultato essere inversamente correlato con la loro età alla biopsia in maniera significativa. Tuttavia i livelli proteici del recettore nel lisato totale e nella frazione citosolica sono risultati significativamente più bassi di circa il 60% nel tessuto muscolare dei pazienti rispetto ai controlli. Per validare i dati, ho quantificato la purezza dell'estratto nucleare, valutando l'arricchimento del marker nucleare PARP rispetto al marker citosolico  $\beta$ -tubulina mediante Western Blot rispetto al citosol e al lisato totale. Ho trovato una quantità sei volte maggiore di PARP nella frazione nucleare ( $p < 0.001$ ).
2. Ho osservato una riduzione significativa della massa mitocondriale nel tessuto dei pazienti, espressa come riduzione del numero di copie di mtDNA (40%) e del segnale positivo all'NADH deidrogenasi (50%) in sezioni trasversali di muscolo colorate istochimicamente, avvalorando i dati di altri collaboratori che avevano trovato in precedenza: un decremento dell'attività della citrato sintasi (40%), una normale attività dei complessi della catena respiratoria ed una normale espressione e presenza proteica di geni mitocondriali o coinvolti nella biogenesi dei mitocondri, quali NRF1, TFAM, COX4, MnSOD, MFN1, MFN2, PGC-1 $\alpha$ , PGC-1 $\beta$  e ERR $\alpha$ . Ho, inoltre, confermato il normale funzionamento mitocondriale, mediante la quantizzazione dei supercomplessi mitocondriali con BN-PAGE e Western Blot, non riscontrando alcuna anomalia nel tessuto dei pazienti. Tali dati indicano che nel muscolo dei pazienti SBMA sono presenti meno mitocondri, che hanno una normale attività. Questa riduzione non è dovuta a una compromessa biogenesi mitocondriale.
3. Ho valutato gli Indici di Atrofia e di Ipertrofia nel tessuto muscolare di pazienti SBMA e controlli. Ho trovato nel muscolo dei pazienti valori molto elevati di entrambi gli Indici, che però non correlavano con il numero di copie di mtDNA quantizzate mediante RT-PCR.
4. Per spiegare la riduzione della massa mitocondriale, ho valutato il processo autofagico. Ho trovato un aumento significativo dei livelli proteici di LC3-II (49%), Beclin-1 (174%) e LAMP1 (529%), coinvolte nell'autofagia, nel lisato totale del muscolo SBMA rispetto ai controlli e un incremento significativo della presenza proteica di BNIP3 (187%), PINK1 (338%) e ubiquitina (200%), coinvolte nel processo autofagico, nei mitocondri isolati dal muscolo dei pazienti SBMA rispetto ai controlli.

L'espressione degli stessi geni, invece, è risultata essere non alterata. Per avvalorare i dati, ho quantificato la purezza dell'estratto mitocondriale, valutando l'arricchimento del marker mitocondriale TOM20 rispetto al marker citosolico  $\beta$ -tubulina mediante Western Blot rispetto al lisato totale. Ho trovato una quantità circa otto volte maggiore di TOM20 nella frazione mitocondriale ( $p < 0.001$ ).

5. Ho confermato i dati Western Blot di auto-mitofagia mediante indagine morfometrica, ovvero eseguendo una doppia colorazione del tessuto muscolare di pazienti SBMA e controlli con Ab anti-LC3 (marcatore dei lisosomi) e Ab anti-ATPasi (marcatore dei mitocondri) ed osservando mediante imaging sia un incremento significativo del numero di vacuoli autofagici (2 volte) che un incremento significativo del segnale di colocalizzazione dei due anticorpi (3,5 volte) nel muscolo SBMA rispetto ai controlli. I dati ottenuti mediante immunofluorescenza, dunque, hanno confermato quelli ottenuti mediante WB e cioè l'associazione tra la riduzione della massa mitocondriale con l'incremento del processo auto-mitofagico.
6. Ho misurato i livelli di espressione di Drp1 e hFis1, proteine coinvolte nella frammentazione del network mitocondriale, evento che precede la mitofagia, i quali sono risultati normali. Al contrario, sia nel lisato totale che nei mitocondri isolati ho trovato un aumento non significativo di Drp1 (37%) e un aumento significativo di hFis1 (72%) nel muscolo dei pazienti rispetto ai controlli.
7. Per chiarire il collegamento tra l'accumulo di AR nel nucleo dei pazienti e l'eliminazione dei mitocondri attraverso il macchinario auto-mitofagico, ho valutato la composizione lipidica delle membrane mitocondriali dei pazienti SBMA e controlli mediante spettrometria di massa. E' stata trovata una riduzione significativa del 52% della quantità di cardiolipina, il principale fosfolipide strutturale della membrana mitocondriale interna, e un aumento forse compensatorio del 49% della fosfatidiletanolamina e del 104% della fosfatidilserina, mentre è risultata normale la composizione delle cardiolipine. Alla luce dei risultati di De Primo et al. (Genome Biol. 2002; 3) e Wang et al. (Oncogene 2006; 25:7311-7323), nel muscolo dei pazienti SBMA ho valutato i livelli di espressione della cardiolipina sintasi (CRLS1), che sono risultati ridotti significativamente del 51% rispetto ai controlli. Questi dati sono in linea con quanto recentemente dimostrato da Halievski et al. su topi Tg femmine SBMA trattate con testosterone (PLoS One 2015, 10:e0118120), dati che riguardano la variazione dei livelli di espressione di proteine coinvolte nella biogenesi delle membrane dei mitocondri.

## Conclusioni

Lo studio da me condotto ha dimostrato la riduzione della quantità di mitocondri nel tessuto muscolare dei pazienti SBMA, osservata mediante analisi molecolari (riduzione del numero di copie di mtDNA), biochimiche (attività della citrato sintasi) e morfologiche (imaging su colorazione istochimica NADH-DH del tessuto muscolare). Tale riduzione non è dovuta ad alterata biogenesi mitocondriale ma a un aumento della rimozione dei mitocondri mediante meccanismo auto-mitofagico. Queste alterazioni sono associate a un accumulo di poli-Q AR nel nucleo del tessuto muscolare SBMA e a una significativa riduzione dei livelli di espressione della cardiolipina sintasi e della quantità di cardiolipina nelle membrane mitocondriali, parzialmente compensata da un aumento della fosfatidiletanolamina. Questi dati mostrano per la prima volta un meccanismo causa-effetto di accumulo nucleare di poli-Q AR associato a una riduzione della massa mitocondriale nel muscolo di pazienti SBMA, probabilmente dovuta a un'alterazione della struttura della membrana mitocondriale.

## Collaborazioni

In collaborazione con la dott.ssa M. Pennuto dell'Università di Trento, ho valutato nel muscolo scheletrico di topi knock-in (AR 113Q) affetti da SBMA e WT, trattati o meno con una dieta iperlipidica (Low Fat and High Fat diet), i seguenti parametri:

1. Numero di copie di DNA mitocondriale mediante RT-PCR: Ho quantizzato il numero di copie di mtDNA nel quadricipite di topi maschi WT e 113Q a 2, 3 e 6 mesi. Dai risultati è emerso che il numero di copie di mtDNA non varia nei topi 113Q di 2 mesi, mentre a 3 mesi in alcuni si osserva un decremento e a 6 mesi tutti i topi SBMA hanno meno copie di mtDNA rispetto ai WT. In seguito, ho fatto lo stesso tipo di valutazione sul quadricipite e il gastrocnemio di 4 topi WT LF, 4 topi 113Q LF, 4 topi WT HF e 4 topi 113Q HF, tutti maschi e a 6 mesi di vita. I dati ottenuti hanno confermato la riduzione significativa del numero di copie di mtDNA nel quadricipite dei topi 113Q a 6 mesi rispetto ai WT (50%). Interessante è il recupero significativo che ho osservato nei topi 113Q alimentati con una dieta di grasso, infatti essi avevano una quantità di mtDNA simile ai WT. Nessuna differenza, invece, è emersa nel gastrocnemio dei topi 113Q, indicando quindi un interessamento muscolo specifico dell'AR mutato.
2. Attività di enzimi glicolitici mediante analisi spettrofotometrica nei lisati totali: E' stato ipotizzato che nel quadricipite dei topi 113Q ci fosse una compromissione della glicolisi, che quindi poteva giustificare il rescue che si osservava alimentando i topi con il grasso. Per questo motivo ho valutato l'attività enzimatica di 3 proteine coinvolte in tale via metabolica (fosfofruttochinasi, piruvato chinasi e lattato deidrogenasi) nel quadricipite di 5 topi WT LF, 4 topi 113Q LF, 5 topi WT HF e 4 topi 113Q HF. Dai risultati è emerso che l'attività della lattato deidrogenasi è ridotta in maniera significativa al 68% nel muscolo dei topi 113Q LF rispetto ai WT e non alterata negli altri. L'attività degli altri due enzimi, invece, è risultata essere invariata nei topi 113Q sia LF che HF rispetto ai WT.
3. Esochinasi mediante WB nel lisato totale: i livelli proteici dell'esochinasi nei topi SBMA LF sono risultati significativamente ridotti del 66% rispetto ai controlli, con un parziale rescue significativo (80%) dei valori normali con dieta iperlipidica (HF).
4. Esochinasi mediante WB nei mitocondri isolati: i livelli proteici dell'esochinasi nei topi SBMA LF sono risultati ridotti significativamente al 20% rispetto ai controlli, con un parziale rescue significativo (58%) dei valori normali con dieta iperlipidica.
5. Quantità dei mitocondri come attività della citrato sintasi e analisi di imaging di sezioni di muscolo colorate istochimicamente per NADH-DH. L'attività della citrato sintasi, misurata mediante analisi spettrofotometrica nei lisati totali e normalizzata per mg di proteine mitocondriali, è risultata significativamente più alta nel muscolo dei topi SBMA LF e HF rispettivamente del 52% e 72% rispetto ai topi WT LF. La dieta iperlipidica non ha avuto alcun effetto sui topi WT HF. Tali dati suggeriscono un aumento della massa mitocondriale nel tessuto muscolare SBMA rispetto ai WT. Per confermare il dato, ho quantizzato il segnale positivo alla NADH deidrogenasi in sezioni trasversali di muscolo colorate istochimicamente. Tale segnale per campo è risultato aumentato significativamente al 547% e al 359% rispettivamente nel muscolo dei topi SBMA LF e HF rispetto ai WT LF, mentre nessuna differenza è stata trovata tra i due gruppi di topi WT.
6. Attività OXPHOS mediante analisi spettrofotometrica dell'attività enzimatica nei lisati totali: l'attività dei complessi della catena respiratoria (CI, CII, CIII, CI+CIII, CII+CIII e CIV), normalizzata per mg di proteine mitocondriali, è risultata sempre più alta in maniera significativa nel muscolo dei topi SBMA LF e HF rispetto ai WT, mentre non c'era alcuna differenza tra i gruppi di topi WT. Se invece l'attività dei complessi viene normalizzata per attività della citrato sintasi, che è un indicatore dell'abbondanza mitocondriale in un tessuto, non si osserva alcuna differenza tra i quattro gruppi di campioni. Tali dati indicano che nel tessuto dei topi SBMA ci sono più mitocondri, con una normale attività OXPHOS.

In collaborazione con la dott.ssa L. Vergani dell'Università degli studi di Padova, in cellule con una diversa percentuale di mutazione MELAS dell'mtDNA, cibridi di polmone (0%, 35%, 70% e 99% mutati) e cibridi di muscolo (0%, 70%, 80% e 99% mutati), ho valutato:



1. Geni coinvolti nel processo auto-mitofagico e nella dinamica mitocondriale mediante RT-PCR: ho valutato i livelli di espressione di LC3, Beclin-1, BNIP3, p62, PINK1 e Parkin per quanto riguarda il processo auto-mitofagico e di Drp1, hFis1, OPA1, MFN1 e MFN2 per quanto concerne la dinamica mitocondriale.
2. Proteine coinvolte nella dinamica mitocondriale e nella mitofagia mediante Western Blot su mitocondri isolati: ho valutato la presenza proteica di Drp1, hFis1, OPA1, MFN1 e MFN2, coinvolte nei processi di fusione e fissione mitocondriale, e di FUNDC1 e Bcl2, coinvolti nella mitofagia.

I dati da me prodotti hanno aiutato i miei collaboratori ad arrivare alla conclusione che i cibridi di polmone (A549 adenocarcinoma polmonare) favoriscono l' mtDNA wild-type e i cibridi di muscolo (RD rhabdomyosarcoma) favoriscono il DNA mitocondriale mutato. Difatti, tutti i dati ottenuti dimostrano che nei cibridi di polmone la mitofagia e la fissione aumentano con l'aumentare della quantità di DNA mitocondriale mutato, indicando che vi è una attiva rimozione dei mitocondri danneggiati. Interessante è notare che nei cibridi muscolari si verifica l'opposto: aumenta la fusione e la mitofagia diminuisce all'aumentare della percentuale di mutazione. Questi dati ci spiegano perché nei cibridi con background muscolare viene favorito il DNA mitocondriale mutato, e mostrano come possibile causa di questo comportamento la presenza di un alterato meccanismo di quality-control del network mitocondriale che è meno efficiente rispetto a quello dei cibridi con background polmonare.

In collaborazione con il dott. B. Pantic dell'Università di Padova, in cellule muscolari primarie di controlli e pazienti con Distrofia Miotonica immortalizzate e non attraverso una triplice stabile trasfezione con geni per CD1, CDK4 e telomerasi, ho valutato:

1. Numero di foci per nucleo, per valutare se la procedura di immortalizzazione consentiva il mantenimento delle caratteristiche di patogenicità. Non ho trovato differenze tra i due tipi di cellule di pazienti e nulla nei nuclei dei controlli.
2. Livelli proteici di CD1 e CDK4 nel lisato totale delle cellule dei pazienti immortalizzate, per valutarne il mantenimento dei livelli di espressione nel tempo. Non ho osservato variazioni nel tempo.

### **Tecniche di laboratorio acquisite:**

#### BIOLOGIA CELLULARE :

1. Colture cellulari: cellule primarie di mioblasti umane di pazienti SBMA e controlli e cibridi di polmone e muscolo
2. Sortaggio di cellule CD56 positive mediante FACS
3. Differenziazione delle cellule con o senza DHT e Sambutamolo Solfato o Clenbuterolo
4. Trattamento cellule con cloroquina e colorazione dei mitocondri con colorante vitale (mitotracker red)
5. Estrazione cellule satelliti da biopsie muscolari fresche

#### BIOLOGIA MOLECOLARE :

1. Estrazione DNA da cellule e da tessuto muscolare
2. Estrazione proteine da cellule e da tessuto muscolare
3. Estrazione RNA da cellule e da tessuto muscolare mediante trizol
4. Retrotrascrizione RNA in cDNA
5. Quantizzazione mtDNA umano e murino mediante RT-PCR
6. Quantizzazione dei geni coinvolti nell'autofagia, biogenesi lisosomiale, fissione e di AR mediante RT-PCR
7. Isolamento mitocondri da tessuto muscolare e cellule
8. Isolamento nuclei e citosol da tessuto muscolare

#### BIOCHIMICA:

1. WESTERN BLOT per analisi delle proteine coinvolte nell'autofagia e di AR e quantificazione mediante analisi densitometriche delle bande

2. Valutazione dell'attività enzimatica dei complessi della catena respiratoria e di enzimi glicolitici con spettrofotometro

#### TECNICHE DI IMAGING :

1. Immunofluorescenza di i) biopsie muscolari umane con Ab anti-ATPasi e Ab anti-LC3-II e osservazione al microscopio confocale; ii) fibrioblasti umani di pazienti SBMA e controllo trattati o meno con cloroquina: visualizzazione mitocondri con mitotracker red e autofagosomi con Ab anti-LC3-II
  2. Analisi di immagini mediante software dedicato (ImageJ)
  3. Quantizzazione dell'indice di fusione e del calibro dei miotubi dopo alcuni gg di differenziamento mediante software Image-Pro Plus
  4. Quantizzazione dell'Indice di Atrofia e di Ipertrofia con software dedicato
- Colorazione istochimica di tessuto muscolare per NADH-DH

#### **Pubblicazioni**

- A. Malena<sup>#</sup>, B. Pantic<sup>#</sup>, **Doriana Borgia**<sup>#</sup>, G. Sgarbi, G. Solaini, E. Perissinotto, I. J.Holt, A.Spinazzola, M. Sandri, A. Baracca, L.Vergani. “*Mitochondrial quality control is cell-type responsive to pathological mutant mitochondrial DNA*”. **Autophagy** - in revisione
- B. Pantic<sup>#</sup>, **Doriana Borgia**, S. Giunco, A. Malena, T. Kiyono, S. Salvatori, A. De Rossi, E. Giardina, F. Sangiuolo; E. Pegoraro, L. Vergani, A.Botta. “*Primary human myoblasts immortalized by cyclin D1, CDK4 and telomerase are reliable and versatile cell models of muscle disease*”. Sottomesso
- A.Rocchi<sup>#</sup>, C. Milioto<sup>#</sup>, S.Parodi, A.Armirotti, **Doriana Borgia**, M. Pellegrini, A. Urciulo, S. Molon, V. Morbidoni, M. Marabita, V. Romanello, P.Gatto, B. Blaauw, P. Bonaldo, F. Sambataro, D. M. Robins, A. P. Lieberman, G. Sorarù, L.Vergani, M. Sandri, M. Pennuto.”*Glycolytic-to-oxidative fiber-type switch and mTOR and PGC1 $\alpha$  activation are early-onset features of SBMA muscle that can be modified by high-fat diet*”. **Acta Neuropathologica** - in revisione
- **Doriana Borgia**<sup>#</sup>, A. Malena, M. Spinazzi, M.A. Desbats, V. Romanello, L.Salviati, G. Querin, E. Pegoraro, G. Sorarù, M.Sandri, A.P. Russel, G.Miotto, L. Vergani. “*Mitochondrial parameters in spinal bulbar muscular atrophy muscle tissue*”. In preparazione

#### **Partecipazione a congressi**

1. **Borgia Doriana**, Malena A., Spinazzi M., Bettio S., Querin G., Pegoraro E., Sorarù G., Russel A.P., Vergani L. “*Mitochondrial parameters in spinal bulbar muscular atrophy muscle tissue*”. **Secondo incontro di aggiornamento sulla malattia di Kennedy. Trento, 18 Aprile 2015**
2. **Borgia Doriana**, Malena A., Spinazzi M., Bettio S., Querin G., Pegoraro E., Sorarù G., Russel A.P., Vergani L. “*Mitochondrial parameters in spinal bulbar muscular atrophy muscle tissue*”.  
**GIBB: Gruppo Italiano di Biomembrane e Bioenergetica. Padova, 20-22 Giugno 2013**

#### **Attività seminariale**

1. **Incontri di patologia neuromuscolare**  
Padova, ogni mercoledì dal 13 marzo 2013 al 29 maggio 2013, Auletta del Dipartimento di Neuroscienze SNPSRR
2. **Riunione annuale GIBB (Gruppo Italiano di Biomembrane e Bioenergetica)**  
Padova 20 – 22 giugno 2013 Aula Magna, Complesso Interdipartimentale Vallisneri
3. **SUMMER SCHOOL – IOV**  
Padova, 23-27 Settembre 2013 Aula Magna – Sezione di Oncologia – Dipartimento di Scienze Chirurgiche, Oncologiche e Gastroenterologiche
4. **Incontro di aggiornamento sulla malattia di Kennedy**

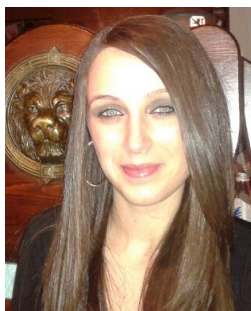
- Padova 30 ottobre 2013 Aula Magna, Complesso Interdipartimentale Vallisneri
5. **NIMR-Padova Symposium on Mitochondrial DNA Segregation, Expression & Survival**  
Londra 1-2 Aprile, NIMR (National Institute for Medical Research)
  6. **Understanding Muscle Stem Cell Functional Decay During Physiological Aging**  
Padova, Martedì 8 Aprile 2014, Aula Seminari del VIMM
  7. **Stem Cells in Silence, Action and Cancer**  
Padova, Mercoledì 7 Maggio 2014, Aula Seminari del VIMM
  8. **Coenzyme Q biosynthesis from yeast to humans**  
Padova, Giovedì 22 maggio 2014, Aula Magna della Clinica Neurologica
  9. **L'organo adiposo e il sistema neuro-muscolare: implicazioni nutrizionali**  
Padova, 28 maggio 2014, Aula Morgagni – Policlinico
  10. **Terapia dell'Epilessia: la gestione del paziente che giunge in Pronto Soccorso**  
Padova, Martedì 13 Gennaio 2015, Aula Magna della Clinica Neurologica
  11. **II° INCONTRO DI AGGIORNAMENTO SULLA MALATTIA DI KENNEDY**  
Trento, Sabato 18 Aprile 2015, Aula Magna (B107) del CIBIO (Centre for Integrative Biology), Università di Trento
  12. **SPRING SCHOOL**  
Bressanone, Venerdì-Sabato 29-30 Maggio 2015, Aula Magna della Casa della Gioventù, Università degli Studi di Padova
  13. **Esercizio fisico, salute e malattia**  
Padova, Giovedì 3 Dicembre 2015, Aula Seminari del VIMM



## *Curriculum vitae*



## INFORMAZIONI PERSONALI



## Doriana Borgia

📍 Via Marco Antonio Calza, 9, 35128, Padova, Italia

☎ 3486383044

✉ [doriana89b@hotmail.it](mailto:doriana89b@hotmail.it)

Skype [doriana89b](#)

👤 Sesso F | 📅 Data di nascita 30/11/1989 | 🇮🇹 Nazionalità Italiana

## ISTRUZIONE E FORMAZIONE

01/01/2013 – 31/12/2015

### Dottore di Ricerca (ammessa all'esame finale)

Laboratorio Neuromuscolare – Dipartimento di Neuroscienze (DNS) – Università degli studi di Padova

- Valutazione di parametri mitocondriali nel tessuto muscolare di pazienti e topi knock-in affetti da Atrofia Muscolare Spino-Bulbare

Gennaio 2013

### Abilitazione all'esercizio della professione di Biologa

Università della Calabria – via Pietro Bucci – Arcavacata di Rende (CS)

Ottobre 2010 – 04/10/2012

### Laurea Magistrale in Biologia (classe LM-6)

Università della Calabria – via Pietro Bucci – Arcavacata di Rende (CS)

- Titolo della tesi: Regolazione da cationi dei sistemi di trasporto umani OCTN1 e OCTN2
- Voto: 110/110 e lode

Ottobre 2007 – 04/10/2010

### Laurea Triennale in Scienze Biologiche (classe 12)

Università della Calabria – via Pietro Bucci – Arcavacata di Rende (CS)

- Titolo della tesi: Trattamento igienico-sanitario delle acque potabili
- Voto: 109/110

## COMPETENZE PERSONALI

Lingua madre

Italiano

Altre lingue

Inglese

COMPRESIONE		PARLATO		PRODUZIONE SCRITTA
Ascolto	Lettura	Interazione	Produzione orale	
B2	B2	B2	B2	B2

Livelli: A1/A2: Utente base - B1/B2: Utente intermedio - C1/C2: Utente avanzato  
[Quadro Comune Europeo di Riferimento delle Lingue](#)

- Competenze comunicative**
- Consolidata attitudine al lavoro di gruppo
  - Ottima capacità di comunicazione e di adattamento
  - Vasta esperienza nell'interazione con personale tecnico-scientifico di vario livello
- Competenze organizzative e gestionali**
- Vasta esperienza nella gestione organizzativa di un laboratorio e nella pianificazione ed esecuzione di esperimenti
- Competenze professionali**
- BIOLOGIA CELLULARE:**
- Colture cellulari: cellule primarie di muscolo (mioblasti e fibroblasti) umani e murini e di ibridi di muscolo (RD) e polmone (A549)
  - Sortaggio di cellule CD56 positive mediante FACS
  - Estrazione cellule satelliti da biopsie muscolari fresche
- BIOLOGIA MOLECOLARE:**
- Estrazione DNA/RNA/proteine da cellule e da tessuto muscolare
  - Retrotrascrizione RNA in cDNA
  - PCR e RT-PCR
  - Digestione enzimatica DNA
  - Elettroforesi su gel di agarosio DNA
- BIOCHIMICA:**
- Isolamento mitocondri da tessuto e cellule muscolari
  - Isolamento nuclei e citosol da tessuto muscolare
  - SDS-PAGE, WESTERN BLOT e quantificazione delle bande mediante analisi densitometriche (Gel-Pro Analyzer)
  - Valutazione dell'attività enzimatica dei complessi della catena respiratoria e di enzimi glicolitici con spettrofotometro
  - Purificazione di proteine ricombinanti over-esprese in E.Coli: cromatografia per affinità su colonne al nichel
  - Ricostituzione proteina purificata in liposomi
  - Valutazione attività di trasporto di proteine della membrana plasmatica ricostituite in liposomi con substrato radioattivo
  - Cromatografia su colonna per gel filtrazione o esclusione molecolare (resina Sephadex G-75)
  - Analisi aspetti funzionali e cinetici dell'attività di trasporto con software dedicato (Grafit 5.0)
- IMAGING:**
- Immunofluorescenza di biopsie e cellule muscolari e osservazione al microscopio confocale
  - Colorazione istochimica tessuto muscolare per NADH-DH
  - Analisi di immagini mediante software dedicato (ImageJ)
  - Quantizzazione dell'indice di fusione e del calibro dei miotubi dopo alcuni giorni di differenziamento mediante software Image-Pro Plus
  - Quantizzazione dell'Indice di Atrofia e di Ipertrofia di tessuto muscolare con software dedicato (ImageJ)

**Competenza digitale**

**AUTOVALUTAZIONE**

Elaborazione delle informazioni	Comunicazione	Creazione di Contenuti	Sicurezza	Risoluzione di problemi
Utente intermedio	Utente intermedio	Utente intermedio	Utente intermedio	Utente intermedio



Altre competenze      Livelli: Utente base - Utente intermedio - Utente avanzato  
Competenze digitali - Scelta per autovalutazione  
Titolo: Complemento in corso di pianoforte, conseguito il 06/09/2006, presso Istituto Musicale Pareggiato P.I. Tchaikovsky - Nocera Terinese (CZ)  
▪ Ottima conoscenza dei programmi del pacchetto Microsoft Office (Word, Excel, PowerPoint)  
Titolo: Diploma di Teoria e Solfeggio, conseguito il 09/09/2004, presso Conservatorio di Musica Stanislao Giacomantonio – Cosenza (CS)  
▪ Ottima capacità di utilizzo di motori di ricerca

Patente di guida      B

## ULTERIORI INFORMAZIONI

---

### Publicazioni

- A. Malena<sup>#</sup>, B. Pantic<sup>#</sup>, **Doriana Borgia<sup>#</sup>**, G. Sgarbi, G. Solaini, E. Perissinotto, I. J.Holt, A.Spinazzola, M. Sandri, A. Baracca, L.Vergani. *"Mitochondrial quality control is cell-type responsive to pathological mutant mitochondrial DNA". **Autophagy*** - in revisione
- B. Pantic<sup>#</sup>, **Doriana Borgia**, S. Giunco, A. Malena, T. Kiyono, S. Salvatori, A. De Rossi, E. Giardina, F. Sangiuolo; E. Pegoraro, L. Vergani, A.Botta. *"Primary human myoblasts immortalized by cyclin D1, CDK4 and telomerase are reliable and versatile cell models of muscle disease"*. Sottomesso
- A.Rocchi<sup>#</sup>, C. Milioto<sup>#</sup>, S.Parodi, A.Amirotti, **Doriana Borgia**, M. Pellegrini, A. Urciulo, S. Molon, V. Morbidoni, M. Marabita, V. Romanello, P.Gatto, B. Blaauw, P. Bonaldo, F. Sambataro, D. M. Robins, A. P. Lieberman, G. Sorarù, L.Vergani, M. Sandri, M. Pennuto. *"Glycolytic-to-oxidative fiber-type switch and mTOR and PGC1 $\alpha$  activation are early-onset features of SBMA muscle that can be modified by high-fat diet"*. **Acta Neuropathologica** - in revisione
- **Doriana Borgia<sup>#</sup>**, A. Malena, M. Spinazzi, M.A. Desbats, V. Romanello, L.Salviati, G. Querin, E. Pegoraro, G. Sorarù, M.Sandri, A.P. Russel, G.Miotto, L. Vergani. *"Mitochondrial parameters in spinal bulbar muscular atrophy muscle tissue"*. In preparazione

### Congressi

- **Borgia D.**, Malena A., Spinazzi M., Bettio S., Querin G., Pegoraro E., Sorarù G., Russel A.P., Vergani L. *"Mitochondrial parameters in spinal bulbar muscular atrophy muscle tissue"*. **Secondo incontro di aggiornamento sulla malattia di Kennedy, Trento, 18 Aprile 2015**
- **Borgia D.**, Malena A., Spinazzi M., Bettio S., Querin G., Pegoraro E., Sorarù G., Russel A.P., Vergani L. *"Mitochondrial parameters in spinal bulbar muscular atrophy muscle tissue"*. **GIBB: Gruppo Italiano di Biomembrane e Bioenergetica. Padova, 20-22 Giugno 2013**